2010

Survey of gas-liquid mass transfer in bioreactors

Enes Kadic
Iowa State University

Survey of gas-liquid mass transfer in bioreactors

by

Enes Kadic

A thesis submitted to the graduate faculty
in partial fulfillment of the requirements for the degree of
MASTER OF SCIENCE

Major: Mechanical Engineering

Program of Study Committee:
Theodore J. Heindel, Major Professor
Ron M. Nelson
Brent H. Shanks

Iowa State University

Ames, Iowa

2010

Table of Contents

List of Figures

List of Tables

Abstract

Bioreactors are becoming more important in the production of biobased products such as proteins, medicines, and renewable fuels. The economic viability of these processes is dependent on the bioreactor's ability to aid the microorganism and provide a friendly environment. One of the important microorganism requirements is proper gas concentrations so that the microorganism has the necessary inputs for proper metabolism. These gas concentrations are obtained and maintained through optimized gas-liquid mass transfer and mixing, also known as hydrodynamics. Other bioreactor responsibilities include damage mitigation and bioreactor volume utilization. A proper bioreactor design should also maximize profitability through ease of use, maintenance, and construction.

This thesis work provides a survey of gas-liquid mass transfer theories, applications, and dependencies in major bioreactor and several novel designs. The major reactor designs include the stirred tank bioreactor, bubble column, airlift bioreactor, and fixed bed bioreactor. Variations of these major designs are also considered such as the slurry bubble column, internal- and external-loop airlift, draught-tube bioreactor, and trickle, packed, and flooded bed bioreactor.

Since the microorganisms used in biological processes are diverse, a best or preferred bioreactor design is not feasible. Rather, bioreactor options can be presented based on the microorganism properties and production scale. Stirred tank bioreactors generally produce the largest gas-liquid mass transfer rates, but they also tend to cause high shear rates and variations, which can be very harmful to microorganisms. The impeller often limits the operating range, scale, process time, especially with non-Newtonian liquids. The bubble column and internal-loop airlift bioreactor have similar gas-liquid mass transfer rates; however, the bubble column has significant backmixing while the airlift bioreactor has lower bioreactor volume utilization. The external-loop airlift bioreactor provides more process and mixing control and generally has lower shear rates, but the attainable gas-liquid mass transfer rate and volume utilization tend to be lower. The fixed bed

bioreactors protect and support microorganisms very well. On the other hand, the phase flow rates are much lower than in the other bioreactor designs. In other words, each bioreactor design has important advantages and disadvantages, and the microorganism may very well determine the optimal design.

The bioreactor designs may be described as complementary rather than competitive. Each design and design variation has been implemented to fill a void caused by the original form. This design mentality has led to highly complex bioreactor relationships and the inability to identify the single best bioreactor because that was not the intent. Future research and development can be taken into two different directions. First, a design variation could be approached with the clear intent of superiority for biological processes. Such a device could possible use a mixture of airlift and stirred tank bioreactor attributes. Second, research could be oriented towards the continued niche creation. Each design improvement would be implemented with the intent of improving a certain bioreactor attribute or application with a specific type of microorganism. For example, the fixed bed bioreactor research could investigate new packing that would provide better support and shear protection for very sensitive microorganisms such mammalian cells.

Acknowledgements

This material is based upon work supported by ConocoPhillips Company. Any opinions, findings, conclusions, or recommendations are those of the author and do not reflect the views of ConocoPhillips Company. The author acknowledges Dr. Theodore Heindel for the guidance, ideas, and support as well as the committee members, Dr. Ron Nelson and Dr. Brent Shanks.

1 Introduction

The biological production of renewable fuels and chemical, medicines, and proteins is not possible without a properly functioning bioreactor. Bioreactors are expected to meet several basic requirements and create conditions favorable to the biological matter such that the desired production is maximized. The basic requirements may include minimal damage to the biological matter, maximize reactor volume utilization, maximum gas-liquid mass transfer, and/or maximum mass transfer from the liquid to the biological species (Bliem and Katinger, 1988a). Even though gas-liquid mass transfer is often the limiting reaction process, the biological species may incur additional limitations. For example, biological species can be very sensitive to shear while others may not grow well in low power concentrations and thrive in very turbulent conditions (Bliem and Katinger, 1988a; Hoffmann et al., 2008). In other words, the reactor has to accommodate very specific environmental conditions, and the operator has to be mindful of those when choosing bioreactors design and operating condition.

Once the broadness of the problem is absorbed, it becomes clear that one bioreactor design or design ideology is insufficient to meet the spectrum of needs (Bliem and Katinger, 1988a). Therefore, each bioreactor design tries to produce a very specific set of conditions applicable to a certain cell or bacteria line. In order to help with this decision process, this thesis work provides a survey of relevant gas-liquid and gas-liquid-solid bioreactors, defines the bioreactors' pros, cons, and hydrodynamics, and identifies research needs and figures of merit that have yet to be addressed. Since a large portion of the bioreactor designs have been ported over from the chemical and petrochemical industries, a significant portion of the research work also origninated from those areas. Hence, bioreactors will often be referred to as simply reactors in order to signal that some of the research used for the discussion and conclusion have been adapted from non-biological research areas.

2 Modes of Operation

Batch, semi-batch, and continuous modes of operation are classified by the flow rates in and out of the system. Virtually all reactor types are capable of operating in these modes. This section will review the different modes by presenting some general information, operating procedures, and advantages and disadvantages.

2.1 Batch Bioreactors

The batch reactor is the oldest and most used bioreactor in industry (Bellgardt, 2000; Branyik et al., 2005). Its historical and most familiar use is in the production of alcoholic beverages (beer, wine, whiskey, etc.) and bread. Batch bioreactors combine all the necessary ingredients and then operate until the desired product concentration is reached at which point the product is extracted. In well-known processes where the final product is relatively cheap, product concentration can be correlated to time, leading to some process automation, lower capital needs, and lower operational costs (Bellgardt, 2000). Batch reactor systems are also useful in modeling environmental issues (Fogler, 2005).

Biological application and experience has led to differentiation based on substrate input or sterilization frequency. The simplest and least applicable variant is the batch cultivation system (Bellgardt, 2000). Reactor sterilization is undertaken prior to the start of the process, followed by the medium being fed into the reactor creating a high substrate concentration (Bellgardt, 2000; Williams, 2002). Inoculated microorganisms are introduced to the batch reactor at a low concentration to allow proper growth which is practically uncontrollable until the process is finished. Ideally, the product is extracted once a satisfactory concentration is achieved, but the product in the batch cultivation system is also extracted if a necessary ingredient has been exhausted (Bellgardt, 2000). Finally, the reactor is cleaned, and the process starts over again with reactor sterilization.

The need for more control over the biological process created the fed-batch (also known as the semi-batch) cultivation system, which is the most widely used batch reactor. This deviation is a variable volume process that introduces additives, gradually creating a more responsive and friendly growth environment (Bellgardt, 2000). In other words, the bacteria receives the right amount and type of nutrients at the appropriate growth stage, creating a more efficient and controllable process. The final result is a product that can be adjusted or extracted when it achieves the desired properties.

The fed-batch and batch cultivation systems share the same cleaning and sterilization process. This stoppage creates considerable costs and operational downtime. The repeated or cyclic system, which can be applied to both batch and fed-batch cultivation, may be installed in order to maximize productivity. The cyclic cultivation system does not enter the cleaning and sterilization process, but rather preserves part of the batch for the next cycle. Another method to increase productivity is cell retention techniques such as fluidized beds, membranes, or external separators. These options allow multiple cycles without cleaning and sterilization, which is initiated only if it is deemed that mutation risks exceed tolerable levels (Bellgardt, 2000).

Batch bioreactor variants try to limit problems or expand applications of batch reactors, but some systematic advantages and disadvantages exist. For the most part, batch bioreactors have lower fixed costs due to the simple concept, design, and process control (Bellgardt, 2000; Donati and Paludetto, 1999; Williams, 2002); however, variable costs are generally higher for several reasons. First, cleaning and sterilization often add significant downtime and labor costs (Donati and Paludetto, 1999; Williams, 2002). These costs, however, can be limited in the cyclic cultivation system. Second, batch bioreactors have heat recovery difficulties leading to high environmental impact and energy consumption (Donati and Paludetto, 1999; Schumacher, 2000; Williams, 2002). Third, the additive nature of fed-batch and cyclic cultivation systems force the operator to prepare several subcultures for inoculation, which adds further variable cost pressures (Williams, 2002).

Lastly, batch bioreactors are not steady-state processes. The biological matter grows uncontrollably, leading to a changing environment which can bring about safety issues, runaway growth, or unexpected products (Westerterp and Molga, 2006).

Runaway reactions are unlikely in biological systems, but the variable environment can create conditions that change the competitive situation favoring a different bacterial species than the initially dominant one (Hoffmann et al., 2008). Batch reactors have limited, albeit relatively simple, process control which can lead to inconsistent or unwanted product, especially in a batch cultivation system. This problem can get even more pronounced in operations with a high potential contact amid pathogenic microorganisms or toxins, adding to variable costs if more stringent cleaning and sterilization procedures are needed (Williams, 2002).

The fed-batch cultivation system makes process control more challenging by creating a variable volume process. Any control mechanisms, therefore, require much more labor or capital (Bellgardt, 2000; Donati and Paludetto, 1999; Simon et al., 2006; Williams, 2002). According to Simon et al. (2006), a fed-batch system can have thousands of control variables requiring a modern and powerful supervisory control and data acquisition system, programmable logic controllers, trained personnel, and an eight year upgrade cycle, all of which eliminate or limit upgradability of older systems or construction of larger batch bioreactor systems (Heijnen and Lukszo, 2006; Simon et al., 2006). The complexity limits practical batch bioreactor application beyond a certain size, while other bioreactor modes enjoy economies of scale for much larger operations (Donati and Paludetto, 1999; Heijnen and Lukszo, 2006; Simon et al., 2006; Williams, 2002).

Some of the batch system costs can be offset by its flexibility. Batch bioreactors are able to produce the desired product consistently. They are also capable of producing several types of products with the same equipment or making the same type of product with different equipment. Significant product modifications can also be implemented online (Donati and Paludetto, 1999; Heijnen and Lukszo, 2006). These traits offer flexibility and competitive advantages to batch

reactor operations; however, many problems and complications are encountered when these reactor schemes are used for multiple separation processes, which is often the case in industry (Barakat and Sorensen, 2008).

Most batch reactors operate in a changing external environment especially with respect to product and ecological demands (Heijnen and Lukszo, 2006). Researchers are able to take batch bioreactors and investigate reactions, both chemical and biological, for which data are unavailable or have never been documented, while limiting contamination and experimental or dangerous risks (Donati and Paludetto, 1999). These research reactors should be used for scaling purposes with care since most reactions and biological growth are affected by hydrodynamics, which are a function of reactor scale and type.

Ultimately, batch bioreactors contain biological matter that tends to mutate. Growth periods, therefore, need to be kept short and controlled to prevent these microbial mutations, which could produce inconsistent or undesirable products (Williams, 2002). Some fermentation processes, however, are characterized by biological matter that mutates very little allowing for long reaction times (Donati and Paludetto, 1999). Either way, a positive side effect of the controlled growth period is a higher conversion level (Williams, 2002).

A specific batch bioreactor application depends on multiple internal and external factors; however, general rules of thumb and process specific improvements can be employed to make a smarter and more profitable selection. Batch bioreactor selectivity is based on the following factors: economic balance, production scale, reaction times, production flexibility, and the nature of the process and product (Donati and Paludetto, 1999). Typically, batch bioreactors are used for smaller operations, specialty products, long growth periods (reactor of choice by elimination), operations in which flexibility is vital, unsteady processes, and experimental development (Donati and Paludetto, 1999; Simon et al., 2006; Williams, 2002).

Batch bioreactor operation can be made more efficient by implementing several simple managerial procedures. First, a disturbance strategy should be developed by which personnel are trained to respond and actively scan for problems in the process leading to "lines of defense" that limit contamination and loss of product (Westerterp and Molga, 2006). These "lines of defense" should include an operating condition within which personnel and management are comfortable, an early warning system, and a reaction procedure to accidents and malfunctions including proper training and equipment (Westerterp and Molga, 2006). Second, a decision support framework (DSF) should be developed so all personnel and management are familiar with operating costs, benefits, objectives, etc. The DSF will make production more efficient and profitable; it provides a clear outline of benefits and costs associated with general and specific options. General models, such as ANSI/ISA88 or ANSI/ISA95, are available and can be applied to all batch reactors (Heijnen and Lukszo, 2006). Lastly, two improvement strategies can be implemented to make batch reactions more efficient. The "cook book" or "recipe" approach has been shown to improve yields in batch process operations. The user is able to adjust the biological reaction online as needed and is able to draw upon extensive experience and/or knowledge to have better process control and product quality and consistency. The second strategy, production schedule optimization, has been proven effective in situations where products are made with different equipment, or equipment is used to make different products by optimizing capacity utilization (Schumacher, 2000).

2.2 Continuous Bioreactors

Continuous bioreactors have several intrinsic properties that differentiate them from batch bioreactors. The largest distinction is that substrate and product continuously flow in and out of the reactor, which does not allow for a cleaning or sterilization processes and extracts product regardless of identity or qualities (Bellgardt, 2000). If output does not meet specifications, the resulting product has to be either discarded or separated and recycled back into the reactor. Either option creates a negative economic impact by increasing (i) initial investment due to the necessary

installation of a recycling system and (ii) variable costs due to the discarded product and the associated inputs (Williams, 2002). Product properties are controlled by substrate residence time which, by design, can only be controlled by material flow rate and reactor geometry. In order to ensure a homogeneous product, the process is assumed to be steady-state and conditions within the bioreactor are typically assumed to be independent with time (Williams, 2002). Therefore, continuous bioreactors are agitated mechanically and/or by gas injection. Substrate input is not used for agitation so as to decouple it from reactor hydrodynamics. In order to make the steady-state conditions easier to achieve and maintain, most continuous bioreactors are run in a constant volume setting, which induces uniform volumetric substrate and product flow rates. Efficiency is enhanced using cell retention techniques such as fluidized beds, membrane reactors, or cell recycle (Bellgardt, 2000). The semi-continuous bioreactor, a hybrid between the batch and continuous bioreactor, is run in batch mode during start-up. Once necessary conditions are achieved, this bioreactor is operated continuously unless the product has not achieved the necessary properties, in which case the reactor is operated in batch mode until the desired specifications are met (Williams, 2002).

Any continuous bioreactor discussion is ultimately related to batch systems which are seen as a proven technology with processes designed around their capabilities and properties. In addition, operators have more experience and are more comfortable dealing with batch disturbances (Branyik et al., 2005). Continuous bioreactors, however, offer many advantages such as control, production, and the potential for optimization (Williams, 2002). Control can be achieved with several schemes. Substrate and cell concentrations or reactor conditions can be modified online to influence bacterial growth rates which, in turn, modify reactor and reaction dynamics (Bellgardt, 2000; Gonzalez et al., 1998; Ramaswamy et al., 2005; Reddy and Chidambaram, 1995; Sokol and Migiro, 1996). These changes provide an indirect influence over product type and properties (Ramaswamy et al., 2005).

The continuous bioreactor offers more operational control and flexibility over batch bioreactors. Practical production is made simpler and more profitable due to the possibility for automation and the lack of cleaning and sterilization processes (Bellgardt, 2000). The added equipment cost is offset with operational savings while control schemes, which are limited to a few hundred variables, are often much simpler than the corresponding batch reactor systems (Simon et al., 2006; Williams, 2002).

In addition to the control advantages, the steady-state operation of continuous bioreactors allows for the production of a consistent and economically attainable product quality (Williams, 2002). It also rectifies a major downside in the batch system – the bacterial concentration is very low in the initial stages while growth rates are sluggish at maturity, both leading to decreased productivity. The continuous system allows high bacterial concentrations throughout the process, boosting production capacity and consistency (Bellgardt, 2000). Combined with the lack of cleaning and sterilization processes, continuous bioreactors maximize production time while providing lower labor and variable costs and maximum capital utilization (Bellgardt, 2000; Williams, 2002).

Lastly, continuous bioreactors allow for optimization. Operators are able to vary inputs and reactor conditions online, creating an optimized environment for the growth stage and age of the cell culture, resulting in a more consistent output (Bellgardt, 2000; Williams, 2002). In some series reactor applications, process augmentation is necessary to prevent wash-out or inconsistent product (in case of a upstream disturbance and varying substrate concentration). These disturbances and variances are often experienced when a batch reactor or other limiting cycles are used to prepare a substrate for the continuous process (Ramaswamy et al., 2005).

Disturbance management depends greatly on the ability to investigate the cause of the disturbance. Batch reaction systems have complicated procedures to identify the cause of disturbances with the operator often left guessing (Schumacher, 2000). The continuous process provides a clear plan of attack. The effect of changing one variable while keeping all others constant

allows for a clear relationship and better understanding (Williams, 2002). Researchers are able to form global correlations or models aiding development, adoption, or on-going operations.

Much higher production capacity, efficiency, capital utilization, and lower variable costs for continuous bioreactors may make operations appear efficient, but continuous systems have a number of disadvantages. Biological growth typically requires a batch start-up period to achieve conditions within the reactor to promote optimal production (Bisang, 1996; Gonzalez et al., 1998; Williams, 2002). In addition, bacterial matter, especially in recycle and retention processes, age and mutate which negatively impacts their productivity and efficiency and may even lead to the production of unwanted products (Branyik et al., 2005; Domingues and Teixeira, 2000). If so, a continuous system is either unable to produce the prescribed product quality or requires more equipment and control systems (Williams, 2002). Long lasting processes also have contamination problems and biological growth on the walls, requiring the reactor to be controlled more closely; otherwise, faster growing cultures overtake the desired ones (Bellgardt, 2000; Williams, 2002).

Controlling continuous production is also made more difficult because it is usually non-linear (Ramaswamy et al., 2005; Reddy and Chidambaram, 1995). Several control mechanisms exist, but most make the mistake of varying substrate or bacterial concentrations based on indirect data, such as temperature or pH, and assuming a first order response (Bellgardt, 2000; Ramaswamy et al., 2005). This type of control mechanism usually results in a system that is too slow and has stability problems (Reddy and Chidambaram, 1995). Non-linear controllers are available, but been have shown to be unreliable and complicated and usually report excessive variations (Gonzalez et al., 1998; Reddy and Chidambaram, 1995). Operators may also be limited to a certain gas or liquid input range. Bacteria require a certain amount of gas for proper growth, and a low gas flow rate could suffocate the bacteria or create a hostile environment decreasing reactor productivity. On the other hand, too much gas may create suboptimal conditions and have a negative impact on bacterial growth or reactor hydrodynamics (Bellgardt, 2000).

The flexibility, reliability, efficiency, and cost reductions which the continuous systems are supposed to deliver can be offset by control issues, making the pure continuous bioreactor ineffective and even more expensive to operate than batch systems (Williams, 2002). In addition, some fermentation processes, such as beer production, are not able to easily use continuous systems since they change basic product properties, such as taste, color, and/or odor (Branyik et al., 2005).

Several scenarios exist for which continuous bioreactors are feasible and preferred, such as high volume production, use of mutation resistant bacteria culture, wastewater treatment, and processes which do not require a sterile environment. Currently, continuous bioreactors are used for the production of vinegar, baker's yeast, alcohols, and solvents and for wastewater treatment (Bellgardt, 2000; Simon et al., 2006; Williams, 2002). Proper control systems also allow continuous principles to be used in other production systems. These requirements include that the process does not necessitate a sterile environment or that it can be easily controlled through alternative means such as flocculation, substrate and cell concentrations, or the use of secondary or genetically altered cell cultures (Bellgardt, 2000; Bisang, 1996; Domingues and Teixeira, 2000; Gonzalez et al., 1998; Ramaswamy et al., 2005; Reddy and Chidambaram, 1995; Simon et al., 2006; Sokol and Migiro, 1996; Williams, 2002). The most practical option for the use of the continuous system would be with the semi-continuous bioreactor. This variant would require a smaller initial investment, offer productivity and optimization possibilities, and have less control problems than a continuous bioreactor (Williams, 2002). It would allow for start-up, residence time variations, more flexibility, and some positive batch reactor traits.

2.3 Summary

The batch bioreactor is the oldest and most widely used bioreactor. The advantages of using a batch bioreactor are lower fixed cost, flexibility, and operational simplicity. Operational costs can be lowered if the process is well-known. These reactors are preferred for use in smaller operations, specialty products, long growth periods, operations in which flexibility is vital, unsteady-state processes, and experimental development. Continuous bioreactors, on the other hand, provide for more production optimization, automation, and capital utilization. If the continuous process is used properly, the larger initial investment can be easily offset by lower variable costs and faster production times. Therefore, this process is preferred for high volume production, processes using mutation resistant bacteria, and processes that do not require a sterile media. The production of alcohols, solvents, vinegar, or baker's yeast and wastewater treatment are a few examples that take advantages of the continuous process.

Although the choice may seem simple, the experience has been otherwise. The continuous process has had a hard time breaking into industries that have traditionally used batch bioreactors. Some operators have found the switch to a continuous process to be laborious. The unknown provides a situation which could be critical to the project's survival. For example, even though the continuous process offers huge time savings in the production of beer, the batch bioreactor remains the most popular. More risk loving and high volume operators, such as producers of industrial alcohols and solvents and wastewater treatment plants, find the continuous system to be a huge economic advantage. The choice should be made with an understanding of risk capacity for the particular application. The analysis should also include an economic sensitivity analysis and foresight into equipment availability. The process selection may ultimately limit the type of bioreactor used or its operational conditions.

3 Gas-Liquid Mass Transfer Models

Mass transfer operations in biological systems depend on a myriad of intermediate and parallel processes. Reactors for gas-liquid applications, which account for about 25% of all chemical reactions (Tatterson, 1994), fulfill two needs: dispersion and absorption (Oldshue, 1983). Dispersion requires that the entire reactor volume be used to mix the gas into the liquid. This step, however, is usually easily achieved or is not the critical system constraint (Oldshue, 1983). The low solubility of most gases limits gas absorption to the point that gas-liquid mass transfer becomes the rate limiting step for the overall reaction (Bouaifi et al., 2001; Fogler, 2005; Garcia-Ochoa and Gomez, 1998; Linek et al., 1996a; Moo-Young and Blanch, 1981; Ogut and Hatch, 1988; Oldshue, 1983; Vazquez et al., 1997). This limitation is even more severe in systems using very low solubility gases, such as carbon monoxide found in synthesis gas, some of which are very important in industrial applications (Moo-Young and Blanch, 1981). Thus, the easiest way to increase the productivity for these processes is to increase the gas-liquid mass transfer (Kapic, 2005).

Two transfer coefficients may be considered at the gas-liquid interface. The liquid-phase mass transfer coefficient is represented by k_L, whereas the gas-phase mass transfer coefficient is identified by k_G. Since the gas-phase mass transfer resistance is typically much smaller than the liquid side, $k_G >> k_L$ and gas-liquid mass transfer is controlled by k_L (Chisti, 1989); this value is modulated by the specific (gas-liquid) interfacial area, a. The driving force for mass transfer is the gas concentration gradient between the gas phase, C^*, and the dissolved gas, C. The mass transfer rate is then determined by

$$\frac{dC}{dt} = k_L a\left(C^* - C\right) \tag{3.1}$$

The volumetric gas-liquid mass transfer coefficient, k_La, is typically used when determining the mass transfer coefficient because it is difficult to measure k_L or a independently. Variances in volumetric mass transfer coefficient during operation are often thought to be a direct result of

changes in the interfacial area (Hoffmann et al., 2007; Stenberg and Andersson, 1988b), which would imply that homogeneous (bubbly) operation is more desirable than heterogeneous flow (Bouaifi et al., 2001). However, according to Linek at al. (2005b), concise conclusions are often troublesome because liquid-phase mass transfer coefficient is calculated using the gas-liquid mass transfer coefficient (k_L) and the specific interfacial area (a). Any measurement errors in either variable cause false conclusions or improper use of mass transfer models.

Many mass transfer models exist, but most of them depend on three assumptions and are simplified versions of actual mass transfer mechanisms, many of which occur simultaneously. The first assumption is that the different phases and the phase interface offer resistance to mass transfer in series, in a similar fashion to heat transfer resistances. The second assumption maintains that mass transfer is controlled by the phase equilibrium near the interface which changes more quickly than the bulk phase equilibrium (Azbel, 1981). In other words, mass transfer occurs at the microscale (van Elk et al., 2007). Lastly, gases are assumed to be single component. Multiple component problems are more complicated because each individual gas component making up the mixture has to be considered for the limiting gas-liquid mass transfer step. The complexity grows further once the relationships between each gas component and the bacteria are considered.

Single component gases are preferred for research purposes because direct and mechanistic relationships can be drawn. However, air has been used in many oxygen mass transfer studies because it is easily accessible; in this case, air is assumed to be composed of two components, oxygen and an inert gas comprised primarily of nitrogen. Nevertheless, its utilization in gas-liquid processes is often seen as inferior relative to other gases such as pure oxygen, carbon monoxide, carbon dioxide, or hydrogen (Bliem and Katinger, 1988b; Worden and Bredwell, 1998). For experimental purposes, air is treated as a single component gas with the realization that the driving force could change due to non-transferred gases (Worden and Bredwell, 1998). Multiple

component gases, however, are often encountered in industrial settings mainly due to biological or chemical reactions. Therefore, mass transfer models and correlations should be used to provide mass transfer and possibly production bounds.

The oldest and most simplistic mass transfer model, which is often presented in undergraduate chemical reaction engineering textbooks (e.g., Fogler, 2005), is the film model originally presented by Nernst in 1904. The interface is assumed to be infinitesimally thin and its resistance is usually ignored. The liquid phase has a constant and definite boundary layer, or film, of thickness $\underline{\delta_{eff}}$ which limits mass transfer (Azbel, 1981). Since these assumptions are made about the boundary layer characteristics, mass transfer is concluded to occur in a steady-state environment. Other limiting factors are the molecular diffusivity, D, and the driving force represented by the concentration gradient. The film model equation, therefore, predicts mass flux J as

$$J = \frac{-D}{\delta_{eff}}\left(C^* - C\right) \tag{3.2}$$

Molecular diffusivity and film thickness are combined into the liquid-phase mass transfer coefficient, k_L, such that

$$J = k_L\left(C^* - C\right) \tag{3.3}$$

This model has several limitations. The film model assumes that mass transfer is controlled by the liquid phase film, which is often not the case because the interface characteristics can be the limiting factor (Linek et al., 2005a). The film thickness and diffusivity may not be constant over the bubble surface or swarm of bubbles. Experiments also indicate that mass transfer does not have a linear dependence on diffusivity. Azbel (1981) indicates that others have shown that turbulence can have such a significant effect on mass transfer such that eddy turbulence becomes the controlling mechanism in which diffusivity does not play a role. In most instances, however, eddy turbulence and diffusivity combine to play a significant role in mass transfer (Azbel, 1981).

The Border Diffusion Layer Model was introduced as an amendment to the film model to present a more realistic description. It accounts for an undefined film thickness, turbulence effects, and the role of molecular diffusion. When the flow is turbulent, the flow around the bubble is split into four sections: the main turbulent stream, the turbulent boundary layer, the viscous sublayer, and the diffusion sublayer. Eddy turbulence accounts for mass transfer in the main turbulent stream and the turbulent boundary layer. The viscous sublayer limits eddy turbulence effects so that the flow is laminar and mass transfer is controlled by both molecular diffusion and eddy turbulence. Microscale eddy turbulence is assumed to be dominant in the viscous sublayer. Mass transfer in the diffusion sublayer is controlled almost completely by molecular diffusion (Azbel, 1981).

This model can be used as a rough estimate. It is still plagued by the steady-state assumption which is oftentimes an inadequate description of mass transfer. The diffusion sublayer, δ, is a function of viscosity (ν), diffusivity (D), and viscous sublayer thickness (δ_0), but realistic measurements are difficult, if not impossible, to obtain. An empirical correlation has been suggested for δ (Azbel, 1981).

$$\delta = \left(\frac{D}{\nu}\right)^{1/n} \delta_0 \tag{3.4}$$

The power n is an experimental variable with a value of about two for gas-liquid mass transfer. The liquid-phase mass transfer coefficient can therefore be related to diffusivity as (Azbel, 1981; Moo-Young and Blanch, 1981)

$$k_L \approx D^{1/n} \tag{3.5}$$

The Higbie penetration model for mass transfer compensates for transient behavior. It assumes that mass transfer occurs during brief phase contacts which do not allow enough time for steady-state conditions. In other words, the phases collide, but do not have a definitive and continuous interface with respect to time. The mass transfer is prompted by turbulence which refreshes the

interface, and the refresh rate is the limiting step in mass transfer. Eddies approach the surface at which point mass transfer by molecular diffusion is initiated and is described by (Azbel, 1981):

$$\frac{\partial C}{\partial t} = -D\frac{\partial^2 C}{\partial y^2} \tag{3.6}$$

Equation (3.6) assumes that the gas phase is not reacted during the mass transfer process at the interface. Fast reactions, however, predominantly occur very close to the interface and have to be accounted for by (van Elk et al., 2007):

$$\frac{\partial C}{\partial t} = -D\frac{\partial^2 C}{\partial y^2} - r_C \tag{3.7}$$

where r_C represents the reaction rate of the gas phase at the interface. In this case, fast reactions are assume to occur when $Ha > 2$, where Ha is the Hatta number defined as the ratio of species absorption with and without reaction. The reactive absorption provides the advantage of separating the investigation of the interfacial area from the mass transfer coefficient (Hoffmann et al., 2007).

All eddies spend approximately the same amount of time at the interface defined by τ. This interface contact time is assumed to be proportional to the amount of time it takes the bubble to rise one bubble diameter, $d_{B,}$ or

$$\tau = \frac{d_B}{U_B} \tag{3.8}$$

where U_B is the bubble velocity. The Higbie penetration model predicts (Azbel, 1981; Moo-Young and Blanch, 1981)

$$k_L = 2\left(\frac{D}{\pi\tau}\right)^{1/2} \tag{3.9}$$

The assumption that each eddy spends the same amount of time at the interface is unrealistic. Modified penetration models, such as Danckwerts' surface renewal theory model, allow each eddy

to have an independent, variable interface contact time based on a statistical probability function. It uses a fractional renewal, *s*, to account for the rate of surface renewal, in which case:

$$k_L = (Ds)^{1/2} \tag{3.10}$$

The surface renewal theory model still shares the same power as the two previous models (Azbel, 1981). The difficulty with the surface renewal model is that the unknown variable, *s*, depends on operational conditions and reactor geometry. Hence, it would be difficult to use this model as a scaleup guide.

Later research concluded that reality lies somewhere between the film and penetration models. These film-penetration models, such as those of Hanratty and Toor (Azbel, 1981; van Elk et al., 2007), concluded that the original film model is accurate for highly diffusive gases, large interface contact times, or a small boundary layer thickness (relative to a penetration depth). If a penetration model is used during these situations, predicted mass transfer will be too high (van Elk et al., 2007). Other penetration-type or hybrid models allow for further modifications making their predictions more accurate or applicable for certain conditions. A common ground has been found in the exponential dependence of the diffusivity. Gas-liquid applications show the power n ranging from 0.5 to 1. If water is used as the liquid, the power ranges from 0.65 to 0.985 (Azbel, 1981).

Current research falls into one of two schools of thought: Calderbank's slip velocity model and Lamont and Scott's eddy turbulence model (Linek et al., 2004; Linek et al., 2005b). Even though both models are penetration-type models, they make very different assumptions. The slip velocity model assumes different behavior for small and large bubbles. It also assumes a significant difference between average velocities for the two phases. The slip velocity and the surface mobility control mass transfer and, in terms of penetration theory, surface renewal.

Small bubbles with a diameter $d_B < 1$ mm act as rigid spheres with an immobile surface and slipless interface (Linek et al., 2005a; Scargiali et al., 2007). The surface and its phase interface limit mass transfer. In this case, turbulence indirectly affects mass transfer by influencing the terminal

bubble rise velocity and, therefore, the residence time (Poorte and Biesheuvel, 2002). Larger bubbles, those with d_B > 2.5 mm, have a mobile, ellipsoidal surface experiencing much larger drag forces than rigid spherical bubbles with the same total volume (Scargiali et al., 2007). Therefore, mass transfer in large bubbles is limited by eddy turbulence. In this case, other penetration models can properly describe mass transfer behavior. The transition area is highly variable. Bubble surface mobility in this region is dependent on liquid properties and surfactants (Linek et al., 2005a).

The eddy turbulence model, or simply eddy model, assumes that small scale eddies control surface renewal and, subsequently, mass transfer. This model acknowledges a scale dependence. Macro scale movements, those represented by the Reynolds number ,*Re*, are assumed to have a small impact on surface renewal. The Reynolds number is defined as

$$\mathrm{Re} = \frac{U d_B}{\nu} \tag{3.11}$$

where U is the velocity, d_B is the (hydraulic) bubble diameter, and ν is the fluid kinematic viscosity. The eddy model postulates that small bubbles would not know the difference. Small scale effects are needed to incur a relative impact. Eddies are assumed to pound the bubble surface and cause surface renewal regardless of bubble size and interface properties (Linek et al., 2004; Linek et al., 2005a; Linek et al., 2005b).

Some of these models predict opposing results. For example, the slip velocity model predicts mass transfer to decrease with increasing turbulence once the bubble surface becomes rigid. The eddy turbulence model predicts the opposite. These theories represent effects that occur concurrently. The strength of each mode depends on the reactor type and process. For example, complex reactions, such as polymerization or cellular cultures, are highly sensitive to micromixing (Nauman and Buffman, 1983). Mass transfer during these highly complex processes are affected more by micro- than macromixing (Hoffmann et al., 2008). These models and their predictions will be revisited in the appropriate reactor sections. Furthermore, the models do not account for

surfactant effects on the interface, nor its influence on mass transfer behavior (Vazquez et al., 1997).

The fundamental gas-liquid mass transfer models lack the ability to obtain and process all necessary information and factors integral to reactor operation. Gas-liquid systems are simply too complex. Therefore, a theoretical equation, that is widely applicable, does not exist (Garcia-Ochoa and Gomez, 2004). Empirical correlations have been developed to simplify analysis and design and have become exclusive in literature and practice (Kawase and Moo-Young, 1988). Parameters are chosen that are thought to influence the operation, and their powers and constants are fitted to the experimental data. They are used for design and scaleup while mass transfer models are used to explain the influence of various operational inputs.

4 Stirred Tank Reactors

4.1 Introduction

Stirred tank reactors (STRs) are one of the standard reactors in the chemical industry and have therefore been widely implemented for biological applications (Williams, 2002). They are used with viscous liquids, slurries, very low gas flow rates, and large liquid volumes (Charpentier, 1981; Fujasova et al., 2007; Garcia-Ochoa and Gomez, 1998; Kawase and Moo-Young, 1988). Stirred tank reactors are also popular because a well-mixed state is easily achieved, which aids in providing necessary substrate contact, pH and temperature control, removal of toxic byproducts, uniform cell distribution, clog prevention, and particle size reduction (Branyik et al., 2005; Hoffmann et al., 2008). This chapter provides an overview of STR operation and summarizes issues related to gas-liquid mass transfer. Additional information is provided by Oldshue (1983), Tatterson (1991, 1994), Ulbrecht and Patterson (1985), Harnby et al. (1992), McFarlane and Nienow (1995, 1996a, 1996b), McFarlane et al. (1995), and Linek et al. (1987, 1996a, 1996b, 2004).

Stirred tank reactors are widely applied in industry because of their low capital and operating costs (Williams, 2002). Popular applications are fermentation (Cabaret et al., 2008; Fujasova et al., 2007; Garcia-Ochoa and Gomez, 1998; Hoffmann et al., 2008; Scargiali et al., 2007; Vasconcelos et al., 2000), carbonation, oxidation (Oldshue, 1983; Scargiali et al., 2007), chlorination (Fujasova et al., 2007; Oldshue, 1983; Scargiali et al., 2007), hydrogenation (Fujasova et al., 2007; Murthy et al., 2007; Scargiali et al., 2007; Shewale and Pandit, 2006), dissolution, polymerization (Shewale and Pandit, 2006), chemical synthesis, and wastewater treatment (Cabaret et al., 2008; Ogut and Hatch, 1988; Shewale and Pandit, 2006). Stirred tank reactors are preferred if high gas-liquid mass transfer coefficients are needed (Bredwell et al., 1999). These reactors are usually made out of stainless steel for industrial units or out of clear materials, such as glass or certain plastics, for experimental applications (Williams, 2002).

Typical STR units (Figure 4.1) have a small height-to-diameter ratio relative to other reactor types (Charpentier, 1981). The diameter D_T can vary from about 0.1 m for experimental units to 10 m for industrial applications (Harnby et al., 1992). As shown in Figure 4.1, the impeller and baffle dimensions, as well as the impeller clearance are typically a specified fraction of the tank diameter. The aspect ratio, defined as the liquid height-to-diameter ratio, is highly variable and depends on the number and arrangement of impellers and the reactor application. Single impeller systems typically have an aspect ratio of 1 (Charpentier, 1981; Tatterson, 1991), but certain exotic applications call for designs with aspect ratios up to 3 (Nielsen and Volladsen, 1993; Tatterson, 1991). Industrial multiple impeller designs are mostly limited to an aspect ratio of less than ~4 due to practical considerations (Charpentier, 1981).

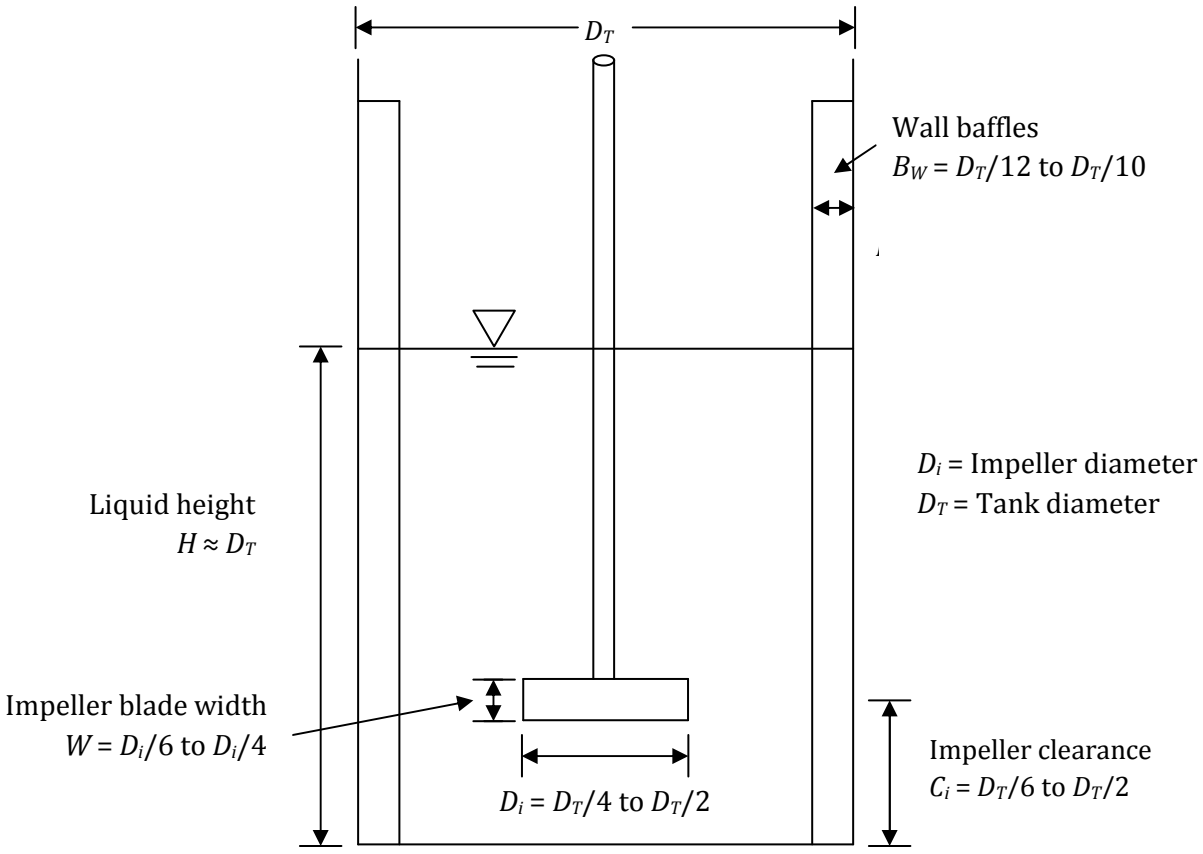

Figure 4.1: Standard single impeller stirred tank reactor design (Adopted from Tatterson (1991)).

Reactor shape, specifically the bottom, can vary greatly. The standard reactor design is cylindrical with a flat bottom (Ulbrecht and Patterson, 1985), but dished, conical, or curved bottoms have also been used (Harnby et al., 1992; Tatterson, 1991). The bottom shape does not seem to affect gas-liquid mass transfer or gas dispersion significantly, but the dished bottom is preferred for solid suspensions and mixing (Oldshue, 1983). Other reactor shapes, such as spherical or semispherical, are in use (Oldshue, 1983) but the standard design is preferred for gas-liquid dispersion due to operational experience and cost. Even though standard reactor designs exist in the chemical industry for liquid-liquid processes, customized STR use for biological and gas-liquid applications preclude an optimized stirred tank reactor design for all applications (Tatterson, 1991).

4.2 Stirred Tank Reactor Flow Regimes

Superficial gas velocity, defined as the volumetric gas flow rate divided by the STR cross-sectional area, influences gas-liquid mass transfer through two mechanisms: gas-filled cavities and gas holdup. The sweeping action of the impeller creates a low pressure void that quickly fills the sparged gas. These gas-filled cavities are the mechanism for gas dispersion and gassed power reduction (McFarlane et al., 1995). These cavities ultimately influence impeller loading, gas dispersion, and liquid circulation such that the impeller creates specific flow regimes which are of great importance for STR optimization.

4.2.1 Radial Flow Impellers

Radial flow impellers expel the fluid from the impeller region in the radial direction. The Rushton-type impeller is a standard example of radial flow impeller operation, which is often used as the basis for the typical flow regimes identified in radial flow impeller operation. As shown in Figure 4.2, three stable cavity groups are observed using this impeller: vortex cavities, clinging cavities, and large cavities. Vortex cavities form at constant impeller speeds and small gas flow rates. They are defined by two rolling vortices, one at the top and the other at the bottom of the

impeller blade. Clinging cavities are formed with an increase in gas flow rate. They are larger than vortex cavities and cling to the blade backside, but still produce vortices at the gas tail. Large cavities, which form with another increase in the gas flow rate, are larger, smoother, and behave differently in terms of hydrodynamics (Nienow et al., 1985; Smith and Warmoeskerken, 1985).

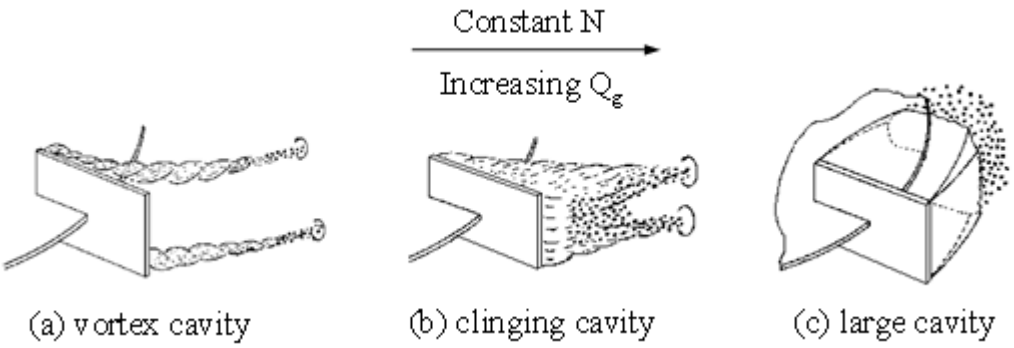

Figure 4.2: Cavity types for the Rushton-type impellers where N is the impeller speed and Q_G is the volumetric gas flow rate (Smith and Warmoeskerken, 1985).

Turbulent action forces the gas to break away from the cavity and exit the impeller zone. This breakage is the source of gas dispersion in stirred tank reactors. The large cavity deserves special attention because it induces gas breaking away less violently than the other cavity types. Large cavities also have an advantage in that they hold more gas and have more surface area from which gas can break away. Since these cavities form at higher gas flow rates and thus superficial gas velocities, they are able to sustain a higher gas dispersion rate than the other two cavity types; however, there is a breakeven point. Cavities can become too large and hamper gas-liquid mass transfer. For example, if the cavity volume to surface area ratio is too large, gas dispersion will decrease (Nienow et al., 1985; Smith and Warmoeskerken, 1985).

Cavities also reduce the energy transfer between the impeller and liquid. A higher superficial gas velocity induces more gas dispersion at a lower power input. However, if too much gas is present and the cavities are too large, the energy transmission is reduced and the impeller's gas dispersion and mixing capabilities are hampered. In this case, the cavities produce an unwanted energy loss and a state described as flooding (Ogut and Hatch, 1988).

The exact nature of these events is accompanied by changes in the cavity structures for the Rushton-type turbine (Figure 4.3). Vortex and clinging cavities form symmetric structures (i.e., their size and shape are similar for every impeller blade). Although these transfer energy well, they do very little for gas dispersion making them undesirable for gas-liquid processes. If the gas flow rate is increased, a 3-3 structure is formed, which is defined by alternating large and clinging cavities. Its importance comes from its stability and gas handling capacity. It offers the optimal gas dispersion for the lowest power input (i.e., most efficient). If the gas flow rate is increased further, the impeller is flooded. At this point, the stable 3-3 structure is replaced by a structure formed by large, unstable ragged cavities, which are inefficient for gas-liquid mass transfer and gas dispersion (Nienow et al., 1985; Smith and Warmoeskerken, 1985). The instability can also lead to varying impeller power draw which can damage the motor and gearbox system.

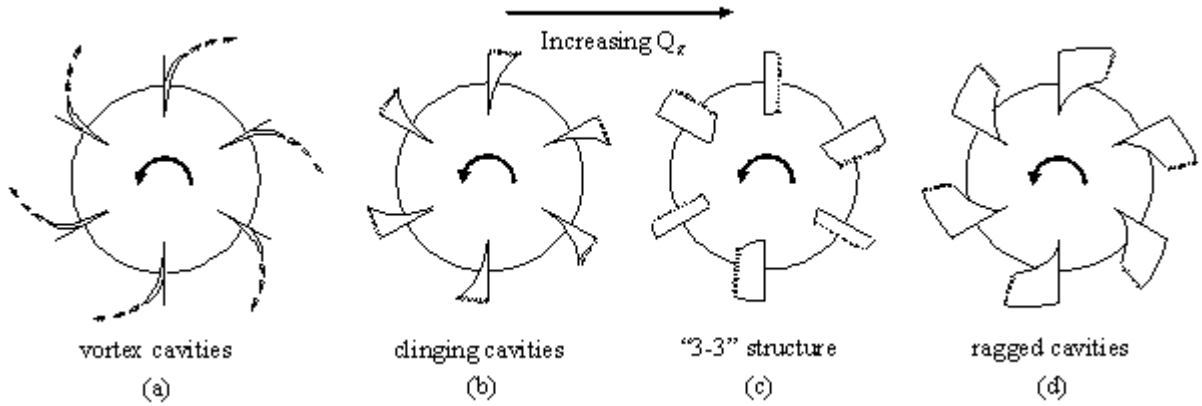

Figure 4.3: Cavity structures for the Rushton-type impeller (Nienow et al., 1985; Smith and Warmoeskerken, 1985).

These events have inspired improvements to the Rushton-type turbine to increase the gas handling capacity of the impeller to allow more gas and, hence, higher gas concentrations in the reactor. To accomplish this, impellers should create smaller cavities in similar structures while minimizing flooding. The concave blade disk turbine has been shown to accomplish these goals.

The gas cavities on the impeller influence the gas dispersion and bulk flow regimes in a STR. For single impeller radial flow systems, five bulk flow regimes (Figure 4.4) have been defined (Nienow

et al., 1977). The different regimes occur at increased impeller speeds while holding the gas flow rate constant. At low impeller speeds, the power input is very small and negligible dispersion occurs (regime (1) in Figure 4.4). Increasing the impeller speed begins to disperse the gas phase (regime (2)). The bulk flow above the impeller acts like a bubble column while the lower section is not contacted by the gas phase. Further increasing the impeller speed allows the gas to be recirculated in the upper reactor section, and some gas dispersion occurs in the lower region (regime (3)). Regime (4) is identified by gas recirculation throughout the reactor. This condition is optimal for gas-liquid mass transfer and mixing processes. At the highest impeller speeds (regime (5)), significant circulation loops and gross recirculation are observed and high turbulence at the surface promotes gas entrainment (surface aeration) (Nienow et al., 1977). The progression of these bulk flow regimes are also shown in Figure 4.5 (Nienow et al., 1985).

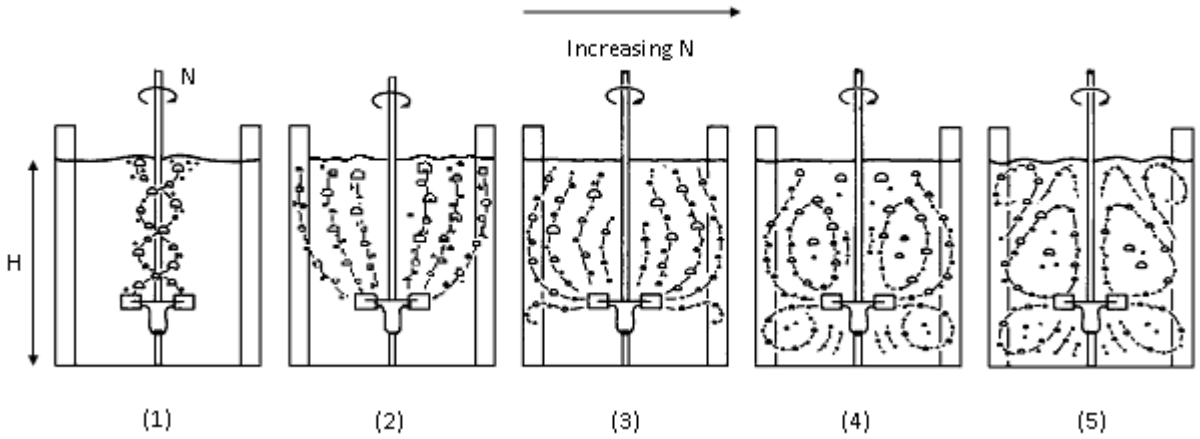

Figure 4.4: Bulk flow patterns for radial flow impellers at constant U_G (Nienow et al., 1977).

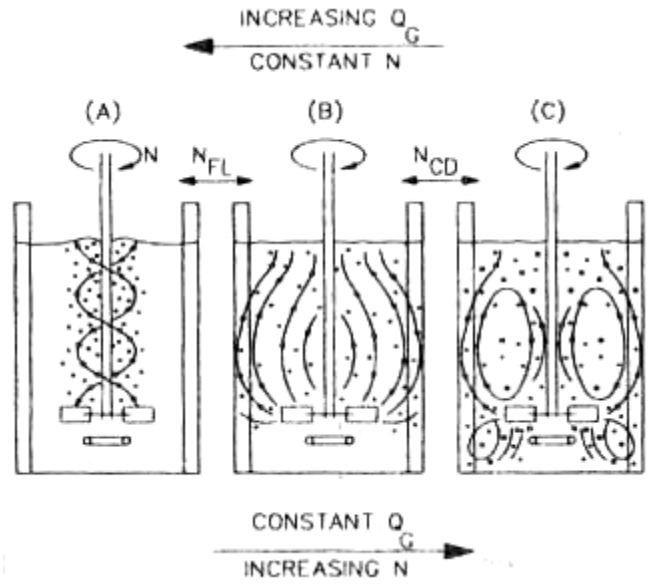

Figure 4.5: Loading regimes and transitions for radial flow impellers where N_{FL} indicates a transition from flooded to loaded regimes and N_{CD} defines the transition to completely dispersed flow regime (Nienow et al., 1985).

Nishikawa et al. (1984) determined that when negligible gas dispersion occurs, impeller type, location, or separation are irrelevant. In other words, if the total power input to the system is dominated by the sparged gas, the mixing in the stirred tank reactor approximates a bubble column. This effect was, however, recognized to occur at small power inputs, and the impeller power would start to dominate hydrodynamics and mass transfer at 30 W/m^3 for Rushton-type impellers (Gagnon et al., 1998). This power level is almost never observed in application since most gas-liquid dispersion with STRs occurs in the range of 500-4000 W/m^3 (Bliem and Katinger, 1988b; Bredwell and Worden, 1998; Oldshue, 1983).

The flow regime transitions can be determined from a gassed power number (or gassed-to-ungassed power ratio) vs. flow number graph where the flow number is defined as:

$$Fl_G = \frac{Q_G}{ND^3} \tag{4.1}$$

where Q_G, N, and D_i are the volumetric flow rate, impeller speed, and impeller diameter, respectively. Generic and experimental examples are shown in Figure 4.6 and Figure 4.7,

respectively. Flooding occurs at a local maximum of this graph represented by a flooding transition impeller speed N_F. It has also been defined as the transition point from (3) to (2) or (4) to (3) (by decreasing N). The local minimum for the graph holds a special place. It represents the minimum power input required to achieve bulk flow regime (4), also known as complete dispersion or recirculation. The reactor should be operated such that $N > N_{CD}$; this represents the most economical operation in terms of power usage and gas utilization. Mixing time, which is defined as the time required to mix incoming fluid homogeneously into the existing liquid volume, is also optimized, but it is still higher than in an unaerated system (Hadjiev et al., 2006). If the impeller speed is increased beyond the complete dispersion impeller speed, the power use increases (Nienow et al., 1985; Smith and Warmoeskerken, 1985).

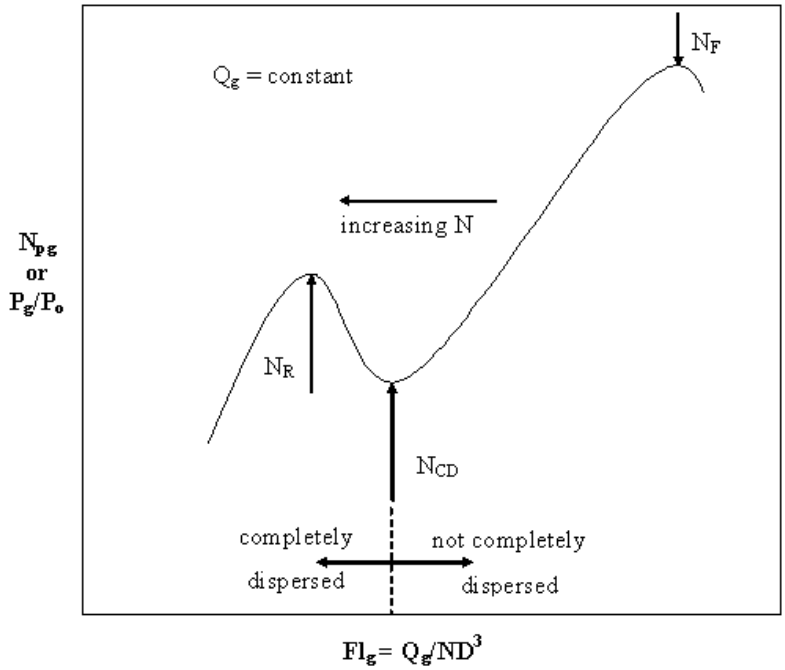

Figure 4.6: Generic transition plot where N_{pg} is the gassed power number (Kapic, 2005).

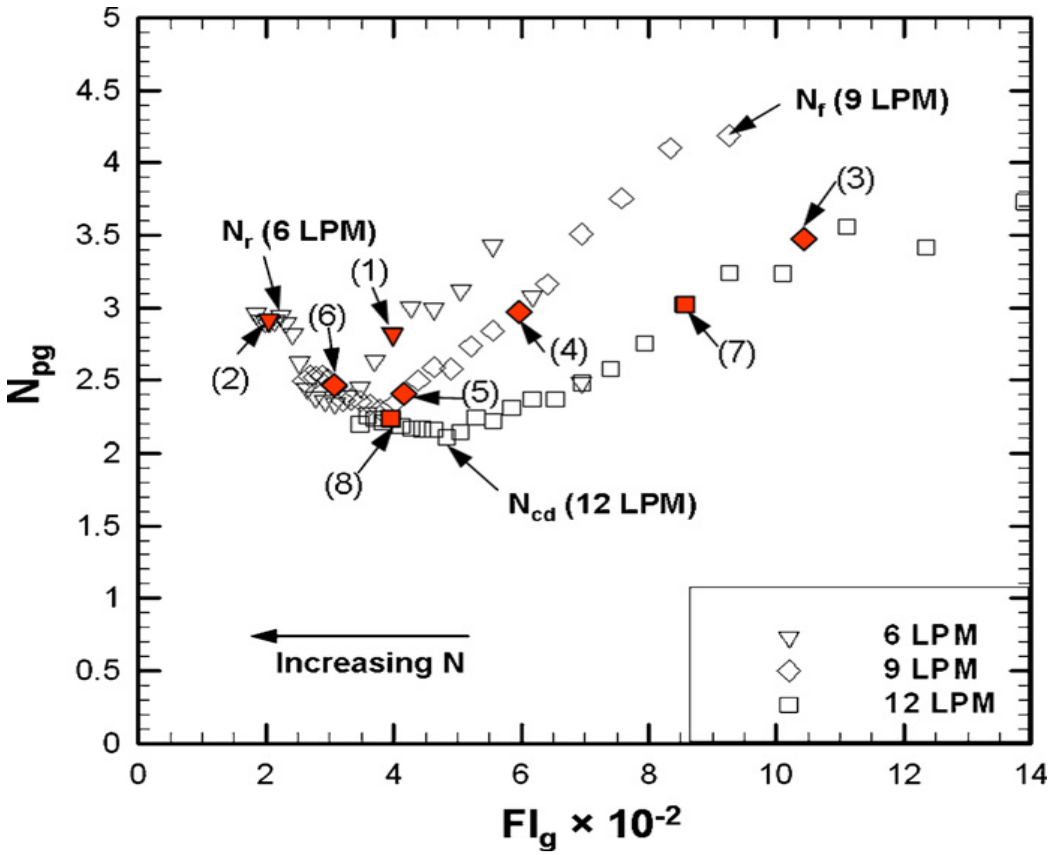

Figure 4.7: Experimental transition plot. The numbered data points represent specific conditions tested by Ford et al. (2008).

A second local maximum that follows represents the transition to the gross recirculation flow regime. This impeller speed, identified by N_R, should be avoided because it leads to inefficient gas utilization and gas entrainment. If an oxygen probe were to be positioned near the entrained gas, oxygen depletion would be a matter of time and a reduction in k_La would be recorded. In other words, the impeller should be operated between N_{CD} and N_R to achieve maximum efficiency. The transition between these flow regimes and their representative impeller speeds have been shown to be a function of impeller type, D_i/D_T, and scale. Given a D_i/D_T and impeller type, the transition impeller speeds are scale independent, but the rate at which the transitions occur are not. Larger vessels have a gradual transition while smaller ones experience transition over a limited flow number range (Nienow et al., 1985; Smith and Warmoeskerken, 1985). As shown in Figure 4.6, increasing the gas flow rate leads to smoother and delayed transitions.

4.2.2 Axial Flow Impellers

Axial flow impellers direct the fluid flow within the STR along the axis of the rotating shaft. Simple propeller-type impellers offer a simple example. In down-pumping axial flow impellers, the fluid is pumped downward while the gas is introduced below the impeller. The cavity propagation of axial flow impellers (Figure 4.8) is similar to the Rushton-type turbine, but gas dispersion differs in that pulsation forces gas to leave the impeller zone via the cavity tail (McFarlane et al., 1995). As shown in Figure 4.8, low impeller speeds and gas flow rates form vortex cavities at the impeller blade tip. Increasing the gas flow rate leads to the creation of a clinging cavity. The creation of larger cavities on axial flow impellers requires an increase in the gas flow rate and the impeller speed. A minimum impeller speed is needed to support larger cavities. If this minimum is not met, axial flow impellers experience vortex shedding such that the vortex detaches from the blade, leading to the next vortex creation cycle. This shedding can cause variations in torque and power draw, but usually do not cause any problems (McFarlane et al., 1995).

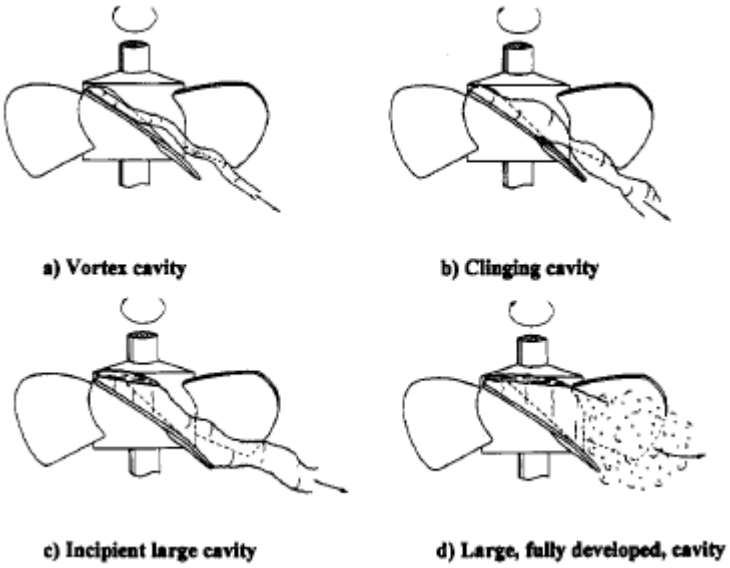

Figure 4.8: Cavity types for axial flow impellers (McFarlane et al., 1995).

Incipient large cavities are formed in axial flow impellers if the gas flow rate is increased and the minimum impeller speed requirement is met. This cavity type occupies more space than the clinging cavity, but disperses gas in a similar pulsating fashion. At a higher gas flow rate, large, fully developed cavities form, which occupy almost the entire blade area, but they do not extend beyond the impeller blade edge. When large cavities are present, the liquid and gas are discharged predominately in a radial direction from the impeller zone. Prior to flooding, the large cavity loses its defined boundary and blends into the flow. Once the impeller is flooded, the cavity structure is completely lost and gas simply passes through the impeller zone without any breakage or dispersion (McFarlane et al., 1995).

Unlike the Rushton-type turbine, cavities on axial flow impellers are rarely stable and frequently change shape, size, and identity, which can induce different gas loading regimes and torque and power draw variations. If gas enters the impeller zone via the impeller induced liquid flow, the impeller is said to be loaded indirectly. In contrast, direct loading is defined by sparged gas controlled flow into the impeller zone. In other words, the impeller generated flow is not able to deflect the sparged gas. The transition leads to changes in the cavity size, shape, and identity, which are significant for large cavities (McFarlane et al., 1995).

Downward pumping axial flow impellers exhibit different bulk flow regimes at low and high gas flow rates due to the effects or large cavities; this phenomenon differentiates axial from radial flow impellers; however, the major regimes (flooding, loading, and complete dispersion) have similar characteristics. McFarlane et al. (1995) used an A-315 (axial flow impeller) for visualization purposes and noted that other downward pumping axial flow impellers exhibit similar behavior. Figure 4.9 depicts A-315 behavior as described by McFarlane et al. (1995) for low gas flow rates (relative to scale and power draw). The figures progress from (a) to (d) in terms of increasing impeller speeds. In (a), the impeller is flooded at a low impeller speed. Gas rises easily through the impeller zone and behaves similarly to flooded radial flow impellers. Increasing impeller speed

induces minor recirculation loops in the impeller vicinity and the impeller is said to be directly loaded. The transition between (b) and (c) signals the direct-indirect transition such that the impeller is partially directly and indirectly loaded. Increasing the impeller speed further leads to indirect loading (c). Cavity oscillations cause the bulk flow to vary between asymmetric (i) to occasional symmetric (ii) flow patterns. Variations in cavity type and loading are not damaging to the motor and gearbox because the flow remains mostly axial throughout the process such that the torque and power draw variations are limited. Further increase leads to complete dispersion as shown in (d) (McFarlane et al., 1995).

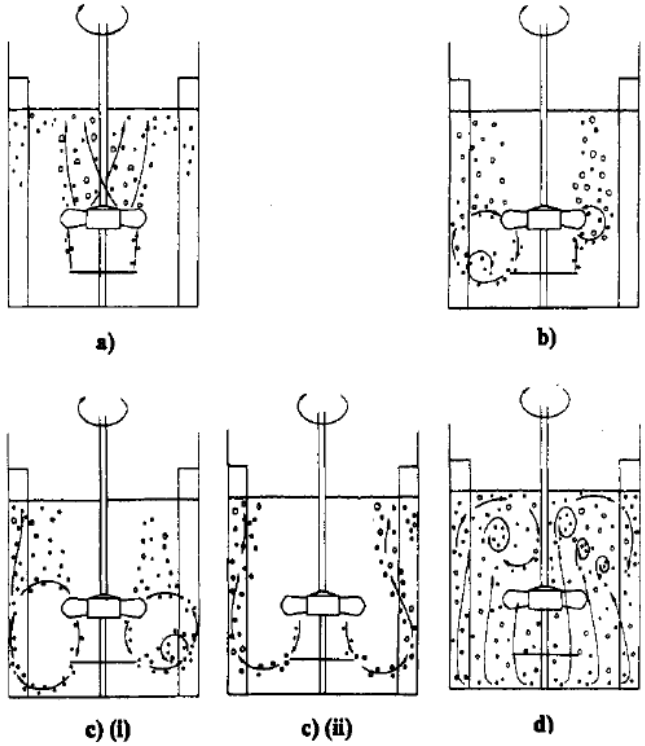

Figure 4.9: Bulk flow regimes generated by downward pumping A-315 at low gas flow rates (McFarlane et al., 1995).

McFarlane et al. (1995) describe different flow patterns when relatively high gas flow rates are present (Figure 4.10). At higher gas flow rates and beyond a minimum impeller speed, large cavities form and have a significant impact on flow stability and bulk flow regimes. Flooding occurs in the same manner as with low gas flow rates (a). If the impeller speed is above a threshold, large cavities

form causing a significant loss in pumping capacity; this is accompanied by direct loading and a significant radial and axisymmetric flow pattern as shown in (b). The impeller cavity distribution is also axisymmetric. The transition from direct to indirect loading is shown in (c). An increase in the impeller speed induces oscillations between predominantly radial (i) and axial (ii) flow. Occasional cavity shedding induces impeller dominance which would force gas to the tank bottom (iii); however, this event is temporary, and flow eventually reverts back to radial or oscillating dominance. This series of events occurs over a very short impeller speed range and a subsequent increase results in proper loading and dispersion (d).

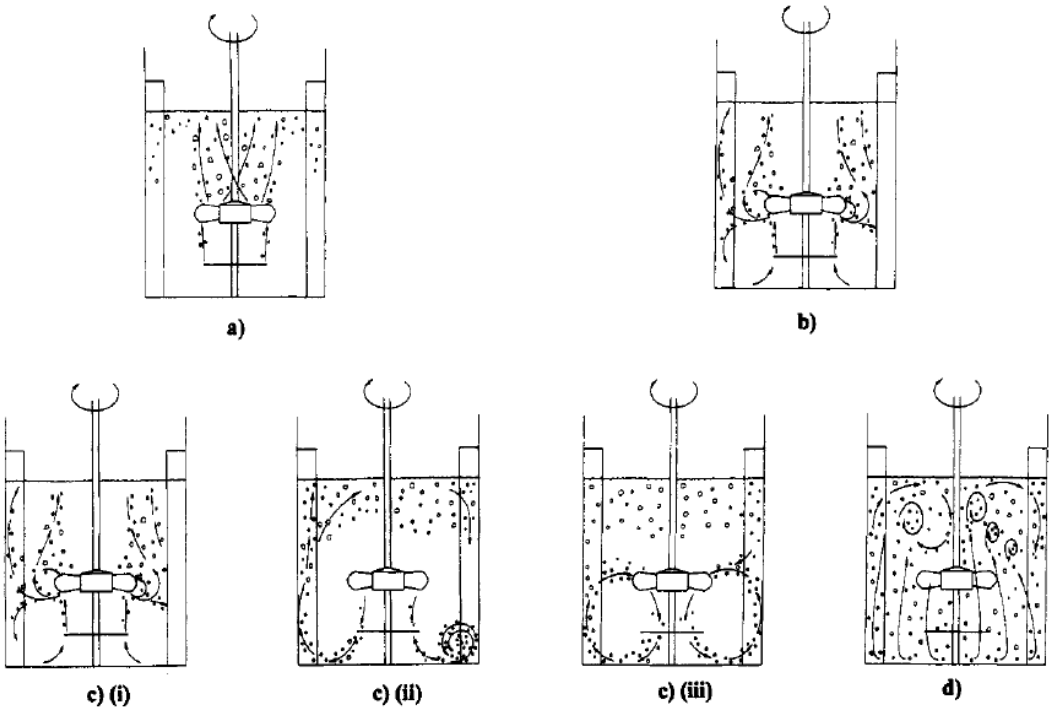

Figure 4.10: Bulk flow regimes generated by downward pumping A-315 at high gas flow rates (McFarlane et al., 1995).

The oscillation in cavity size and flow direction (Figure 4.10c) can produce large and significant variations in power draw and torque such that the power number for the down-pumping A-315, for example, can vary between 0.84-1.48 at a frequency of 1-2 minutes. The variations in torque and power draw can have damaging effects on the motor and gear assembly (Tatterson, 1994) and can lead to vessel vibration (Sardeing et al., 2004b). Additionally, large cavities tend to create

asymmetric flow which can produce a significant bending moment on the impeller shaft, resulting in shaft damage. Smaller impellers at low power concentrations experience these problems much earlier because large cavities are able to form with a smaller amount of gas at these scales. Up-pumping axial flow impellers have a more stable oscillation because the sparged gas enters the impeller zone in the same direction as the fluid (McFarlane et al., 1995).

The detrimental effects of large cavity formations can be minimized by increasing the impeller speed. Reactor design improvements can be made such that large cavities require more gas or that the minimum impeller speed for large cavity formation is reduced. The goal is to reduce the impact on the normal operating range such that the event is outside normal parameters or induces fluctuations that are within the design specifications for the motor and gear assembly (McFarlane et al., 1995).

4.3 Effects of Impeller Design and Arrangement

The impeller provides mechanical agitation and gas dispersion. It is responsible for bubble breakup in gas-sparged stirred tank reactors and for solid suspension in gas-liquid-solid stirred tank reactors. Numerous impeller designs exist to meet various needs, and the economic success of a project depends on the evaluation and selection of a proper impeller in concert with reactor geometry (Ungerman and Heindel, 2007). A few standard impellers in gas-liquid dispersion are documented. Normal impeller-to-tank diameter ratio, D_i/D_T, is typically between 1/4 and 2/3 (Harnby et al., 1992) with the standard ratio being 1/3 (based on industrial experience) and rarely going above 1/2 (Tatterson, 1991). This geometry minimizes cost and is capable of providing a well-mixed state for the liquid phase and complete dispersion of the gas phase. An impeller with a larger D_i/D_T ratio proves inefficient and unnecessary. The impeller power draw is proportional to the impeller speed to the third power and the impeller diameter raised to the fifth power. It is, therefore, cheaper to operate an impeller at a faster speed than a larger diameter if more dispersion or blending is needed. Impeller clearance, defined as the distance between the impeller and tank

bottom, is typically in the range $D_T/6$-$D_T/2$ (Tatterson, 1994) depending on the liquid viscosity, impeller type, sparger-impeller separation, and number of impellers.

Impellers can be classified into groups based on the liquid viscosity used in the reactor (Harnby et al., 1992). Propellers, turbines, and paddles have a higher tip speed relative to other impeller types and are used for low viscosity Newtonian liquids which are encountered in most processes (Ogut and Hatch, 1988). Propellers are usually operated faster and paddles slower than turbines. The standard three-bladed propeller has poor gas-liquid dispersion and contacting characteristics and will be excluded from further discussion.

4.3.1 Radial Flow Impellers

A more common impeller classification is by flow leaving the impeller zone. Impellers can be classified into radial or axial flow impellers. Some examples of radial flow impellers are the Narcissus impeller (NS), concave blade disc turbine (Figure 4.11), (Chemineer) BT-6, and the multi-bladed disc turbine. A six-bladed disc turbine, shown in Figure 4.12, is often referred to as a Rushton-type turbine (RT) (Ulbrecht and Patterson, 1985). The standard blade is $D_i/4$ long and $D_i/5$ wide (Oldshue, 1983). Increasing the number of blades (12 or 18) produces similar recirculation as the standard RT, but reduces the power draw drop upon gassing (Smith et al., 1977). Increasing the number of blades, however, increases the ungassed power number from ~5 to 8-9 (Nienow, 1996), which diminishes the use of disc turbine with higher blade numbers as a mixing device (Nienow et al., 1995). Turbine designs using retreating, angled, or hollow faced blades are in existence, but have not been able to compete with the Rushton-type turbine for gas-liquid dispersion tasks (Harnby et al., 1992; Williams, 2002).

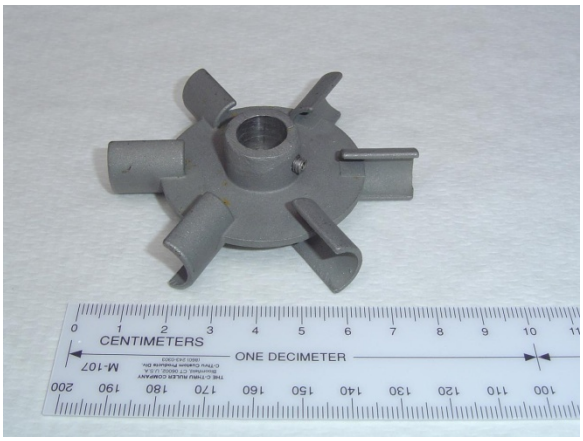

Figure 4.11: Concave impeller.

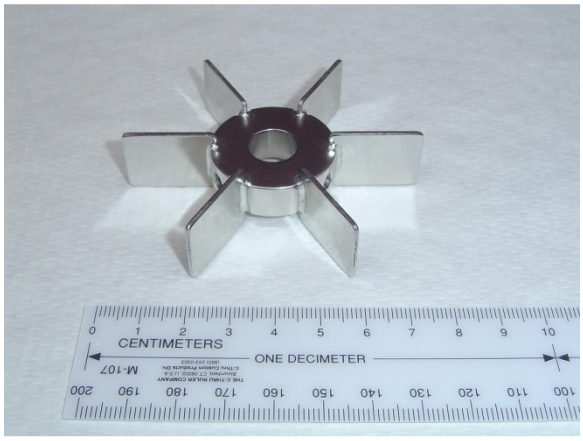

Figure 4.12: Rushton-type turbine.

The RT is the most popular impeller for gas-liquid dispersion since the 1950s (Nienow, 1996). It has very good bubble breakup and gas dispersion capabilities leading to good mass transfer characteristics (Cabaret et al., 2008; Williams, 2002). It is the measuring stick to which other gas-liquid impellers are compared. The high power number of the Rushton-type turbine, which is a disadvantage for mixing purposes, is an advantage for gas-liquid dispersion. The RT is capable of creating higher maximum shear zones and produce smaller bubbles. Smaller bubbles lead to a higher interfacial area, which in turn increases the mass transfer capacity. In addition, the disc feature of the RT prevents gas bubbles from passing through the lower shear region and forces the gas flow through the high shear impeller tip region (Oldshue, 1983; Tatterson, 1991). These

features give the Rushton-type turbine k_La values that are an average of 50% higher than other impellers operating under similar conditions (Sardeing et al., 2004a).

Although commonly used, Rushton-type turbines exhibit several negative traits. Some are design specific, but others are shared by all radial flow impellers. This is mainly due to the fact that newer radial impellers were designed with the goal of improving on a small number of disadvantages (Nienow, 1996). The RT experiences a power draw drop upon gassing of 50-65% (McFarlane and Nienow, 1996b). This weakness is purely operational, but forces the reactor to have a complicated gearbox design (Ulbrecht and Patterson, 1985) which adds to the installation and maintenance costs. Concave (hollow) and 12 or 18 blade disc turbines can be used to minimize this effect. They form smaller cavities on the blade backside relative to the standard RT (Smith et al., 1977). The smaller cavities lead to much smoother power curves and less variation in power draw upon gassing (Ungerman and Heindel, 2007), and hence lead to simpler gearbox designs (Ulbrecht and Patterson, 1985).

Concave blade disc turbines are of interest in gas-liquid dispersion because they are able to handle more gas than Rushton-type turbines before flooding (Smith et al., 1977; Vasconcelos et al., 2000). The mass transfer capacity for the concave blade disc turbine is very similar to the Rushton-type turbine, but Chen and Chen (1999) found that the blade curvature could be optimized for a certain power input to produce higher gas-liquid mass transfer coefficients. Unlike the Rushton-type turbine, the concave blade disc turbine requires the cup orientation to be in the direction of impeller rotation (Tatterson, 1994).

Vasconcelos et al. (2000) investigated the influence of the impeller blade shape, shown in Figure 4.13, on gas-liquid mass transfer. They concluded that the importance of blade shape was negligible for disc turbines as long as the power number, power draw drop upon gassing, and gas flow rate were similar. Other authors have come to a similar conclusion, but also stipulated that the process has to be in the turbulent regime (Nienow, 1996). Angled, concave, and lancelet blade disc

turbines provided lower impeller power numbers, but also offered smaller power draw drops upon gassing and smaller, if any, gas cavities. Hence, they are more efficient and capable of handling gas. Increasing the impeller diameter could discount the power draw disparity while allowing retrofitting to be easily accomplished. As such, the retrofitted system would provide similar gas-liquid mass transfer performance and would handle more gas, potentially allowing for an increased operational range and gas-liquid mass transfer.

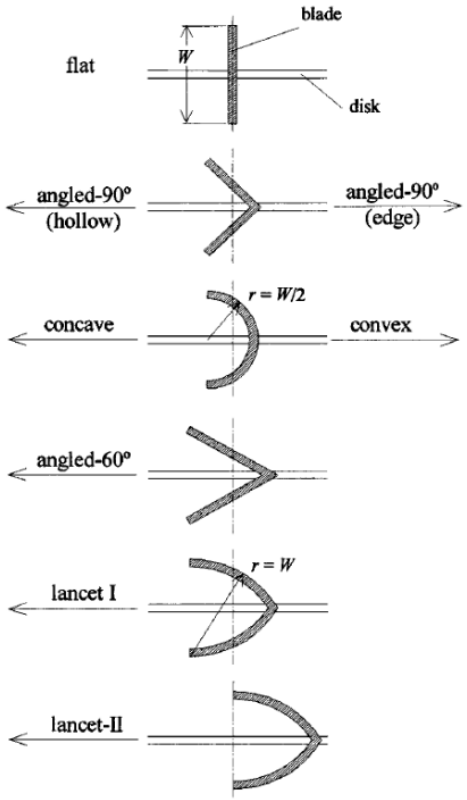

Figure 4.13: Possible blade shapes for use with disc turbines (Vasconcelos et al., 2000).

Another major weakness for radial flow impellers stems from one of the strengths: the high shear rates. The power dissipation (or shear) rates are concentrated at the blade tips (Gagnon et al., 1998) and are not uniformly distributed throughout the reactor (Fujasova et al., 2007; Ungerman and Heindel, 2007). This unbalanced shear distribution can lead to stagnant zones in the outer reactor region (Bellgardt, 2000) and higher mass transfer in the impeller stream relative to the working volume (Stenberg and Andersson, 1988a, 1988b). According to Stenberg and Andersson

(1988b), 50% of the energy is dissipated in the impeller stream, 20% in the immediate impeller vicinity, and 30% is dissipated through the rest of the reactor. This disparity leads to radial flow impellers, especially the RT, providing very poor top-to-bottom mixing (McFarlane and Nienow, 1995), particularly in more viscous fluids.

If a constant impeller speed scaleup rule is used, the impeller tip energy dissipation rate will increase due to its connection to the impeller diameter (Bliem and Katinger, 1988b). The power decay is more pronounced in larger vessels and contributes to scaleup issues (Figueiredo and Calderbank, 1979). This concentration leads to the local energy dissipation rate in the impeller vicinity being up to 270 times higher than the average. Furthermore, the local rate experiences large fluctuations creating problems in scaleup and reactor design comparisons. These high shear fluctuations can be harmful to some bioreactor microorganisms (Bliem and Katinger, 1988a, 1988b; Bredwell and Worden, 1998).

Lastly, the fluid can experience low bulk circulation leading to low gas holdup in the bottom reactor section (Fujasova et al., 2007; Ungerman and Heindel, 2007) and gas compartmentalization (Moucha et al., 2003). Gas compartmentalization is to be avoided since it poses the danger of spent gas entrainment or gas starvation. Spent gas is inactive in production and limits the practical working volume (Fujasova et al., 2007) while gas starvation can limit the effectiveness of the microorganisms (Pollack et al., 2008).

As scale increases, a proper mixing state gains in importance which can lead to radial flow impellers providing very poor mixing conditions in a significant portion of the reactor volume (McFarlane and Nienow, 1995). The solution has been to simply operate the impeller at a faster speed which can have detrimental effects on microorganisms, power usage, and impeller characteristics. Retrofitting a system with a larger radial flow impeller to resolve some of these problems is not usually possible because different turbine diameters produce very different torques. The higher torque of a larger diameter turbine can be damaging for the motor and drive

train to the point that this practice is seen as high-risk-low-reward and rarely implemented (McFarlane and Nienow, 1995). The smoother power curves of the concave blade turbine are very promising for this purpose and should be seriously considered.

Chen and Chen (1999) investigated the possible replacement of the RT. The comb blade and perforated blade disc turbine were found to have higher k_La values than the standard RT at similar power inputs. They came to the conclusion that bubble breakup was not only a function of the shear gradient magnitudes, but also the amount of time the gas phase remained in the shear field. By spatially increasing the shear field, bubbles spent longer time periods in this region and decreased the probability that larger bubbles would pass through this region without significant breakup. The results were that the comb and perforated blade disc turbine produced k_La values that were almost 12% and 30%, respectively, higher than the Rushton-type turbine at the same power input and superficial gas velocity while producing lower shear gradient magnitudes. Currently, there is no available information of these impellers being used in processes involving microorganisms.

4.3.2 Axial flow impellers

Many attempts have been made to replace radial flow impellers with axial flow impellers. Examples of axial flow impellers include the Lightnin A-310 (Figure 4.14), Lightnin A-315 (Figure 4.15), Pitched Blade Turbine (PBT) (Figure 4.16), Techmix 335 (TX), Prochem Maxflo T, SuperMIG (EKATO), marine propeller, A-3 impeller, or a multibladed paddle. The PBT and hydrofoil impellers, such as the Lightnin A-315, are the most commonly used axial flow impellers. These devices have much lower power numbers than radial flow impellers which makes them ideal for mixing purposes. Their blending prowess is due to the fact that the mixing time is independent of the impeller type (Nienow, 1996). Hence, the operation can be accomplished at a lower cost with axial flow impellers; however, as shown in Figure 4.17, axial flow impellers are usually inferior to radial flow impellers for mass transfer purposes. They usually produce flow in the axial direction, but can

create some radial flow if $D_i/D_T > 0.5$ (Tatterson, 1991). This situation is usually avoided since the standard low viscosity impellers have a D_i/D_T ratio of about 1/3 (Harnby et al., 1992).

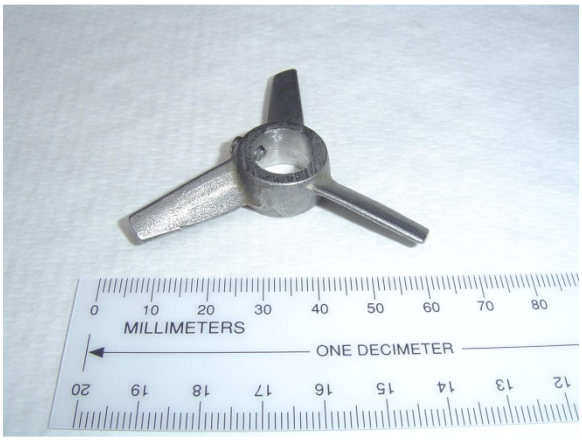

Figure 4.14: Lightnin A-310 axial flow impeller.

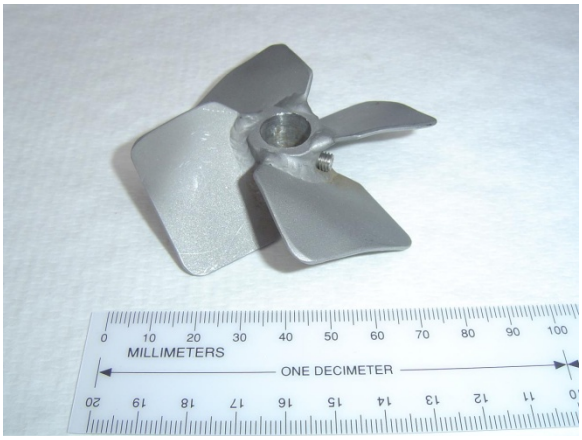

Figure 4.15: Lightnin A-315 axial flow impeller.

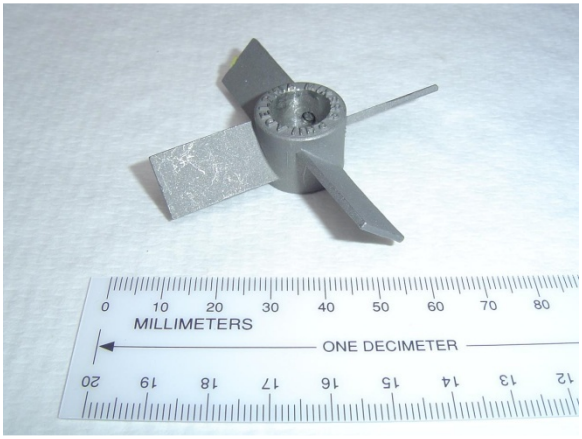

Figure 4.16: Pitched blade turbine (PBT) axial flow impeller.

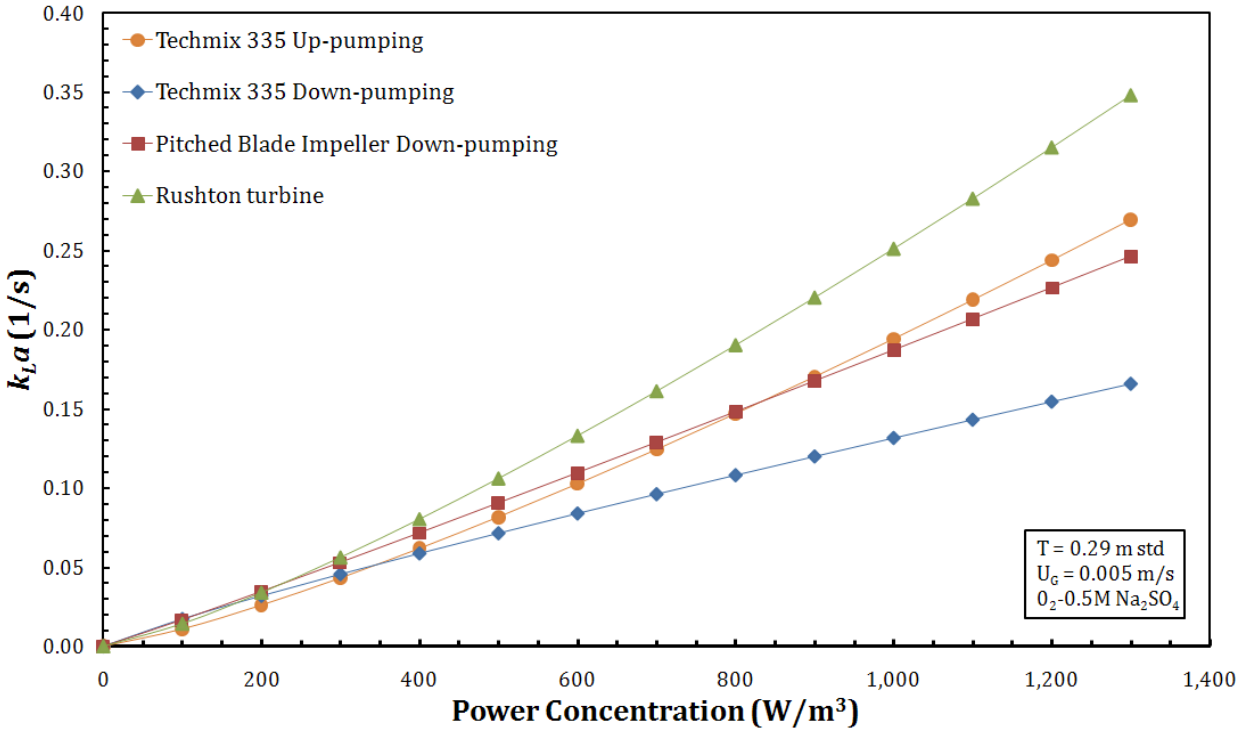

Figure 4.17: Gas-liquid mass transfer for various impeller types (Adopted from Moucha et. al (2003)).

Axial flow impellers used in low bottom clearance tanks can also create radial flow if the direction of the flow is downward. In this case, the flow can leave the impeller zone only by flowing in the radial direction (Tatterson, 1991). This phenomenon is usually not observed since the standard bottom clearance for low-viscosity impellers in gas-liquid dispersions is between one impeller diameter and one half the tank diameter (Ulbrecht and Patterson, 1985). The hydrofoil impeller discharge is affected by the impeller Reynolds number based on the impeller diameter and speed. If the system is operated with a viscosity such that Re is about 5000, the flow becomes more and more radial. This change could have a significant impact on mixing and gas dispersion and would be especially important for viscous non-Newtonian processes (McFarlane and Nienow, 1995).

The PBT discharges fluid from the impeller zone at an angle of 45°-60°. The standard design has flat blades that are 45° from the horizontal and have a 1/5 blade width-to-diameter ratio. This discharge angle causes a significant radial component regardless of the impeller size or position

which has led to the PBT to being classified as a mixed impeller in the axial family (McFarlane and Nienow, 1995). These features make the PBT an excellent mixing device. The mixing (blending) time is reduced and heat transfer is improved; however, the PBT makes a bad impeller for gas breakup. Gas bubbles are led to the blade tip where they are sliced apart, but the blade shape does not accumulate bubbles in a sufficient manner. Therefore, a large number of bubbles pass through the impeller zone without interacting with the breakup mechanism (Martín et al., 2008b). The solidity ratio, which relates the impeller blade area to the impeller swept area, is about 0.43 for the PBT (Oldshue, 1983). Low solidity ratio impellers flood before radial flow impellers and high solidity ratio impellers, so their use in gas-liquid processes in single impeller systems is atypical (Ungerman and Heindel, 2007).

In order to reduce flooding, high efficiency hydrofoil impellers, distinguished by their profiled blades (McFarlane and Nienow, 1995), were introduced. These impellers, such as the Lightnin A-315 (see, for example, Figure 4.15), have a much higher solidity ratio of about 0.87, flood later (Ungerman, 2006), and have a smaller power draw drop upon gassing (30-50%) (McFarlane and Nienow, 1996b) than radial flow impellers. It is therefore capable of handling more gas than the radial or PBT impellers (Chen and Chen, 1999). In fact, it can handle 86% more gas than a Rushton-type turbine before flooding (Yawalkar et al., 2002) and 40% more gas than the PBT before the onset of gas loading transition (described in Section 4.2.2) (McFarlane and Nienow, 1996b). However, the A-315 is still an axial flow impeller and produces lower shear gradients relative to the Rushton-type turbine. The advantage of using the A-315 over a RT depends upon the gas flow rates and shear sensitivity of the microorganisms. If neither of these situations is important, the RT is still the better choice. If the gas flow rates are of importance but shear sensitivity is not, the concave blade disc turbine is the more effective impeller.

The axial flow direction makes particulate suspension easier relative to radial flow impellers (Tatterson, 1991). Axial flow impellers are also better blending devices because they have a lower

power number – hence power usage – and shorter blending times; however, results for gas-liquid contact have been unimpressive relative to the Rushton-type turbine, and axial flow impellers tend to have smaller gas-liquid mass transfer coefficients. Additionally, large reactors using axial flow impellers have shown highly asymmetric and oscillating gas holdup distributions with periods of up to several minutes (Bakker and Oshinowo, 2004). Therefore, their use has been limited to mixing and shear normalizing in multiple impeller gas-liquid systems (Bouaifi et al., 2001) and mixing and solid suspension in single impeller systems (Oldshue, 1983).

The direction of the flow, up or down, depends on the geometry and rotation of the axial flow impeller. In general, up-pumping impellers push the gas to the surface faster (lower gas holdup) while down-pumping impellers induce recirculation and longer residence times, defined as the time a particle spends in the reactor, which leads to higher gas holdup (Moucha et al., 2003). These circulation loops are important with respect to gas holdup and contribute to multiple impeller systems offering 30% higher gas holdup values than single impeller systems (Bouaifi et al., 2001). The down-pumping impeller also offers shorter mixing times, which can lead to lower operational costs in systems where mixing is important (Gogate and Pandit, 1999).

Some researchers, on the other hand, do not find a preference for up- or down-pumping axial flow impellers (Fujasova et al., 2007) or find the up-pumping configuration produces more macromixing than down-pumping systems, which led to smaller bubble diameters (Majirova et al., 2004; Sardeing et al., 2004b). Sardeing et al. (2004b) observed that gas holdup in the up-pumping configuration was determined to be 10-25% higher than the down-pumping orientation. The gas holdup conclusions were drawn based on constant impeller speed data. Down-pumping axial flow impellers also have significant stability and hydrodynamic problems in certain operating ranges, which may have contributed to the up-pumping axial flow impeller's superior gas holdup performance (McFarlane and Nienow, 1995; McFarlane et al., 1995). Sardeing et al. (2004b) focused on power concentration, which they indicated to be more relevant, and the down-pumping PBT was

determined to be more efficient than the up-pumping PBT, confirming similar conclusions made by Moucha et al. (2003), Bouaifi et al. (2001a), and Gogate and Pandit (1999).

4.3.3 Multiple Impeller Systems

Multiple impeller STR designs, schematically represented in Figure 4.18, are very popular in practice (Nocentini et al., 1998) and were implemented due to shortcomings of the single impeller system and industrial requirements. For example, when a single impeller system is used in an industrial-scale reactor, it may not provide proper agitation and gas dispersion in large reactors. Additionally, viscous or non-Newtonian liquids do not mix well in a single impeller system. Large gas-filled cavities on the back of the impeller blades also limit the amount of gas that can be properly dispersed in a single impeller STR (Cabaret et al., 2008).

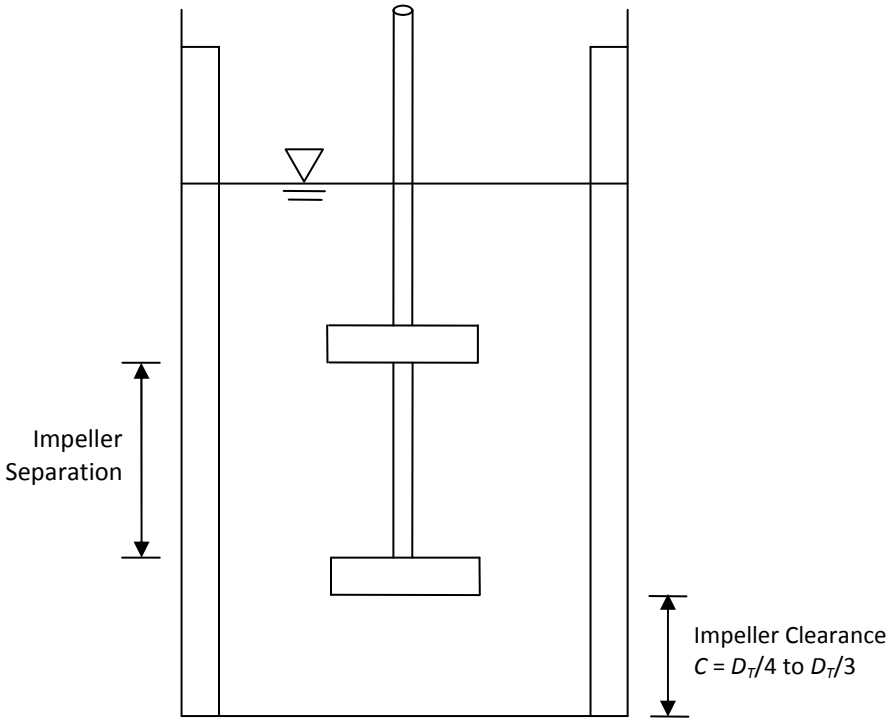

Figure 4.18: Standard multiple stirred tank reactor design.

Multiple impeller systems are able to distribute energy throughout the reactor more efficiently, which leads to a more homogeneous shear rate distribution. Liquid circulation and gas dispersion are also improved, leading to longer gas-phase residence times. These factors lead to better gas

utilization, higher gas-liquid mass transfer coefficients (Bouaifi and Roustan, 2001; Cabaret et al., 2008; Fujasova et al., 2007; Moucha et al., 2003; Nocentini et al., 1998), longer gas phase residence times, better bulk flow characteristics (Shewale and Pandit, 2006), and higher gas holdup (Bouaifi et al., 2001; Bouaifi and Roustan, 2001; Shewale and Pandit, 2006) relative to single impeller systems. The industrial implementation of multiple impellers can be made to single impeller systems with minimal retrofitting and without changes to the motor and gearbox (Lines, 2000), especially if the addition is an axial flow impeller (McFarlane and Nienow, 1995).

In order to achieve a proper working condition, however, proper impeller placement has to be considered. The bottom clearance for most multiple impeller designs is between $D_T/4$ and $D_T/3$. If the impellers are too close to each other, impeller-impeller interference can lead to inefficient operation and an inability to separate operational inputs; this would add complications without enhancing efficiency. Interference also provides limited, if any, increase in k_La (Nishikawa et al., 1984). The power draw for a multiple impeller configuration will be normal upon startup, but may decrease to about 70% of the initial value and remain at those levels throughout the process when the impellers are too close. The flow patterns of interfering impellers may also exhibit characteristics of a single impeller system (Mishra and Joshi, 1994) leading to negligible improvements and increased costs (Oldshue, 1983). For example, a second RT has been reported to increase k_La by 74% if placed correctly, but would provide no improvement if interference occurred (Nishikawa et al., 1984).

The separation between impellers depends on the impeller type, but should be a minimum of $1D_i$ (Linek et al., 1996b). The Rushton-type turbine, for example, requires a separation of $1.5D_i$, but $2D_i$ would be preferred to ensure independence (Fujasova et al., 2007). Linek et al. (1996b) found that if the impellers were acting independently, each impeller's mass transfer characteristics could be evaluated as a single impeller system. The overall mass transfer coefficient could be calculated using a weighted average, with the lower and upper section having a weight of 0.25 and 0.75,

respectively (Linek et al., 1996a). However, this approach failed using non-coalescing media and was not proven at larger scales (Linek et al., 1996b).

The impeller is the key component for proper STR operation, especially for multiple impeller systems. A proper selection procedure has to consider numerous options and their applicability to the particular process of interest. A mixed configuration using a radial and axial flow impeller is assumed to be more efficient for gas dispersion and mixing in a low viscosity Newtonian fluid than a dual axial or radial configuration, even though the Rushton-type turbine combination provides better k_La (see, for example, Figure 4.19). Efficiency, in this case, is defined as the capability to maximize gas-liquid mass transfer while minimizing power input (Gagnon et al., 1998). It is often advantageous to use a Rushton-type or concave blade turbine as the bottom impeller. This impeller would provide optimal bubble breakage. The upper impeller can be a downward pumping axial flow impeller to enhance gas-liquid circulation (Puthli et al., 2005).

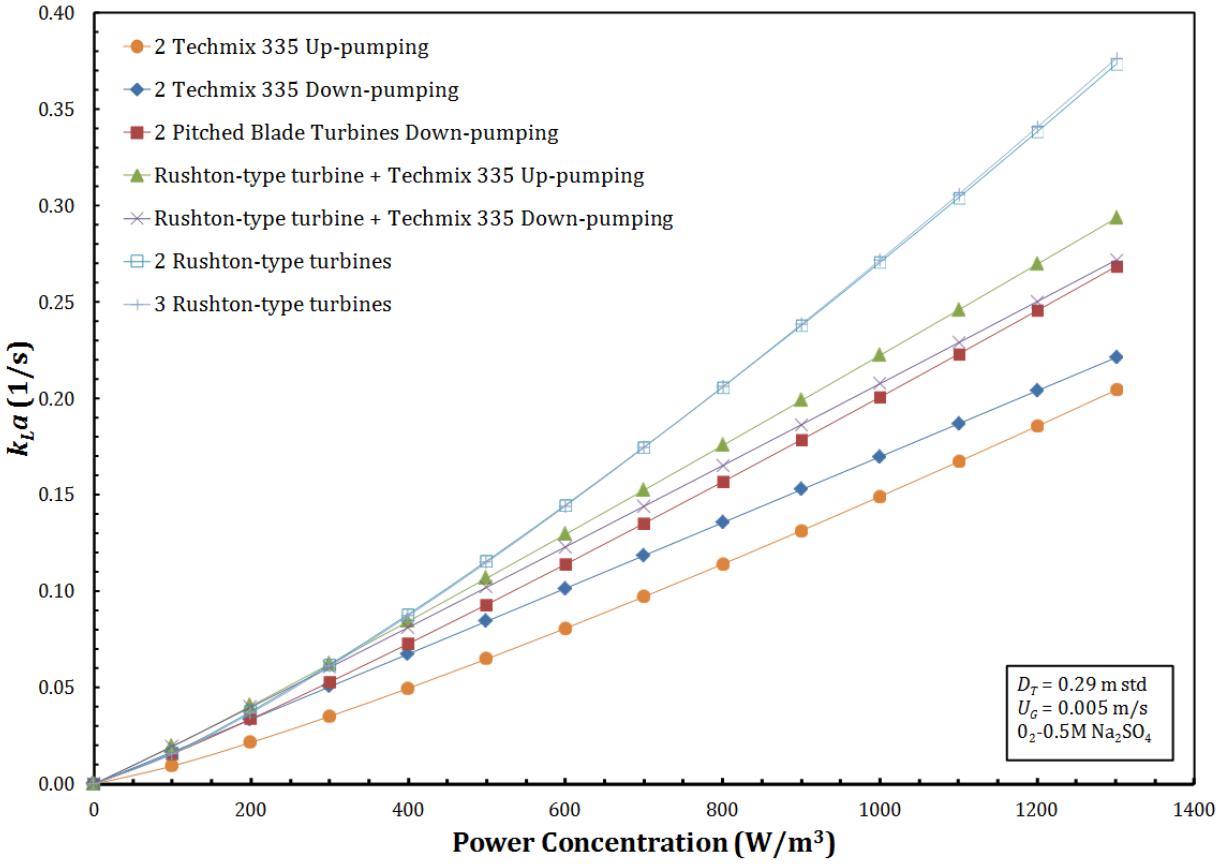

Figure 4.19: Effects of multiple impellers on gas-liquid mass transfer in a STR (Adopted from Moucha et al. (2003)).

Experiments using a radial setup are often performed to set the bar for mass transfer comparisons. Gagnon et al. (1998) contributed to this discussion by investigating the effect of adding impellers to the same reactor. A second Rushton-type turbine increased gas holdup, gas residence time, and the gas-liquid mass transfer coefficient. The addition of a third Rushton-type turbine increased these further, but at a much lower amount. They came to the conclusion that gas holdup and, subsequently, gas-liquid mass transfer does not increase linearly with the number of impellers and power drawn. Moucha et al. (2003) came to a similar conclusion when going from 1RT to 2RT but, as shown in Figure 4.19, the additional mass transfer was negligible when the increase was made from 2RT to 3RT.

The mixed configuration efficiency and the declining increase in k_La with increasing number of turbines are determined by the impeller loading. The bottom impeller is loaded directly (by sparged gas) while the other impeller(s) are loaded indirectly (by impeller generated flow loops). Direct loading enhances gas dispersion capabilities of the Rushton-type turbine, while indirect loading puts more emphases on liquid mixing efficacy. Impeller loading is a more important consideration in experimental-scale reactors. Larger industrial-scale reactors require more effective blending and top-to-bottom mixing than the Rushton-type turbine can provide (Bouaifi and Roustan, 2001; Fujasova et al., 2007). The Rushton-type turbine is oftentimes limited in this regard, and the conditions created in these impeller zones (cells) are more geared towards axial flow impellers (McFarlane and Nienow, 1995).

Furthermore, radial flow impellers' discharge divides the reactor volume into well-mixed systems with minimal interchange (Nienow, 1996). As a result, radial flow impellers in large-scale systems may produce compartmentalization, caverns (impeller is encased by its flow field while most of the reactor is stagnant), higher gas recirculation, and low volumetric exchange zones (Nocentini et al., 1998). For large STRs, the combination of a radial flow impeller on the bottom and a down-pumping axial flow impeller on the top enhances the reactor fluid mixing such that the reactor volume contact is maximized with minimal power input (Fujasova et al., 2007; Vasconcelos et al., 2000).

Some discrepancies and opposing suggestions in the literature can be explained by using the studies of Linek et al. (1996a) and Nocentini et al. (1998). They found unequal amounts of gas pass through each impeller section regardless of loading type, resulting in gas distribution nonuniformity which can lead to the bottom impeller being flooded far earlier than the others. Since the bottom impeller contacts the most gas and is responsible for initial bubble breakup, flooding of this impeller is severely detrimental to system operation (Nocentini et al., 1998).

Linek et al. (1996a) concluded that the bottom impeller section had gas holdup and mass transfer values that were 15% and 45%, respectively, lower than the upper section when the STR was filled with non-coalescing media (0.5M Na_2SO_4). Similar conclusions were reached when using water, with the upper section producing higher k_La values by 15%. This also implies that impeller power consumption was not balanced, i.e., one of the impellers consumed more power and created higher shear gradients than the other, producing higher k_L and a values for the upper reactor section. The problem is made worse due to the fact that gas tends to coalesce faster and easier in regions of low power (relatively speaking), creating larger bubbles which reduce the interfacial surface area and possibly lowers k_L. Coalescence, however, would be far less likely in non-coalescing media which should explain Linek et al. (1996a) results.

Bouaifi et al. (2001) found that the average bubble diameter was larger in the bottom section of the reactor than the upper section. They concluded that bubbles formed a distribution such that the larger bubbles were in a region outside the impeller stream and were up to four times larger than the bubbles entrained in the impeller stream. More specifically, gas in these setups would concentrate about the impeller shaft, impeller tip, and within the radial area between the impeller and reactor walls (Boden et al., 2008; McFarlane and Nienow, 1996a). These observations were made for an axial system, but are very similar to those made by Stenberg and Andersson (1988b) for a 1RT setup, which produced a similar qualitative mass transfer behavior for these impeller types.

Bouaifi et al. (2001) also observed that a “very heterogeneous bubble distribution” would form in a dual axial flow impeller system once the bottom impeller was flooded. If the impeller was properly loaded and complete dispersion occurred, 50-60% of the bubbles had a diameter of 1-3 mm. Thus, it was more effective to operate in the loaded and complete dispersion regime. These experiences confirm and explain the unbalanced mass transfer performance observed by Linek et

al. (1996a, 1996b) and Gagnon et al. (1998) in multiple impeller systems and by Bellgardt (2000), Moilanen et al. (2008), and Stenberg and Andersson (1988a, 1988b) in single impeller systems.

The impeller choice in multiple impeller reactors is therefore vital. A proper selection requires a minor power increase of ~15% to produce similar k_La of a Rushton-type setup but with a much friendlier environment for microorganisms and larger scales (Fujasova et al., 2007). The required radial and axial flow impeller often depends on the operational conditions. The simplest configuration includes a Rushton-type turbine for the lower impeller and a down-pumping PBT for the upper turbine(s). Since these impellers tend to flood relatively early, it has been proposed to replace the Rushton-type turbine and down-pumping PBT to extend the operational use. For example, Pinelli et al. (2003) did not find an advantage to using two Rushton-type turbines over two BT-6 impellers (asymmetric concave blade impellers designed by Chemineer). Gas holdup and macromixing were observed to be very similar, which would imply that the concave blade disc turbine could replace a Rushton-type turbine in a single or multiple impeller system without major hydrodynamic implications while providing more gas handling capacity (Vasconcelos et al., 2000). While holding power concentration and superficial gas velocity constant, Chen and Chen (1999) observed much higher mass transfer potential and smaller bubbles by replacing the RT with a comb and perforated blade disc turbine. The A-315 could replace the down-pumping PBT if a higher gas capacity is necessary. A more homogeneous environment is also expected with this replacement at larger scales because the A-315 (e.g., Figure 4.15) provides better recirculation exchange and interaction with the other impeller(s) (Bouaifi et al., 2001).

It is common to use multiple impeller systems in operations that are expected to undergo significant changes in viscosity and rheology. These processes are operated in the laminar regime which puts more emphases on the viscous behavior of the fluid. Multiple impellers have been determined to produce better gas-liquid mass transfer in viscous fluids than the commonly used helical ribbon impeller. Most researchers, however, spend time investigating low viscosity impeller

combinations for viscous non-Newtonian applications (Tecante and Choplin, 1993). These low clearance impellers can require large amounts of power, making their operation impractical, especially for very viscous non-Newtonian liquids (Gagnon et al., 1998). In these cases, the operation is simply shut down if the impellers are not capable of providing proper conditions (Ogut and Hatch, 1988).

Cabaret et al. (2008) and Gagnon et al. (1998) concluded that better mixing and higher product conversion can be achieved if a close clearance impeller, such as the helical ribbon, is used in conjunction with a radial flow impeller such as the RT in a highly viscous system. The Rushton-type turbine provides proper gas dispersion, while the close clearance impeller attempts to contact most of the reactor volume and provides proper bulk mixing, shear distribution, lower apparent viscosity, and minimal stagnant zones (Tecante and Choplin, 1993). These effects also lead to higher reactor utilization and can decrease power requirements.

4.3.4 Surface Aeration

Stirred tank reactors are highly turbulent mixers which can induce a high degree of surface turbulence. Although the effects of turbulence in the reactor volume are known, the interaction at the gas-liquid surface can be complicated. Unbaffled vessels can experience flow destructive vortices and solid-body motion at normal operating impeller speeds. If the vessel is baffled, these vortices tend to be minor, but their influence on mass transfer can be important. Highly turbulent surfaces allow the STR to entrain head space gas, effectively adding to the sparged gas flow rate. This phenomenon is referred to as surface aeration. Therefore, direct sparging, which has been the only option discussed so far, is not required. However, this form of indirect sparging affects impeller performance and reactor hydrodynamics in the same fashion as direct sparging (Patwardhan and Joshi, 1998).

Surface aeration is used in wastewater treatment, water aeration (fishing ponds for example), and processes requiring the gas phase conversion to be maximized (toxic or highly valuable gases). If the system requires the gas phase to be recycled, surface aeration allows the reactor to be capped creating a dead end system. Hence, a recycle gas compressor is not necessary which minimizes fixed costs (Patwardhan and Joshi, 1999). Such reactor designs limit potentially toxic exposure, increase work reliably, and have limited maintenance costs. The lack of a sparger can further extend these benefits for processes containing an excessive amount of a solid phase such as wastewater treatment (Patwardhan and Joshi, 1998).

Surface aeration is most common in multiple impeller systems and/or semibatch and batch processes (Lines, 1999). Multiple impeller designs place an impeller relatively close to the surface which can induce surface aeration at relatively low impeller speeds. Most authors do not check for this phenomenon, and it is often unclear as to which models are used for the mass balance in the gas phase. The exclusion of a dynamic gas holdup term (assuming dynamic conditions) does not affect the results if surface aeration is limited; however, if surface aeration is significant, experimental errors could be large (Figueiredo and Calderbank, 1979).

The critical impeller speed for surface aeration (N_{CSA}) can be identified using indirect sparging. A simple k_La vs. N graph produces a sharp increase in k_La at N_{CSA}. Direct sparging makes this identification more difficult. Although gas may be entrained, additional gas dispersion does not occur until the impeller speed is increased by about 20% above the initial entrainment speed. Other factors controlling surface aeration are impeller type and diameter, tank diameter, impeller clearance and submergence, baffling, and gas and liquid properties (Patwardhan and Joshi, 1998).

Surface aerators are, however, highly limited by impeller submergence and require an impeller to be very close to the surface in order to be effective. Furthermore, the operation becomes hampered with scaleup such that dead zones are common (Lines, 1999; Patwardhan and Joshi, 1998). Design and scaleup for surface aerated systems are even more challenging than a standard

STR (Lines, 1999). As such, this reactor design is not capable of competing with conventional designs. However, surface aeration is an important phenomenon that occurs in stirred tank reactors (Patwardhan and Joshi, 1998). Although it may not have a significant impact on gas-liquid mass transfer, it should be kept in mind especially if comparisons are to be made between competing designs. Many experimental reactors include an operating range that is much higher than traditional industrial applications (Benz, 2008). These designs may induce surface aeration and artificially increase mass transfer performance.

4.3.5 Self-Inducing Impellers

Self-inducing impellers are also used for indirect sparging purposes. The spinning action of the impeller creates a low pressure region at the impeller intake. Orifice holes are exposed to this low pressure region and connected by a hollow shaft to the atmosphere or head space (for dead end systems) (Patwardhan and Joshi, 1999; Vesselinov et al., 2008). As such, the gas flow rate is a function of the impeller speed. The "atmospheric" pressure can be adjusted by pressurizing the shaft entrance such that additional gas is pumped into the system (Patwardhan and Joshi, 1999).

Self-inducing impellers are classified by the flow in and out of the impeller zone. Type 11 impellers are shown in Figure 4.20a and are defined by the gas being the only phase at the inlet and outlet. The most common and simplest design is a hollow pipe with orifice holes at the ends. The hollow pipe impeller induces gas flow through Bernoulli's equation. Gas induction occurs once the pressure differential is large enough to overpower the liquid hydrostatic head. Type 12 impellers (Figure 4.20b) have a gas phase at the inlet and a gas-liquid flow at the outlet. Gas induction occurs in a similar fashion to Type 11, but Type 12 impellers mix the phases in the impeller zone through some intricate designs. Type 22 impellers (Figure 4.20c) are intricate devices which have a two-phase inlet and outlet composition. The impeller induces a large vortex until the impeller is able to induce phase interface ("surface") aeration. The design calls for an axial gas-liquid inlet and radial outlet. An optional impeller hood prevents gas outlet in the axial direction, inducing a pressure

differential so that the liquid is pumped into the impeller zone from the bottom reactor section (Patwardhan and Joshi, 1999).

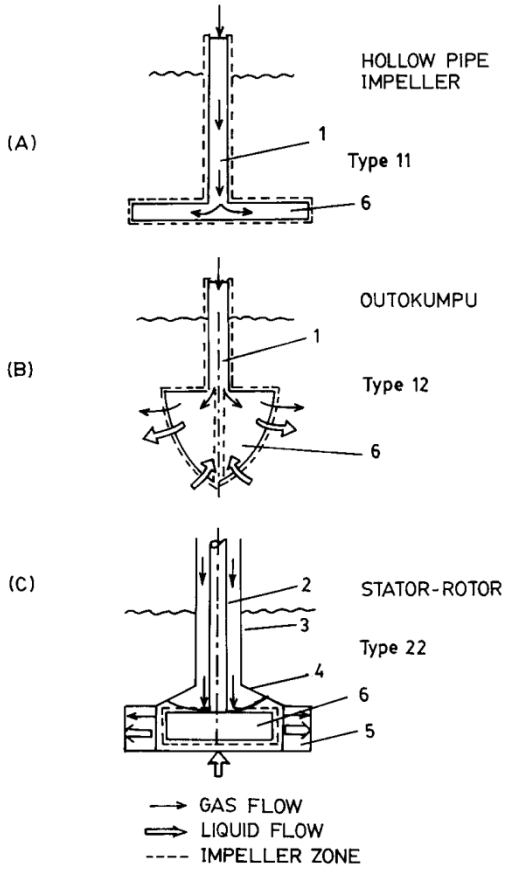

Figure 4.20: Self-inducing impeller types (Patwardhan and Joshi, 1999).

These impellers have both advantages and disadvantages. Type 12 and 22 impellers force the gas phase to travel through a high shear volume, creating smaller average bubble diameters and higher interfacial area in the outlet flow. These designs also allow for a reduction in power usage, but this usually comes at a cost of reduced residence time which can have a negative impact on conversion. Since dead end zones are feasible, this design provides similar advantages to surface aerators. The disadvantages of self-inducing impellers are usually their complicated designs, diminished control (with power input often being the only control variable), and gas-liquid mass transfer performance comparable to “standard” stirred tank reactors. Unless the gas phase is highly

toxic or the gas recycling system too expensive, self-inducing impellers have little to offer in microorganism systems.

4.4 Superficial Gas Velocity

The superficial gas velocity, U_G, is a description of the amount of gas present in the reactor volume and is defined as the volumetric gas flow rate per unit cross-sectional area of the reactor. This definition is easily quantifiable and has been used by many researchers as a correlation parameter for gas holdup and gas-liquid mass transfer. Most researchers cited in this chapter, with the exception of Linek et al. (2005), have proposed a positive correlation of superficial gas velocity with gas-liquid mass transfer; however, its specific influence on mass transfer is often confusing.

If the impeller is operated below a minimum tip speed (2.25 m/s for RT), the reactor hydrodynamics are dominated by the gas flow and the reactor acts as a bubble column. At this point, gas-liquid mass transfer has an exclusive dependence on the superficial gas velocity (Charpentier, 1981). Since the intent of the stirred tank reactor is to provide agitation that would be superior to gas sparging alone, stirred tank reactors are operated such that impeller agitation dominates the hydrodynamics (Nishikawa et al., 1981).

The superficial gas velocity is often recognized to influence gas-liquid mass transfer through gas holdup (Nocentini et al., 1993) and its influence on the interfacial surface area (Garcia-Ochoa and Gomez, 2004). It is generally assumed that the interfacial surface area can be increased by entraining more gas in the reactor, and this results in increased gas dispersion and gas-liquid mass transfer.

Bubble-bubble interaction and coalescence have to be considered when the superficial gas velocity is increased. Coalescence occurs through a three step process. First, bubbles collide and form a liquid layer (typically 10^{-3} to 10^{-4} cm thick). Second, the film drains assuming that the collision force is sufficient to deform the bubble interface and that the bubbles spend enough time in contact for the film to drain. Third, assuming a critical film layer thickness ($\sim 10^{-6}$ cm) is achieved,

the film breaks and the bubbles combine (Martín et al., 2008b; Tse et al., 1998). The entire sequence of events is completed in milliseconds for coalescing liquids (Tse et al., 1998), but may take up to 15 seconds for liquids containing surface active agents (Laari and Turunen, 2005), which will be discussed in Section 4.6. Coalescence is, therefore, influenced by the collision frequency, collision force, bubble deformation, and coalescence efficiency (Bredwell et al., 1999; Martín et al., 2008b), and is controlled by the film drainage rate (Tse et al., 1998).

Superficial gas velocity has an influence over the collision frequency. If more gas is present, there is a higher probability of collision (Martín et al., 2008b). Coalescence efficiency and drainage rate depend on the film properties which are a function of the liquid properties. The collision force, however, is the controlling factor because the bubble diameter is a function of the power input (Bouaifi et al., 2001; Nocentini et al., 1993).

Thus, increasing the superficial gas velocity may initially increase k_La because there will be more gas bubbles and a larger gas-liquid interfacial area. However, further increasing superficial gas velocity could lead to bubble coalescence, which would increase the average bubble diameter and bubble rise velocity and lower the gas residence time (Moilanen et al., 2008). All of these factors would lower gas-liquid mass transfer (Charpentier, 1981). Under these conditions, the impeller fails to disperse the gas properly, and bubbles form a heterogeneous distribution (Bouaifi et al., 2001) and rise easily (Ford et al., 2008). Even if a higher k_La is achieved by increasing U_G, a lower residence time can still lead to lower fermentation conversion levels (Bredwell et al., 1999).

The effect of increasing gas holdup on a is often ambiguous. This is a special situation for the stirred tank reactor because the power input determines the bubble diameter and hydrodynamics (Bouaifi et al., 2001; Nocentini et al., 1993), while the gas flow rate has a driving influence on bubble dynamics in other reactor designs (to be discussed in other chapters). In other words, gas holdup information does not necessarily contain any (quantitative or qualitative) information about bubble diameter and interfacial surface area for STRs such that an increase in gas holdup

does not necessarily increase a (Moilanen et al., 2008). However, gas holdup is still reported as an indicator of hydrodynamic performance, gas distribution (Boden et al., 2008), and gas-liquid contacting (Garcia-Ochoa and Gomez, 2004).

Gas-liquid mass transfer correlations, however, typically fail to reflect STR hydrodynamics and predict an increase in mass transfer with an increase in the superficial gas velocity. If these correlations are used improperly, such as during scaleup or outside its representative size and operating conditions, inaccurate k_La estimates will result. In other words, the correlation form is simply incapable of representing the hydrodynamic situation and fails to decouple events occurring due to the superficial gas velocity and those occurring due to the power concentration. The current state-of-the-art k_La correlations with respect to STR conditions will be described in detail in Section 4.12, but it is important to realize that a correlation that is capable of communicating a more complete hydrodynamic picture still remains elusive.

4.5 Power Input

Power dissipation has a direct impact on the gas-liquid mass transfer in STR. As the power dissipation increases, the bubble diameter decreases (Bouaifi et al., 2001; Nocentini et al., 1993), which, in turn, increases the interfacial surface area. Bubbles break apart because the surface tension forces are overcome by a higher power density. Coalescence behavior is reduced because bubbles are not allowed enough contact time for film drainage between adjacent bubbles. At the same time, however, a higher power density implies that the collision force is also increased which would enhance coalescing. Thus, an equilibrium point is reached. As the bubble diameter is reduced to d_B < 1 mm, the effect of increased power concentration is decreased. These small bubbles tend to have immobile interfaces which are more resistant to mass and energy transfer. These diminishing returns cause low viscosity Newtonian fluids to have an optimal bubble diameter distribution of 1-3 mm (Bouaifi et al., 2001) unless surfactant stabilized microbubbles are produced (Bredwell and Worden, 1998; Worden and Bredwell, 1998).

The power dissipation influence on the liquid-phase mass transfer coefficient (k_L) is highly debated in stirred tank reactors, especially at higher power densities. The slip-velocity and eddy turbulence models have been used to explain mass transfer, but they come to different conclusions with respect to power. The slip-velocity model predicts a decrease in mass transfer with increasing power dissipation while the eddy turbulence model predicts an increase. Linek et al. (2004) postulate that the main reason for the confusion stems from the miscalculation of k_L. They investigated different measurement methods and models used by others and concluded that the slip-velocity models were underestimating k_La and, hence, k_L.

It was recognized that both models represent parallel mass transfer processes, but that stirred tank reactors were prone to induce higher rates of eddy diffusion and turbulence (rather than molecular diffusion and surface rigidity control) over surface renewal and mass transfer. Hence, shear rates in stirred tank reactors regulate surface renewal during normal operating conditions. A similar conclusion could be drawn from the Border Diffusion Layer Model (Azbel, 1981). It stipulates, for example, that the eddy diffusion coefficient is three orders of magnitude higher than the molecular diffusivity in the viscous sublayer. If power rates were increased, the viscous sublayer would decrease, which in turn would limit the effect of molecular diffusion on mass transfer and the liquid-phase mass transfer coefficient would increase.

Other researchers have taken an engineering approach. Nocentini et al. (1993) concluded that k_L changes relatively little with power dissipation with respect to a. Thus, any changes in k_La during an operation are dominated by changes in a and k_L is of little interest (Hoffmann et al., 2007; Stenberg and Andersson, 1988b). STR flow patterns should also be considered and neglecting them can lead to a fivefold underestimation in gas-liquid mass transfer (Linek et al., 2004).

One may conclude that power dissipation is the only variable that definitely and directly influences gas-liquid mass transfer in STRs. It has direct control over bubble diameter (interfacial area) and the liquid-phase mass transfer coefficient; however, increasing the impeller speed to

achieve higher gas-liquid mass transfer rates can be inefficient. Stirred tank reactors also operate under an economical constraint. The impeller speed is related to the power draw by an exponential factor of three. Along with operational limitations such as the motor and gearbox assembly and microorganism shear constraint, most gas-liquid mass transfer processes operate in the power dissipation range of 3,000-4,000 W/m^3 (Bredwell and Worden, 1998; Oldshue, 1983). Certain specialized processes require extreme power dissipations of 40,000-100,000 W/m^3 (Gezork et al., 2000, 2001). Operation below 30 W/m^3 is not practical with a stirred tank reactor (Gagnon et al., 1998).

Superficial gas velocity does not necessarily control the interfacial area or liquid-phase mass transfer in stirred tank reactors directly, but influences the gas dispersion efficiency and power dissipation rate. It is very difficult to disconnect the superficial gas velocity from the power concentration in stirred tank reactors, even under experimental settings. Thus, most k_La correlations include the power concentration and superficial gas velocity as variables with the power concentration having a larger role than the superficial gas velocity; this will be discussed in more detail in Section 4.12.

4.6 Liquid Properties

Liquid properties affect gas-liquid mass transfer in STRs through their influence on impeller and reactor hydrodynamics and bubble coalescence. Impeller loading, flow patterns, and power dissipation rates depend on the viscosity of the fluid. The power draw is influenced by the dynamic viscosity during laminar operation while density is the main parameter during turbulent conditions. The transition regime is very large for STRs ($10 < Re < 20{,}000$) (Nienow, 1998) during which the power draw is influenced by both liquid properties simultaneously (Tatterson, 1994).

More importantly, however, is the viscosity's influence over coalescence and impeller loading. Increased viscosity dampens turbulent eddies, and the viscosity gradients force gas towards the impeller zone (Kawase and Moo-Young, 1988). If the fluid is highly viscous, it can lead to

compartmentalization, dead zones, poor gas dispersion, and excessive gas accumulation in the impeller zone highlighted by large and stable gas cavities. Gas accumulation leads to impeller flooding at lower gas flow rates and may limit the amount of the gas that can be sparged. These events also effectively reduce the working volume, requiring large reactors for very viscous and/or non-Newtonian processes (Ogut and Hatch, 1988).

Liquid properties have a direct influence on gas-liquid mass transfer through liquid film behavior and bubble coalescence. Liquid properties influence the boundary layer thickness, surface tension, and surface pressure which determine the coalescence frequency, coalescence efficiency, mixing time, residence time, and liquid-phase mass transfer coefficient. Liquid viscosity influences the thickness of the boundary layer which affects eddy turbulence and diffusion at the gas-liquid interface (Worden and Bredwell, 1998). As the turbulence is reduced, liquid surface renewal is dampened as well.

The thicker boundary layer also means that the mass transfer resistance offered by the liquid film increases. Boundary layer thickness, surface tension, and surface pressure influence surface rigidity. As the bubble surface becomes more rigid, eddy turbulence encounters a higher resistance to the diffusive sublayer penetration. These effects combine to decrease eddy diffusion, molecular diffusion, and, consequently, the liquid-phase mass transfer coefficient (Azbel, 1981). Surface mobility is also an important factor in determining residence time. As the surface rigidity increases, the drag force decreases allowing the bubble to rise faster than those with mobile surfaces (Scargiali et al., 2007).

The effect of liquid viscosity has been investigated by many authors by adding CMC (carboxymethyl cellulose) to water (Puthli et al., 2005). The solution viscosity increases with CMC concentration while providing a negligible influence on bubble coalescence (Fujasova et al., 2007) and bulk flow patterns (McFarlane and Nienow, 1996a). The results show that k_L and k_La decrease as viscosity increases (Charpentier, 1981; Fujasova et al., 2007; Linek et al., 2005a; Puthli et al.,

2005). The gas-liquid interfacial area tends to decrease in these situations as well because the larger cavities and large cavity formations at lower gas flow rates induce a lower power draw (McFarlane and Nienow, 1996a) and larger average bubble diameters (Cabaret et al., 2008). The power draw drop and flow pattern changes are more gradual such that torque and power draw oscillations are reduced. This behavior is attributed to more stable gas-filled cavities that form at lower gas flow rates in high viscosity liquids. The power draw drop, however, can be too smooth for some hydrofoil impellers such that it becomes difficult to identify N_{CD}, requiring purely visual identification (McFarlane and Nienow, 1996a).

The influence of various liquids on coalescence has led to their categorization into coalescing or non-coalescing liquids. Coalescing liquids, such as water or ocenol solution (anti-foaming agent), do not reduce, or may even enhance, bubble coalescence. The bubble film in these liquids tends to be relatively thin and provides minimal resistance to film drainage. Non-coalescing liquids have surface tension reducing properties which, together with turbulence, determine the bubble diameter (Garcia-Ochoa and Gomez, 2004). As surface tension decreases, the turbulent forces provided by impeller agitation are able to decrease the bubble diameter. The smaller bubbles provide more interfacial area increasing the gas-liquid mass transfer coefficient (Charpentier, 1981). Impeller performance and bulk flow patterns are not retarded using non-coalescing liquids even if gas residence time and holdup are increased such that the qualitative interaction is analogous to an air-water system (McFarlane and Nienow, 1996a).

Although water is often used for experimental studies and flow visualization (McFarlane and Nienow, 1996a), it is of little industrial importance according to Linek et al. (1996a) because it is not able to mimic the hydrodynamic behavior of industrial mixtures (McFarlane and Nienow, 1996a). Gas-liquid processes, especially in fermentation (McFarlane and Nienow, 1996a), utilize inputs and/or outputs which are surface active agents such as sugars, alcohols, or electrolytes. Surface active agents exhibit non-coalescing behavior while dampening bubble interface activity

(Stenberg and Andersson, 1988b), potentially reducing the liquid-phase mass transfer coefficient by 75% (Bredwell and Worden, 1998). As the bubble shrinks, the resistance offered by the liquid film changes significantly, further hindering surface velocity and turbulence (Bredwell and Worden, 1998). The gas-liquid mass transfer is therefore determined by the balance of increased interfacial area and decreased liquid-phase mass transfer coefficient (Garcia-Ochoa and Gomez, 1998).

The exact effect on k_La depends on the particular surface active agent(s) and its concentration. Generally speaking, surface active agents increase mass transfer at low concentrations and decrease it at higher ones (Fujasova et al., 2007). Electrolytes (like Na_2SO_4) can be used to describe the general behavior and is also representative of low-viscosity Newtonian fluids such as alcohol (Bouaifi et al., 2001). Na_2SO_4 causes an increase in k_La up to a certain concentration (0.2M), above which its coalescence-inhibiting effects are cancelled by k_L retardation. Increasing the concentration above 0.5M leads to a decrease in k_La (Linek et al., 2004).

Gas holdup may increase by up to 40% with the addition of electrolytes regardless of concentration (Majirova et al., 2004), but the resulting increase in a (and k_La) is offset by the potentially dominating decrease in k_L. These effects are unique to stirred tank reactors because dispersion and agitation are controlled by the impeller and its energy dissipation rate. Glycerol may be used to simulate viscous Newtonian liquids and has a non-coalescing influence in concentration of 5-50% by weight. The maximum k_La is exhibited at 45% by weight (Nocentini et al., 1993). Sokrat44, which has comparable viscosity properties to CMC TS.20 (produced by Lovochemie, Czech Republic), caused a reduction of 40-80% in k_La (Linek et al., 2005a), but has been shown to behave qualitatively similar to electrolytes (Fujasova et al., 2007).

The chemical industry has developed two classes of special surface active agents which are of importance in biological gas-liquid processes: surfactants and anti-foaming agents. Surfactants are used in processes containing coalescence-prone liquids or requiring minimal bubble diameters. The name itself is derived from surface active agent, but is meant to distinguish the industrial products

with coalescence inhibiting properties from other surface active agents which occur naturally, especially in fermentation broths (Kawase and Moo-Young, 1988; van der Meer et al., 1992), or exhibit coalescence inciting properties. A common surfactant is soap. Common surfactants for research purposes are Tween 80 (polysorbate 80) and PEG 1000 (polyethylene glycol). They are nonionic surfactants, which make them less effective for non-coalescing duties, but they are fairly benign, safe, and quite common in the food industry.

Surfactants are amphiphilic and tend to accumulate at the gas-liquid interface, which provides the bubble with a stabilizing interface effect. The formation of these clusters, referred to as micelles, requires a critical micelle concentration, CMC (not to be confused with carboxymethyl cellulose which shares the same abbreviation). This shielding effect is achieved by the surfactant construction. Standard surfactants have a nonpolar hydrophobic tail and polar hydrophilic head. The charged nature of the hydrophilic head would repel two stabilized micelles (bubbles) and not allow enough contact time for the film to drain. Because the interface rigidity is increased, the bubbles are more likely to simply bounce off each other and not form a proper interface connection for drainage. The result is that surfactants may lead to smaller bubbles, higher interfacial surface areas, and higher gas-liquid mass transfer coefficients (Cheng and Sabatini, 2007).

Surfactants provide similar negative impacts on the liquid-phase mass transfer coefficient as other surface active agents with two exceptions. The first is that surfactants usually do not change surface tension relative to non-surfactant solutions, but the surface tension remains steady while stirring (Vazquez et al., 1997). The second is that soluble surfactants do not impede diffusion of small molecules (Bredwell and Worden, 1998) and may not affect the film resistance (but this is rare). On the other hand, the polar group induces an energetic barrier for the turbulence to overcome and is usually seen as decreasing the surface renewal rate. The exact nature of the barrier depends on the polarity and molecular weight of the hydrophilic head, the length of the hydrophobic tail, and the surfactant orientation at the gas-liquid interface (Linek et al., 2005a). An

increase in the ionic strength, for example, would decrease coalescence frequency, decrease bubble diameter, and increase the interfacial surface area (Charpentier, 1981; Stenberg and Andersson, 1988b). The overall impact of surfactants on the interface is represented by a 75% decrease in k_L (Bredwell and Worden, 1998).

The downside of using surfactants is economical and practical in nature. Surfactants are sold by the chemical industry and would add to the product cost. Surfactants also have a tendency to attach to the product or microorganisms and wash out, which would require a surfactant separation and/or recovery system. The recovery system would minimize the surfactant cost, but would add a fixed cost element. Most separation or recovery units for gas-liquid processes use a charged filter, which cannot be reused, to attract the polar head (Cheng and Sabatini, 2007). If microorganisms are involved in gas-liquid processes, surfactants could suffocate or expose them to an unfriendly environment. For example, hand soap is designed to lyse bacteria. Other design options usually exist to increase gas-liquid mass transfer, which do not carry the added fixed or variable costs associated with surfactants.

The exception to the surface active agent rule is provided by anti-foaming agents, such as ocenol. These surface active agents are used by the chemical industry in processes that create excessive foaming which limits gas disengagement at the reactor surface (Bliem and Katinger, 1988b). Anti-foaming agents are designed to induce bubble coalescence such that gas disengagement is maximized. This requires large bubbles and causes a rapid decline in k_La up to a certain concentration where the rate of decline stabilizes (Linek et al., 2005a). In addition to a lower k_La, anti-foaming agents require higher energy inputs and down-stream processing that is similar to surfactants. Anti-foaming agents also denaturize the biological components. Therefore, anti-foaming agents have limited application in most gas-liquid processes (Bliem and Katinger, 1988b) and are usually avoided.

A more challenging situation is presented for viscous non-Newtonian liquids or, more commonly, processes which change a low viscous Newtonian fluid into a viscous non-Newtonian fluid with a complex rheology. Common non-Newtonian processes are encountered in fermentation due to mycelin growth and polymerics produced by the involved microorganisms (Cabaret et al., 2008; McFarlane and Nienow, 1996a). Mycelin growth is simulated using a material with similar macroscopic structure resembling fungal hyphae suspended in water, commonly achieved with paper-pulp suspensions. The polymeric effect on viscosity is simulated using CMC, Carbopol (carboxypolymethylene), or Xanthan gum (Kawase and Moo-Young, 1988; McFarlane and Nienow, 1996a). The viscosity of the solution is simulated by increasing the concentration of those additives over time.

Operations with these types of complex fluids proceed fairly efficiently while the fluid is Newtonian, even if it turns viscous; however, once the liquid becomes non-Newtonian, it adds an additional dampening effect that is very hard to overcome. It becomes very hard to provide proper mixing and dispersion and the reactor volume experiences a wide array of possible Reynolds numbers (Tecante and Choplin, 1993) and energy dissipation rates (Ogut and Hatch, 1988). As a matter of fact, stagnant regions outside the impeller zone and cavern and channel formation are very common. Furthermore, the impeller is easily flooded due to the viscosity gradients which force the gas into the impeller zone (Kawase and Moo-Young, 1988). Hence, the gas flow rate must be limited and increasing the impeller speed is a disadvantage (Ogut and Hatch, 1988).

The result is a poor gas and nutrient distribution and reduced productivity (Gagnon et al., 1998), which in turn causes the process time to be governed by the final 10-20% conversion (Lines, 2000) and requires greater vessel size relative to Newtonian processes (Ogut and Hatch, 1988). The solution has been to simply stop the process once the viscosity reaches a certain level (Ogut and Hatch, 1988) or to implement shear normalizing setups using traditional axial or nontraditional helical impellers which produce a lower apparent viscosity solution (Tecante and Choplin, 1993).

4.7 Baffle Design

Whirlpool effects are often troublesome for STR operation with low-viscosity liquids because they diminish mixing and dispersion (Williams, 2002). Multiphase systems that are mixed with impellers can experience a central vortex which causes recirculation, low power consumption, minimal mixing (Patwardhan and Joshi, 1998), and phase separation (Tatterson, 1994). If the impeller speed is increased even further, this vortex can reach the impeller (Patwardhan and Joshi, 1998). Baffles are often used to alleviate these effects in low viscosity Newtonian liquids, but are avoided with viscous and/or non-Newtonian liquids (Cabaret et al., 2008; Harnby et al., 1992; Williams, 2002). A secondary advantage is that baffles reduce the liquid velocity forcing a larger differential with the impeller velocity. The consequence is that the ungassed power draw is higher in baffled than unbaffled vessels, potentially increasing eddy turbulence and gas-liquid mass transfer. These events are exclusive to turbulent operation, and baffles are unnecessary in the laminar regime (Tatterson, 1994). Gassed power draw can be expected to be similar in baffled and unbaffled vessels while the impeller is loaded (Gagnon et al., 1998). A less common application for baffles in gas-liquid processes is as fins for heat transfer purposes or as gas or liquid feeding device.

Baffle designs are quite numerous and include half, finger, triangle, partition, and bottom baffles with vertical, horizontal, or spiral direction and a wide array of cross-sectional shapes. The basic design, however, is by far the most common because the advantages of non-standard designs are often limited and because the standard design has been widely researched with easily accessible information, scaleup data, and design specs (Ungerman, 2006). The standard design specifies 4-8 equally spaced, vertical plates (Williams, 2002) with a width between $D_T/12$ to $D_T/10$ (Oldshue, 1983; Tatterson, 1991, 1994). Baffles are often offset from the reactor wall to discourage dead zones. The standard wall clearance is about 1.5% D_T (Paul et al., 2004). Baffles are either welded or bolted to the vessel (Bakker and Oshinowo, 2004). If the vessel is made from or lined by a fragile

material, baffles can be supported by a ring placed on top of the tank. The mounting limits these vessels to one or two baffles (Torré et al., 2007).

Prefixes are often used to describe the length or shape. For example, full baffles describe standard baffles having a length equal to the reactor height, half baffles have a length equal to half the height, etc. The shape is often distinguished by a prefix affiliated with a common object. For example, beavertail baffles have a shape that looks like a beavertail (wide in the bottom and tappers off at the top), C-baffles have a semi-circular cross-sectional shape, etc.

Several STR baffle arrangements have been tested to optimize gas-liquid mass transfer or process time. Surface baffles, which are half baffles located in the upper half of the reactor, limit vortex formation while increasing surface turbulence (Patwardhan and Joshi, 1998). This baffle design induces small vortices which entrain gas more effectively, increasing gas holdup and k_La. The limitation of baffle usage in the lower portion of the reactor volume allows for higher turbulence and enhances sparged gas and power utilization (Gagnon et al., 1998); however, Sivashanmugam and Prabhakaran (2008) noted that such nonstandard baffles also lead to lower impeller power draw, which may decrease mass transfer in that portion of the tank. Regardless, this setup has limited application for batch and semi-batch operation.

Lines (2000) came to a different conclusion in addressing similar goals of enhanced operation for batch and semi-batch modes. He concluded that half baffles in the lower portion of the reactor volume allow for more efficient operation that would induce surface aeration without allowing large vortices to reach deep into the vessel and influence the impeller. The limitation, of course, is the liquid height. The baffles break even at a liquid height to reactor diameter ratio of 1.1 for single impeller systems. A 2 beavertail baffle system can be used to extend the range to a ratio of 1.5 and any further increase in reactor height relative to its diameter negates this advantage.

These two examples help to point to a common occurrence: the prescription of opposing systems. Both researchers are correct, and their suggestions are useful for their particular task, but they are not universal. Each system and process has an optimal design - including baffles - that may differ from the standard. It is recommended that a proper baffle design be investigated in the initial design stages and should be compared to the standard option; however, most prefer to avoid this situation and use full baffles due to their simplicity, reduced design costs, and known operation compared to non-standard designs (Oldshue, 1983; Tatterson, 1991, 1994).

4.8 Sparger Design

Spargers are used to input gas into the reactor and affect impeller power consumption (Ni et al., 1995), critical impeller speed for complete dispersion, and critical impeller speed for suspension (Murthy et al., 2007). Spargers are typically located underneath the impeller with the distance and size being dependent on impeller type. The most common placement is $1D_i$ below the impeller. The sparger diameter is usually smaller than the impeller diameter (Birch and Ahmed, 1997). The orifice holes are usually placed on the sparger bottom. This placement prevents the holes from getting plugged during processes that use high viscosity fluids, a solid phase, or fine particles (Patwardhan and Joshi, 1998). The conditions in the sparger orifice have to be such that the gas flow Reynolds number is in excess of 2100 to ensure that all holes are operational (Rewatkar and Joshi, 1993).

Standard sparger designs include ring (Figure 4.21), single orifice (point) (Figure 4.22), pipe, porous (Figure 4.23), and membrane spargers. A ring sparger with equally spaced holes is the most commonly used design for stirred tank reactors since it provides the most consistent results, uses less power, causes a smaller power drop upon gassing, and is thought to provide higher gas holdup and gas-liquid mass transfer coefficients than other sparger types. To be more exact, a small ring sparger is preferred because it produces higher k_La values than the large ring sparger or quadruple pipe sparger (Bakker, 1992).

Figure 4.21: Ring sparger (Micromold Products, 2008).

Figure 4.22: Orifice sparger (Canadian Process Technologies, 2008).

Figure 4.23: Porous spargers (Chand Eisenmann Metallurgical, 2008).

4.8.1 Spargers for Axial Flow Impellers

The selection of the sparger design has to include a discussion of the accompanying impeller type. An improper selection is often used to explain inconsistencies in published data (Ungerman and Heindel, 2007). The most common source of error is to simply use the standard ring sparger design for all impeller types. This may lead to problems with the down-pumping axial flow impellers (Birch and Ahmed, 1996, 1997; McFarlane and Nienow, 1995; McFarlane et al., 1995; Sardeing et al., 2004b). The standard ring sparger forces gas to flow in the opposite direction of the impeller flow field and induces direct loading such that variations in torque and power draw are easily realized. Larger orifice diameters exasperate this problem by increasing the rate at which cavities are allowed to grow on the impeller blades (Murthy et al., 2007). Replacement of a ring sparger with a pipe sparger can reduce gas holdup by 25% (Rewatkar et al., 1993) and does not address the flow issue since gas is sparged in a similar manner. A single orifice sparger enhances the problem since most of the gas is sent into the impeller center promoting cavity formation (McFarlane et al., 1995).

The influence on axial flow impellers can, however, be negated by using a large ring sparger such that gas exhausts in the impeller periphery. Direct loading is avoided and power draw and torque variations are reduced (McFarlane and Nienow, 1996a) because the gas is sparged into a strong downward stream such that the probability of indirect loading is increased. This regime provides the down-pumping axial flow impeller with steady operation (McFarlane et al., 1995), a lower critical impeller speed for complete dispersion and suspension, while flooding is avoided. Particle suspension is achieved with less power and gas is distributed more uniformly for this arrangement (Murthy et al., 2007). Increasing the impeller diameter has also proven to increase stability (Birch and Ahmed, 1996) and suspension efficiency (Sardeing et al., 2004a). Large axial flow impellers solve the problem due to their stable vortex formations and inherent “periodic vortex shedding” (McFarlane and Nienow, 1995).

Another solution for the loading problem, which is not always practical, is to increase the distance between the sparger and impeller, which makes it more likely that the gas is diverted away from the axial flow impeller by the flow stream, leading to more indirect loading (McFarlane et al., 1995). Increasing the distance also tends to delay the power drop upon gassing, making the separation distance an important design parameter (Garcia-Ochoa and Gomez, 1998). The advantage, however, decreases with increasing viscosity (McFarlane and Nienow, 1996a).

Sparger placement for down-pumping axial flow impellers is suggested to be $0.8D_i$ below the impeller. Larger distances increase the flow instabilities and affect the operating range (McFarlane et al., 1995) while smaller distances increase the frequency at which impeller loading fluctuates (McFarlane and Nienow, 1996a). The exact sparger position is often determined by other equipment, and the impeller position requirement such that most designs place the sparger $1D_i$ below the impeller and optimize the proper sparger size and type to provide maximum gas holdup and minimum power drop upon gassing (Birch and Ahmed, 1996; Ungerman, 2006).

4.8.2 Spargers for Radial Flow Impellers

One may think that sparger design may have an important role in the initial bubble diameter and, as such, will influence the interfacial surface area and gas-liquid mass transfer coefficient (Bouaifi et al., 2001; Garcia-Ochoa and Gomez, 1998). Designers should choose a sparger that would offer a smaller initial bubble diameter to increase the efficiency of the operation. However, it has been shown that Rushton-type impellers control the bubble diameter and dispersion such that the sparger choice is noncritical (Garcia-Ochoa and Gomez, 1998). Even if the bubble diameter originating from the sparger is very large, the bubbles are broken apart by the time they reach the impeller and do not affect cavity size, impeller loading, gas-liquid interfacial area, and gas-liquid mass transfer. However, in order to ensure that bubbles pass through the high shear impeller zone, the sparger diameter is suggested to be smaller than the impeller diameter with a standard of $0.8D_i$ (McFarlane et al., 1995; Tatterson, 1991).

This discussion sheds light into the superior performance of a multiple impeller system with a radial-axial flow impeller combination, with a radial flow impeller in the lower position and an axial flow impeller in the upper position. The radial flow impeller is not affected by the sparger type and is able to efficiently disperse small bubbles. The upper impeller is loaded indirectly by the flow field, which it generates, and is able to provide proper mixing conditions. As such, the sparger choice does not affect the performance of the other impellers. If the impellers operate independently, impellers are optimally loaded for gas dispersion and liquid mixing such that progressive reduction in k_La is minimized and the desired process time can be reduced by more than 30% (Lines, 2000).

4.9 Microbial Cultures

Microbial cultures are used as catalysts in bioreactors. Bacteria are the most commonly used culture, but animal, plant, or insect cells have also been implemented (Bliem and Katinger, 1988a). Stirred tank reactors are popular for microorganism growth (Vazquez et al., 1997) because STRs enhance feedstock contact, provide pH and temperature uniformity, and maximize mixing (Hoffmann et al., 2008). Their impact on reactor hydrodynamics is mostly indirect. Occasionally, microorganisms retard turbulence if the organic holdup is above 11-15% depending on the species. The other possibility is that the microorganisms produce surface active agents (van der Meer et al., 1992); however, their most common impact on hydrodynamics is that reaction kinetics may be limited by the environment such that the operational range (power concentration, superficial gas velocity, etc.) may be reduced. As such, it is more constructive to concentrate on the impact that hydrodynamics have on microorganisms.

The most influential factor is for shear gradients which most commonly hinder productivity regardless of the mass transfer situation (Bliem and Katinger, 1988a, 1988b; Hoffmann et al., 2008). Shear gradients damage microorganisms through several mechanisms. The simplest one is cell wall (physical) damage. This mechanism also separates animal and plant cell applications from bacterial

ones. Bacteria are usually smaller and have stronger cell walls relative to their size than animal or plant cells such that bacterial processes use a power range of 1-5 W/kg (comparable to chemical processes) while cellular processes use 0.0005-0.1 W/kg (Bliem and Katinger, 1988a). In other words, smaller cultures are usually able to withstand higher shear gradients because the most damaging eddies have to be on the order of the cell size. As such, animal cell growth rate has been found to be reduced with eddies smaller than 130 μm (Bliem and Katinger, 1988b).

Shear gradients may also interfere with cell-to-cell interaction, cell-to-substrate adhesion, and microbial competition. Additionally, certain microorganisms prefer to flocculate. Hoffmann et al. (2008)[1] concluded that bacteria, which tended to form elongated filaments, were more prone to shear induced damage than those which formed cocci (spherical formations). Although the elongated filaments were more advantageous for food collection during calmer operation, the introduction of strong turbulence provided a competitive advantage for cocci forming bacteria such that those dominated the population at the end of the experiment.

The bacteria's spatial juxtaposition (awareness relative to other bacteria) may also be hindered by turbulence. In the worst case scenario, the bacteria are not able to make significant contact and are not able to achieve the necessary cell density for optimal operation (Bliem and Katinger, 1988b) or are not able to make syntropic relationships with other bacterial cultures (Hoffmann et al., 2008). The result is that startup performance is very poor with minimal or insignificant conversion while long term performance is not hindered in a bacterial mixture that allows competition and has at least one shear tolerant species. Conditioning with feast and famine cycles improved recovery time and tolerance to feed and shear shocks (Hoffmann et al., 2008).

---

[1] The conclusions are based on a particular set of microbial species and have not been verified by other researchers. According to their published article, Hoffmann et al. (2008) experimented with different sized vessels at the same impeller speed. Since turbulence is more intense and power concentration higher with scale, their results and conclusions may not be universally applicable.

Thus, bioreactors using shear sensitive microorganisms have to minimize cellular damage, maximize feedstock transfer to microorganisms, and maximize mixing. The latter requirements are important because the bacterial structure may change during starvation mode to make the culture even more susceptible to cell wall degradation. This situation is true for mycelia (fungi) and may be applicable to other branching bacteria. A healthy specimen, shown in Figure 4.24a, has relatively thick branches without vacuoles (empty pockets). As the bacteria starves (Figure 4.24b), it reduces the number of branches and starts to consume its internal reserves, which leads to the formation of vacuoles. As the number and size of vacuoles increases, the cell wall strength and its ability to resist environmental stresses decreases. As starvation is extended, the specimen will consume as much of its own mass as it can (which depends on the species) and vacuoles will dominate its structure, as can be seen in Figure 4.24c. At this point, the microorganism is easily and significantly damaged by shear gradients (Hoffmann et al., 2008). Energy and mass is diverted to the tip, as pointed out in Figure 4.24c, in order to search for a food source. This tip is of solid construction relative to the main body. Insufficient mixing can have similar effects in that the reactor volume is partially in starvation mode and not producing an optimal amount (if any) of product in those regions (Shewale and Pandit, 2006).

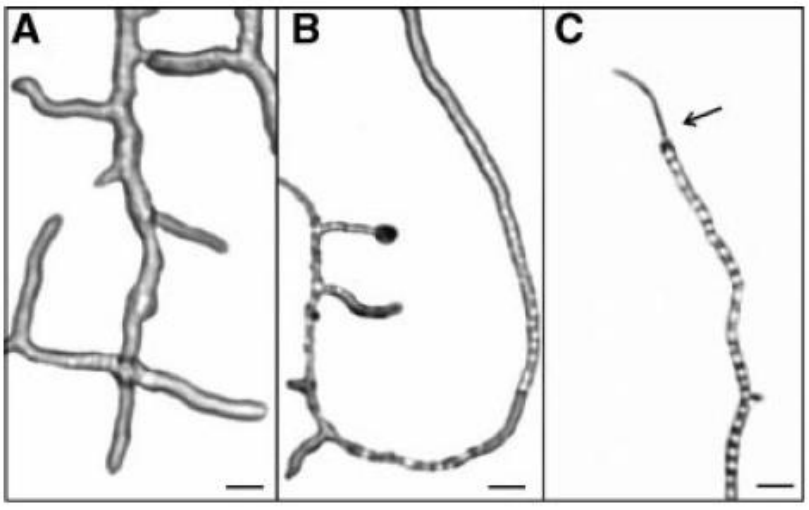

Figure 4.24: Bacteria starvation; (a) a healthy specimen, (b) a bacterium under starvation conditions, and (c) extensive starvation with the formation of many vacuoles (empty pockets) (Hoffmann et al., 2008).

Microorganisms and their reaction kinetics may start out being gas-liquid mass transfer limited, but the process and changing environment may change the limiting factor to temperature or pH level. Bacteria are classified by their temperature preference into mesophilic or thermophilic families. Mesophilic bacteria operate optimally at about 30°C with a sharp drop-off in efficiency as temperature approaches 50°C. These cultures are used more widely because they are easier to control and produce a more consistent product, but are generally able to convert only 40% of the biological matter in 30 to 40 days. Thermophilic bacteria, on the other hand, prefer temperatures of about 60°C and have proven conversion rates up to 48% in just 10 days (Demirel and Yenigün, 2002; Ros and Zupancic, 2002). Acidity is quite variable (although not for a specific bacterial culture) and can range from pH 4.3 to pH 7.9 for anaerobic bacteria (Demirel and Yenigün, 2002). Output can be maximized for acid sensitive processes using syntropic relationships (i.e., volatile fatty acids oxidizing bacteria and hydrogen utilizing methanogens) (Hoffmann et al., 2008).

Furthermore, the production and conversion process often introduces unwanted byproducts or creates products which negatively affect bioreactor operation. For example, protein producing microorganisms, which are often used in pharmacokinetics, produce a mixture over time that is damaging to the bacteria aside from the surface active agent properties of the protein. Shear is tolerated by the microorganisms in this mixture, but air-liquid interfaces, which are naturally very common in gas-liquid processes, can lead to denaturation (Titchener-Hooker and Hoare, 2008). Batch and semibatch stirred tank bioreactors are also influenced by the accumulation of products in the volume, which can significantly change liquid phase properties. Although the production is certainly welcome, it can lead to the process being tail dominated (process time controlled by last 20%, for example) or creating an extremely viscous liquid phase, which, in most cases, forces the operation to cease.

Many industries, in which the stirred tank bioreactors are being implemented, require production to be very consistent and/or the design phase to be completed quickly. For example, it is common in the biopharmaceutical industry to start the design phase once approval of a drug has been secured; however, the design process requires a significant amount of time during which the patent clock is ticking. Hence, costly delays are very common (Titchener-Hooker and Hoare, 2008).

The need for better results has led to the implementation of process and genetic engineering. Process engineering is described throughout this section. Its goal is to optimize the conditions such that production and/or conversion are increased; however, it can be difficult to predict hydrodynamic effects on microorganisms. The answer has been to carefully test microorganism on the micro (experimental) scale and implement genetic engineering techniques to create more shear resistant strains (Zeng and Deckwer, 1996). Process engineering, however, prevails in practice as genetic engineering has not been able to produce very resistive strains (although productivity has been increased) such that stirred tank bioreactors are limited in their power dissipation rates.

4.10 Solid Suspension

A solid phase is often used to represent microorganisms or, more commonly, feedstock used by the microbial culture. Solids have a similar impact on hydrodynamics as surface active agents. The liquid-phase mass transfer coefficient is decreased considerably due to decreased interfacial mobility (Charpentier, 1981; Scargiali et al., 2007; Vazquez et al., 1997). Furthermore, the apparent viscosity is increased (Charpentier, 1981) such that turbulence is reduced and energy dissipation is dampened. The final result is a degradation in both k_L and a.

The solid phase is required to be dispersed throughout the reactor volume to provide optimal conversion. This dispersion requires a minimum (critical) impeller speed, which depends on the impeller type, particle size, solid loading, and other solid and liquid properties affecting particle drag. Lowering the critical impeller speed is important because it implies that suspension is more efficient, distribution is more uniform (Murthy et al., 2007), and conversion is increased.

The behavior of suspended solids depends on the forces acting on the particle: gravity, drag, and lift force (Basset and virtual mass forces may also be considered). Particles with a similar density as the liquid are fluidized and have a velocity approximately equal to the liquid velocity. If the particles are heavier, their velocities are different (usually lower). Much lighter particles tend to disengage from the mixture at the surface and may require some form of surface aeration if uniformity is desired (Paul et al., 2004).

Increased particle size and solid loading require more power to suspend the material such that impeller power and torque draw are increased. The higher load occurs due to the increased mass of solids that need to be lifted from the tank bottom and kept in suspension. The liquid phase (or gas-liquid mixture) has to impart more power to the solid phase, and the impeller is the only significant power source for normal stirred tank reactor operation. The higher power need is met by increasing the impeller speed, but larger impeller diameters may also be advantageous.

Solid suspension leads to the formation of a gas-liquid-solid mixture. The solid phase is regarded as increasing the apparent viscosity of the mixture so that power dissipation is dampened. Generally, as particle size and solid loading increase, the apparent viscosity increases, which lowers the level of turbulence and increases the impeller power draw. The lower level of turbulence translates to a decreased level of mixing, which may decrease uniformity in the reactor volume as well. On the other hand, particles smaller than the liquid film thickness (assuming small solid loading) are able to penetrate the interface film and actually increase turbulence and induces gas-solid mass transfer at the bubble interface. Therefore, the effective liquid-phase mass transfer coefficient is increased (Kluytmans et al., 2003; Patwardhan and Joshi, 1998). This phenomenon is often referred to as the shuttle (or grazing) effect (Kluytmans et al., 2003; van der Meer et al., 1992). Uniformity, which is defined as solid phase concentration variation with a coefficient of 0.05, is important since it allows starvation to be avoided and provides optimal growth conditions (Paul et al., 2004).

The solid phase requires special considerations for stirred tank reactor designs. For example, batch STRs require 10-25% more power for solid suspension relative to continuous operation because continuous flow provides another bottom lifting source. Startup of stirred tank reactors with a settled solid phase may require water or air to help the impeller loosen the packed mass. This problem is often encountered in the mining industry, but is usually avoided in chemical and biological applications; however, the torque draw is going to be higher during startup until particle suspension is achieved (Oldshue, 1983).

Impellers and their arrangements also require modification for solid suspension. Impellers used in single impeller configurations for solid suspension are preferred to have a bottom clearance up to $D_i/3$. This clearance is dependent on the process and impeller type. In order to provide proper mixing, the tanks are shorter than standard gas-liquid designs with a H/D_T ratio about 0.6 to 0.7, and a second impeller is warranted for H/D_T above 1. Solids will settle and stack around the wall if the reactor has a diameter that is too large or an impeller that is too small relative to the tank diameter (Tatterson, 1994). The bottom impeller in a multiple impeller arrangement is more important for solid suspension because the upper impeller can only suspend as much as is fed by its partner (Oldshue, 1983); however, an improper spacing can cause the upper impeller to interfere with the bottom impeller, usually degrading suspension (Tatterson, 1994).

Certain impellers create flow patterns that induce suspension at lower impeller speeds. For example, the down-pumping PBT is more efficient at solid suspension due to its axial bottom-lifting flow than the RT or the up-pumping PBT. The standard Rushton-type turbine is not an efficient suspension impeller (Tatterson, 1994) because the particle lifting occurs through axial flow impeller suction which usually uses about half the impeller flow. Therefore, the Rushton-type turbine requires as much as three times the power for the same level of suspension as the down-pumping PBT (Oldshue, 1983). The advantage and the use of down-pumping axial flow impellers for solid suspension places more relevance on the selection and performance of the sparger design.

Operators are potentially presented with an awkward choice of achieving better gas breakage with a radial flow impeller or better suspension with an axial flow impeller. The decision depends on the gas flow rate. Since most biological processes require a significant amount of gas to proceed efficiently, the instabilities present in the down-pumping PBT and necessary gas-liquid mass transfer have led to a close clearance Rushton-type turbine (clearance of $H/4$ and D_i=$D_T/2$) to be the safest impeller choice for three phase systems if the impeller is operated under complete dispersion conditions (Ulbrecht and Patterson, 1985). The close clearance RT has a significant axial component while still preserving some of its gas breakage capabilities (Harnby et al., 1992).

Standard baffle designs for gas-liquid systems can be used with solids that have a similar density as the liquid. If the solid phase is denser than the liquid, baffles should be much thinner if they are used at all. This is due to the fact that the decreased level of turbulence may lead to stratification, dead zones, and/or recirculation loops near the baffles. These occurrences can cause excessive buildup of solid material and poor performance. Therefore, baffles used for this purpose may have a plate thickness up to $D_T/24$ (Oldshue, 1983).

The presence of the solid phase requires the tank bottom to be adjusted as well. Flat-bottomed tanks are modified with corner fillets to prevent buildup in those lower turbulence areas (Oldshue, 1983), but dished (Paul et al., 2004) or contoured (Ulbrecht and Patterson, 1985) tank bottoms are more effective (in terms of critical impeller speed for suspension) for solid suspension. Although bottom roughness is usually ignored, solid suspension can benefit from a rough finish depending on the particle size. If turbulent eddies created by bottom roughness are of similar size as the particle, their energy is high enough to lift the particle and aid suspension. Surface roughness may also limit the contact between particles and the reactor bottom, lowering the likelihood of a momentum losing interaction. If the eddies are significantly smaller than the particle, their momentum and energy is not capable of influencing the particle. In fact, smaller eddies can contribute to the

(parasitic) drag force experienced by the particle such that bottom roughness may increase the critical impeller speed for suspension for larger particles (Ghionzoli et al., 2007).

The necessity of a solid phase decreases the hydrodynamic performance; however, little gas-liquid mass transfer information and data are present for three phase STRs, especially using CFD modeling (Murthy et al., 2007). Therefore, three phase designs use gas-liquid systems as a starting point, which, of course, provides very optimistic predictions for gas-liquid mass transfer (Vazquez et al., 1997). A proper design procedure should be conducted using a three phase experiment as a basis or using microreactors to obtain the next iterations. Scaleup from these microreactors has to be handled with care since a general scaleup strategy does not exist (Gill et al., 2008).

4.11 Novel Stirred Tank Reactor Designs and Modifications

Novel STR designs tend to be hybrid systems; an example of which is an impeller system is integrated into an airlift reactor. Such modifications will be covered in Section 8.3. Torus reactors are seldom-used mechanically agitated reactors for biological applications although they are oftentimes brought up as alternatives. They are very similar to stirred tank reactors except that torus reactors are horizontal reactors with the stirrer entering the vessel from the side, as shown in Figure 4.25. The most significant difference between a torus and stirred tank reactor is that the torus reactor is a mechanical loop reactor. The torus reactor has a much more defined flow and backmixing is less prevalent. Hence, microorganisms that prefer less turbulent environments or polymerization processes perform better with the torus reactor than the stirred tank reactor. For example, Laederach and Widmer (1984) observed a 40% higher biomass production in a batch torus reactor than a batch stirred tank reactor. The limited amount of backmixing also tends to minimize foam production and dead zones. At the same time, the lack of turbulence can be less appealing for shear resistive microorganisms and non-foaming liquids. A continuous torus reactor also experiences some complexities due to the flow altering behavior of the injection and extraction points (Pramparo et al., 2008).

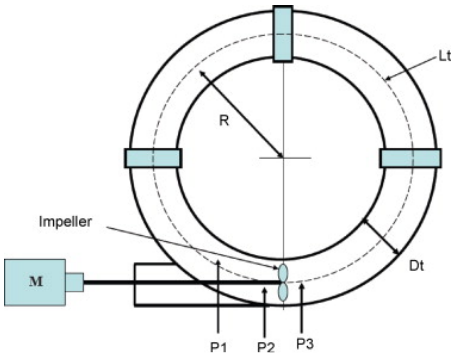

Figure 4.25: Torus reactor example (Nouri et al., 2008).

A much more common approach is to adjust stirred tank reactor components, especially the impeller design and setup. New impeller designs are quite numerous and tend to produce marginal improvements and are usually variations of existing impellers. An interesting impeller type for gas-liquid mass transfer is the spinning disk. As the name implies, the impeller is a disk without blades. Recent research has been concentrated on using these impellers for microbubble generation and mineral flotation due to their bubble break-up characteristics. The spinning disk has lower shear rates than the Rushton turbine at both the tip and stream; however, the spinning disk dissipates 97-98% of its energy at the impeller tip under unaerated conditions. When aerated, energy dissipation increased by 40-60% at the impeller tip and in the impeller stream. This increase is countered by a decrease in the bulk flow intensity. These properties make the spinning disk excellent as bubble breakup devices, but the disk impeller is not capable of mixing a significant amount of liquid (Deglon et al., 1998). A spinning disk could be used in a multiple impeller system, although research has not addressed this possibility. One possible reason is that its strength, high shear rates, may also be its weakness for some biological applications.

Another popular adjustment, that covers a significant number of impeller modifications, is to change the shape or pitch of the blades. For example, Pinelli et al. (2003) experimented with asymmetric blades (i.e., Chemineer BT-6). The BT-6, shown in Figure 4.26, is a concave impeller, which has a top edge longer than the bottom. The result is that the BT-6 has a shallower power curve, which leads to smaller torque fluctuations and broader gas flow operating ranges than

hydrofoil impellers or Rushton turbines. Although the BT-6 cannot compare to the Rushton turbine's bubble breakup characteristics, it is a much better mixing impeller that floods much later. The user can either exchange bubble breakup performance for lower power consumption or use the BT-6 as a pumping device in combination with a Rushton turbine.

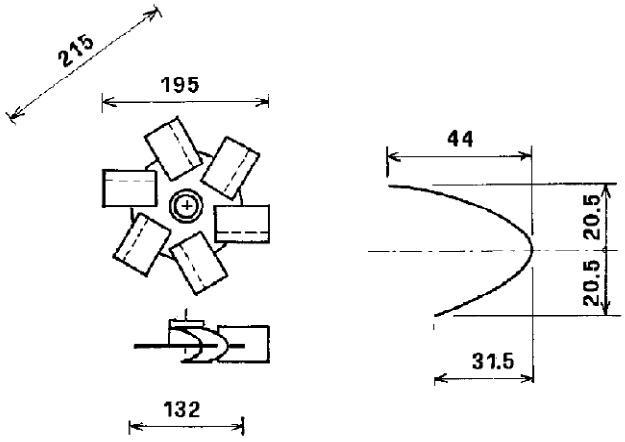

Figure 4.26: Chemineer BT-6 schematic (Pinelli et al., 2003).

Impellers usually enter the vessel from the top; however, very large or novel vessels find it useful for the impeller to enter from the bottom or side (Harnby et al., 1992) because it can minimize the amount of structural steel needed to support the shaft and impeller (Aden et al., 2002). Impeller shafts usually have a circular cross-section and are oriented perpendicular to the reactor bottom and placed along the tank centerline. Other impeller shaft placement relative to the centerline, known as impeller eccentricity, has been practiced (Tatterson, 1991). Off-centering the impeller shaft has been shown to improve mixing, minimize the appearance of vortices (Oldshue, 1983), and produce smaller bubbles in the turbulent regime (Cabaret et al., 2008). Shaft eccentricity (changing the cross-sectional shape) minimizes vortices and can be used in place of baffles. In these applications, mixing time decreases while power input increases. Industrial applications may find this configuration undesirable due to construction and maintenance costs (Cabaret et al., 2008).

Although common shafts are standard, dual shaft systems have been investigated. Dual shafts allow the impellers to spin at independent speeds and directions. Although this configuration adds to setup and maintenance costs, it provides operational flexibility. Since the amount of gas that passes through each impeller zone differs, independent controls allow optimal operation for each impeller. Cabaret et al. (2008) found that the upper impeller needs to run 20% faster for homogenous gas distribution. Dual shafts can also accommodate counter-rotation. Cabaret et al. (2008) claims that counter-rotating Rushton-type impellers in unbaffled tanks is just as efficient as standard, baffled operation. The costs of implementing dual shafts would usually be expected to outweigh any gains made using dual impellers in low viscosity liquids.

Foam breakers can be introduced in stirred tank reactors as well as aerated vessels (bubble column or airlift reactors) in order to avoid the usage of anti-foam agents. Anti-foam agents tend to form an additional barrier to gas-liquid mass transfer and thus reduce the gas-liquid mass transfer coefficient. A mechanical stirrer can be introduced to break the bubbles that accumulate in the separator allowing for more efficiency gas disengagement (Deshpande and Barigou, 1999).

4.12 Correlation Forms

The mass transfer theories from Chapter 3 have been used to define operational boundaries for stirred tank reactors. The hydrodynamic complexity of gas-liquid flows in STRs has curbed the practical application of theoretical models. Currently, a universal model or correlation has not been successfully developed and applied over a wide range of system configurations, scales, operating conditions, or inputs (Garcia-Ochoa and Gomez, 2004; Kawase and Moo-Young, 1988), which is a major disadvantage of stirred tank reactors. The situation is even worse in gas-liquid-solid processes due to lack of relevant data and increased hydrodynamic complexity (Garcia-Ochoa and Gomez, 2004; Murthy et al., 2007). Design and scaleup are implemented using an iterative method, where previous works are used as the first step in a trial-and-error process (Benz, 2008), which continues until the reactor produces the desired conditions (Bliem and Katinger, 1988a).

In order to streamline the process, empirical, semi-empirical, or dimensionless group correlations have been proposed of which empirical correlations are the most commonly used (Bliem and Katinger, 1988a; Garcia-Ochoa and Gomez, 2004; Kawase and Moo-Young, 1988). Variables are chosen based on a gas-liquid mass transfer model believed to dominate the process as well as practical considerations. These correlations have been used in design and scaleup, but are only valid for the particular system and operating range (Benz, 2008; Garcia-Ochoa and Gomez, 2004) and have an accuracy of about +/- 30% at best (Benz, 2008) even if they are in dimensionless form (Bliem and Katinger, 1988a).

In general, STR correlations lack the ability to account for reactor variations and the specific hydrodynamic state; however, they can be used as an estimate if the corresponding systems have geometric, hydrodynamic, and flow pattern similarity. Industrial designs based on experimental setups should be referenced to systems that properly reflect the desired industrial settings and circumstances (Bliem and Katinger, 1988b; Kapic and Heindel, 2006; Kapic et al., 2006). For example, most experimental setups are operated in a Reynolds range of 5,000-10,000 while large industrial units operate in the range 10,000-100,000 (Bliem and Katinger, 1988b). The disconnect becomes more obvious when we consider that a significant number of experiments include data in a power range of 5-10 kW/m^3, while industrial units are rarely operated beyond 3 kW/m^3 (Benz, 2008) or below 500 W/m^3 (Bliem and Katinger, 1988b). This is mainly due to the theoretical models' requirement of a well-mixed state for the liquid phase while industrial units require minimal costs. Hence, mixing and process time often grows much quicker with scale than anticipated and often leads to production difficulties (Nienow, 1996).

A simple approach for finding an appropriate gas-liquid mass transfer correlation is to break k_La down into its components (a and k_L) and find separate correlations for each, after which those would be combined to generate a k_La correlation. It is very convenient to start with the interfacial

area since an applicable theoretical correlation is readily available (Figueiredo and Calderbank, 1979)

$$a = \frac{6\varepsilon_G}{d_{Sm}} \tag{4.2}$$

where ε_G is the gas holdup and d_{Sm} is the Sauter mean bubble diameter.

Next, an assumption is made on the mass transfer model, and the two terms are combined. If a film model is used, k_L is assumed to be inversely proportional to d_B. Therefore,

$$k_L a = \frac{\beta \varepsilon_G}{d_B{}^n} \tag{4.3}$$

where d_B is the mean bubble diameter and β and n are fitted constants. If a penetration model is used, k_L is correlated to a power concentration, usually defined in terms of P_G/V_L:

$$k_L a = C\varepsilon_G \left(P_G/V_L\right)^A / d_B \tag{4.4}$$

where A and C are fitted values, P_G represents the gassed power, and V_L is the liquid volume within the STR. It should be noted that Eqns. (4.3) and (4.4) fall in the semi-empirical family of correlations. Gas holdup correlations, which are presented in Table 4.1, could be substituted into Eqn. (4.4) to obtain gas-liquid mass transfer approximations.

Some researchers have found a better statistical fit by using the total power, P_{tot}, defined as the gassed impeller power plus the buoyancy power of the sparged gas (Moucha et al., 2003). This has been done because the sparged gas power has been shown to impact gas-liquid mass transfer in a similar fashion to impeller power (Stenberg and Andersson, 1988b). On the other hand, Gagnon et al. (1998) came to the conclusion that the impeller transfers energy to the fluid in the impeller zone and that the gas phase does not influence this energy transfer directly. Most researchers, therefore, ignore the effect of the buoyancy force and the gas expansion energy in stirred tank reactors. The power dependence can also be accomplished by using the impeller speed N or a combination of the

impeller diameter D_i and N. Correlations based on D_i and N are more scale dependent then the power concentration. Therefore, correlations will be compared on a power concentration basis.

Equation (4.4) has two control and measurement difficulties: gas holdup and bubble diameter. Gas holdup can have dynamic features and its measurement may be difficult to implement in a reactor control scheme. The bubble diameter, especially in heterogeneous flow, is not uniform and its measurement requires visual inspection, which is troublesome in industrial or large-scale experimental units. Therefore, the representative control inputs (power concentration and superficial gas velocity) for the bubble diameter and gas holdup can be used (Moo-Young and Blanch, 1981). The two inputs represent forces acting on the bubbles such as the drag, buoyancy, inertial, and the surface tension forces. These substitutions have led to the most widely used empirical correlation form:

$$k_L a = C\left(\frac{P_G}{V_L}\right)^A U_G{}^B \tag{4.5}$$

where A, B, and C are fitted constants and U_G is the superficial gas velocity. Correlations based on Eqn. (4.5) are presented in Table 4.2.

Although Eqn. (4.5) has been widely used in practice (Kawase and Moo-Young, 1988), it conveys very little information about the particular system and mass transfer mechanism (Moucha et al., 2003). For example, impeller operating regimes, flow patterns, forces, and liquid and gas properties are not accounted for in this correlation. The particular results are global representations of the system and have little hope of representing microscale effects which are vital in gas-liquid mass transfer (Bouaifi et al., 2001). As shown in Figure 4.27, these issues have caused wide variability in the available gas-liquid mass transfer (and gas holdup) correlations and their dependence on power concentration and superficial velocity (Yawalkar et al., 2002). For example, the power concentration exponent ranges from 0.32 (Gagnon et al., 1998) to 1.32 (Linek et al., 1996a), and the U_G exponent ranges from 0 (Linek et al., 2005a) to 0.77 (Moucha et al., 2003).

Hence, depending on the particular correlation, estimated k_La values may vary by a factor of two or more for a fixed power concentration.

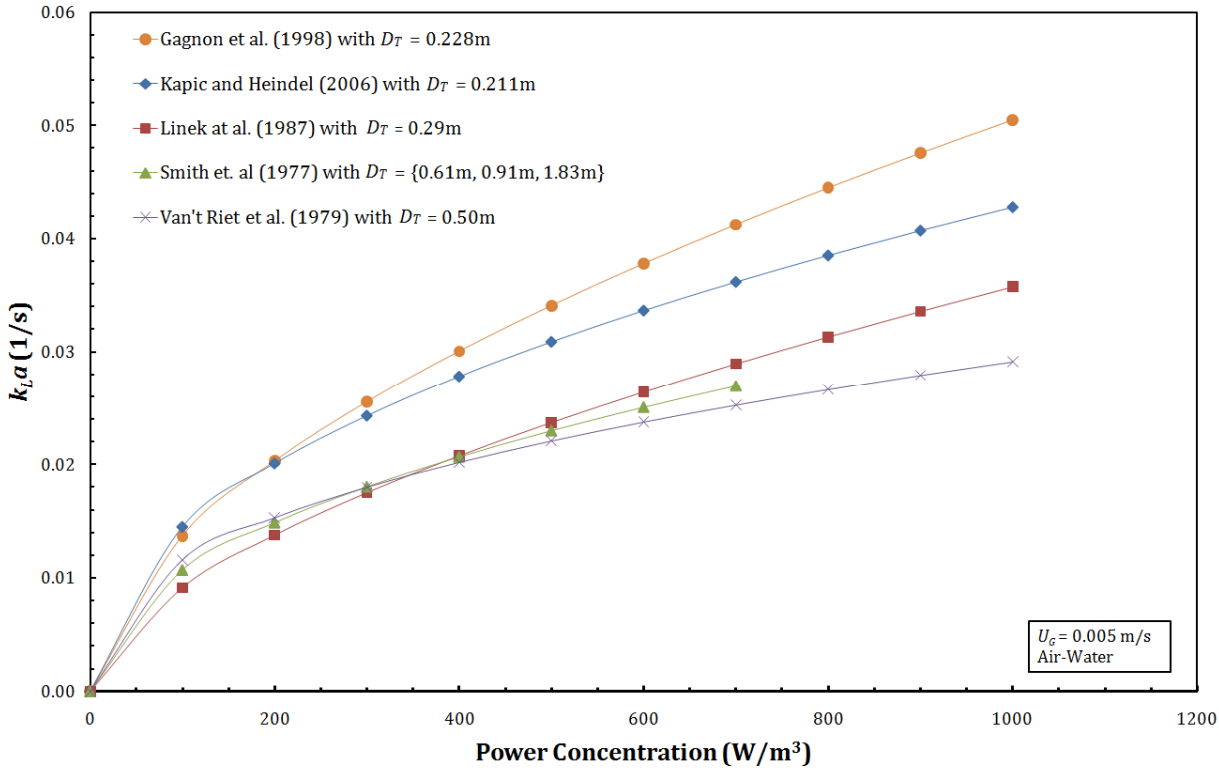

Figure 4.27: Sample mass transfer results for an STR with a single Rushton-type impeller from the correlation based on Eqn. (4.5).

It would be fair to conclude that the choice of fitted variables is based on statistical methods with little thought to implications on mass transfer models and forces acting on the system, thus reducing the usefulness outside the experimental range. For example, the exponents depend on the reactor size (Stenberg and Andersson, 1988b), system geometry, experimental range, and experimental method (Figueiredo and Calderbank, 1979). Therefore, one may conclude that Eqn. (4.5) is leaving out major variables.

A second problem with Eqn. (4.5) is that the two measured variables, power concentration and superficial gas velocity, are inherently connected through hydrodynamics. Their experimental and statistical separation is a very difficult task and is rarely achieved (Garcia-Ochoa and Gomez, 2004; Stenberg and Andersson, 1988b). As stated in the STR literature, questionable measurement

techniques (Linek et al., 1996a) and experimental assumptions (Nocentini, 1990) make a large number of the STR correlations inadequate and conflicting (Nishikawa et al., 1984).

The need to define the system more accurately has led to several improvements on Eqn. (4.5). Fujasova et al. (2007) and Moucha et al. (2003) have added a power term, N_{Pg}, to account for the impeller type:

$$k_L a = C\left(\frac{P_{tot}}{V_L}\right)^A U_G{}^B N_{Pg}{}^D \tag{4.6}$$

where A, B, C, and D are fitted constants. The (gassed) power number is defined as:

$$N_{Pg} = \frac{P_G}{\rho N^3 D^5} \tag{4.7}$$

where ρ is the liquid density and P_G is the gassed impeller power draw. Cavity effects are reflected by a decrease in the gassed power draw and hence the gassed power number. Although the power number helps to identify the particular impeller type, it does not identify the flow regime in which the impeller is operating.

Fujasova et al. (2007) and Linek et al. (1996a, 1996b) went further and attempted to account for multiple impellers. Linek et al. (1996a, 1996b) pointed to the fact that different amounts of gas pass through each impeller zone. It was suggested that one correlation should be formulated for the bottom section while the other impellers were packaged into a separate correlation. Linek et al. (1996a) presented a weighed power term that could be used in Eqn. (4.5). The bottom impeller would account for 25% of the power draw while the other impellers accounted for 75%. Fujasova et al. (2007) added a gassed to ungassed power ratio term that would account for the different amounts of gas passing through each impeller and communicate the impeller performance upon gassing relative to its ungassed state (McFarlane and Nienow, 1996b). Hence, the total mass transfer coefficient was determined from an average of the mass transfer coefficients of each impeller section which was calculated using:

$$k_L a = C P_{tot}^{\ A} U_G^{\ B} \left(P_G/P_0\right)^D N_P^{\ E} \tag{4.8}$$

where *A*, *B*, *C*, *D*, and *E* are fitted constants and P_0 is the ungassed power.

The previous equations assume that liquid properties do not change throughout the process or hope that any viscosity changes or liquid type is reflected in the power concentration term (Ni et al., 1995). These circumstances lead Eqn. (4.5) to fail when the fluid viscosity changes during the process or if the fluid exhibits or becomes non-Newtonian. Several authors have suggested the inclusion of a viscosity term to account for these effects (Garcia-Ochoa and Gomez, 1998, 2004; Linek et al., 2005a; Ogut and Hatch, 1988; Tecante and Choplin, 1993):

$$k_L a = C\left(\frac{P_G}{V_L}\right)^A U_G^{\ B} \mu_a^{\ C} \tag{4.9}$$

where *A*, *B*, *C*, and *D* are fitted constants and μ_a is the apparent viscosity based on the Ostwald-de Waele model. A Casson viscosity (Garcia-Ochoa and Gomez, 1998, 2004) and a liquid-to-water viscosity ratio (Nocentini et al., 1993) have also been used successfully. Unfortunately, Eqn. (4.9) also shares the same disadvantages as Eqn. (4.5) – it is limited to similar systems operating over similar ranges.

Flow patterns and impeller loading conditions have not been considered thus far. They are important characteristics of a system, but are identified through indirect and inefficient means. Yawalkar et al. (2002a, 2002b), Kapic (2005), Kapic and Heindel (2006), and Kapic et al. (2006) have attacked this prospect using a correlation based on a complete dispersion impeller speed N_{CD}. It defines the point at which complete gas dispersion is achieved at the minimal power input (e.g., see Figure 4.6 and Figure 4.7). Yawalkar et al. (2002) proposed

$$k_L a = C\left(\frac{N}{N_{CD}}\right)^A U_G^{\ B} \tag{4.10}$$

where *A*, *B*, and *C* are fitted constants. Various correlations of this form are summarized in Table 4.3. It was noted that this $k_L a$ correlation was independent of reactor geometry, impeller type,

position of the impeller, and sparger if operated at the same N/N_{CD} ratio. For example, Kapic and Heindel (2006) correlated data from several different sources and STR sizes into a single correlation[2]:

$$\frac{k_L a}{U_G^{\ A}} = C\left(\frac{N}{N_{CD}}\right)^B \left(\frac{D}{T}\right)^D \tag{4.11}$$

where A, B, C, and D are fitted constants. These results are shown in Figure 4.28. This correlation does a good job of fitting the experimental data for a variety of tank sizes. However, the correlation is valid only for STRs with Rushton-type impellers operating in the completely dispersed flow regime.

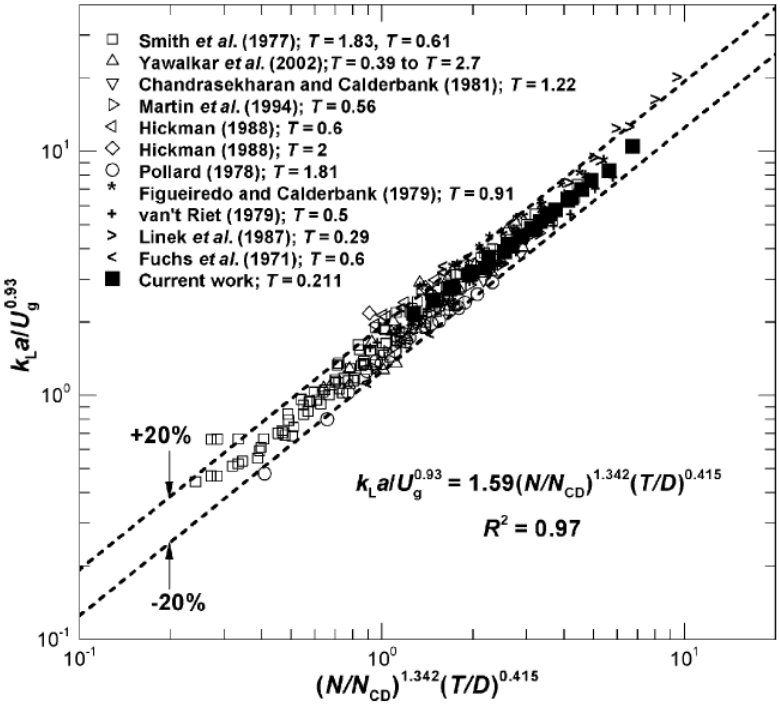

Figure 4.28: Scaleup correlations developed by Kapic and Heindel (2006).

[2] The original correlation in Kapic and Heindel (2006) inadvertently transposed the D/T fraction.

In order to achieve more consistent scaleup success, full-scale and pilot reactors should have geometric and hydrodynamic similarity. The pilot reactor used for preliminary design should have operational relevance to the full-scale unit especially with respect to the impeller speed (Kapic and Heindel, 2006). Yawalkar et al. (2002a) went further to address the question of scaleup by defining Eqn. (4.10) in terms of gas volume per unit liquid volume per minute (*vvm*):

$$k_L a = C\left(\frac{N}{N_{CD}}\right)^A (vvm)(T)^B \tag{4.12}$$

where *A*, *B*, and *C* are fitted constants. Eqn. (4.12) proved more effective at predicting $k_L a$ for larger volumes. This scaling approach is, however, limited because it requires the pilot reactor to provide a *vvm* ten to twenty times higher than the full-scale version (Benz, 2008).

A much simpler approach can be taken with systems having geometric and hydrodynamic similarity. It is often thought the gas-liquid mass transfer coefficient could be increased by increasing the amount of gas in the reactor volume. This idea has been in extensive use in multiple impeller systems because of the difficulty in determining k_L (Moucha et al., 2003). Gas holdup ε_G was used to represent this concept (Moucha et al., 2003) and is defined as:

$$\varepsilon_G = \frac{V_G}{V_G + V_L} \tag{4.13}$$

where V_G and V_L are the gas and liquid volume, respectively. A very simple form of the gas-liquid mass transfer coefficient proposed by Stenberg and Andersson (1988b) is

$$k_L a = C\varepsilon_G \tag{4.14}$$

where *C* is a fitted value.

Stenberg and Andersson (1988b) found that Eqn. (4.14) accounted for over 93% of their data. It was concluded that the gas-liquid mass transfer coefficient variations in a system are explained by changes in the interfacial area due to its connection to gas holdup by Eqn. (4.2). They also found that a large error in the bubble diameter would create a relatively small error in $k_L a$, which was

shown using Eqn. (4.3). Unfortunately, the correlation does not communicate any information regarding the mass transfer process, hydrodynamics, or fluid properties and is somewhat unconventional since no other authors have presented their work in this form. The reactor design and operational uniqueness are not accounted for with Eqn. (4.14). In addition, Moucha et al. (2003) found that axial flow impellers, which could provide higher gas holdup, would still underperform radial flow impeller in term of mass transfer due to their inability to provide smaller bubble diameters (Moucha et al., 2003). Therefore, Eqn. (4.14) will fail during scaleup, but could be used as a first approximation for a similar design and size.

The scaleup problems arise from the fact that all STR gas-liquid mass transfer correlations are empirical. They are, for the most part, unable to account for hydrodynamic or liquid property changes with scale and time. Extensive attempts have been made in using nondimensional groups, especially towards solving gas-liquid processes involving non-Newtonian liquids. These correlations tend to be more complicated and require numerous static, but only few dynamic, inputs. One of the simplest correlations is presented by Ogut and Hatch (1988) which involves four dimensionless groups and requires six inputs. One of the more complicated forms, proposed by Nishikawa et al. (1981), uses 12 dimensionless groups because the model tries to explain operation during low power input leading to the stirred tank reactor behaving like a bubble column. A general word of warning would be that if a correlation is based on statistical fitting, it runs the risk that the fit is achieved by probability rather than causality. The result could be that the correlation predicts improbable outcomes when extended beyond the operating range (Stenberg and Andersson, 1988b).

4.13 Needed Research

A few basic research needs are left to be explored for the stirred tank reactor. The hydrodynamics are known for the standard impellers, but the explanation of the physics behind each of the phenomena is not well understood. If a new impeller is designed, its predicted effects are determined based on its similitude to standard impellers rather than the impeller design. Since stirred tank reactors use a wide variety of shear producing impellers, the gas-liquid mass transfer correlations are highly specific on the type of impeller. Current correlations are not capable of accounting for the impeller type and usually cannot be applied to other impellers without significant error. A correlation that would have this capacity would be incredibly helpful. An issue tied to the impeller type is scaleup procedures and guidelines, which may not agree on the predicted effects. The worst case scenario is that the impeller power law is ignored, which would lead to practically irrelevant comparisons. The best case is that the guideline helps to maintain a constant variable of interest such as shear rates in the impeller zone. Unfortunately, other variables, which can have a significant impact on microorganism production, often change unpredictably such as the level of mixing in the scaled vessel. A holistic, although complicated, approach could be helpful.

The use of multiple impeller systems should be customized towards a particular application and its goals. Optimization should be an attainable goal. Research could be directed towards determining which impeller combinations should be preferred for process specfic goals (i.e., mixing, gas-liquid mass transfer, shear). It would be helpful to develop a suggestion matrix such that a user could look up a range of possible impeller combinations for a given maximum shear rate. Then, the user could decide between mixing and gas-liquid mass transfer. For example, if the microorganism is somewhat shear resistant, but it also forms potentially toxic byproducts due to secondary reactions or concentrations, mixing might be more important than gas-liquid mass transfer.

Stirred tank bioreactor research and design is not focused enough on microorganism applications. A majority of research is conducted with and by the chemical fields. If the application is biological in nature, several different requirements have to be met. For example, little research has been completed with live microorganisms, which leads many scaleup procedures into the unknown. Microorganism behavior, such as flocculation, is often not accounted for. Such properties could be studied by simulating microorganisms using fibers. Fibers could also be studied as a microorganism support carrier to better protect microorganisms from shear.

Microorganism tend to produce proteins and other byproducts that may significantly alter liquid properties. Non-Newtonian liquids are often left out of hydrodynamic research work or non-Newtonian behavior is investigated on its own; however, microorganisms change several liquid properties in parallel and through different means. For example, the proteins may cause the fluid to become non-Newtonian, but the microorganisms may also flocculate. The current research is not capable of predicting hydrodynamics in such a case. The only conclusion that could be drawn is that gas-liquid mass transfer will decrease and mixing will be significantly hampered. This question could be investigated by adding fibers to non-Newtonian mixtures.

Naturally, impeller designs could also be investigated to fit the needs of microorganisms. In such a world, honeycombed impellers might become less attractive since they might kill microorganisms in the high shear impeller zone. In addition, multiple impeller arrangements could be investigated or designed better so that the impellers aid each other's operation. For example, the axial impeller would mix the reactor so that the radial impeller is loaded properly and the radial impeller would not allow the gas phase to enter the axial impeller zone in such a way to cause axial impeller loading instabilities. It would be feasible that the optimum designs and combination do not have the standard separation distance.

4.14 Summary

Stirred tank reactors are one of the standard bioreactor designs used in biological applications because gas-liquid mass transfer can be easily increased through faster impeller speed and higher gas flow rate. Stirred tank reactors come in many different flavors and scales. Small and experimental scale STRs can be serviced by a single impeller while most industrial applications use multiple impellers. The best choice for single impeller STRs is a radial disc impeller, but other designs may be more advantageous depending on the application. For example, retrofitting with some radial flow impeller, such as the Rushton-type turbine, may be difficult due to its high torque; however, replacement or addition of an axial flow impeller, such as the A-315, is easily achieved without further stress on the motor and gearbox. Therefore, a multiple impeller design with a non-interfering radial flow impeller (bottom) and axial flow impeller(s) is preferred.

Theoretical models explaining mass transfer are in place, but a k_La equation, which is applicable over a wide array of designs and operational range, is still not available. The interaction between the impeller and the gas and liquid phases is very complicated and a lot of ambiguity and controversy exists. Literature is often filled with contradictory suggestions and explanations. Hence, practical design procedures, such as scaleup or retrofitting, can be very complicated and results are often hard to predict correctly. Furthermore, microorganisms add another level of complication because they may be sensitive to the reactor conditions so that production declines even if gas-liquid mass transfer, the supposed limiting factor, increases. These interactions in turn have led to industrial applications often being dominated (in terms of time) by the last 10-20% of conversion (relative).

Therefore, great care has to be used in designing, operating, or retrofitting stirred tank reactors for biological applications. Scaleup may be more successful if the experimental and industrial scale designs have hydrodynamic and geometric similarity because the probability of similar conditions is increased. In such cases, it is expected that production would also meet predicted values. In

addition, the implemented scaleup strategy has to account for increased turbulence with scale. A common error is to use a constant impeller speed scaleup strategy, which leads to much higher levels of turbulence and power costs at the industrial scale. In fact, a global scaleup strategy does not exist, and any designs and modifications have to be thoroughly tested. The trial and error method cannot be avoided, but hydrodynamic and geometric similarity reduces the time and cost required to achieve satisfactory results.

Table 4.1: Gas holdup correlations for stirred tank reactors.

$\varepsilon_G = C(P_G/V)^a U_G^b$

Researchers	C	a	b	U_G range (mm/s)	P_G/V range (W/m^3)	Gas	Liquid	Impeller Configuration	H (m)	T (m)
Bouaifi et al. (2001)	22.4	0.24	0.65	3.7-18.1	0-1,000	Air	Tap water	2 (PBT, A310, A315)	0.86	0.43
	24.8	0.24	0.65					2 (RT, PBT, A310, A315)		
Figueiredo and Calderbank (1979)	0.34	0.25	0.75	n/a	n/a	n/a	n/a	n/a	n/a	n/a
Linek at al. (1994)	0.23	0.31	0.73	n/a	n/a	n/a	Water	2 (RT)	n/a	n/a
	0.05	0.49	0.58				0.5M Na_2SO_4			
Linek at al. (1996)	0.07	0.36	0.54	0-0.00848	0-4,000	Nitrogen and oxygen	Water	4 (RT)	0.19, 0.38, 0.57, 0.76	0.19
	0.29	0.30	0.73							
	0.02	0.59	0.44				0.5M Na_2SO_4			
	0.05	0.46	0.52							
Moucha at al. (2003)	0.02	0.63	0.52	2.12, 4.24, 8.48	0-1,300	Oxygen	0.5M Na_2SO_4	1 (TXU)	0.29, 0.58, 0.87	0.29
	0.05	0.49	0.57					2 (TXU)		
	0.17	0.42	0.75					3 (TXU)		
	0.05	0.42	0.53					1 (TXD)		
	0.14	0.32	0.59					2 (TXD)		
	0.26	0.36	0.74					3 (TXD)		
	0.05	0.47	0.58					1 (PBD)		
	0.08	0.52	0.71					2 (PBD)		
	0.35	0.29	0.80					3 (PBD)		
	0.19	0.44	0.75					3 (RT, 2TXU)		
	0.24	0.45	0.82					3 (RT, 2TXD)		
	0.10	0.52	0.71					3 (RT, 2PBD)		
	0.03	0.51	0.50					2 (RT, TXU)		
	0.11	0.42	0.66					2 (RT, TXD)		
	0.05	0.50	0.57					2 (RT, PBD)		
	0.02	0.62	0.57					1 (RT)		
	0.05	0.49	0.58					2 (RT)		
	0.04	0.54	0.58					3 (RT)		
Pinelli et. al (2003)	0.10	0.28	0.48	7.0-14.0	200-2,600	Air	Water	2 (BT-6)	0.96, 1.44	0.48
	0.25	0.24	0.65							
Vasconcelos et al. (2000)	0.10	0.37	0.65	n/a	n/a	n/a	Water	2 (RT)	n/a	n/a
Whitton and Nienow (1993)	1.28	0.26	0.66	11.8-33.1	1.4-1.7 rps	n/a	n/a	1 (RT)	n/a	0.61, 2.67
Yawalker et. al (2002)	0.56	0.25	0.41	4.0-15.7	0.7-8.3 rps	Air	Water	1 (PBD)	0.57	0.57
	0.52	0.25	0.40							

Note: The correlations by Calderbank (1958), Hickman (1988), Linek et al. (1987), Smith and Warmoeskerken (1985), Van't Riet (1979), Whitton and Nienow (1993), and Zhu et al. (2001) are as cited by Yawalkar et al. (2002b).

Table 4.2: Standard gas-liquid mass transfer **c**orrelations based on Eqn. (4.5).

$k_L a = C(P_G/V)^A U_G^B$

Researchers	C	A	B	U_G range (mm/s)	P_G/V range (W/m^3)	Gas	Liquid	Impeller Configuration	H (m)	T (m)
Bouaifi et al. (2001)	0.022	0.50	0.60	3.72-18.10	0-1,000	Air	Tap water	2 (RT, PBT, A310, A315)	0.86	0.43
Fujasova et al. (2007)	0.006	0.74	0.53	2.12, 4.24, 8.48	0-1,200	Air	Water	3 (RT in bottom; PBD, PBU, TXD, LTN, NS)	0.29, 0.58, 0.87	0.29
	0.001	1.22	0.51				0.5M Na2SO4			
	0.002	0.95	0.58				Sokrat 44			
	0.006	0.69	0.53				Water			
	0.001	1.25	0.57				0.5M Na2SO4			
	0.001	1.00	0.50				Sokrat 44			
	0.006	0.69	0.53				Water			
	0.001	1.20	0.58				0.5M Na2SO4			
	0.001	0.95	0.53				Sokrat 44			
	0.005	0.72	0.50				Water			
	0.000	1.22	0.45				0.5M Na2SO4			
	0.002	0.95	0.57				Sokrat 44			
Gagnon et. al (1998)	0.5	0.01	0.86	0-1.2	0.001-30	Air	Water	1 (RT)	0.55	0.23
	0.8	0.02	0.92					2 (RT)		
	0.2	0.02	0.72					2 (RT)		
	0.3	0.03	0.79					3 (RT)		
	0.4	0.01	0.87		0.001-100			HR		
	0.5	0.06	0.88					HRB		
	12.2	0.57	0.47		30-10,000			1 (RT)		
	2.9	0.83	0.50					2 (RT)		
	3.2	0.79	0.48					2 (RT)		
	9.2	0.60	0.50					3 (RT)		
	15.4	0.32	0.50		100-10,000			HR		
	31.1	0.38	0.65					HRB		
Gezork et al. (2001)	0.005	0.59	0.27	0-130000	0-100,000	Air	Water	1 or 2 (RT)	0.29	0.29
	0.004	0.70	0.18				0.2M Na2SO4			
Hickman (1988)	0.043	0.40	0.57	2-17	50-3,500	Air	Water	1 (RT)	n/a	0.6
	0.027	0.54	0.68							2
Kapic and Heindel (2006)	0.040	0.47	0.60	0.5-7.2	6.7-13.3 rps	Air	Tap water	1 (RT)	0.21	0.21
Kapic et al. (2006)	0.026	0.61	0.61	0.5-7.2	6.7-13.3 rps	CO	Water	1 (RT)	0.21	0.21
	0.001	1.23	0.55			Air	0.5M Na2SO4	2 (RT)		
Linek at al. (1987)	0.005	0.59	0.40	2.12, 4.24	100-3,500	Air	Water	1 (RT)	n/a	0.29
	0.001	0.95	0.40				0.5M Na2SO4			
Linek et al. (1990)	0.000	1.24	0.40	n/a	n/a	Air	Water	n/a	n/a	n/a
Linek et al. (1994)	0.000	1.21	0.40	n/a	n/a	Air	0.3M Na2SO4	3 (RT)	n/a	n/a
Linek et al. (1996)	0.009	0.63	0.54	0-8.48	0-4,000	Nitrogen and oxygen	Water	4 (RT)	0.19, 0.38, 0.57, 0.76	0.19
	0.006	0.68	0.50							
	0.001	1.17	0.46				0.5M Na2SO4			
	0.001	1.32	0.33							

Table 4.2 cont.: Standard gas-liquid mass transfer correlations based on Eqn. (4.5).

$k_L a = C(P_G/V)^A U_G^B$

Researchers	C	A	B	U_G range (mm/s)	P_G/V range (W/m^3)	Gas	Liquid	Impeller Configuration	H (m)	T (m)
Linek et. al (2005)	0.00003	1.18	0.00	1.8, 3.6, 5.4	10-1,500	Pure oxygen or air	0.8M Na2SO4	1 (RT)	0.12	0.12
	0.00003	1.16	0.00				0.8M Na2SO4 and Sokrat44 (3% vol)			
	0.00004	1.08	0.00				0.8M Na2SO4 and CMC TS.5 (0.2 wt%)			
	0.00022	0.77	0.00				0.8M Na2SO4 and CMC TS.5 (0.6 wt%)			
	0.00013	0.73	0.00				0.8M Na2SO4 and Ocenol (3 ppm by vol)			
	0.00003	1.15	0.00				0.8M Na2SO4 and PEG 1000 (100 ppm by mass)			
Moucha at al. (2003)	0.001	1.25	0.63	2.12, 4.24, 8.48	0-1,300	Oxygen	0.5M Na2SO4	1 (TXU)	0.29, 0.58, 0.87	0.29
	0.002	1.20	0.74					2 (TXU)		
	0.002	1.20	0.70					3 (TXU)		
	0.018	0.88	0.77					1 (TXD)		
	0.006	1.01	0.69					2 (TXD)		
	0.009	1.01	0.75					3 (TXD)		
	0.002	1.05	0.46					1 (PBD)		
	0.001	1.11	0.39					2 (PBD)		
	0.001	1.15	0.51					3 (PBD)		
	0.003	1.01	0.54					3 (RT, 2TXU)		
	0.003	1.04	0.51					3 (RT, 2TXD)		
	0.001	1.14	0.46					3 (RT, 2PBD)		
	0.001	1.06	0.36					2 (RT, TXU)		
	0.002	1.02	0.47					2 (RT, TXD)		
	0.001	1.13	0.43					2 (RT, PBD)		
	0.000	1.24	0.34					1 (RT)		
	0.001	1.23	0.56					2 (RT)		
	0.001	1.24	0.47					3 (RT)		
	0.001	1.19	0.55					All Data		
Ni et. al (1995)	1.645	0.50	0.64	0.5 vvm	0-10,000	Air	Yeast and feed	2 (RT)	0.195 0.37	0.12 0.24 3
Nocentini et al. (1993)	0.015	0.59	0.55	0.1-0.7 vvm	100-10,000	Air	Water and glycerol	4 (RT)	0.70, 0.93	0.23
Pinelli et. al (2003)	0.018	0.37	0.29	7.0-14.0	200-2,600	Air	Water	2 (BT-6)	0.96, 1.44	0.48
	0.005	0.59	0.40							

Table 4.2 cont.: Standard gas-liquid mass transfer correlations based on Eqn. (4.5).

$k_L a = C(P_G/V)^A U_G^B$

Researchers	C	A	B	U_G range (mm/s)	P_G/V range (W/m^3)	Gas	Liquid	Impeller Configuration	H (m)	T (m)
Puthli et al. (2005)	0.0001	0.58	0.43	1.7-6.4	300-600 rpm	Air	Water	1 (RT)	0.22	0.13
	0.0001	0.61	0.43					2 (RT, PBT)		
	0.0002	0.67	0.53					3(RT, 2PBT)		
	0.0001	0.68	0.53				0.25% (w/v)CMC	3(RT, 2PBT)		
	0.0001	0.66	0.54				0.375% (w/v)CMC			
	0.0022	0.36	0.56				0.50% (w/v)CMC			
Riggs and Heindel (2006)	0.051	0.51	0.65	0.5-2.88	200-600 rpm	CO	Water	1 (RT)	0.21	0.21
Smith et. al (1977)	0.010	0.48	0.40	4.0-20.0	20-5,000	Air	Water	1 (RT)	0.60 0.61 0.91 1.63	0.44 0.61 0.91 1.83
	0.020	4.75	0.40	4.0-46.0	0-700	Air	0.11 Na_2SO_4			
Van't Riet (1979)	0.026	0.40	0.50	n/a	n/a	n/a	Coalescent	1 (RT)	n/a	n/a
	0.020	0.70	0.20				Non-coalescent			
Vasconcelos et al. (2000)	0.006	0.66	0.51	n/a	n/a	n/a	Water	2 (RT)	n/a	n/a
Zhu et. al (2001)	0.031	0.40	0.50	1.0-7.5	100-1,500	Air	Water	1 (RT)	n/a	0.39

Note: The correlations from Linek et al. (1987), Van't Riet (1979), and Zhu et al. (2001) are as cited by Yawalkar et al. (2001a). The correlation from Linek et al. (1994) is as cited by Fujasova et al. (2007).

Table 4.3: Gas-liquid mass transfer correlations based on Eqn. (4.10).

$k_L a = C(N/N_{CD})^A U_G^B$ (Adopted from Yawalkar et al. (2002a))

Researchers	C	A	B	U_G range (mm/s)	N/N_{CD}	Gas	Liquid	Impeller Configuration	H (m)	T (m)
Chandrasekharan and Calderbank (1981)	2.7	1.15	0.96	3.5-18	0.85-1.56	Air	Water	1 (RT)	n/a	1.22
Calderbank (1958), van't Riet (1979)	2.8	1.14	0.97	5-36	0.67-2.65	Air	Water	1 (RT)	n/a	0.5
Hickman (1988)	4.3	1.35	1.04	2-17	066-1.61	Air	Water	1 (RT)	n/a	0.60, 2
Linek et. al (1987)	5.2	1.69	1.09	2.12-4.24	1.4-3.8	Air	Water	1 (RT)	n/a	0.29
Smith et. al (1977)	2.4	1.38	0.96	4.4-46	0.25-2.44	Air	Water	1 (RT)	0.61 0.91 1.63	0.61 0.91 1.83
Smith (1991)	6.5	1.44	1.12	n/a	n/a	Air	Water	1 (RT)	n/a	0.6, 2.7, 2.7
Smith and Warmoeskerken (1985)	12.6	1.54	1.27	n/a	n/a	Air	Water	1 (RT)	n/a	0.44
Whitton and Nienow (1993)	3.5	1.17	1.00	n/a	n/a	Air	Water	1 (RT)	n/a	0.61, 2.67
Yawalker et. al (2002)	3.4	1.46	1.00	n/a	n/a	Air	Water	1 (RT)	n/a	
Zhu et. al (2001)	3.3	1.14	0.97	1.0-7.5	n/a	Air	Water	1 (RT)	n/a	0.69

5 Bubble Column Reactors

5.1 Introduction

Bubble columns (BC) belong to a family of pneumatic bioreactors. The concept, in which compressed air is injected into the base of a cylindrical vessel, is a cheap and simple method to contact and mix different phases (Díaz et al., 2008). The liquid phase is delivered in batch or continuous mode, which can be either counter- or cocurrent. The batch bubble column is the more common form, but the cocurrent version, shown in Figure 5.1, is also encountered. Countercurrent liquid flow is rarely used in industry as it provides minor, if any, advantages and multiple complications (Deckwer, 1992), with separation by evaporation being one of the few exceptions (Ribeiro and Lage, 2005).

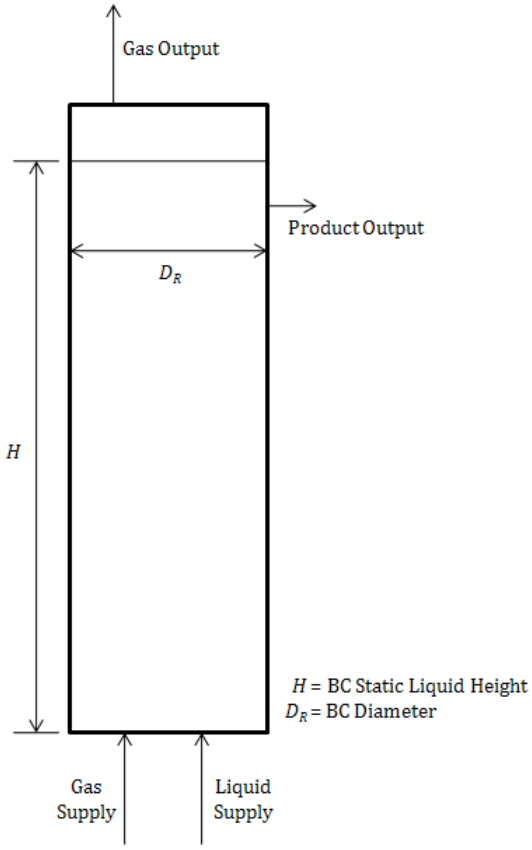

Figure 5.1: Bubble column schematic; if the liquid is also flowing continuously, in the same direction as the gas then the bubble column would be identified as cocurrent.

The gas throughput has a significant impact on the column design. Superficial gas velocity in BCs is limited to U_G = 0.03-1 m/s with most applications operating at the lower end. The exact value is scale and flow regime dependent and only large industrial projects would use $U_G \approx 1$ m/s. Such flow rates lead to very fast-rising bubbles (Deckwer, 1992; Krishna et al., 2001).

Bubble columns tend to be tall vessels with a large aspect ratio (H/D_R) because the height is a controlling factor for the process and residence times, especially for batch and semi-batch operations (Roy and Joshi, 2008). Biochemical processes require an aspect ratio between 2 to 5, even for experimental work. Industrial applications require much taller vessels with an aspect ratio of at least 5 (Kantarci et al., 2005), but it is fairly common to have vessels with an aspect ratio greater than 10 (Bellgardt, 2000). An aspect ratio greater than 5 is also preferred because it does not influence bubble column hydrodynamics (Ribeiro, 2008).

The upper section of the bubble column is often widened to encourage gas separation. Bubble column volume is dependent on the application. The chemical production industry uses columns with volumes on the order of 100-200 m^3 while the biotechnology industry and wastewater treatment use columns that may be up to 3,000 and 20,000 m^3, respectively (Deckwer, 1992).

Bubble columns require very little maintenance or floor space and have low operating costs compared to other reactor types (Ribeiro, 2008). The low operating and maintenance costs are mainly due to the lack of moving parts. Compressed gas is capable of producing a friendlier and uniform environment, which is important for processes involving shear sensitive microorganisms or pressure sensitive catalysts (Kantarci et al., 2005). Compressed gas is also a more effective power source for very large reactor volumes (up to 500 m^3) (Bellgardt, 2000). The pneumatic power source typically produces lower energy dissipation rates compared to stirred tank bioreactors. Furthermore, BC designs allow for online modification of microorganism concentrations (Kantarci et al., 2005) and handling of materials that may cause erosion or plugging (Ribeiro, 2008).

The above advantages make bubble columns ideally suited for a variety of process industries including the chemical, petrochemical, biochemical, pharmaceutical, food, environmental, and metallurgical industries, and are used in operations such as oxidation, chlorination, alkylation, polymerization, and hydrogenation. Bubble columns are also widely used for the treatment of wastewater and manufacture of synthetic fuels (through fermentation), enzymes, proteins, and antibiotics (Kantarci et al., 2005).

The major disadvantage of bubble column reactors is the difficulty in controlling the complex hydrodynamics found in the reactor, which have a controlling effect on the transport and mass transfer characteristics (Kantarci et al., 2005). The flow patterns, which are not well-defined (Bellgardt, 2000), create considerable backmixing and a large pressure drop through the column. These phenomena are due to the complex bubble interactions and their coalescence behavior (Martín et al., 2008a), which limit the designer's ability to control reactor performance (Dhaouadi et al., 2008; Roy and Joshi, 2008; Vial et al., 2001). The result is that bubble column behavior is fairly unknown, especially if reactor geometries, liquid properties, or operating ranges are varied in parallel (Godbole and Shah, 1986; Vial et al., 2001). Hence, design and scaleup are difficult (Ribeiro, 2008; Vial et al., 2001) and require a tedious and iterative process (Godbole and Shah, 1986). Guidelines have been developed to shorten this method and will be addressed in the relevant sections below. Additional information on bubble columns is provided by Beenackers and Van Swaaij (1993), Deckwer (1992), Godbole and Shah (1986), Han and Al-Dahhan (2007), Kantarci et al. (2005), Lau et al. (2004), and Ribeiro and Lage (2005).

5.2 Flow Regimes

Gas-liquid mass transfer behavior in bubble columns is closely tied to gas holdup through the various flow regimes identified in Figure 5.2. The two principal and industrially useful flow regimes are the homogeneous and heterogeneous flow regimes (Mena et al., 2005). At low gas flow rates, the bubbly or homogeneous flow regime develops (Figure 5.2a). The regime is characterized by small bubbles which are a few millimeters in diameter and uniformly distributed in the radial direction and, therefore, rise uniformly. The bubble diameter in the homogeneous regime tends to be controlled by the sparger design and liquid properties. There is limited bubble-bubble interaction in this regime and bubble coalescence and breakup are negligible. So, if the sparger is capable of producing smaller bubbles, these bubbles tend to stay stable at the smaller diameter.

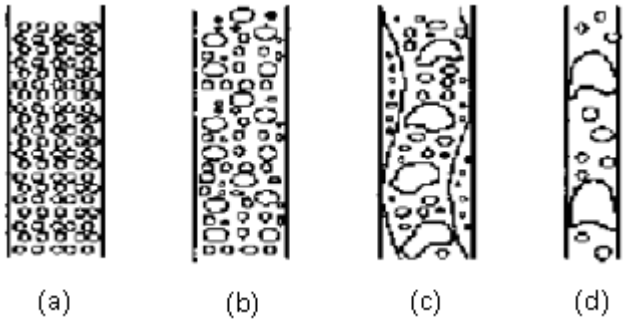

Figure 5.2: (a) Homogeneous, (b) transition, (c) heterogeneous, and (d) slug flow regimes (Kantarci et al., 2005).

As the gas flow rate increases, more bubbles are created without affecting the bubble diameter or distribution significantly. Hence, the interfacial area and gas holdup increase almost linearly (Kantarci et al., 2005). Mixing is minimal, which leads to very fast average bubble rise velocity (20-30 cm/s) and short residence times, even in very tall bubble columns (Deckwer, 1992). Therefore, better performance can be achieved at the subsequent flow regimes, which have much better mixing features; however, a significant amount of research has been directed towards the stability of the homogeneous flow regime because certain biochemical processes require the calm environment experienced in this regime. The size of most industrial units makes it difficult for the

homogeneous flow regime to be used because the amount of gas throughput and mixing is often inadequate (Kantarci et al., 2005). There are additional geometric restraints on the homogeneous flow regime which will be discussed in the geometry section.

As the gas flow rate is increased, the flow evolves into an unstable structure, referred to as the transition regime (Figure 5.2b). The flow regime transition in terms of gas holdup as a function of superficial gas velocity is shown in Figure 5.3. Bubbles collide and distinct bubble classes are formed. The nature of the transition can occur through two different paths. The first is described by line "a" in Figure 5.3. The gas holdup and interfacial area are still increasing within the transition regime up to a local maximum. This effect is mainly due to the balancing act between more gas being present in the reactor and coalescence phenomenon, which lead to larger bubbles and faster bubble rise velocities, leading to a local gas holdup maximum (Kantarci et al., 2005). Another reason for the increase is that the larger bubbles tend to breakup and coalesce frequently, adding to turbulence (Dhaouadi et al., 2008).

After the maximum has been reached, gas holdup and interfacial area decrease as the larger bubbles start to take control of gas holdup behavior (Kantarci et al., 2005). The second path, described by line "b" in Figure 5.3, occurs much faster and is identified by a continuous increase in gas holdup, albeit at a shallower slope, once the flow reaches the heterogeneous flow regime. Line "c" in Figure 5.3 represents a pure heterogeneous flow regime, which may occur with viscous liquids, large orifices, and/or small bubble column diameters (Ruzicka et al., 2003; Ruzicka et al., 2001b).

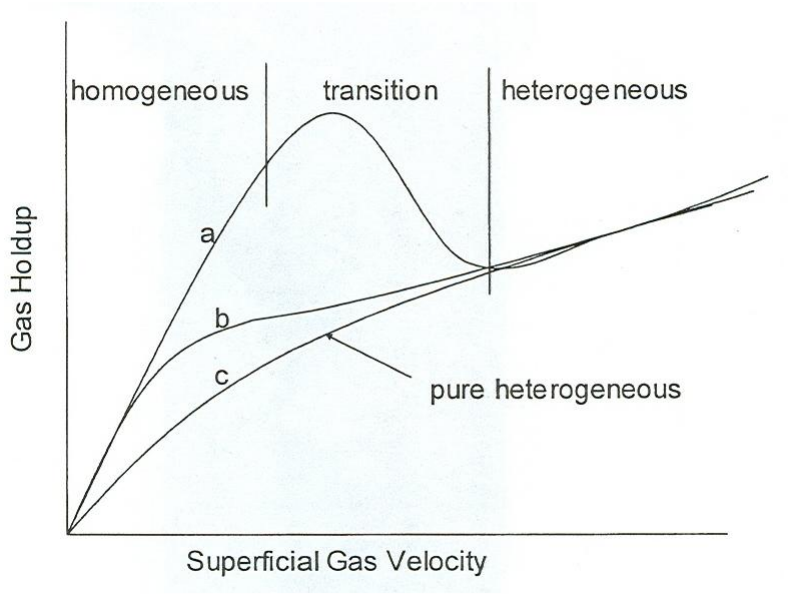

Figure 5.3: Flow regime progression (Su, 2005).

The instability that triggers the flow regime transition is mainly due to the bubble size and shape – smaller bubbles with rigid interfaces stabilize the flow because these bubbles have an inherent aversion to coalescence and breakup (León-Becerril and Liné, 2001). If the colliding bubbles are deformable, the collision is inelastic and will have an easier time forming a liquid channel to drain the liquid film, which separates the two bubbles. If, on the other hand, the colliding bubbles are non-deformable (rigid), the bubbles have a higher probability of simply bouncing off each other or separating quickly (Martín et al., 2008a). Hence, experimental results show that spherical bubbles correlate to a transition from homogeneous flow at about U_G = 5 cm/s while ellipsoidal bubbles have a transition at a lower superficial gas velocity of U_G = 3 cm/s. Therefore, the transition regime is dependent on bubble behavior in the homogeneous regime. If the homogeneous flow regime is more stable, the transition regime will be better defined, shorter, and occur at a higher superficial gas velocity (León-Becerril et al., 2002). In the practical application, the transition superficial gas velocity also tends to deviate with the column dimensions, sparger design, and liquid properties (Kantarci et al., 2005). In general, coalescence starts to occur at U_G = 2 cm/s while the actual transition to heterogeneous flow occurs U_G = 4-5 cm/s (Deckwer, 1992).

Even though the transition regime may offer a maximum for the gas holdup and interfacial area, it is not desired for industrial processes due to its unstable and unpredictable nature. The instability has made the identification of the transition point nearly impossible. Although computational fluid dynamics and other methods are capable of predicting the other flow regimes, these methods are not capable of predicting the transition point or the hydrodynamic behavior near it (Olmos et al., 2003). Hence, even if the operator wanted to work in the transition regime, it would be nearly impossible to achieve consistent results.

The evolution to the next flow regime, the churn-turbulent or heterogeneous flow regime (Figure 5.2c), is signaled by an increase in gas holdup and interfacial area with increasing gas flow rate. This growth is fairly small (less than linear) and tends to trail off. The mean bubble diameter, which tends to be on the order of a few centimeters, is controlled by coalescence and breakup mechanisms in the center section of the bubble column. Even though the gas-liquid mass transfer coefficient is lower in the heterogeneous regime than the homogeneous regime, most industrial units operate in this flow regime (Ruzicka et al., 2001a) because it offers significantly better mixing and acceptable gas holdup and interfacial area values. Furthermore, selectivity and productivity requirements force a large number of industrial operations to be highly turbulent, which is an advantage of the heterogeneous regime (Jakobsen et al., 2005). Phase backmixing is a characteristic of the heterogeneous flow regime and represents a major disadvantage. It causes very complex hydrodynamic behavior, which leads to significant problems for the design and scaleup of bubble columns. The backmixing and recirculation are induced by a differential static pressure between the central and wall region (Zahradnik et al., 1997).

As the flow transitions to the heterogeneous flow regime, two different bubble classes emerge, small and large, and behave differently with a unique influence on gas holdup. In the transition regime, the gas holdup for large bubbles increases much faster than the gas holdup contribution due to the small bubbles. This trend continues until the coalescence rate of smaller bubbles

increases so that the growth in gas holdup and interfacial area caused by large bubbles cannot account for the decrease caused by the shrinking number of small bubbles.

As the heterogeneous flow regime is entered, bubble coalescence and breakup rates stabilize, and the gas holdup due to the large bubble class increases consistently, but at ever decreasing rates while the smaller bubble class gas holdup is relatively constant (Kantarci et al., 2005). This progression can be seen in Figure 5.4; it is due to the very high bubble rise velocity of the large bubble class ($U_R \approx 160$ cm/s at $U_G = 20$ cm/s) while the rise velocity for the small bubble class remains relatively unchanged ($U_R \approx 21$ cm/s at $U_G = 20$ cm/s) (Schumpe and Grund, 1986).

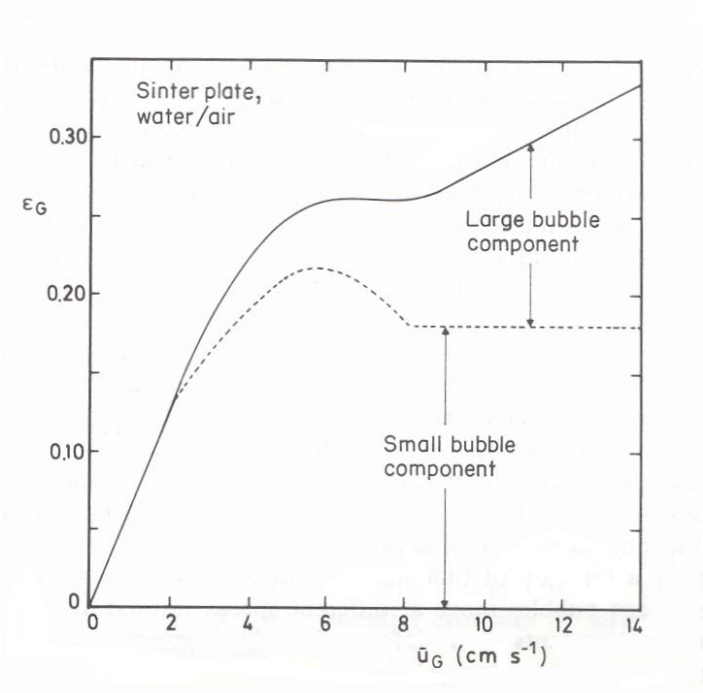

Figure 5.4: Bubble class contributions to gas holdup (Deckwer, 1992).

For small column diameters ($D_R < 0.15$ m), a fourth flow regime is feasible: slug flow (Figure 5.2d). It is characterized by a train of large bubbles, which spans the entire column diameter, dominating the flow. This flow regime is not practical and is not achieved in industrial units. Another flow regime that is not often encountered is the foaming flow regime, which is present under high superficial gas velocities, viscosity, and pressure (Kantarci et al., 2005; van der Schaaf et al., 2007).

Since most industrial processes are performed in the heterogeneous flow regime, studies have been directed towards its macroscopic flow patterns. Tzeng et al. (1993) classified these macroscopic flow structures into four regions using a 2D bubble column: descending flow, vortical flow, fast bubble flow, and central plume. The central region of the bubble column is made up of a central plume through which relatively small bubbles ascend. This central plume is surrounded by a fast bubble flow that is made of larger bubbles. At the edge of this motion, vortices form that trap bubbles and liquid, forming the vortical flow region. These vortices direct bubbles near the column wall to descend (descending flow region). Chen et al. (1994) arrived at similar macroscopic structures using a 3D bubble column. The fast and descending bubble flows, however, flowed in a spiral pattern. In addition, the homogeneous flow regime also displayed a descending flow structure near the wall region. A graphic depiction of the heterogeneous flow regime described by Chen et al. (1994) is presented in Figure 5.5.

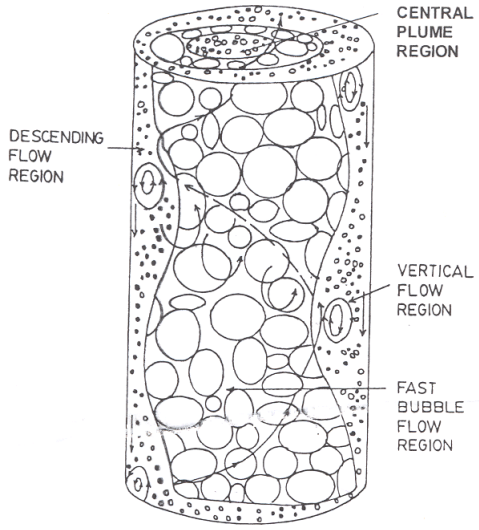

Figure 5.5: Macroscopic flow structure in the heterogeneous flow regime (Chen et al., 1994).

The progression and behavior of these flow regimes is often quite complicated and depends on the superficial gas velocity, liquid properties, column dimensions, operating temperature and pressure, sparger design, and the solid phase properties (if present) (Kantarci et al., 2005). This

dependence is derived from the controlling factors determining the bubble diameter. The influence of each will be addressed in the relevant sections below.

Gas holdup and superficial gas velocity effects on gas-liquid mass transfer are analyzed based on the previously mentioned bubble interactions and flow regime progression. Global gas holdup is assumed to be directly correlated to the gas-liquid mass transfer coefficient because local variations in the interfacial area and gas holdup coincide. Having reviewed the flow regimes, it can be concluded that the transition regime offers a dilemma. Its hydrodynamics are not linear and do not follow general behavior in the homogeneous and heterogeneous flow regimes (Chaumat et al., 2005). Therefore, errors in the gas-liquid mass transfer coefficient are expected to be greater around the transition region, and better approximations are expected for correlations that take into account the regime identification.

The flow regime identification is often assumed to be based on the superficial gas velocity (all else being equal). If a correlation is based on a certain design with a specific process in mind, adjustments could be incorporated into operation while assuming that the results will be close to the predicted values. At the same time, most correlations neglect any changes in the liquid-phase mass transfer coefficient. If operation is expected to include rheological changes, which may have a significant effect on the liquid-phase film resistance, the correlation could fail. It would produce additional variations in the gas-liquid mass transfer correlation that could not be accounted for by variations in the interfacial area and its codependent variations in gas holdup. Therefore, a proper gas-liquid mass transfer study should attempt to separate the approximation of the liquid-phase mass transfer coefficient and the interfacial area under such circumstances.

5.3 Column Geometry

5.3.1 Column Diameter

The gas-liquid mass transfer coefficient and gas holdup tend to decrease with increasing bubble column diameter in the homogeneous and transition flow regime (Zahradnik et al., 1997) up to a critical value (Deckwer, 1992; Shah et al., 1982; Zahradnik et al., 1997), which is usually cited to be D_R = 0.15 m (Kantarci et al., 2005); however, gas holdup has been influenced by column diameters greater than 0.15 m in the homogeneous and heterogeneous flow regimes (Ruzicka et al., 2001a; Vandu and Krishna, 2004), and the critical diameter is more accurately described to lie in the range of 0.1-0.2 m (Zahradnik et al., 1997).

The diameter dependence is created by several factors such as wall effects (Lau et al., 2004), which are negligible for water-filled columns larger than 0.10 m (Kantarci et al., 2005; Lau et al., 2004), and the flow and mixing conditions (Krishna et al., 2001; Zehner, 1989). The wall effect on gas holdup is summarized in Figure 5.6. Figure 5.6A and 5.6C represent radial gas holdup profiles in small bubble columns ($D_R \leq$ 0.060 m) while Figure 5.6B and 5.6D represent more realistic effects in larger bubble columns. Hence, smaller bubble columns distort gas holdup behavior and may also misrepresent bubble diameter measurements (if done visually). Column diameter also has a strong influence on flow stability, defined by a critical gas holdup and gas flow rate at which the onset of the transition flow regime occurs. A larger diameter causes instability and earlier transition while a smaller diameter would induce the opposite behavior (Ruzicka et al., 2001a).

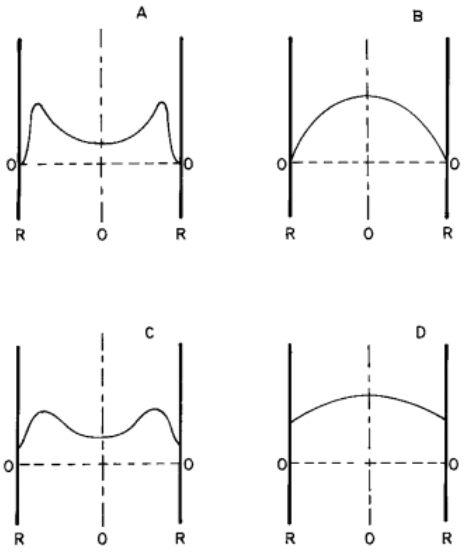

Figure 5.6: Radial gas holdup profiles for small (A and C) and large (B and D) bubble column diameters (Veera and Joshi, 1999).

Although the slug flow regime is defined by low gas holdup and is observed in small bubble columns, small bubble columns do not necessarily have low gas holdup. The smaller bubble column diameter may limit the bubble size distribution, which can lead to smaller bubbles, increase stability, and sustain a higher gas holdup. Once the column diameter is larger than 0.10-0.15 m, the bubble size distribution is controlled by the coalescence and breakup mechanisms (Lau et al., 2004). This effect has been confirmed by Bouaifi et al. (2001) who investigated different gas distributors and column sizes; their results are shown in Figure 5.7.

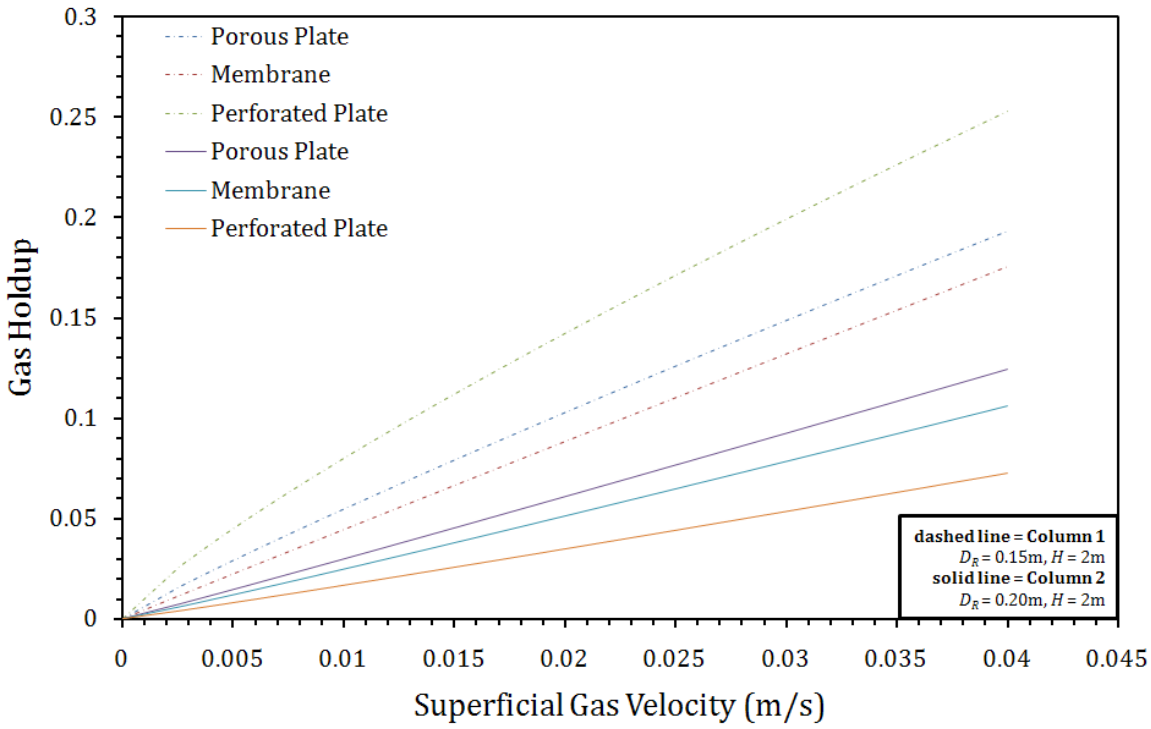

Figure 5.7: Gas holdup dependence on column diameter and gas distributor (adopted from Bouaifi et al. (2001)).

It is often observed that the smaller bubble class is not affected by bubble column diameter while the larger one is (Kantarci et al., 2005; Li and Prakash, 2000). Larger bubble columns experience a larger degree of recirculation, which may lead to a higher degree of coalescence, higher bubble rise velocities, and lower gas holdup values (Krishna et al., 2001; Zehner, 1989). It is also feasible to observe lower gas holdup values in a smaller bubble column if it is operated in the slug flow regime, which is dominated by very large and fast rising bubbles. Larger columns cannot maintain this mode of operation so that a direct comparison at a higher gas flow rate may lead to the conclusion that larger columns have larger gas holdup values (Daly et al., 1992). This effect can be seen in Figure 5.8 where the bubble column with the largest diameter shows the best gas holdup performance. A fairer comparison would be made on a gas flow rate per unaerated liquid volume basis.

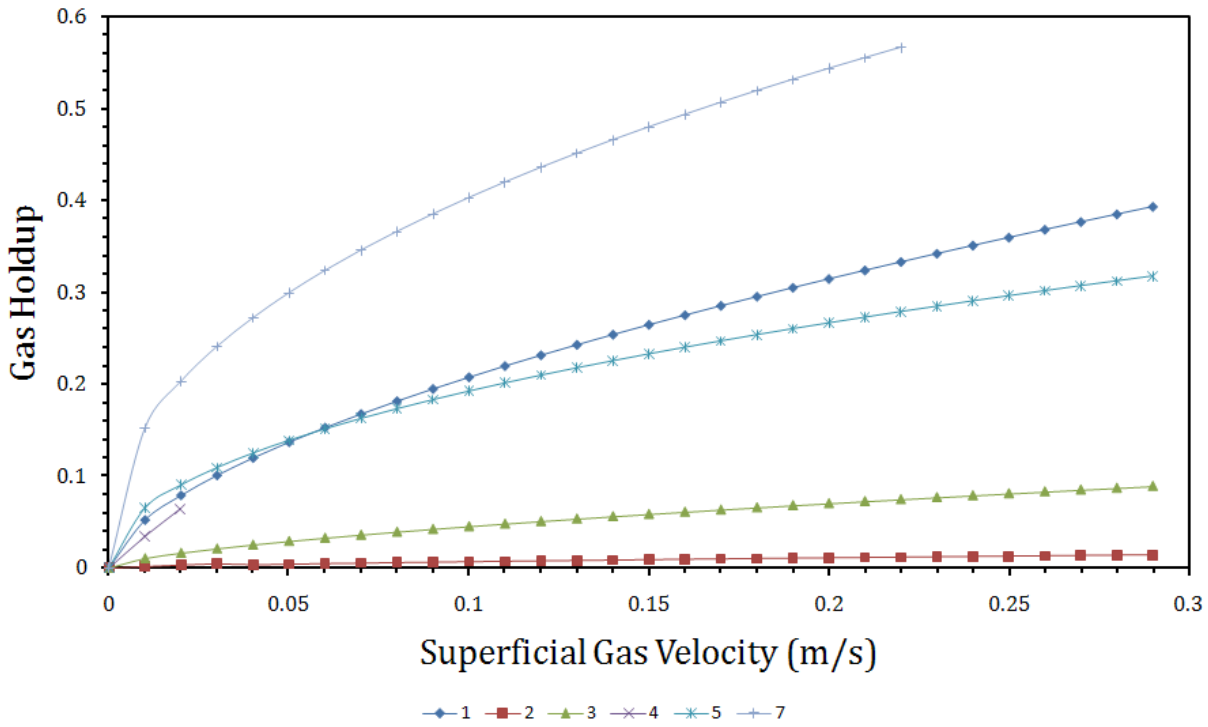

Figure 5.8: Gas holdup correlation sample using tap water at 15°C as liquid phase: (1) Anabtawi et al. (2003) (H = 0.60, D_R = 0.074 m), (2) Deckwer (1992) (D_R = 0.14 m), (3) Godbole et al. (1982), (4) Hammer (1984), (5) Hikita and Kikukawa (1974) (D_R = 0.10 m), (6) Hughmark (1967) (D_R = 0.0254-0.10 m), and (7) Reilley et al. (1986) (D_R = 0.30 m).

Research work by Krishna et al. (2001) and Zehner (1989) concluded that most studies did not account for the flow regime dependence. For example, the heterogeneous flow regime, for which significant column geometry research exists, has a positive effect due to the higher degree of liquid recirculation. The homogeneous flow regime, on the other hand, has limited liquid recirculation by design. Instead, the larger bubble column diameter leads to faster bubble rise velocities, especially in the central region, which leads to lower gas holdup and gas-liquid mass transfer. Unfortunately, a significant number of gas holdup and gas-liquid mass transfer studies fail to identify the flow regime in which the bubble column is operating, which makes meaningful comparisons often difficult.

The effect of column diameter on bubble size and flow regime has led to the introduction of flow regime maps, such as the one presented in Figure 5.9. These maps plot the regimes depending on the superficial gas velocity and bubble column diameter and attempt to predict the gas holdup;

however, the maps are only examples and cannot be applied universally. Flow regimes and bubble behavior are also influenced by the gas distributor design and physiochemical properties of the liquid phase. Changes in these factors bring about significant variations, which are not accounted for by flow regime maps. Nonetheless, these maps may be used as operating instructions for a reactor design that has been extensively studied.

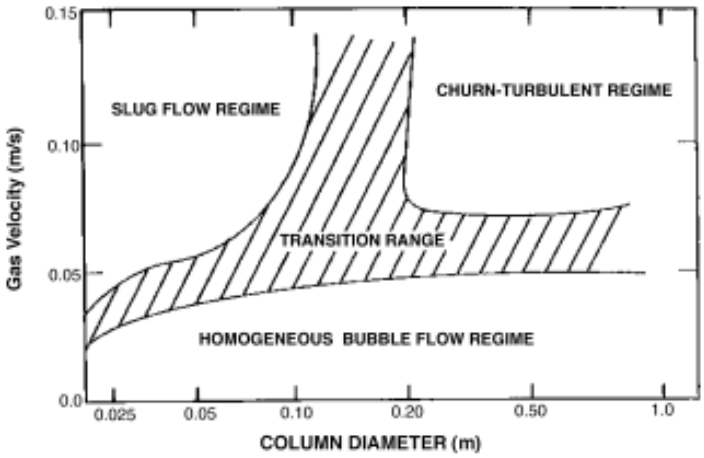

Figure 5.9: Flow regime dependence on column diameter (Kantarci et al., 2005).

5.3.2 Unaerated Liquid Height

The bubble column height, defined by the static liquid level, regulates the residence time over which the bubbles are allowed to go through the coalescence and breakup process. In other words, the column height may allow enough time for equilibrium to be reached. Hence, shorter columns often experience smaller bubble size distributions and higher gas holdup values (Kantarci et al., 2005; Wilkinson, 1991; Zahradnik et al., 1997). A height greater than 1-3 m or an aspect ratio greater than 5 usually ensures that equilibrium has been established. Even though the gas holdup behavior indicates that operation with shorter bubble columns is more effective (Kantarci et al., 2005), the practical application is limited. The residence time is simply too short and would require extensive gas recycle and a very large column footprint for meaningful bubble column volumes; however, the idea can be advantageous and has been applied to microreactors, which will be reviewed at a later time.

The column height may lead to bubble behavior stratification. For example, the top of the bubble column may experience high gas holdup due to foaming. The volume surrounding the sparger behaves differently depending on the gas distributor design. If the gas distributor is capable of producing smaller bubbles, the gas holdup is higher; however, this effect is limited only to the immediate area. The reactor bulk (middle section) usually behaves according to coalescence and breakup principles and the prevailing flow regime. Hence, the bulk region would be expected to have smaller gas holdup values (Ruzicka et al., 2001a). If the column is tall enough, such as a height greater than 1-3 m or an aspect ratio greater than 5, the sparger and foaming effects on gas holdup become negligible and the bulk region dominates reactor hydrodynamics (Veera and Joshi, 1999; Wilkinson et al., 1992; Zahradnik et al., 1997); however, foaming should still be avoided since it may damage any microorganisms.

5.3.3 Aspect Ratio

Bubble columns are assumed to decrease gas holdup with increased size, but an aspect ratio above 5 does not seem to affect hydrodynamics significantly and is usually ignored. Comparisons based on aspect ratio have failed in the past due to large gas holdup data scatter. A good fit could not be obtained such that scaleup rules still need to be based on column diameter and height individually (Ruzicka et al., 2001a). Aspect ratios below 5 are rarely used in industry and are often ignored in experimental settings.

5.4 Other Operating Conditions

5.4.1 Pressure

Pressure affects bubble dynamics and, therefore, has an important influence on gas holdup and gas-liquid mass transfer. It should be noted that correlations often fail to account for pressure and provide poor predictions if pressure variances are encountered, as is often the case in industrial applications (Dhaouadi et al., 2008). Generally, increased pressure is seen as decreasing the bubble surface tension and increasing bubble inertia (Kantarci et al., 2005; Luo et al., 1999) and gas solubility (Dhaouadi et al., 2008). These factors decrease the average bubble diameter, which allows for higher interfacial area and gas holdup values (Kojima et al., 1997). Thus, the higher interfacial area leads to higher gas-liquid mass transfer coefficients (Lau et al., 2004). In addition, as the bubble diameter decreases with increasing pressure, the bubble rise velocity also decreases, leading to an increased gas residence time and a more efficient gas-liquid mass transfer performance.

The effect on the liquid-phase mass transfer coefficient is most likely neutral to positive. Past experience has been that the liquid-phase mass transfer coefficient is only dependent on the phase data (Gestrich et al., 1978), but current research efforts have presented contradictory evidence (Han and Al-Dahhan, 2007), likely due to the previously discussed k_L calculation method in Chapter 3. It is probable that the effect on k_L is negligible at lower pressures due to the much more important changes in the bubble diameter; however, the solubility dependence on pressure could be significant, especially at higher pressure (Kojima et al., 1997).

The extent of the effect often depends on the pressure increase, liquid properties, and gas flow rates. It is often cited that pressures below 1 MPa have a negligible impact on bubble size and gas holdup; however, the references usually point to older articles which used stirred tank reactors and have significantly different power characteristics than bubble columns (Stegeman et al., 1995). More recent work, on the other hand, suggests that pressure, even below 1 MPa, has a significant

impact on gas holdup and the interfacial area. Furthermore, pressurization has been determined to have a more significant impact in viscous liquids and slurries, and when operating in the heterogeneous flow regime (Lau et al., 2004).

As the liquid becomes more viscous, bubbles have a tendency to coalesce more readily. The increased pressure serves as a detriment to coalescence and decreases the average bubble diameter. Hence, systems with a slurry phase benefit from pressurization (Luo et al., 1999). Bubble characteristics in the heterogeneous flow regime are defined by bubble breakup and coalescence frequencies. Once again, higher pressure tends to suppress coalescence and decrease the average bubble diameter. For example, Lau et al. (2004) varied pressure and gas flow rate in their study and found that increasing the pressure from 0.1 to 2.86 MPa led to a 130% increase in k_La at a gas flow rate of 10 cm/s. When the same pressure increase was implemented at a gas flow rate of 20 cm/s, an increase of 187% was observed. These results can be seen in Figure 5.10. It should be noted that the gas holdup failed to predict gas-liquid mass transfer increase as pressure increased. This effect can be clearly seen when a comparison is made between Figure 5.10 and Figure 5.11, which related gas holdup to pressure.

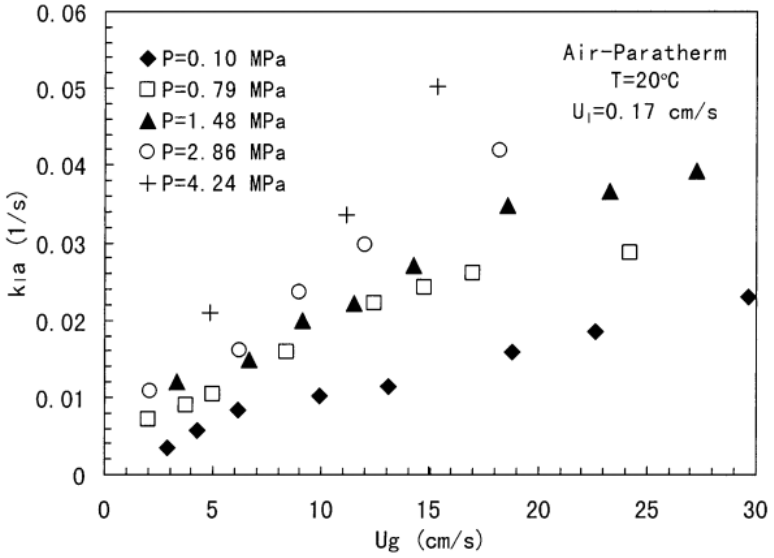

Figure 5.10: Pressure effects on gas-liquid mass transfer in a 10.16 cm bubble column with a single nozzle gas distributor (Lau et al., 2004).

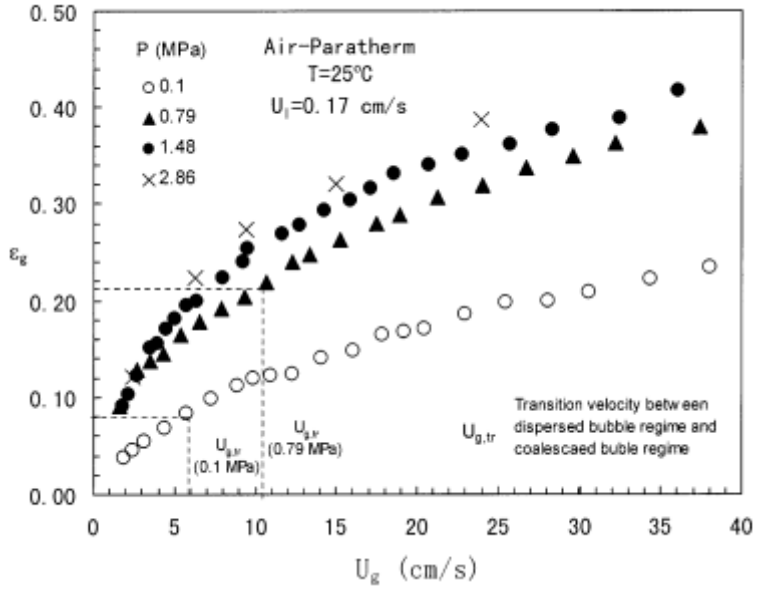

Figure 5.11: Pressure effects on gas holdup in a 10.16 cm bubble column with a single nozzle gas distributor (Lau et al., 2004).

The gas holdup data of Lau et al. (2004) are basically parallel while the gas-liquid mass transfer data have different slopes. Furthermore, the gas holdup increase of 1.48 MPa versus 2.86 MPa is modest (~10%) while the gas-liquid mass transfer is a more impressive, especially at higher gas flow rates. This would lead one to conclude that interfacial area increased significantly from 0.1 MPa to 1.48 MPa while the liquid-phase mass transfer coefficient seems to become important in the increase from 1.48 MPa to 2.86 MPa. More data points for gas-liquid mass transfer would give a larger resolution and more confidence in this conclusion.

Even more surprising was the increase in k_La with liquid velocity at high pressures observed by Lau et al. (2004). Usually, the superficial liquid velocity is ignored and is cited as having an insignificant or negative effect on gas-liquid mass transfer because a higher superficial liquid velocity is thought to decrease the gas residence time and, therefore, k_La (Chaumat et al., 2005). At a pressure of 2.86 MPa, Lau et al. (2004) observed a k_La increase by 30% when the superficial liquid velocity was increased from U_L = 0.17 to 0.26 cm/s.

5.4.2 Temperature

Temperature is a much more contentious issue. It is thought that higher temperatures reduce the liquid viscosity and bubble surface tension, which lead to a higher stability of small bubbles and higher interfacial area. In addition, the liquid-phase mass transfer (k_L) is thought to increase with an increase in temperature due to the lower viscosity according to Calderbank's slip velocity model. At the same time, k_L is thought to decrease due to lower surface tension and turbulence. Therefore, the liquid-phase mass transfer coefficient could go in either direction according to a balancing act of the two forces as temperature is increased.

Lau et al. (2004) also varied temperature with the gas flow rate and concluded that higher temperatures lead to higher gas-liquid mass transfer coefficients at constant gas flow rates. For example, an increase in temperature from 25 to 92°C at a superficial gas velocity of 20 cm/s led to an increase in the gas-liquid mass transfer coefficient of 470% while gas holdup increased by only 25%. Although this temperature increase is huge, Lau et al. (2004) noticed a significant increase in the gas-liquid mass transfer coefficient with even a few degree Celsius change in temperature. At the same time, gas holdup did not show any significant variation.

A secondary effect of higher temperatures would be that the rate of reaction is often directly correlated to temperature and (partial) pressure. An industrial process may benefit further with a higher rate of reaction in the bulk as well as at the interface. The reaction, which may occur at the interface, is often ignored during experimental measurements and correlation formulations as these are not significant in pure liquids without the presence of bacteria; however, industrial processes may experience a significant degree of interfacial reaction. Therefore, industrial processes would be expected to perform better than experiments might suggest due to the application of higher temperatures and pressures. At the same time, the microorganisms may limit the extent of the operating range.

Hence, the conclusion is made that higher temperature (most likely) and pressure lead to an increase in the liquid-phase mass transfer coefficient and gas-liquid mass transfer coefficient. The more troublesome aspect for most gas-liquid mass transfer correlations is that gas holdup is decoupled from gas-liquid mass transfer. This review has not encountered any correlations that includes these operating conditions directly. Instead, most correlations attempt to quantify this effect with changes in liquid properties, which are much harder to measure in industrial settings.

5.5 Liquid Properties

Liquid properties influence the behavior of the bubble interface and, consequently, have a strong effect on both the liquid-phase mass transfer coefficient and the interfacial area. It should be noted that research using organic liquids, which would be very useful for bioreactor and gas-liquid mass transfer optimization, are scarce due to measurement difficulties (Jordan et al., 2002). Interestingly enough, liquids behave similarly regardless if they are pure or mixed. The only important factor seems to be that the liquids have similar properties such as viscosity and surface tension (Ozturk et al., 1987). Hence, researchers have mixed a variety of constituents with tap water to simulate a wide array of mixtures including organic liquids.

The mixing has contributed to the wide array of gas holdup and gas-liquid mass transfer results. Even with all the care, obtaining quality data is extremely challenging. For example, salt water is often simulated using a sodium chloride additive (NaCl); however, salt water includes a wide array of salts, and the exact constituencies depend on the salt water source. As a result, real salt water actually has higher coalescence-inhibiting abilities than an equivalent NaCl mixture. In other words, the real mixture could have synergies between the different constituents, which are traditionally not addressed (Merchuk et al., 1998).

5.5.1 Viscosity

The liquid viscosity determines the degree to which the bubbles are deformable. As the viscosity increases, the bubbles become more deformable, coalescence occurs much easier and faster (Martín et al., 2008a), and breakup is suppressed (Zahradnik et al., 1997). Deformable bubbles allow for the bubble interface to drain much easier and allow coalescence to occur in a shorter amount of time. Bubble breakup is suppressed because the higher viscosity tends to have a negative effect on turbulence. A second negative effect is that the larger bubbles have a higher rise velocity and lead to a shorter residence time for the gas phase (Zahradnik et al., 1997). Hence, higher viscosity liquids are observed to have larger bubbles and smaller gas holdups and interfacial areas (Li and Prakash, 1997; Zahradnik et al., 1997).

The preference of larger bubbles with viscosity often favors the heterogeneous flow regime and may even suppress the homogeneous and transition flow regime above a critical viscosity ($\mu_L \approx 8$ mPa s) (Ruzicka et al., 2003; Ruzicka et al., 2001b). Zahradnik et al. (1997) studied the influence of viscosity by increasing the sugar concentration in an aqueous saccharose solution. The results are summarized in Figure 5.12. As the sugar concentration increased, the mixture's viscosity increased as well. They found that distilled water, which has a viscosity of about 1 mPa s at room temperature, showed the familiar flow regime pattern in a gas holdup versus superficial gas velocity graph as shown by line "a" in Figure 5.3. A similar pattern was observed with a 30% sugar mixture which had a viscosity of 3 mPa s; however, a 43% mixture (viscosity of 8.2 mPa s) failed to produce the homogeneous flow regime. These results may have a significant negative impact on processes which rely on the presence of the homogeneous flow regime and high viscosity liquids.

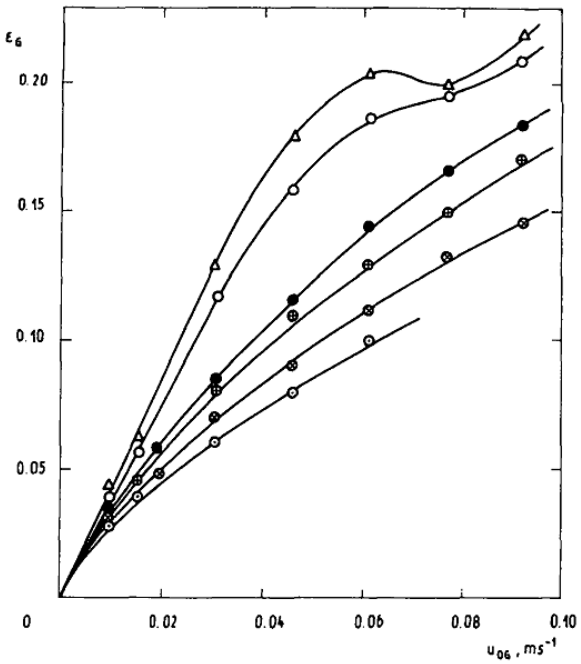

plate parameters: $\varphi = 0.2\%$, $d_0 = 0.5$ mm (△) distilled water; aqueous saccharose solutions: (○) $c = 30$ wt. %, $\mu_L = 3$ mPa s; (●) $c = 43$ wt. %, $\mu_L = 8.2$ mPa s; (⊕) $c = 52$ wt %, $\mu_L = 19$ mPa s; (⊗) $c = 55$ wt %, $\mu_L = 30$ mPa s; (⊙) $c = 64.5$ wt. %, $\mu_L = 110$ mPa s.

Figure 5.12: Viscosity effect on the stability of the homogeneous flow regime (D=0.15m; H/D=3.5) (Zahradnik et al., 1997).

Viscosity also affects the liquid-phase mass transfer coefficient through the Stokes-Einstein effect. Einstein proposed that the diffusion coefficient could be expressed as

$$D_L = \frac{RT}{N_A} \frac{1}{6\pi\mu_L r_U} \tag{5.1}$$

where R, T, N_A, μ_L, and r_U are the gas constant, temperature, Avogadro number, viscosity, and radius of the gas particle, respectively (Sharma and Yashonath, 2006). Hence, a higher viscosity could significantly reduce the diffusivity, which in turn would decrease the liquid-phase mass transfer coefficient (Chaumat et al., 2005; Lau et al., 2004; Sharma and Yashonath, 2006; Waghmare et al., 2008); however, the decrease in the interfacial area is expected to dominate the decrease in the liquid-phase mass transfer coefficient.

Ruzicka et al. (2003) observed, in opposition to most published work, an increase in gas holdup and stabilization of the homogeneous flow regime at a very low viscosity, μ_L = 1-3 mPa s. This may

be attributed to an increased in bubble layer stability due to the low viscosity (Ruzicka and Thomas, 2003), which does not show major negative effects described previously.

5.5.2 Surface Tension and Additives

Surface tension is a liquid property that tends to counter bubble deformation and encourages bubble breakup (Akita and Yoshida, 1974; Mehrnia et al., 2005; Walter and Blanch, 1986). The result is a more stable bubble interface which leads to smaller bubble diameters, a more stable flow regime (Lau et al., 2004; Schäfer et al., 2002), and higher gas holdups and interfacial areas (Kluytmans et al., 2001). It is also thought that a lower surface tension leads to a higher contact time because the liquid flow over the bubble surface is slowed (Lau et al., 2004).

Surface tension is influenced by the presence of surfactants (Kantarci et al., 2005), which act in the same fashion as described in Section 4.6. Surfactants attach themselves to the bubble interface and form a hydrophilic boundary at the bubble surface. The result is a much smaller bubble size, which offers a more rigid surface. This surface, in turn, lowers the bubble surface tension and further reduces the bubble rise velocity.

Surfactants may offer several advantages. First, the homogeneous and transitional flow regimes benefit from the additional stability (Zahradnik et al., 1997) while the heterogeneous flow regime benefits from much smaller bubbles (Krishna et al., 2000). Second, the negative effects due to viscosity can be reversed with the use of surfactants (Zahradnik et al., 1999a; Zahradnik et al., 1999b). Lastly, industrial processes often produce surfactants (such as certain proteins or alcohols) naturally (Kantarci et al., 2005). It should be noted that, just like stirred tank reactors, bubble columns experience diminishing returns with increasing surfactant concentration (Krishna et al., 2000) and a reduction in the liquid-phase mass transfer coefficient (due to barrier effects) (Álvarez et al., 2008).

Electrolytes have been shown to increase gas holdup and decrease the bubble diameter (Kantarci et al., 2005) even at high concentrations where they usually have a higher surface tension

than pure water (Levin and Flores-Mena, 2001). At relatively low concentrations, electrolytes decrease surface tension and reduce the film drainage speed, leading to higher gas holdup (Kluytmans et al., 2001). Anti-foam agents, on the other hand, caused a decrease in gas holdup due to higher surface tension and bubble diameters (Veera et al., 2004). Other impurities, especially of organic origin, tend to increase gas holdup and create immobile bubble interfaces; however, most research is conducted using inorganic mixtures or pure liquids (Chaumat et al., 2005).

Alcohols create smaller bubbles and higher gas holdups because they are either amphiphilic or have a lower surface tension so that the aqueous mixture supports smaller bubbles. This behavior has been observed for a large number of alcohols in an aqueous saccharose solution. The only exception proved to be methanol. The theory, which was successfully tested experimentally by Zahradnik et al. (1999b), is that the longer carbon chains increase the effectiveness (of alcohols as coalescence suppressants) and cause methanol, the simplest alcohol, to lose its usefulness at a much lower concentration relative to the other alcohols (Zahradnik et al., 1999a; Zahradnik et al., 1999b).

5.6 Gas Properties

Gas properties are often not considered and effect on gas holdup and gas-liquid mass transfer have not been extensively investigated. It is perceived that the gas identity is immaterial or does not have a significant impact within a process and operating range since the gas phase mass transfer resistance is almost always negligible relative to the liquid phase mass transfer resistance (Hughmark, 1967). The research that provided and verified these conclusions, such as work by Ozturk et al. (1987), was often conducted using low densities and superficial gas velocities; however, Jordan et al. (2002) have shown that higher pressures and superficial gas velocities result in a much stronger effect. For example, Ozturk et al. (1987) found a low power of the gas density of 0.04 while Jordan et al. (2002) calculated a much higher value of 0.24.

The explanation for the different results can be attributed to Kelvin-Helmholtz instabilities of larger bubbles. The theory stipulates that the mean slip velocity (relative velocity of the gas and liquid phases) at the interface leads to wave formation. Once these waves become too large, the bubble breaks. This critical wave length has a nonlinear dependence on gas density. Hence, lower gas densities do not lead to the formation of this critical wave length, and researchers, such as Ozturk et al. (1987), did not find a relationship. In addition, the mean slip velocity is highly correlated to the superficial gas velocity such that high superficial gas velocities also aggravate the interfacial waves. In other words, the Kelvin-Helmholtz instability is rarely observed at relatively low gas densities and superficial gas velocities (Jordan and Schumpe, 2001; Jordan et al., 2002).

5.7 Solid/Slurry Phase Properties

The mixture present in the gas-liquid-solid bubble column is referred to as slurry. Hence, the gas-liquid-solid bubble column is often called a slurry bubble column (SBC) or slurry column. In the special scenario in which the liquid phase is not present, the gas-solid bubble column can also be referred to as a fluidized bed reactor because the solid phase is usually well dispersed and acts as a fluid.

The slurry bubble column is generally modeled and thought of as a bubble column with a higher liquid phase apparent viscosity (Krishna et al., 2000). It is also thought that solids decrease gas holdup and gas-liquid mass transfer, especially in the heterogeneous flow regime, due to a decrease in turbulence. Gas-liquid mass transfer correlations for gas-liquid bubble columns may be applied to gas-liquid-solid bubble columns if the density difference between the solid and liquid phase is small or if the liquid viscosity is high; however, such action does not account for any solid phase effects on the bubble interface, possible surface reaction, and often provide highly variable results. It should be noted that microorganisms are technically very small solid phase particles, but are almost always neglected and assumed to form a pseudo-homogeneous mixture with the liquid phase. It is also common for microorganisms to have non-Newtonian properties at higher

concentrations, which is usually not addressed in bubble column discussions and correlations and yet represents an important feature of bioreactor behavior (Beenackers and Van Swaaij, 1993).

The effect and understanding of solid loading on gas-liquid interactions is currently ambiguous, contradictory, or inadequate and requires further research. The main reason is that recent work has shown an important correlation between the dominant flow regime and solid loading while most research does not identify the flow regime under which the experiment was operated (Mena et al., 2005). In the case of low solids loading (less than 5% by volume), a SBC indeed acts like a BC. As the solids loading increases, the behavior of the SBC starts to deviate from that of the BC. For solids loading up to 25% by volume, the gas holdup decreases significantly. Beyond this concentration, gas holdup increases slightly as small bubbles start to accumulate because of the decrease the bubble rise velocity (Kantarci et al., 2005). Three-phase bubble columns could see an improvement in fluidization characteristics through the introduction of a screw-like promoter element (Ramesh et al., 2009).

The particle type and size can have a positive effect as it does with the stirred tank reactor. If the particle is wettable, a repelling force is observed against the gas phase, which creates a buffer zone between gas bubbles (Kluytmans et al., 2001), slows film drainage, and suppresses bubble coalescence (Mena et al., 2005). Hence, wettable particles usually increase gas holdup while non-wettable particle decrease it.

Particles are thought to be too big to contribute to gas-liquid mass transfer in a positive way and simply increase the apparent viscosity; however, fine particles with a particle diameter less than 10 μm are able to penetrate the bubble surface (creating smaller bubbles), increase film density (suppresses bubble coalescence and decreases bubble rise velocity) (Kluytmans et al., 2001; Mena et al., 2005; Sada et al., 1986), or create reactions at the bubble interface. Another possibility is that the smaller particles stick to the bubble interface, which would block or diminish surface reactions (Langmuir-Hinshelwood mechanism) or physically get in the way of particle

diffusion. At the same time, the nested particles could increase the active area or destabilize the bubble interface. Very large particles are thought to decrease the bubble rise velocity and increase gas holdup by simply being in the way (Beenackers and Van Swaaij, 1993).

The exact particle size at which these events would occur is system dependent and may be defined using the Reynolds number based on the particle diameter. Particles which cause $Re < 2$ are defined as small while medium and large particles are associated with $Re = 2\text{-}300$ and $Re > 500$, respectively (Mena et al., 2005). Beenackers and Van Swaaij (1993) defined particles more specifically. Particles with $d_P < 100$ μm and a concentration by volume $c_s < 0.6$ % cover the bubble surface, which stabilizes the bubble interface and leads to smaller bubbles. This effect, in turn, leads to an increase in the interfacial area by more than a factor of 2. Particles with $d_P = 100\text{-}1000$ μm (the range has been tightened more recently by Luo et al. (1999) to $d_P = 44\text{-}254$ μm) or $d_P < 100$ μm and $c_s > 0.6$ % may have an inconclusive effect on hydrodynamics, which supports the idea that a qualitative decision rule is also needed. Beenackers and Van Swaaij (1993), unlike Mena et al. (2005), did not find convincing data and information, especially for particle densities similar to the liquid phase, to justify any prediction on the effects of $d_P > 1000$ μm. Since Mena et al. (2005) work is more recent, it would give their conclusions more credence.

Kluytmans et al. (2001) investigated the effect of carbon particles with a mean particle diameter of 30 μm. They found a critical carbon particle concentration, which was determined to lie between 0.2 to 0.5 g/L, above which gas holdup did not increase. In addition, the bubbles, which were created using a carbon concentration of 0.5 g/L, were larger than the bubbles using a 0.2 M electrolyte solution. Kluytmans et al. (2001) also investigated the effects of adding carbon particles to an electrolyte solution. The homogeneous flow regime did not benefit as the gas holdup was comparable to bubble columns with only carbon particles or electrolytes. The heterogeneous flow regime, on the other hand, benefited greatly with an increase of about 50% and 100% in gas holdup

relative to a 0.1 M electrolyte solution and 1.0 g/L carbon particle concentration, respectively. It was unclear if the addition of carbon particles and/or electrolytes affected the transition point.

Low solids loading ($c_s \leq 3\%$) tends to stabilize the homogeneous flow regime, increasing the critical flow rate and gas holdup 11-13%, while higher loading ($c_s > 3\%$) leads to instability. At much higher solids loading ($c_s > 20\%$), the solid phase decreases gas-liquid mass transfer by simply occupying too much volume. In effect, bubble-bubble interactions are increased and coalescence is encouraged (Mena et al., 2005). This may be of importance if the process requires operation in a specific flow regime. The current problem with gas-liquid-solid systems is that these effects work in parallel. The nature of the relationship is not well-understood such that solids may increase, decrease, or have a neutral effect on gas holdup and gas-liquid mass transfer, which has led to the wide array of discussion, conclusions, and results.

Fiber slurries offer a special type of solid phase used in bubble columns. The fibers, depending on type, are flexible and have a large aspect ratio. These traits make fiber characteristics an important influence on bubble column hydrodynamics (Su and Heindel, 2004). Although gas-liquid-fiber slurries are currently found in the pulp and paper industry in relation to flotation deinking and extensive research has been accomplished in the area (Su, 2005; Su and Heindel, 2004, 2005a, 2005b; Su et al., 2006; Tang and Heindel, 2005a, 2005b, 2006a, 2006b, 2007), their application could expand. The addition of fibers cause drag reduction, lower levels of fouling, and possible gas holdup improvement (Tang and Heindel, 2005a, 2006a). Gas holdup enhancement may occur due to coalescence suppression and longer gas phase residence time; however, gas holdup may also decrease due to enhanced bubble coalescence (bubble trapping) and reduced bubble velocity and interface fluctuations (Tang and Heindel, 2005a). A particular characteristic of fiber suspensions is its flocculation properties. Hence, gas-liquid-fiber slurries could be used as well-characterized model microorganism systems in future gas holdup and gas-liquid mass transfer studies.

5.8 Gas Distributor Design

Gas distributors used in bubble columns include sintered, perforated, or porous plates, membrane or ring-type distributors, arm spargers, and single-orifice nozzles. The sintered plate (Figure 5.13a), which is usually made out of glass or metal, produces very small bubbles; however, the sintered plate is rarely used for industrial applications because they can plug easily and require cocurrent operation; it is preferred for laboratory use. Perforated plates (Figure 5.13b), which are normally made out of rubber or metal, usually have holes 1-5 mm in diameter and are the most common gas distributor for bubble columns. The total aeration open area is usually maintained between 0.5 to 5% of the cross-sectional area of the reactor. Single-orifice nozzles (Figure 5.13c) are simple tubes, which are able to produce uniform flow some distance into the column. The flow, however, tends to be somewhat unstable. Bubble columns may also use ring spargers (Figure 5.13d) that are used with stirred tank reactors. Ring spargers are able to produce uniform and stable flow, but are usually unable to produce smaller bubbles (Deckwer, 1992) and lead to earlier transition to the heterogeneous flow regime than the perforated plate (Schumpe and Grund, 1986).

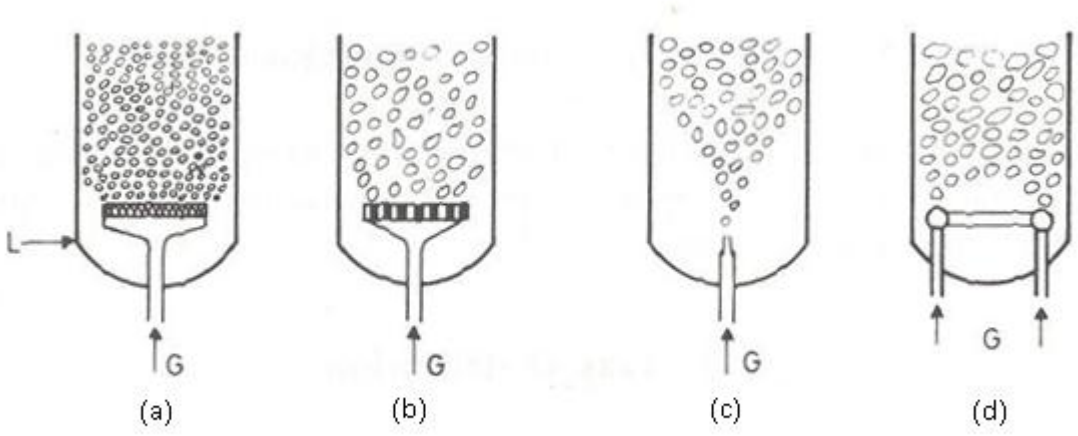

Figure 5.13: (a) sintered plate, (b) perforated plate, (c) orifice nozzle, and (d) ring sparger (Deckwer, 1992).

The effects of gas distributor design and its extent depends on the superficial gas velocity and flow regime in which the bubble column operates. In the case of heterogeneous flow, the sparger

has a negligible influence on the bubble size and gas-liquid mass transfer because the bubble dynamics are determined by the rate of coalescence and breakup, which are controlled by the liquid properties and the nature and frequency of bubble collisions (Chaumat et al., 2005). Hence, the sparger effect is more pronounced for U_G < 0.15 m/s while it is much less important at U_G > 0.20 m/s and nonexistent at U_G > 0.30 m/s (Han and Al-Dahhan, 2007). Viscous liquids are also not affected by the gas distributor design if the column is sufficiently tall (Zahradnik et al., 1997).

Furthermore, the mechanisms that dominate gas holdup (e.g., surface tension, particle wettability, ionic force of surfactant, viscosity, and density) require consideration. If the liquid undergoes viscosity or density changes through, for example, particle addition, the initial bubble diameter does not affect gas holdup in the heterogeneous flow regime. If, on the other hand, the other mechanisms are affected or adjusted, such as the addition of surfactants or electrolytes, the heterogeneous flow regime is affected by the initial bubble diameter up to a relatively high superficial gas velocity (of about 0.5 m/s) and, hence, gas distributor design is important. Once a high enough superficial gas velocity is reached, the probability and frequency of bubble collision increases greatly and a precipitous decrease in gas holdup is observed (Kluytmans et al., 2001).

The homogeneous and transition regimes are highly influenced by the gas distributor design. A sparger, which is able to produce smaller initial bubble diameters, is able to produce a higher number of bubbles at the same flow rate and a more stable homogeneous flow regime (Álvarez et al., 2008). If the sparger is able to produce smaller bubbles in the homogeneous regime, the sparger would also be able to produce higher gas holdups and interfacial areas (Bouaifi et al., 2001). Hence, these spargers are also able to produce higher gas-liquid mass transfer coefficients under the homogeneous flow regime (Verma and Rai, 2003).

The distributor effect can be quite significant such that the gas-liquid mass transfer correlation can vary by up to a factor of 2 (Lau et al., 2004). The extent to which the gas distributor affects gas holdup and bubble dynamics depends on the bubble column geometry and superficial gas velocity.

The taller the column is, the smaller the influence of the initial bubble diameter will be on the global gas holdup. A higher superficial gas velocity increases the probability and frequency of bubble collision and decreases the effect of the initial bubble diameter and gas distributor design.

The assumption made to this point is that the spargers are indeed capable of producing all flow regimes; however, Wilkinson (1991) noted that the discussion was irrelevant if the orifice diameter was larger than 1-2 mm because it would create bubbles that are too large and would be affected by the macroscopic flow pattern alone. In order to create significant influence, the aeration holes have to be smaller than 1 mm. Zahradnik et al. (1997), however, investigated the performance of a perforated plate and concluded that the hole diameter has to be smaller than 0.5 mm for a significant effect. A perforated plate with an orifice diameter of even 0.6 mm only created the heterogeneous flow regime using different liquids.

The open area ratio, defined as the total aeration orifice area divided by the column cross sectional area, was investigated and led to many conflicting conclusions. Different researchers approached the subject from different aspects. One camp has chosen to adjust the number of holes while keeping the orifice diameter constant while the other increases the orifice diameter while keeping the number of holes equal. Both approaches are potentially troublesome. If the open area ratio is increased by increasing the number of holes and keeping the orifice diameter constant, the holes could be spaced too closely such that they act as a single sparger hole. This sparger behavior is caused by immediate coalescence from neighboring bubbles as they are created and prior to their disengagement from the sparger orifice (Martín et al., 2008a; Su and Heindel, 2005a). If the holes are made larger while the number is held constant, the homogeneous flow regime could be skipped entirely (Zahradnik et al., 1997). Regardless, the agreement exists that if the open area ratio decreases, gas holdup increases, but the homogeneous flow regime stability may not necessarily be affected (Su and Heindel, 2005a). Naturally, the open area ratio did not affect gas holdup in the fully developed heterogeneous flow regime (Kantarci et al., 2005; Su and Heindel, 2005a).

Bubble formation and orifice activity are two important factors determining stability. Synchronous bubble formation, where almost all holes are active, tend to produce uniform bubble and gas holdup distribution. This, in turn, leads to a more stable homogeneous flow regime, lower liquid recirculation, and higher gas holdup and gas-liquid mass transfer. Asynchronous orifice operation is often accompanied by alternating or oscillating orifice activity which leads to flow instability. The instability creates more bubble-bubble interaction and leads to lower gas holdup and gas-liquid mass transfer. Hence, the gas distributor affects the critical superficial gas velocity at which the transition regime is detected.

Perforated plates are defined by a critical flow rate above which the orifice operation is asynchronous and the flow is relatively unstable. As the hole spacing is decreased, the critical flow rate would decrease as well. At the same time, perforated plates require a minimum pressure drop in order to achieve uniform orifice activity. In other words, a critical flow rate is also created at the lower end such that a lower flow rate would lead to instability as well (Kang et al., 1999; Ruzicka et al., 2003; Su and Heindel, 2005a). This effect would produce additional complications in making comparative analysis between research works using different open area ratio adjustment methods.

Vial et al. (2001) compared different gas distributor designs and made several interesting observations. The single-orifice nozzle tended to produce highly non-uniform flow while the porous plate and multiple-orifice sparger produced a fairly uniform flow pattern. This led the single-orifice sparger to always operate in the heterogeneous flow regime. Furthermore, the multiple-orifice sparger proved to be the most dependable. It produced the homogeneous flow regime until the superficial gas velocity reached about 4 cm/s. The heterogeneous flow regime would be fully developed at 11-12 cm/s. The porous plate, on the other hand, was sensitive and provided different results depending on the startup procedure.

Kluytmans et al. (2001) compared initial bubble diameters produced by different gas distributors and found that a 30 μm porous plate produced much smaller bubble diameters (0.2-0.5 mm) than the 0.5 mm perforated plate (1-2 mm). The higher gas holdup performance of the porous plate was attributed to the creation of these smaller bubbles.

Bouaifi et al. (2001) used two different columns (Column 1 with D_R = 0.15m; Column 2 with D_R = 0.20m; H = 2m) and found that the porous plate generally produced higher gas holdup, followed by the membrane distributor and perforated plate. They agreed that smaller bubbles would lead to higher gas holdup values, but also concluded that the power consumption can vary significantly. For example, the membrane gas distributor would create very small bubbles with 80% of the bubble population being in the 3.5-4.5 mm range, which compared well with the results of the porous plate and its range of 2.5-4.5 mm. The membrane gas sparger, however, used much more power to obtain similar results. This is usually not a concern in an experimental setting, but may be of concern in (larger) industrial operations. Bouaifi et al. (2001) are the only researchers to account for the power usage of the different gas distributor designs. This is most likely due to the often ignored or relatively minor cost of compressed gas.

5.9 Correlations

Correlations attempt to reflect the reactor environment as closely as possible. This goal is most often achieved through empirical data fitting, similar to the technique for stirred tank reactors. Analytical expressions are rarely used because they are burdensome with regard to the required data (Dhaouadi et al., 2008). A single correlation, based on first principles, does not exist due to the complexities discussed above. For example, Tang and Heindel (2006b) described what is needed to develop a dimensionless correlation for gas holdup in a bubble column based on the Buckingham-Pi Theorem, and they identified 9 dimensionless parameters containing 13 variables representing 3 basic dimensions:

$$\varepsilon_G = f\left\{R_A, \frac{H}{D_R}, \frac{d_0}{D_R}, \frac{\rho_G}{\rho_L}, \frac{\mu_G}{\mu_L}, \frac{U_G}{U_L}, Re_L, Fr, We\right\} \tag{5.2}$$

where R_A, H, D_R, d_0, ρ_G, ρ_L, μ_G, μ_L, Re_L, Fr, and We are the gas distributor open area ratio, bubble column height, bubble column diameter, gas distributor orifice diameter, gas and liquid phase densities, gas and liquid phase viscosities, gas and liquid phase superficial velocities, liquid phase Reynolds number, Froude number, and Weber number, respectively.

Unfortunately for industrial settings, a majority of gas holdup and gas-liquid mass transfer correlations require inputs which are not easily collected for large tanks used in mass production settings. For example, commonly used inputs for gas holdup are the average bubble diameter and superficial gas velocity. Although superficial gas velocity is easily collected, average bubble diameter data are very hard to obtain. Large reactors have a great deal of spatial variation. In addition, industrial tanks are made out of steel and include nontransparent liquids. Visual bubble diameter observations, which are commonly used in experimental settings, would be unlikely to yield proper bubble size approximations. The changing environment would also provide many problems for process automation. Hence, it is rarely used in industrial-sized reactors.

Furthermore, many of the inputs are interdependent, which is a similar problem encountered in stirred tank reactor correlations. One cannot change the superficial gas velocity without impacting the average bubble diameter. This leads to the requirement of either a second data stream or an approximation for the bubble diameter, which could be built into the model to begin with. An approximation for the bubble diameter has not been presented within a gas holdup model. Another example would be that a significant number of correlations include the diffusivity and liquid properties as inputs. If the liquid is expected to change rheologically, which often occurs in industrial settings, measurement or approximation of these inputs would be needed. Once again, this is information that is not easily obtained, even in an experimental setting.

A minor inconvenience is that many review, and a few original articles, do not include proper classification of variables and units, which is particularly troublesome when the correlation is not dimensionless. The inputs are not categorized as being in English or SI units. Moreover, some correlations use standard units, such as Pa-s, while others use nonstandard units, such as mPa-s, without acknowledgement. Many review articles also do not define the reactor or the phases involved. The classification and definition of variables are made more difficult if the correlation is based on a theoretical derivation. These correlations often include terms that are left as constants, and further work is required to define these more accurately for practical applications. Temperature or pressure readings are usually not included as inputs, but are of significant importance for industrial practice.

These problems can be dealt with if the correlation is selected and fit for the process in question. For example, one could easily use a gas holdup correlation such as (Guy et al., 1986)

$$\varepsilon_G = 0.386 N_0 \left(\frac{g D_R^{\,3}}{\nu_L^{\,2}} \right)^{0.025} \left(\frac{U_0}{\sqrt{g d_0}} \right)^{0.84} \left(\frac{d_0}{D_R} \right)^{2.075} \tag{5.3}$$

where ε_G, N_0, g, D_R, ν_L, U_0, and d_0 are gas holdup, a sparger dependent constant, gravitational acceleration, bubble column diameter, liquid viscosity (kinematic), gas velocity in the sparger orifice, and sparger orifice diameter, respectively. A separate gas-liquid mass transfer correlation may then be used, such as (Jordan and Schumpe, 2001)

$$\frac{k_L a d_b^{\,2}}{D_L} = A \left(\frac{\nu_L}{D_L} \right)^{0.5} \left(\frac{g \rho_L d_b^{\,2}}{\sigma} \right)^{0.34} \left(\frac{g d_b^{\,3}}{\nu_L^{\,2}} \right)^{0.27} \left(\frac{U_G}{\sqrt{g d_b}} \right)^{0.72} \left[1 + 13.2 \left(\frac{U_G}{\sqrt{g d_b}} \right)^{0.37} \left(\frac{\rho_G}{\rho_L} \right)^{0.49} \right] \tag{5.4}$$

where $k_L a$, d_b, D_L, A, ν_L, g, ρ_L, ρ_G, σ, and U_G are gas-liquid mass transfer coefficient, average bubble diameter, liquid-phase diffusion coefficient, sparger dependent coefficient, liquid viscosity (kinematic), gravitational acceleration, liquid-phase density, gas-phase density, surface tension, and

superficial gas velocity, respectively. These correlations include almost all required information to define the reactor environment except pressure and temperature.

In contrast, an industrial design has several choices. First and most complicated would be to use the experimental approach, which would be very intensive and costly. Second, a simplified correlation for gas holdup and gas-liquid mass transfer coefficient could be used:

$$\varepsilon_G = C_2 U_G^{\ x} \tag{5.5}$$

$$k_L a = 0.467 U_G^{\ 0.82} \tag{5.6}$$

where ε_G is gas holdup, $k_L a$ is the gas-liquid mass transfer coefficient, U_G is the superficial gas velocity, and C_2 and x are constants. Here, Eqns. (5.5) and (5.6) came from Bouaifi et al. (2001) and Shah et al. (1982), respectively. The constant would include system definitions. This approach would be highly practical and simple, but also non-transferable or limited relative to rheological changes.

Lastly, a cook book approach could be used. As such, a simplified correlation would be used and time-adjusted based on experience and parameter variables like concentrations and temperature/pressure. This approach has a high upfront cost for correlation development, but would not require many data inputs and would have a low variable cost. It would represent a compromise between industrial practicality and scientific reality.

Ultimately, these problems have led to a large degree of variation in results and correlations which can be seen in Table 5.1 for gas holdup, Table 5.2 for the liquid-phase mass transfer coefficient, and Table 5.3 for the volumetric gas-liquid mass transfer correlation. The presented correlations, for example, show a wide degree and range of dependencies and variables. The result, as seen in Figure 5.14, is that some systems have anemic performance while others seem to be superstars of efficiency. Hence, the end user and designer have a great deal of work to ensure logical application of existing data and proper design constraints.

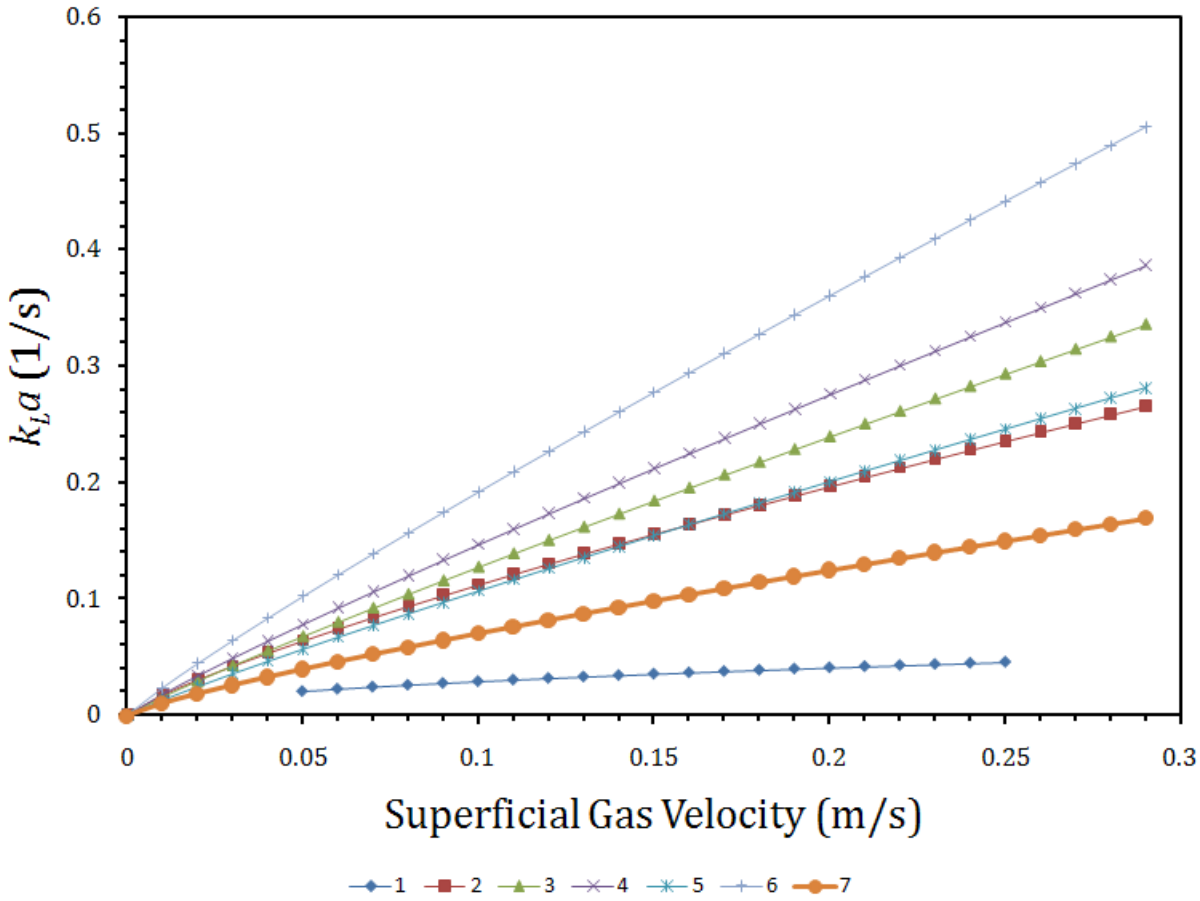

Figure 5.14: Gas-liquid mass transfer by (1) Behkish et al. (2002) (CO-Hexanes mixture without solids, D_R = 0.316 m), (2) Cho and Wakao (1988) (air-aqueous solutions, porous plate; D_R = 0.115 m), (3) Water, (4) Ethanol (96%), (5) 1-Butanol, (6) Toluene from Jordan et al. (2002) (D_R = 0.115 m), and (7) Shah et al. (1982).

5.10 Needed Research

Although a lot of research exists on bubble column gas holdup and gas-liquid mass transfer, little focuses specifically on bioreactors with microorganisms present. Controlled experiments containing actual microorganisms as well as materials able to mimic microorganism behavior, such as fiber suspensions or other liquid additives, need to be incorporated into more comprehensive studies. For example, microorganism flocculation and its effects on hydrodynamics are not commonly studied or simulated, but obviously have serious consequences on bioreactor performance. The goal would be twofold. The first would be to quantify possible surface reactions and other phenomena when microorganisms are present in the reactor environment. The second

goal would be to quantify the quality of currently used substitutes to simulate microorganisms and attempt to identify newer organic possibilities. In connection to these goals, more study is needed on the effect of higher temperature, pressure, and viscosity on microorganisms as well as bioreactor hydrodynamics.

A major study should be attempted to compare the different bioreactor performance characteristics. Comparisons between bubble columns and airlift reactors are available, but a wider array is lacking, but needed. Research towards this end, such as Bouaifi et al. (2001) who compared stirred tank reactors and bubble columns, is sparse. Different bioreactor designs have quite unique scaling abilities and associated costs, and the economic benefits and decisions would be better understood if such studies would be more common.

5.11 Summary

Bubble interactions are tightly connected to hydrodynamics so that gas holdup is usually capable of representing gas-liquid mass transfer trends fairly accurately and, more importantly, predicting reactor hydrodynamics. Thus, any bubble column experiment (or series of experiments) starts with a gas holdup study. The literature provides a wide array of gas holdup information; however, the more detailed experiments, especially those that investigate gas-liquid mass transfer, are much fewer in number and smaller in scope.

Most studies, for example, are based on air-water interaction in an isothermal setting, even though most industrial processes have thermal interactions and complex fluid properties. It is also common for industrial processes to be performed at relatively high temperatures and/or pressure. These settings still lack experimental coverage (Lau et al., 2004). Furthermore, gas holdup and gas-liquid mass transfer are decoupled under thermal operation, and pressure variances are rarely accounted for in currently available correlations.

Gas-liquid mass transfer correlations and their design applications have to be handled very carefully. Bubble-bubble interactions are very complicated processes, which still have not been mastered and are not easily represented with the current set of tools. Although a change in gas holdup can predict the direction of the change in gas-liquid mass transfer, it cannot predict the amount due to the hydrodynamic complexity (Chaumat et al., 2005). Scaleup, design, and application require patience and due diligence. Since most gas-liquid mass transfer correlations use gas holdup data, hydrodynamic and geometric similarity should be attempted in order to maximize the probability of successful prediction. Approximation of gas-liquid mass transfer using third party gas holdup correlations or data have a low probability of success and should be used as a first iteration for scaleup or design. Follow-up investigations are then strongly advised.

Table 5.1: Gas holdup correlations for bubble columns.

Reference	System	Conditions	Correlation
(Akita and Yoshida, 1973)[1]	Air-H_2O, O_2-H_2O, He-H_2O, CO_2-H_2O, Air-Glycol, Air-Aqueous glycol solution, Air-Methanol	α = 0.2 for pure liquids, 0.25 for salt solutions D_R = 0.152 m H = 4.0 m d_0 = 0.5 mm (SO) U_G = 0.5-33 cm/s P up to 0.1 MPa T up to 293K	$\frac{\varepsilon_G}{(1-\varepsilon_G)^4} = \alpha \left(\frac{D_R^2 \rho_L g}{\sigma}\right)^{1/8} \left(\frac{D_R^3 \rho_L^2 g}{\mu_L^2}\right)^{1/12} \frac{U_G}{\sqrt{g D_R}}$
(Anabtawi et al., 2003)[2]	Air-(light oil, machine oil, five different engine oils)	D_R = 74 mm d_0 = 10 mm H = 0.12-0.60 m U_G = 0.18-29 cm/s ρ_L = 906-928 kg/m^3 μ_L = 63-320 mPa s σ = 24.8-35 mN/m	$\varepsilon_G = 0.362 \frac{U_G^{0.60}}{H^{0.38} \mu_L^{0.24}}$
(Bach and Pilhofer, 1978)[3]	Air-(Water, butandiol-1,3, ethylene glycol, n-octanol, tetrabromomethane, cyclohexane, cyclohexanol, ethanol, propanol, ethyl acetate)	D_R = 0.10 m d_0 = 5 mm (PP) U_G = 1-20 cm/s ρ_L = 0.8-2.98 g/cm^3 ν_L = (0.7-124)*10^2 cm^2/s, σ = 21.7-72 mN/m	$\frac{\varepsilon_G}{1-\varepsilon_G} = 0.115 \left(\frac{U_G^3}{\nu_L g \Delta\rho / \rho_L}\right)^{0.23}$
(Bouaifi et al., 2001)	Air-Water	U_G = 0.25-4.0 cm/s Column 1 D_R = 0.15 m H = 2 m Column 2 D_R = 0.20 m H = 2 m	$\varepsilon_G = C_2 U_G^{\,x}$

	Porous Plate		Membrane		Perforated Plate	
	C_2	x	C_2	x	C_2	x
Column 1	3.62	0.91	4.25	0.99	3.66	0.83
Column 2	3.43	1.03	3.12	1.05	2.2	1.06

(Deckwer, 1992)	Air-CMC concentration 0.8-1.8 %wt	D_R = 0.14 m d_0 = 2 mm (PP) and 0.15 or 0.2 mm (SP) μ_L > 50 mPa s	$\varepsilon_G = 0.0322 U_G^{0.674}$ for slug flow regime (U_G > 3 cm/s) $\varepsilon_G = 0.0908 U_G^{0.85}$ for homogeneous flow regime (U_G < 2 cm/s)
(Gestrich and Rahse, 1975)[2]	Air-organic liquids (methanol, ethanol, n-butanol, ethyl acetate, glycol, methylethylketone, $C_2H_4Cl_2$)	H/D_R = 0.26-20 U_G = 1-8 cm/s $\frac{\rho_L \sigma^3}{g \mu_L^4} = 8*10^4 - 5*10^{10}$	$\varepsilon_G = 0.89 \left(\frac{H}{D_R}\right)^{0.035(-15.7+\log K)} \left(\frac{d_B}{D_R}\right)^{0.3} \left(\frac{U_G^2}{g d_B}\right)^{0.025(2.6+\log K)} K^{0.047} - 0.05$ $K = \frac{\rho_L \sigma^3}{g \mu_L^4}$ and d_B = 3 mm
(Godbole et al., 1982)[1]	Air-Viscous media		$\varepsilon_G = 0.239 U_G^{0.634} D_R^{-0.5}$

[1] Adopted from Kantarci et al. (2005)
[2] Adopted from Ribeiro and Lage (2005)
[3] Adopted from Deckwer (1992)

Table 5.1 cont.: Gas holdup correlations for bubble columns.

Reference	System	Conditions	Correlation
(Grover et al., 1986)[1]		D_R = 0.10 m d_0 = 100-120 μm U_G = 0.1-4.5 cm/s T = 303-353K	$\varepsilon_G = \left(\frac{1+b_1P_V}{b_2P_V}\right)\left(\frac{U_G\mu_L}{\sigma}\right)^{0.76}\left(\frac{\mu_L{}^4 g}{\rho_L\sigma^3}\right)^{-0.27}\left(\frac{\rho_G}{\rho_L}\right)^{0.09}\left(\frac{\mu_G}{\mu_L}\right)^{0.35}$ $b_1 = 1.1*10^{-4}$ and $b_2 = 5\text{-}10^{-4}$
(Guy et al., 1986)[2]	Air-Water Air-Aqueous solutions (glycerol, carboxyl methyl-cellulose)	D_R = 0.254 m d_0 = 1 mm U_G = 1-8 cm/s $\frac{U_{b\infty}d_e}{\nu_L} > 4.02\frac{g\mu_L{}^4}{\rho_L\sigma^3}$ $\frac{gd_e{}^2\rho_L}{\sigma} >> 8$	$\varepsilon_G = 0.386N_0\left(\frac{gD_R{}^3}{\nu_L{}^2}\right)^{0.025}\left(\frac{U_0}{\sqrt{gd_0}}\right)^{0.84}\left(\frac{d_0}{D_R}\right)^{2.075}$
(Guy et al., 1986)[2]	Air-Water Air-Aqueous solutions (glycerol, carboxyl methyl-cellulose)	D_R = 0.254 m d_0 = 1 mm U_G = 1-8 cm/s $\frac{U_{b\infty}d_e}{\nu_L} > 4.02\frac{g\mu_L{}^4}{\rho_L\sigma^3}$ $\frac{gd_e{}^2\rho_L}{\sigma} >> 8$	$\varepsilon_G = 0.386N_0\left(\frac{gD_R{}^3}{\nu_L{}^2}\right)^{0.025}\left(\frac{U_0}{\sqrt{gd_0}}\right)^{0.84}\left(\frac{d_0}{D_R}\right)^{2.075}$
(Hammer, 1984)[2]	N_2-Organic liquids (methanol, cyclohexane, cyclehexanol, n-octanol, $C_2H_4Cl_2$)	d_0 = 0.15-2mm U_G = 0.5-2 cm/s ρ_L = 780-1250 kg/m^3 μ_L = 0.31-22 mPa s σ = 21.8-31.9 mN/m	$\varepsilon_G = 0.20\left(\frac{U_G{}^2}{gD_R}\right)^{0.46}\left(\frac{D_R{}^3 g}{\nu_L{}^2}\right)^{0.08}\left(\frac{d_0}{D_R}\right)^{-0.17}$
(Haque et al., 1986)[2]	Air-Aqueous carboxy-methyl-cellulose solutions	D_R = 0.10-1.0 m d_0 = 0.3-2.0 mm U_G > 3 cm/s	$\varepsilon_G = 0.171U_G{}^{0.6}\left[K\left(5000U_G\right)^{n-1}\right]^{-0.22}D_R{}^{-0.15}$ (SI)
(Hikita and Kikukawa, 1974)[2]	Air-Water Air-Aqueous solutions (methanol, sucrose)	D_R = 0.10 and 0.19 m d_0 = 13.0-36.2 mm U_G = 4.3-33.8 cm/s ρ_L = 911-1233 kg/m^3 μ_L = 1-19.2 mPa s σ = 38.2-75.5 mN/m	$\varepsilon_G = 0.505U_G{}^{0.47}\left(\frac{\sigma_w}{\sigma}\right)^{2/3}\left(\frac{\mu_w}{\mu_L}\right)^{0.05}$ (SI)

[1] Adopted from Kantarci et al. (2005)
[2] Adopted from Ribeiro and Lage (2005)
[3] Adopted from Deckwer (1992)

Table 5.1 cont.: Gas holdup correlations for bubble columns.

Reference	System	Conditions	Correlation
(Hikita et al., 1980)[3]	D_R = [0.10,0.19] m H = [1.5,2.4] m d_0 =1.1 cm (SO) U_G=4.2-39 cm/s P up to 0.1 MPa T = 283-303K Non-electrolytes ρ_L = 0.79-1.24 g/cm^3 ρ_G = (0.0837-1.84)*10^{-3} g/cm^3 μ_L = 0.66-17.8 mPa s μ_G = (0.8-1.81)*10^{-2} mPa s σ = 30-76 mN/m Electrolytes ρ_L = 1.01-1.17 g/cm^3 μ_L = 0.9-1.87 mPa s σ = 71.9-79.6 mN/m		$\varepsilon_G = 0.672 f \left(\frac{U_G \mu_L}{\sigma}\right)^{0.578} \left(\frac{\mu_L^4 g}{\rho_L \sigma^3}\right)^{-0.131} \left(\frac{\rho_G}{\rho_L}\right)^{0.062} \left(\frac{\mu_G}{\mu_L}\right)^{0.107}$ Where: f = 1 for electrolytes, $10^{0.0414I}$ for ion strength I<1 g-ion/L, 1.1 for I>1 g-ion/L
(Hughmark, 1967)[1]	Air-(Water, Na_2CO_3 solution, light oil, glycerol, $ZnCl_2$ and Na_2SO_3 solution)	D_R = 0.0254-1.07m (PP) U_G = 0.4-45 cm/s U_L = 0-12 cm/s ρ_L = 777-1698 kg/m^3 μ_L = 0.9-152 mPa s σ = 25-76 mN/m	$\varepsilon_G = \frac{1}{2+\left(\frac{0.35}{U_G}\right)\left[\rho_L \frac{\sigma}{72}\right]^{1/3}}$
(Idogawa et al., 1987)[2]	(Air, H_2, He)-Water Air-organic liquids (acetone, ethanol, methanol) Air-aqueous solutions (ethanol, isoamyl alcohol)	D_R = 0.05 m d_0 = 1 mm U_G = 0.5-5 cm/s ρ_L = 791-1000 kg/m^3 ρ_G = 0.084-120.8 kg/m^3 μ_L = 0.35-3.0 mPa s σ = 22.6-72.1 mN/m	$\frac{\varepsilon_G}{1-\varepsilon_G} = 0.059 U_G^{0.8} \rho_G^{0.17} \left(\frac{\sigma}{\sigma_w}\right)^{-0.22\exp(-P)}$
(Ityokumbul et al., 1994)[2]	Air-Water	D_R = 0.06 m d_0 = 134 μm U_G = 0-2.5 cm/s	$\varepsilon_G = 5.9 U_G$ (SI)
(Jean and Fan, 1987)[2]	Air-Water	D_R = 0.0762 (PP) U_G = 0-12.08 cm/s U_L = 3.27-32.18 cm/s	$\varepsilon_G = 0.00164 U_G^{0.988} \left(28.821 + 0.564 U_L - 0.221 * 10^5 U_L^2\right)$ for $U_G \le 5.19$ cm/s $\varepsilon_G = \frac{0.2933 U_G^{0.34}}{\exp\left(-0.248 U_L U_G^{-0.648}\right) + \exp\left(0.243 U_L U_G^{-0.648}\right)}$ for $U_G \ge 5.19$ cm/s

[1] Adopted from Kantarci et al. (2005)
[2] Adopted from Ribeiro and Lage (2005)
[3] Adopted from Deckwer (1992)

Table 5.1 cont.: Gas holdup correlations for bubble columns.

Reference	System	Conditions	Correlation
(Jordan and Schumpe, 2001)[1]	(Air, N_2, He, CO_2, H_2)-23 different organic liquids	D_R = 0.095-0.115 m d_0 = 1.0-4.3 mm U_G = 1-21 cm/s $\frac{g\rho_L d_b^2}{\sigma} = 825 - 1.55*10^6$ $\frac{U_G}{\sqrt{gd_b}} = 0.06 - 1.22$ $\frac{\rho_G}{\rho_L} = 9.3*10^{-5} - 0.059$	$\frac{\varepsilon_G}{1-\varepsilon_G} = B\left(\frac{g\rho_L d_b^2}{\sigma}\right)^{0.16}\left(\frac{gd_b^3}{\nu_L^2}\right)^{0.04}\left(\frac{U_G}{\sqrt{gd_b}}\right)^{0.70}\left[1+27.0\left(\frac{U_G}{\sqrt{gd_b}}\right)^{0.52}\left(\frac{\rho_G}{\rho_L}\right)^{0.58}\right]$ B is sparger dependent
(Jordan et al., 2002)	(Air, N_2)-(Water, ethanol (96%), 1-butanol, toluene)	D_R = 0.115 m H = 1.370 m U_G = 0.01-0.15 m/s ρ_L = 759-884 kg/m^3 μ_L = 0.58-2.94 mPa s σ = 19.9-32.5 mN/m D_L (10^{-9} m^2/s) = 1.60-4.38 P = 1-10 bar T = 293K	$\varepsilon_G = B\left(U_G\right)^{0.86}\left(\rho_G\right)^{0.24}$ Values for B Water = 1.69 Ethanol (96%) = 1.62 1-Butanol = 1.34 Toluene = 1.95
(Joshi and Sharma, 1979)[1]			$\varepsilon_G = \frac{U_G}{0.3+2U_G}$
(Kang et al., 1999)	Air-(water, aqueous solutions of carboxy-methyl-cellulose)	D_R = 0.152 m d_0 = 1.0 mm U_G = 2-20 cm/s μ_L = 1-38 mPa s P = 0.1-0.6 MPa	$\varepsilon_G = 0.910*10^{-2.10}\left(\frac{D_R U_G \rho_G}{\mu_L}\right)^{0.254}$
(Kato and Nishiwaki, 1972)[2]	Air-Water	D_R = 0.066-0.214 m d_0 = 1.0-3.0 mm U_G = 0-30 cm/s U_L = 0-1.5 cm/s	$\varepsilon_G = \frac{U_G}{31+\beta U_G^{0.8}\left(1-\exp(\gamma)\right)}$ Where: $\beta = 4.5 - 3.5\exp\left(-0.064 D_R^{1.8}\right)$ $\gamma = -0.18 U_G^{1.8}\beta^{-1}$
(Kawase and Moo-Young, 1987)[1]			$\varepsilon_G = 1.07 Fr^{1/3}$ $Fr = \frac{U_G}{\sqrt{gD_R}}$ Where:
(Kawase et al., 1992)[1]			$\frac{\varepsilon_G}{1+\varepsilon_G} = 0.0625\left(\frac{U_G}{\nu_L g}\right)^{1/4}$
(Kim et al., 1972)[2]	D_R = 0.049 m d_0 = 3.175 mm U_G = 0-26 cm/s U_L = 1.4-10.2 cm/s		$1-\varepsilon_G = 1.02\left(\frac{\mu_L^2\rho_G}{D_R g \rho_L}\right)^{-0.009}\left(\frac{U_G\rho_L}{D_R g \rho_G}\right)^{-0.036}\left(\frac{U_G U_L D_R^2}{\nu_G \nu_L}\right)^{-0.015}$

[1] Adopted from Kantarci et al. (2005)
[2] Adopted from Ribeiro and Lage (2005)
[3] Adopted from Deckwer (1992)

Table 5.1 cont.: Gas holdup correlations for bubble columns.

Reference	System	Conditions	Correlation
(Koide et al., 1979)[1]			$\varepsilon_G = \frac{U_G}{31+\beta(1-e)\sqrt{U_G}}$ Where: $\beta = 4.5 - 3.5\exp\left(-0.064 D_R^{1.3}\right)$ and $e = \frac{-0.18 U_G^{1.8}}{\beta}$
(Koide et al., 1984)[1]	Air-Water Air-Aqueous solutions (electrolytes, glycol, glycerol)	D_R = 0.10-0.30 m d_0 = 0.5-2.5 mm (MO) U_G = 1-18 cm/s ρ_L = 997-1178 kg/m³ ρ_s = 2500 and 8700 kg/m³ μ_L = 0.894-17.6 mPa s σ = 51.5-73 mN/m c_s = 0-200 kg/m³ d_s = 47.5-192 μm	$\frac{\varepsilon_G}{(1-\varepsilon_G)^4} = \frac{A\left(\frac{U_G\mu_L}{\sigma}\right)^{0.918}\left(\frac{g\mu_L^4}{\rho_L\sigma^3}\right)^{-0.252}}{1+4.35\left(\frac{c_s}{\rho_s}\right)^{0.748}\left[\frac{\rho_s-\rho_L}{\rho_L}\right]^{0.88}\left(\frac{U_G D_R}{\nu_L}\right)^{-0.168}}$ Where: A = 0.277 for water and non-electrolyte solutions, A = 0.364 for electrolyte solutions
(Kojima et al., 1997)[2]	(N_2, O_2)-Water (N_2, O_2)-Aqueous solutions (enzyme, Na_2HPO_4, citric acid)	D_R = 0.045 m d_0 = 1.38-4.03 mm U_G = 0.5-15 cm/s ρ_L = 1000-1025 kg/m³ μ_L = 0.890-1.075 mPa s σ = 63.36-71.96 mN/m P = 0.1-1.1 MPa	$\varepsilon_G = \varepsilon_0 = 1.18 U_G^{0.679}\left(\frac{\sigma}{0.076}\right)^{-0.546}$ for P = 101 kPa $\varepsilon_G = \varepsilon_0 \exp\left[A\left(\frac{\pi D_R^4 \rho_L U_G^2}{16 d_0^3 \sigma}\right)\left(\frac{P}{P_{atm}}\right)^B\right]$ for P > 101 kPa Where: $A = 1.27*10^{-4}$ and B = 1.0
(Kumar et al., 1976)[1]	Air-H_2O Air-Kerosene Air-40% glycerol Air-2M NaOH solution	D_R = 0.05-0.10 m d_0 = 0.087-0.309 cm (PP) U_G = 0.2-14 cm/s ρ_L = 0.78-1.11 g/cm³ μ_L = 0.88-11.5 mPa s σ = 31.2-74.5 mN/m	$\varepsilon_G = 0.728 U_G^* - 0.485 U_G^{*2} + 0.0975 U_G^{*3}$ $U_G^* = U_G\left(\frac{\sigma\Delta\rho g}{\rho_L}\right)^{1/4}$ Where:
(Lau et al., 2004)	D_R = 0.045-0.45 m H/D_R > 5 d_0 = 1.5 mm U_G = 2.8-67.8 cm/s U_L = 0-0.089 cm/s P up to 22 MPa T up to 250°C ρ_L = 790-1580 kg/m³ ρ_G = 0.97-33.4 kg/m³ μ_L = 0.36-38.3 mPa s σ = 23.3-72.6 mN/m		$\frac{\varepsilon_G}{1-\varepsilon_G} = \frac{2.9\left(\frac{U_G^4\rho_G}{\sigma_G}\right)^{\alpha}\left(\frac{\rho_G}{\rho_m}\right)^{\beta}}{\left[\cosh\left(Mo_m^{0.054}\right)\right]^{4.1}}$ Where: $\alpha = 0.21 Mo_m^{0.0079}$, $\beta = 0.096 Mo_m^{-0.011}$, $Mo_m = \frac{(\xi\mu_L)^4 g}{\rho_m\sigma^3}$, $\ln\xi = 4.6\varepsilon_s\left\{5.7\varepsilon_s^{0.58}\sinh\left[-0.71\exp(-5.8\varepsilon_s)\ln Mo^{0.22}\right]+1\right\}$, and $Mo = \frac{g\mu_L^4}{\rho_L\sigma^3}$
(Lee et al., 2000)[2]	Air-Water	D_R = 0.083-0.15 m d_0 = 4 mm U_G = 0-270 cm/s U_L = 0-23 cm/s	$\frac{\varepsilon_G}{1-\varepsilon_G} = 0.759 U_G^{0.687} U_L^{-0.116}$ (SI)
(Lockett and Kirkpatrick, 1975)[1]			$U_G(1-\varepsilon_G) + U_L\varepsilon_G = V_B\varepsilon_G(1-\varepsilon_G)^{2.39}\left(1+2.55\varepsilon_G^3\right)$

[1] Adopted from Kantarci et al. (2005)
[2] Adopted from Ribeiro and Lage (2005)
[3] Adopted from Deckwer (1992)

Table 5.1 cont.: Gas holdup correlations for bubble columns.

Reference	System	Conditions	Correlation
(Luo et al., 1999)[2]	D_R = 0.1-0.61 m U_G = 5-69 cm/s U_L = 0 m/s ρ_L = 668-2965 kg/m³ ρ_s = 2200-5730 kg/m³ ρ_G = 0.2-90 kg/m³ μ_L = 0.29-30.0 mPa s σ = 19.0-73.0 mN/m φ_s = 0, 0.081,0.181 T = 301K, 351K P = 0.1-5.62 MPa	(Air, He, CO_2, N_2)-Water Air-Organic liquids (methanol, glycol, glycerol, $C_2H_3Br_3$, n-octanol, heptanes, n-butanol, 1,3-butanediol, trichloroethylene) Air-Isopar G, Paratherm F Liquids with and without suspended solids	$\frac{\varepsilon_G}{1-\varepsilon_G} = 2.9\left(\frac{U_G{}^4\rho_G}{g\sigma}\right)^{\alpha}\left(\frac{\rho_G}{\rho_L}\right)^{\beta}\left[\cosh\left(Mo_s\right)^{0.054}\right]^{-4.1}$ Where: $\alpha = 0.21Mo_s^{0.079}$, $\beta = 0.096Mo_s^{-0.011}$, $\rho_s = \varphi_s\rho_s + \varphi_L\rho_L$, $Mo_s = \frac{(\xi\mu_L)^4 g}{\rho_s{}^1\sigma^3}$ $\ln\xi = 4.6\varphi_s\left\{5.7\varphi_s{}^{0.58}senh\left[-0.1562\exp\left(-5.8\varphi_s\right)\ln\left(\frac{g\mu_L}{\rho_L\sigma^3}\right)\right]+1\right\}$
(Mashelkar, 1970)[2]	Air-Water Air-Electrolyte aqueous solutions		$\varepsilon_G = \frac{U_G}{\rho_L(30+2U_G)}\left(\frac{\sigma_w}{\sigma}\right)^{-1/3}$
(Mersmann, 1977)[2]			$\varepsilon_G\left(1-\varepsilon_G\right)^n = 0.14U_G\left[\frac{\rho_L{}^2}{\sigma(\rho_L-\rho_G)g}\right]^{1/4}\left(\frac{\rho_L}{\rho_G}\right)^{5/72}\left(\frac{\rho_L}{\rho_L-\rho_G}\right)^{1/3}\left[\frac{\sigma^3\rho_L{}^2}{\mu_L{}^4(\rho_L-\rho_G)g}\right]^{1/24}$
(Mok et al., 1990)[2]	Air-Water Air-CMC aqueous solutions	D_R = 0.14 m d_0 = 0.3 mm U_G = 0.96-5.04 cm/s ρ_L = 997.1-998.2 kg/m³ σ = 70.5-72 mN/m	$\varepsilon_G = 1.07*10^{-5}\left(\frac{D_R U_G}{\nu_G}\right)^{1.09}\left(\frac{gD_R{}^3}{\nu_L{}^2}\right)^{0.096}\left(\frac{d_0}{D_R}\right)^{-0.19}$
(Mouza et al., 2005)[2]	Air-Water Air-Aqueous solutions (glycerin, n-butanol)	Square column with Width = 0.10 m d_0 = 20 and 40 µm $U_G < U_{trans}$ ρ_L = 991-1173 kg/m³ μ_L = 0.9-22.5 mPa s σ = 48.0-72 mN/m	$\varepsilon_G = 0.001\left[\frac{U_G}{\sqrt{gD_R}}\left(\frac{D_R{}^3\rho_L{}^2 g}{\mu_L{}^2}\right)^{0.1}\left(\frac{D_R{}^2\rho_L g}{\sigma}\right)^{2.2}\frac{D_d}{D_R}\right]^{2/3}$
(Reilley et al., 1986)[1]	D_R = 0.30 m d_0 = 1.5 mm U_G = 0.77-21.7 cm/s ρ_L = 771-1482 kg/m³ μ_L = 0.489-1.29 mPa s σ = 28.3-72 mN/m ρ_G = 0.185-1.48 kg/m³		$\varepsilon_G = 0.009 + 296U_G{}^{0.44}\rho_L{}^{-0.98}\sigma_L{}^{-0.16}\rho_G{}^{0.19}$ can replace ρ_L with ρ_s
(Roy et al., 1963)[1]			$\varepsilon_G = 3.88*10^{-3}\left[\mathrm{Re}_T\left(\frac{\sigma_W}{\sigma_L}\right)^{1/3}\left(1-v_s\right)^3\right]^{0.44}$ for $Re_T > 500$ Where: $v_s = \frac{W_s/\rho_s}{(W_s/\rho_s)+(W_L/\rho_L)}$

[1] Adopted from Kantarci et al. (2005)
[2] Adopted from Ribeiro and Lage (2005)
[3] Adopted from Deckwer (1992)

Table 5.1 cont.: Gas holdup correlations for bubble columns.

Reference	System	Conditions	Correlation
(Sada et al., 1984)[1]	(N_2, He)-(Water, molten $NaNO_3$, molten LiCl-KCl) N_2-Methanol N_2-Aqueous solutions (glycerol, Na_2SO_4)	D_R = 0.073 m d_0 = 1.5-5.7 mm U_G = 0.56-8.3 cm/s ρ_L = 788-1888 kg/m^3 μ_L = 0.45-3.658 mPa s σ = 21.5-130 mN/m	$\varepsilon_G = 0.32\left(1-\varepsilon_G\right)^4 Bo^{0.21} Ga^{0.086} Fr \left(\frac{\rho_G}{\rho_L}\right)^{0.068}$ Where: $Bo = \frac{\rho_L g D_R^{\,2}}{\sigma}$, $Ga = \frac{g D_R^{\,3}}{\upsilon_L^{\,2}}$, and $Fr = \frac{U_G}{\sqrt{g D_R}}$ $\frac{\varepsilon_G}{\left(1-\varepsilon_G\right)^3} = 0.019 U_\infty^{\,1/16} v_s^{\,-0.125 U_\infty^{\,-0.16}} U_G$
(Salvacion et al., 1995)[2]	D_R = 0.14-0.30 m d_0 = 0.5-2.5 mm U_G = 2-15 cm/s ρ_L = 995-997 kg/m^3 ρ_s = 1000-1087 kg/m^3 φ_s = 0-0.20 μ_L = 0.863-0.894 mPa s σ = 55.6-72.0 mN/m		$\frac{\varepsilon_G}{\left(1-\varepsilon_G\right)^4} = \varepsilon_B \left[\frac{1+0.00468\left(D_R^{\,2} g \rho_L \sigma^{-1}\right)^{0.465} f(A)}{1+2.34\varphi_s^{\,0.799}\left(D_R^{\,2} g \rho_L \sigma^{-1}\right)^{-0.0464}}\right]$ Where: A = 0, $\varepsilon_B = 0.277\left(\frac{U_G \mu_L}{\sigma}\right)^{0.918}\left(\frac{g\mu_L^{\,4}}{\rho_L \sigma^3}\right)^{-0.252}$, $f(A) = A^{0.223}\left(1+0.0143A^{0.466}\right)^{-1}$
(Schumpe and Deckwer, 1987)[1]	Bo = 1.4*10^3-1.4*10^5 Ga = 1.2*10^7-6.5*10^{10} Fr = 3*10^{-3}-2.2*10^{-1}		$\varepsilon_G = 0.2 Bo^{-0.13} Ga^{0.11} Fr^{0.54}$ For highly viscous media
(Smith et al., 1983)[1]			$\varepsilon_G = \left[2.25 + \frac{0.379}{U_G}\left(\frac{\rho_L}{72}\right)^{0.31} \mu_L^{\,0.016}\right]^{-1}$ μ_L can be replaced with μ_s, except $\mu_s = \mu_L \exp\left[\frac{(5/3)v_s}{1-v_s}\right]$
(Sotelo et al., 1994)[2]	(Air, CO_2)-water (Air, CO_2)-aqueous solutions (sucrose, ethanol glycerin)	D_R = 0.04-0.08 m d_0 = 30-150 µm U_G = 0.64-4.9 cm/s ρ_L = 928-1147 kg/m^3 ρ_G = 1.18-1.83 kg/m^3 μ_L = 1.0-4.17 mPa s μ_G = 0.0148-0.0191 mPa s σ = 29.8-73.4 mN/m	$\varepsilon_G = 129\left(\frac{U_G \mu_L}{\sigma}\right)^{0.99}\left(\frac{\mu_L^{\,4} g}{\rho_L \sigma^3}\right)^{-0.123}\left(\frac{\rho_G}{\rho_L}\right)^{0.187}\left(\frac{\mu_G}{\mu_L}\right)^{0.343}\left(\frac{d_0}{D_R}\right)^{-0.089}$
(Syeda et al., 2002)[2]	Air-(Water, methanol, glycerol, i-propanol)	D_R = 0.09 m d_0 = 5 mm	$\varepsilon_G = 1.1855\left(\frac{\rho_L d_b}{\sigma}\right)^{0.016}\left(\frac{U_G \mu_L}{\sigma}\right)^{0.578}\left(\frac{\mu_L g}{\rho_L \sigma^3}\right)^{-0.131}\left(\frac{\rho_G}{\rho_L}\right)^{0.062}\left(\frac{\mu_G}{\mu_L}\right)^{0.107}$
(Ulbrecht and Patterson, 1985)[2]	N_2-(Tellus oil, aqueous glucose solution)	D_R = 0.15 and 0.23 m d_0 = 0.5-1.5 mm U_G = 0-25 cm/s ρ_L = 867-1380 kg/m^3 μ_L = 70-550 mPa s σ = 31.0-76.0 mN/m P = 0.1-1.0 MPa	$\varepsilon_G = 0.21 \frac{U_G^{\,0.58} \rho_G^{\,0.3\exp(-9\mu_L)}}{D_R^{\,0.18} \mu_L^{\,0.12}}$

[1] Adopted from Kantarci et al. (2005)
[2] Adopted from Ribeiro and Lage (2005)
[3] Adopted from Deckwer (1992)

Table 5.1 cont.: Gas holdup correlations for bubble columns.

Reference	System	Conditions	Correlation
(Zahradnik and Kastanek, 1979)[2]	Air-Water	D_R = 0.152 and 0.292 m d_0 = 0.87-3 mm U_G = 3.1-27.6 cm/s	$\varepsilon_G = \frac{U_G}{0.3 + 2.0U_G}$ (SI)
(Zahradnik et al., 1997)	Air-Water	D_R = 0.29 m H_0 = 1.5 m U_G = 0.4-16.6 cm/s	$\varepsilon_G = 2.81 U_G^{0.9}$
(Zehner, 1989)			$\varepsilon_G = \frac{U_G / \alpha}{\sqrt{1 + 4\left(U_G / \alpha\right)^{2/3} \frac{V_L(0)}{\alpha}}}$ Where: $\alpha = 1.4\left(\frac{\sigma}{\rho_L}\frac{\rho_L - \rho_G}{\rho_L} g\right)^{1/4}$ and $V(0) = \left(\frac{1}{2.5}\frac{\rho_L - \rho_G}{\rho_L} U_G g D_R\right)^{1/2}$
(Zou et al., 1988)[1]	D_R = 0.10 m d_0 = 10 mm ρ_L = 748.3-997.1 kg/m^3 ρ_G = 1.833-2.161 kg/m^3 μ_L = 0.295-0.894 mPa s σ = 18.77-71.97 mN/m T = 298.15-369.65K		$\varepsilon_G = 0.17283\left(\frac{\mu_L^4 g}{\rho_L \sigma_L^3}\right)^{-0.15}\left(\frac{U_G \mu_L}{\sigma_L}\right)^{0.58}\left(\frac{P + P_{sat}}{P}\right)^{1.61}$

[1] Adopted from Kantarci et al. (2005)
[2] Adopted from Ribeiro and Lage (2005)
[3] Adopted from Deckwer (1992)

Table5.2: Liquid-phase mass transfer correlations for bubble columns.

Reference	System	Conditions	Correlation
(Akita and Yoshida, 1974)[2]	(Air, O_2, He, CO_2)-Water Air-Organic liquids (glycol, methanol) Air-Aqueous solutions (glycol, methanol, glycerol, electrolyte)	D_R = 0.07-0.600 m d_0 = 0.01-5.0 mm U_G = 4.0-33 cm/s ρ_L = 790-1165 kg/m^3 μ_L = 0.58-21.14 mPa s σ = 22.3-74.2 mN/m D_L (10^{-9} m^2/s) = 0.26-4.22	$\frac{k_L d_b}{D_L} = 0.5\left(\frac{\nu_L}{D_L}\right)^{1/2}\left(\frac{d_b^3 g}{\nu_L^2}\right)^{1/4}\left(\frac{g d_b^2 \rho_L}{\sigma}\right)^{3/8}$
(Calderbank and Moo-Young, 1961)[2]	ρ_L = 698-1260 kg/m^3 μ_L = 0.371-8.7 mPa s λ_L = 0.60-27.92 W/(m K) D_L (10^{-4} m^2/s) = 1.9*10^{-6}-0.26		$\frac{k_L d_b}{D_L} = 2.0 + 0.31\left[\frac{d_b^3(\rho_L-\rho_G)g}{\mu_L D_L}\right]^{1/3}$ for d_b < 2.5 mm $k_L\left(\frac{\nu_L}{D_L}\right)^{1/2} = 0.42\left[\frac{(\rho_L-\rho_G)\mu_L g}{\rho_L^2}\right]^{1/3}$ for d_b . 2.5 mm
(Cockx et al., 1995)[2]			$\frac{k_L}{U_G} = \frac{4.47*10^{-2}}{\varepsilon_G}\left(\frac{\nu_L}{D_L}\right)^{-1/2}$
(Fair, 1967)[2]			$\frac{k_L d_b}{D_L} = 2.0\left[1 + 0.276\left(\frac{d_b U_b}{\nu_L}\right)^{1/2}\left(\frac{\nu_L}{D_L}\right)^{1/3}\right]$
(Fukuma et al., 1987)[2]	U_G = 0.30-1.5 cm/s $\frac{g d_b^3}{\nu_L^2} = 3.2*10^5 - 2.6*10^8$ $\frac{g\rho_L d_b^2}{\sigma} = 1.4 - 120$ $\frac{\nu_L}{D_L} = 480 - 1600$		$\frac{k_L d_b}{D_L} = 4.5*10^{-4}\left(\frac{\nu_L}{D_L}\right)^{1/2}\left(\frac{g\rho_L d_b^2}{\sigma}\right)^{-0.2}\left(\frac{g d_b^3}{\nu_L^2}\right)^{0.8}$
(Gestrich et al., 1978)[2]	(CO_2, O_2)-Water (CO_2, O_2)-Aqueous solutions (glycerine, glycerol, electrolyte)		$k_L = 2.23*10^{-4}\left(\frac{g\mu_L^4}{\rho_L\sigma^3}\right)^{-0.180} + 3.85*10^{-3}\left(\frac{H_0}{D_R}\right)^{-0.605} U_G^{\,0.65+0.0335\frac{H_0}{D_R}}$
(Gestrich et al., 1978)[2]	(CO_2, O_2)-Water (CO_2, O_2)-Aqueous solutions (glycerine, glycerol, electrolyte)		$k_L = 2.23*10^{-4}\left(\frac{g\mu_L^4}{\rho_L\sigma^3}\right)^{-0.180} + 3.85*10^{-3}\left(\frac{H_0}{D_R}\right)^{-0.605} U_G^{\,0.65+0.0335\frac{H_0}{D_R}}$
(Hughmark, 1967)[2]	Air-(Water, Na_2CO_3 solution, light oil, glycerol, $ZnCl_2$ and Na_2SO_3 solution)	D_R = 0.0254-1.07 m U_G = 0.4-45 cm/s U_L = 0-12 cm/s ρ_L = 777-1698 kg/m^3 μ_L = 0.9-152 mPa s σ = 25-76 mN/m	$\frac{k_L d_b}{D_L} = 2.0 + 0.0187\left[\left(\frac{U_G d_b}{\varepsilon_G \nu_L}\right)^{0.484}\left(\frac{\nu_L}{D_L}\right)^{0.339}\left(\frac{d_b g^{1/3}}{D_L^{2/3}}\right)^{0.072}\right]^{1.61}$

[1] Adopted from Kantarci et al. (2005)
[2] Adopted from Ribeiro and Lage (2005)
[3] Adopted from Deckwer (1992)

Table 5.2 cont.: Liquid-phase mass transfer correlations for bubble columns.

Reference	System	Conditions	Correlation
(Kawase et al., 1987)[2]			$k_L = \frac{2}{\sqrt{\pi}}\sqrt{D_L}\left(\frac{U_G g}{\nu_L}\right)^{1/4}$
(Kawase and Moo-Young, 1992)[2]			$k_L = \frac{0.28 D_L^{2/3} g^{1/3}}{\nu_L^{1/3}}$ for small bubbles $k_L = \frac{0.47 D_L^{1/2} g^{1/3}}{\nu_L^{1/6}}$ for large bubbles
(Linek et al., 2005a)	O_2-Water O_2-Aqueous solutions (Na_2SO_3 pure and with the addition of Sokrat 44 and carboxy-methyl-cellulose)	D_R = 0.19 m U_G = 0.18-0.54 cm/s ρ_L = 1000-1093 kg/m^3 μ_L = 1.11-3.14 mPa s	$k_L = 0.463\left(g U_G \nu_L\right)^{1/4}\left(\frac{D_L}{\nu_L}\right)^{1/2}$
(Miller, 1974)[2]	Air-Water	D_R = 0.152-0.686 m d_0 = 1.6-6.4 mm U_G = 0.762-15.2 cm/s	$k_L = 1366 d_b^{1.376}\sqrt{\frac{D_L U_b}{\pi d_b}}$
(Nedeltchev, 2003)[2]	N_2-Gasoline, toluene	D_R = 0.316 m U_G = 5-25 cm/s ρ_L = 692-866 kg/m^3 μ_L = 0.46-0.59 mPa s	$k_L = 2.43*10^7 d_b^{2.928}\sqrt{\frac{D_L U_b}{\pi d_b}}$ (SI)
(Ruckenstein, 1964)[2]			$\frac{k_L d_b}{D_L} = 1.252\left[\frac{1-\varepsilon_G^{5/3}}{2+3\left(\varepsilon_G^{5/3}-\varepsilon_G^{1/3}-2\varepsilon_G^{2}\right)}\right]^{1/3}\left(\frac{U_b d_b}{D_L}\right)^{1/3}$
(Sokolov and Aksenova, 1983)[2]	(Air, CO_2)-Water (Air, CO_2)-Aqueous solutions (sucrose, carbonate-bicarbonate buffer)	D_R = 0.05-0.60 m d_0 = 2.25-40 mm U_G = 0.05-4.0 cm/s $\frac{\nu_L}{D_L} = 310-8320$ $\frac{U_G}{\mu_L\sqrt{\rho_L\sigma/g}} = 5-740$	$\frac{k_L\sigma}{D_L\rho_L g} = 0.05\left(\frac{\nu_L}{D_L}\right)^{0.5}\frac{U_G}{U_L}\left(\frac{\rho_L\sigma}{g}\right)^{0.5}$
(Vázquez et al., 2000)	D_R = 0.113 m d_0 = 0.04-0.20 mm (MO) U_G = 0.085-0.181 cm/s ν_L = 1.22*10^{-6} m^2/s σ = 66.00-75.01 mN/m		$k_L = A\sigma^{1.35}U_G^{0.5}$ (SI) Where:

Equivalent pore diameter (10^6 m)	A
150-200	0.17587
90-150	0.18233
40-90	0.18689

[1] Adopted from Kantarci et al. (2005)
[2] Adopted from Ribeiro and Lage (2005)
[3] Adopted from Deckwer (1992)

Table 5.3: Gas-liquid mass transfer correlations for bubble columns.

Reference	System	Conditions	Correlation
(Akita and Yoshida, 1973)[1]	Air-H_2O O_2-H_2O He-H_2O CO_2-H2O Air-Glycol Air-Aqueous glycol solution Air-Methanol	D_R =0.15-0.600 m H = 4.0 m d_0 = 0.5 mm U_G=0.4-32.8 cm/s P up to 0.1 MPa T up to 293K $\frac{U_G}{\sqrt{gD_R}} = 0.0024 - 0.135$ $\frac{gD_R^2\rho_L}{\sigma} = 3050 - 4.85*10^4$ $\frac{\nu_L}{D_L} = 173 - 7.25*10^3$	$\frac{k_L a D_R^2}{D_L} = 0.6\left(\frac{\upsilon_L}{D_L}\right)^{0.5}\left(\frac{gD_R^2\rho_L}{\sigma}\right)^{0.62}\left(\frac{gD_R^3}{\nu_L^2}\right)\varepsilon_G^{1.1}$
(Álvarez et al., 2000)	CO_2-Water CO_2-Aqueous solutions (sucrose, sodium lauryl sulfate)	D_R = 0.113 m d_0 = 0.04-0.20 mm (MO) U_G = 0.085-0.150 cm/s ρ_L = 997-1030 kg/m^3 μ_L = 0.896-1.135 mPa s σ = 65.20-72.49 mN/m D_L (10^{-9} m^2/s) = 1.549-1.897	$k_L a = A\frac{U_G^{2/3}\sigma^{3/4}\rho_L^{3/2}}{\mu_L^{3/4}}$ Where: **Equivalent pore diameter (10^6 m)** / **A (10^7)** 150-200 / 1.924 90-150 / 1.969 40-90 / 2.079
(Behkish et al., 2002)	(H_2, CO, N_2, CH_4)-(hexane mixture, Isopar-M) with and without solids (iron oxides catalyst and glass beads)	D_R = 0.316 m U_G = 5-25 cm/s ρ_L = 680-783 kg/m^3 μ_L = 0.32-2.7 mPa s σ = 27.0-230 mN/m D_L (10^{-9} m^2/s) = 1.33-9.40 $\varphi_s = 0 - 0.36$	$k_L a = 0.18\left(\frac{\nu_L}{D_L}\right)^{-0.16}\left(\frac{\rho_L}{\rho_G}\right)^{-2.84}\left(\rho_G U_G\right)^{0.49}\exp\left(-266\varphi_s\right)$
(Cho and Wakao, 1988)[2]	N_2-aqueous solutions (benzene, CCl_4, $CHCl_3$, $C_2H_4Cl_2$, $C_2H_3Cl_3$)	D_R = 0.11 m U_G = 0.71-5.0 cm/s D_L (10^{-9} m^2/s) = 0.99-2.42	$k_L a = A D_L^{0.5} U_G^{0.81}$ Where: A = 6500 for single nozzle sparger or A = 23000 for porous plate
(Hikita et al., 1981)[3]	D_R = [0.10,0.19] m H = [1.5,2.4] m d_0 =1.1 cm (SO) U_G=4.2-39 cm/s P up to 0.1 MPa T = 283-303K Non-electrolytes ρ_L = 0.79-1.24 g/cm^3 ρ_G = (0.0837-1.84)*10^{-3} g/cm^3 μ_L = 0.66-17.8 mPa s μ_G = (0.8-1.81)*10^{-2} mPa s σ = 30-76 mN/m Electrolytes ρ_L = 1.01-1.17 g/cm^3 μ_L = 0.9-1.87 mPa s σ = 71.9-79.6 mN/m		$k_L a = \frac{14.9gf}{U_G}\left(\frac{U_G\mu_L}{\sigma}\right)^{1.76}\left(\frac{g\mu_L^4}{\rho_L\sigma^3}\right)^{-0.284}\left(\frac{\mu_G}{\mu_L}\right)^{0.243}\left(\frac{\mu_L}{\rho_L D_L}\right)^{-0.604}$ Where: f = 1 for electrolytes, $10^{0.0414I}$ for ion strength I<1 g-ion/L, 1.1 for I>1 g-ion/L

[1] Adopted from Kantarci et al. (2005)
[2] Adopted from Ribeiro and Lage (2005)
[3] Adopted from Deckwer (1992)

Table 5.3 cont.: Gas-liquid mass transfer correlations for bubble columns.

Reference	System	Conditions	Correlation
(Jordan and Schumpe, 2001)	D_R = 0.095-0.115 m d_0 = 1.0-4.3 mm (SO, MO) U_G = 0.80-21 cm/s $\frac{g\rho_L d_b^2}{\sigma} = 1.21 - 5.39$ $\frac{g d_b^3}{\nu_L^2} 825 - 1.55*10^6$ $\frac{U_G}{\sqrt{g d_b}} = 0.06 - 1.22$ $\frac{\rho_G}{\rho_L} = 9.3*10^{-5} - 0.059$ $\frac{\nu_L}{D_L} = 71 - 6.89*10^4$		$\frac{k_L a d_b^2}{D_L} = A\left(\frac{\nu_L}{D_L}\right)^{0.5}\left(\frac{g\rho_L d_b^2}{\sigma}\right)^{0.34}\left(\frac{g d_b^3}{\nu_L^2}\right)^{0.27}\left(\frac{U_G}{\sqrt{g d_b}}\right)^{0.72}\left[1+13.2\left(\frac{U_G}{\sqrt{g d_b}}\right)^{0.37}\left(\frac{\rho_G}{\rho_L}\right)^{0.49}\right]$ Where A is sparger dependent
(Jordan et al., 2002)	(Air, N_2)-(Water, ethanol (96%), 1-butanol, toluene)	D_R = 0.115 m H = 1.370 m U_G = 0.01-0.15 m/s ρ_L = 759-884 kg/m³ μ_L = 0.58-2.94 mPa s σ = 19.9-32.5 mN/m D_L (10^{-9} m²/s) = 1.60-4.38 P = 1-10 bar T = 293K	$k_L a = C\left(U_G\right)^{0.91}\left(\rho_G\right)^{0.24}$ $k_L a = D\left(\varepsilon_G\right)^{1.06}$ **Liquid** / **C** / **D** Water / 0.99 / 0.56 Ethanol (96%) / 1.14 / 0.67 1-Butanol / 0.83 / 0.60 Toluene / 1.49 / 0.72
(Kang et al., 1999)	Air-(water, aqueous solutions of carboxy-methyl-cellulose)	D_R = 0.152 m d_0 = 1.0 mm U_G = 2-20 cm/s μ_L = 1-38 mPa s P = 0.1-0.6 MPa	$k_L a = 0.930*10^{-3.08}\left(\frac{D_R U_G \rho_G}{\mu_L}\right)^{0.254}$
(Kawase and Moo-Young, 1987)[1]			$\frac{k_L a D_R^2}{D_L} = 0.452\left(\frac{\nu_L}{D_L}\right)^{1/2}\left(\frac{D_R U_G}{\nu_L}\right)^{3/4}\left(\frac{g D_R^2 \rho_L}{\sigma}\right)^{3/5}\left(\frac{U_G^2}{D_R g}\right)^{7/60}$
(Khudenko and Shpirt, 1986)[2]	Air-Water	R_{dt} = 0.125-1 $\frac{H_0}{H_b} = 0.25 - 1$ U_G = 0.055-2.1 cm/s T = 17-24°C	$k_L a = 0.041 R_{dt}^{0.18}\left(\frac{U_G}{H_b}\right)^{0.67}$
(Koide et al., 1984)[2]	Air-Water Air-Aqueous solutions (electrolytes, glycol, glycerol)	D_R = 0.10-0.30 m d_0 = 0.5-2.5 mm (MO) U_G = 1-18 cm/s ρ_L = 997-1178 kg/m³ ρ_s = 2500 and 8770 kg/m³ μ_L = 0.894-17.6 mPa s σ = 51.5-73 mN/m c_s = 0-200 kg/m³ d_s = 47.5-192 μm	$\frac{k_L a \sigma}{\rho_L D_L g} = \frac{2.11\left(\frac{\nu_L}{D_L}\right)^{0.5}\left(\frac{g\mu_L^4}{\rho_L \sigma^3}\right)^{-0.159}\varepsilon_G^{1.18}}{1+1.47*10^4\left(\frac{c_s}{\rho_s}\right)^{0.612}\left(\frac{U_P}{\sqrt{D_R g}}\right)^{0.486}\left(\frac{\rho_L g D_R^2}{\sigma}\right)^{-0.477}\left(\frac{\rho_L U_G D_R}{\mu_L}\right)^{-0.345}}$

[1] Adopted from Kantarci et al. (2005)
[2] Adopted from Ribeiro and Lage (2005)
[3] Adopted from Deckwer (1992)

Table 5.3 cont.: Gas-liquid mass transfer correlations for bubble columns.

Reference	System	Conditions	Correlation
(Lau et al., 2004)	(Air, N_2)-(water, Paratherm NF heat-transfer fluid) (Air, N_2, CO, He, H_2)-9 different organic liquids	D_R = 0.045-0.45 m H/D_R > 5 d_0 = 1.5 mm (PP) U_G = 2.8-67.8 cm/s U_L = 0-0.089 cm/s ρ_L = 790-1580 kg/m^3 ρ_G = 0.97-33.4 kg/m^3 μ_L = 0.36-38.3 mPa s σ = 23.3-72.6 mN/m P up to 22 MPa T up to 250°C	$k_L a = 1.77\sigma^{-0.22}\exp\left(1.65U_L - 65.3\mu_L\right)\varepsilon_G^{1.2}$
(Nakanoh and Yoshida, 1980)[2]	Air-Water Air-Aqueous solutions	D_R = 0.14 m d_0 = 4 mm U_G < 10 cm/s ρ_L = 995-1230 kg/m^3 ν_L (10^{-6} m^2/s) = 0.804-8.82 D_L (10^{-9} m^2/s) = 1.06-2.6	$\frac{k_L a D_R^{\,2}}{D_L} = 0.09\left(\frac{\nu_L}{D_L}\right)^{1/2}\left(\frac{D_R^{\,3} g}{\nu_L^{\,2}}\right)^{0.39}\left(\frac{g D_R \rho_L}{\sigma}\right)^{0.75}\frac{U_G}{\sqrt{g D_R}}$
(Ozturk et al., 1987)[2]	(Air, N_2, CO_2, He, H_2)-organic liquids	D_R = 0.095 m d_0 = 3 mm (SO) U_G = 0.80-10 cm/s $\frac{g\rho_L d_b^{\,2}}{\sigma} = 1.2-5.4$ $\frac{g d_b^{\,3}}{\nu_L^{\,2}} = 830 - 1.5*10^6$ $\frac{U_G}{\sqrt{g d_b}} = 0.043 - 0.6$ $\frac{\rho_G}{\rho_L} = 9.3*10^{-5} - 2.0*10^{-3}$ $\frac{\nu_L}{D_L} = 32 - 1.5*10^5$ P = 0.1 MPa T = 293K	$\frac{k_L a d_B^{\,2}}{D_L} = 0.62\left(\frac{\mu_L}{\rho_L D_L}\right)^{0.5}\left(\frac{g\rho_L d_B^{\,2}}{\sigma}\right)^{0.33}\left(\frac{g\rho_L^{\,2} d_B^{\,3}}{\mu_L^{\,2}}\right)\left(\frac{U_G}{\sqrt{g d_B}}\right)^{0.68}\left(\frac{\rho_G}{\rho_L}\right)^{0.04}$
(Salvacion et al., 1995)[2]	Air-Water Air-Aqueous solutions (methanol, ethanol, n-butanol, n-hexanol, n-octanol)	D_R = 0.14-0.30 m d_0 = 0.5-2.5 mm (MO) U_G = 2-15 cm/s ρ_L = 995-997 kg/m^3 ρ_s = 1000-1087 kg/m^3 $\varphi_s = 0 - 0.20$ μ_L = 0.863-0.894 mPa s σ = 55.6-72.0 mN/m	$\frac{k_L a \sigma}{\rho_L D_L g} = 12.9\left(\frac{\nu_L}{D_L}\right)^{1/2}\left(\frac{g\mu_L^{\,4}}{\rho_L \sigma^3}\right)^{-0.159}\left(\frac{g\rho_L D_R^{\,2}}{\sigma}\right)\left(1 + 0.62\varphi_s\right) f(B)$ $f(B) = 0.47 + 0.53\exp\left(-41.4\frac{B\varepsilon_G}{U_G}\sqrt{\frac{\varepsilon_G}{d_b \mu_L \rho_L U_G}}\right)$ Where: B = 0 for water
(Schumpe and Grund, 1986)[1]	Air-Water	D_R = 0.30 m H = 4.4 m d_0 = 1 mm U_G < 20 cm/s T = 20°C	$k_L a = K U_G^{\,0.82}\mu_{eff}^{\,-0.39}$ Where: K=0.063 (water/salt solution) or 0.042 (water/0.8M Na_2SO_4 solution)

[1] Adopted from Kantarci et al. (2005)
[2] Adopted from Ribeiro and Lage (2005)
[3] Adopted from Deckwer (1992)

Table 5.3 cont.: Gas-liquid mass transfer correlations for bubble columns.

Reference	System	Conditions	Correlation
(Shah et al., 1982)[3]			$k_L a = 0.467 U_G^{0.82}$
(Shpirt, 1981)[2]	Air-Aqueous solutions of NH_4Cl	D_R = 0.107 m H_0 = 0.30-1.0 m U_G = 0.094-0.75 cm/s T = 20°C	$\frac{k_L a d_b^{\,2}}{D_L} = A\left(\frac{U_G d_b}{\nu_L}\right)^{0.45}\left(\frac{H_0}{d_b}\right)^{-0.30}$ Where: A = 0.007 for heterogeneous flow regime Or A = 0.0136 for homogeneous flow regime
(Sotelo et al., 1994)[2]	CO_2-Water CO_2-Aqueous solutions (sucrose, ethanol, glycerin)	D_R = 0.04-0.08 m d_0 = 30-150 μm (MO) U_G = 0.064-0.49 cm/s ρ_L = 998-1147 kg/m^3 μ_L = 1.00-4.17 mPa s μ_G = 1.48-1.53 mPa s σ = 29.8-73.4 mN/m D_L (10^{-9} m^2/s) = 0.51-1.78	$\frac{k_L a U_G}{g} = 16.9\left(\frac{U_G \mu_L}{\sigma}\right)^{2.14}\left(\frac{\mu_L^{\,4} g}{\rho_L \sigma^3}\right)^{-0.518}\left(\frac{\mu_G}{\mu_L}\right)^{0.074}\left(\frac{\nu_L}{D_L}\right)^{-0.038}\left(\frac{d_0}{D_R}\right)^{-0.908}$
(Vasquez et al., 1993)[2]	CO_2-Water CO_2-Aqueous solutions (glycerin, glucose, sucrose)	ρ_L = 997-1151 kg/m^3 μ_L = 0.896-6.42 mPa s σ = 66.9-73.4 mN/m D_L (10^{-9} m^2/s) = 0.40-1.92	$k_L a = 0.779 D_L^{0.5} \mu_L^{-0.2} Fl_G^{1/6}$ (SI)

[1] Adopted from Kantarci et al. (2005)
[2] Adopted from Ribeiro and Lage (2005)
[3] Adopted from Deckwer (1992)

6 Airlift Reactors

6.1 Introduction

The airlift reactor (ALR) is a pneumetic device which attempts to reconcile bubble column shortcomings and provide more control to the operator. Two general families of airlift reactors exist: internal- and external-loop airlift reactors (ILALRs and ELALRs, respectively). The internal-loop variant is sectioned by a baffle (Figure 6.1a) or draught tube (Figure 6.1b). The external-loop airlift reactor (Figure 6.2) connects the up- and down-flowing regions with additional piping. These basic designs can be modified extensively to create a wide array of application specific requirements (Fu et al., 2004; Fu et al., 2003; Karamanev et al., 1996; Merchuk et al., 1999; Wei et al., 2000a; Wei et al., 2000b).

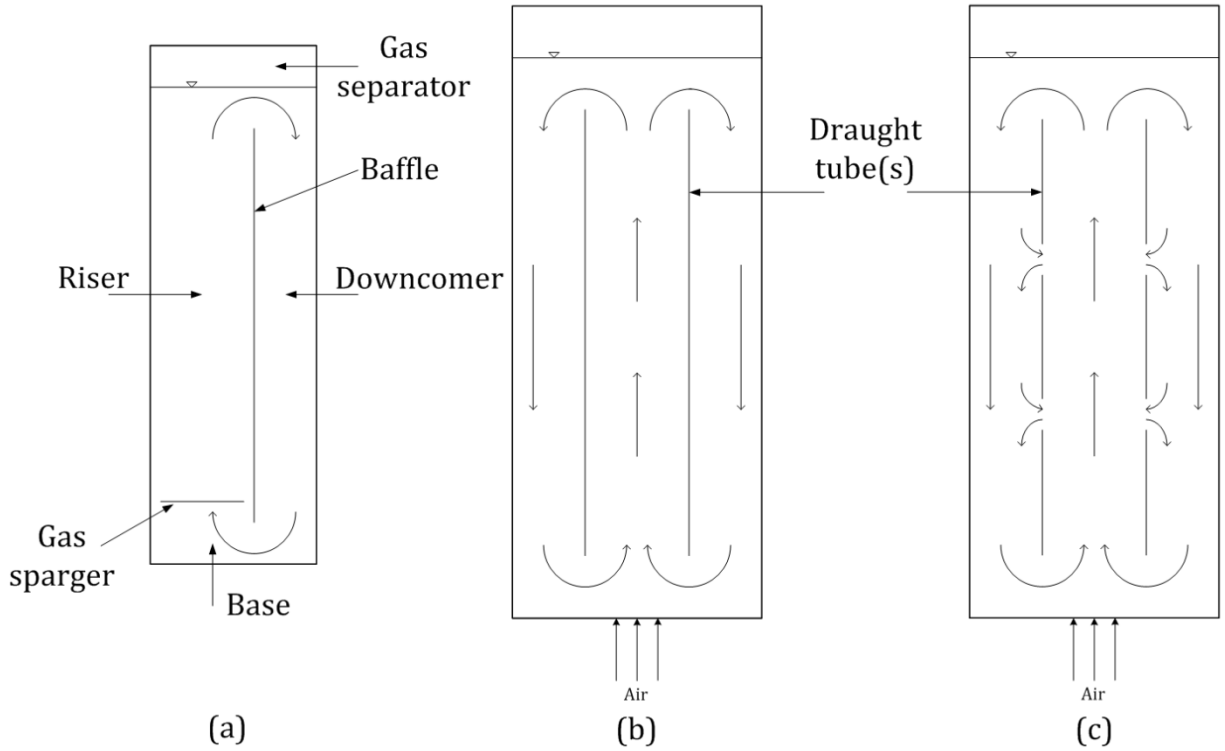

Figure 6.1: Internal-loop airlift reactor with (a) a baffle separating the riser and downcomer, (b) a continuous draught tube separating the riser and downcomer, and (c) a sectioned draught tube separating the riser and downcomer.

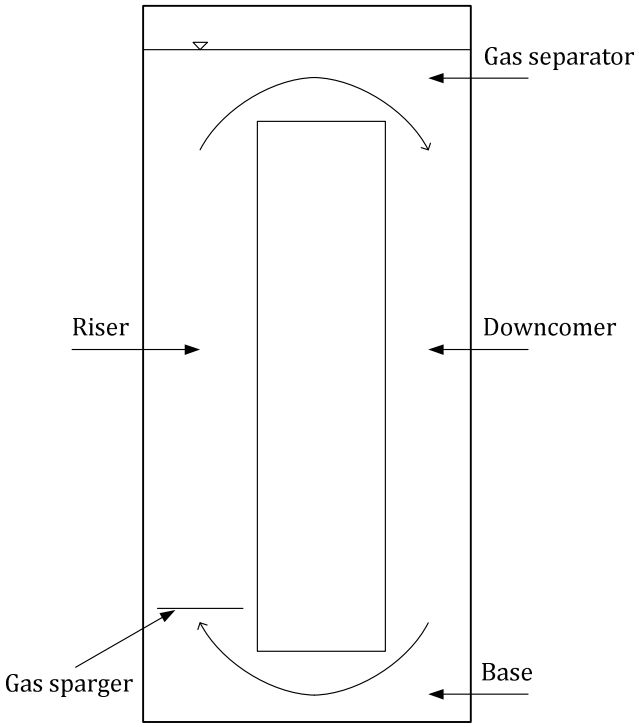

Figure 6.2: External-loop airlift reactor schematic.

Airlift reactor construction is very simple and similar to that of a bubble column (Al-Masry, 1999; Blazej et al., 2004b). There are four basic sections: riser, gas separator, downcomer, and base. The riser is the up-flowing section of the airlift reactor. The gas sparger is oriented such that gas is injected into the riser. The gas sparger location may be within the riser or the base, which is simply the region that connects the downcomer to the riser. The gas separator is at the top of the reactor. As the name implies, gas disengages from the liquid phase (or slurry) in the gas separator. The downcomer is defined as the region in which down-flowing phases are present.

Airlift reactors tend to be taller vessels. Industrial units have a height and diameter up to 10-40 and 2-10 m, respectively. The dimensions are a function of process requirements. Industrial scale units may operate with a liquid circulation velocity up to about 1 m/s and gas residence time of approximately 1 minute (Giovannettone et al., 2009; van Benthum et al., 1999a; van Benthum et al., 1999b). Hence, the height is adjusted to achieve the necessary conversion (van Benthum et al.,

1999b). Pilot scale bioreactors tend to have volumes of 0.05-0.30 m^3. Biological applications use industrial volumes of approximately 10 m^3, but certain applications, such as wastewater treatment, may use reactors up to 1000 m^3 in size (Joshi et al., 1990).

Biological applications use smaller scale vessels because turbulence increases with scale, which leads to an increase in shear stresses as well. Airlift reactors have become popular in mammalian cell suspension applications for which shear stresses become important above 20 L. Increasing the reactor size leads to increased mechanical damage and lower cell densities (Martin and Vermette, 2005).

Airlift reactors can be viewed in two different lights. One is that the ALRs are variations of the bubble column. The bubble-bubble interactions, forces, construction, and reactor applications in ALRs are very similar with those of the bubble column. On the other hand, ALR hydrodynamics are based on interactions between the riser and downcomer gas holdup. The gas separator in conjunction with gas injection in the riser section generally leads to the gas holdup in the riser section being larger than in the downcomer. This effect creates a hydrodynamic pressure difference, which leads to the liquid and/or gas phases circulating in a fairly controlled manner. This mechanism is a source of many advantages unique to the airlift reactor.

Additionally, the liquid and gas phase flow rates may be controlled independently of each other (Williams, 2002). This ability introduces much more control, making the airlift reactor ideal for industrial applications. The phases are circulated by design, which allows much higher gas and liquid flow rates over that of bubble columns (Figure 6.3) without the requirement of a complicated recycle system. The difference between Figure 5.6a and 6.6b is that Figure 5.6a can be achieved through a throttling device. In other words, mixing, heat transfer, and residence time can be optimized while providing the ability to protect any microorganism or catalyst.

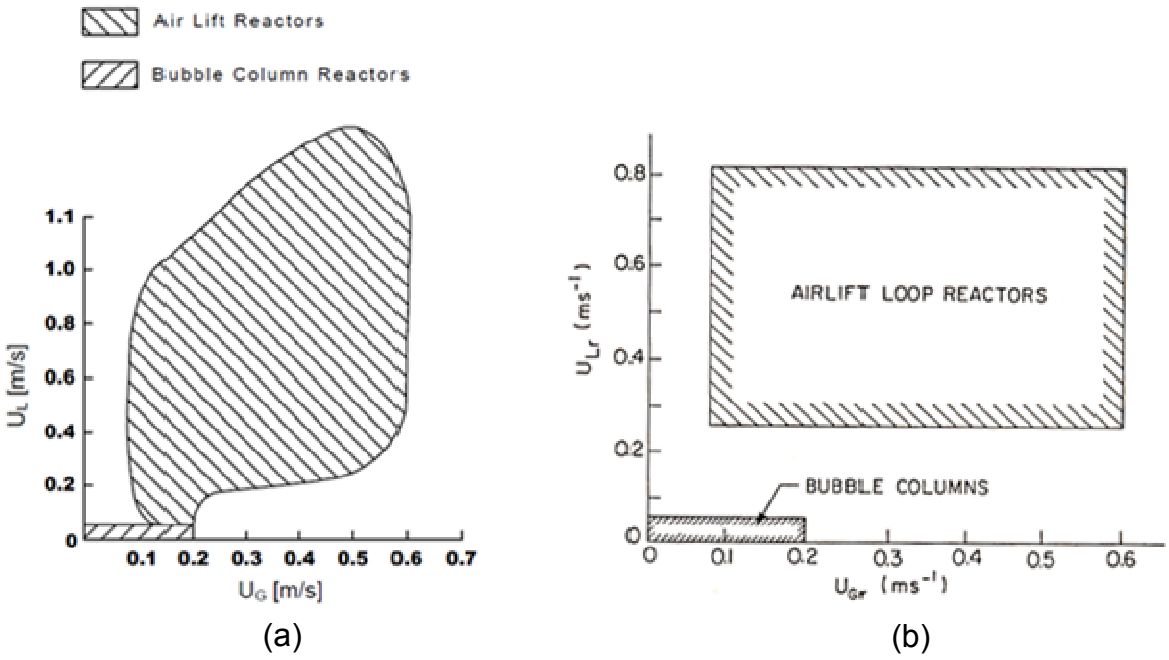

Figure 6.3: Comparison between superficial liquid and gas velocities in bubble columns and airlift reactors from (a) Merchuk (1986) and (b) Chisti (1989).

Dead or high shear zones are minimized in airlift reactors because the influence of sparged gas is limited and the gas phase distribution tends to be practically homogeneous throughout the riser volume, although a non-uniform phase distribution may be observed for approximately the first meter in the riser, which introduces variability in relatively short columns (h_R < 4 m) (Giovannettone et al., 2009). The only possible high shear areas are caused by turns (Merchuk et al., 1999), but these can be eliminated or minimized.

The price for these advantages in ALRs is that the capital investment is usually larger relative to bubble columns. The higher costs can be offset with a liquid and/or gas input increase that is not feasible in a bubble column, which would lead to higher output; however, operation at larger flow scales in airlift reactors can lead to increased variable costs associated with additional gas throughput and pressurization. Foaming also becomes more likely at high gas and liquid flow rates, which leads to inefficient gas separation and recirculation of spent gas bubbles (Wei et al., 2000; Williams, 2002). Complete mixing typically requires 4-9 cycles (the number of times that the liquid

circulates in the ALR) (Karamanev et al., 1996), which would cause further problems if continuous operation is required. Luckily, external-loop airlift reactors can be designed to have much better mixing performance over that of bubble columns.

6.2 Circulation Regimes

The airlift reactor and bubble column have very similar bubble-bubble interactions and behavior, which leads to almost identical gas flow regimes and progression. These have been covered in detail in Section 5.2; however, more attention is placed on liquid flow behavior in airlift reactors since the liquid phase is a significant source of momentum and gas recirculation.

The process of gas entrainment and circulation is complicated and not easily quantified. Problems arise from an abstract relationship between the liquid and gas phase. On one hand, the gas flow rate affects the liquid flow rate through the gas holdup and hydraulic pressure differential relationship. As the gas flow rate increases, larger bubbles with high bubble rise velocities could form, which would lead to lower downcomer gas holdup and increase the circulation velocity. A higher circulation velocity, in turn, would decrease the slip velocity and make entrainment easier. On the other hand, if the liquid velocity is higher than the bubble rise velocity, bubbles would experience a drag (lift) force, which would aid entrainment.

Quantification of this process becomes complex very quickly, and a theoretical measure or technique does not exist. Researchers, instead, have to rely on empirical techniques. Nevertheless, a rough understanding of the circulation process exists and is very helpful in the empirical understanding of ALRs. ALR circulation can be sectioned into three general regimes, as shown in Figure 6.4. At very low gas flow rates, which correspond to $U_{Gr} < 0.012$ m/s, the induced liquid circulation velocity is not strong enough to entrain gas bubbles into the downcomer. Note that U_{Gr} is the superficial gas velocity in the riser. The gas phase is able to almost completely disengage from the liquid phase (regime 1). This regime, referred to as the bubble free regime, is usually not significantly influenced by the liquid properties simply because the amount of gas present in the

system is still fairly low. In order for the liquid properties to become more important, a higher degree of bubble-bubble interaction is needed.

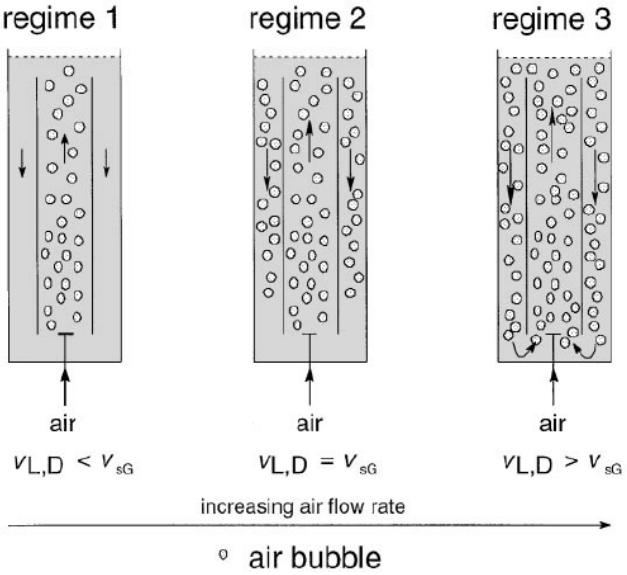

Figure 6.4: Circulation regime progression in a draught tube internal-loop airlift reactor (van Benthum et al., 1999b) where $v_{L,D}$ is the downcomer liquid velocity and v_{sG} is the gas slip velocity.

The liquid is capable of entraining only very small bubbles (d_B < 1 mm) in regime 1. The resulting downcomer gas holdup is usually small with a maximum of about 3%. Once these small bubbles are entrained in the downcomer, they are not transported very far and are expected to reach depths up to 30% of the downcomer height (Albijanic et al., 2007). Any increase in the superficial gas velocity leads to a significant increase in the liquid circulation velocity (Blazej et al., 2004b; van Benthum et al., 1999b). The basic guideline is that the bubble free regime exists as long as the downcomer superficial liquid velocity is lower than the average slip velocity (van Benthum et al., 1999a).

Once the gas is in the downcomer, the liquid has to flow even faster to cause circulation. Gas bubbles are still lighter than the liquid and have a buoyant force, which propels them to rise against the flow. The liquid phase momentum has to provide the power to overcome the buoyant force and create a net downward force in order to cause forward motion and eventual circulation. In effect, a

superficial liquid velocity exists at which gas bubbles can be suspended or are stagnant in the downcomer (regime 2 in Figure 6.4). Hence, this circulation regime is referred to as the transition regime.

When the liquid velocity in the downcomer is about equal to the average slip velocity, an approximate stationary bubble behavior can be observed. In addition, bubble-bubble interactions become more frequent, and liquid properties start to have more influence on reactor performance (Albijanic et al., 2007). Unlike regime 1, the liquid velocity does not deviate significantly and stays approximately constant in regime 2, but the transition regime is not very stable and minor variations in the superficial gas velocity can lead to regime transition. Unfortunately, a theoretical prediction of gas holdup is very challenging and experimental values vary over a wide range (van Benthum et al., 1999b). Regime 1 and the beginning of regime 2 can be described as homogeneous, while the later portion of regime 2 occurs in the bubble column transition flow regime described in Section 5.2 (Merchuk et al., 1998; van Benthum et al., 1999b).

If the downcomer liquid velocity is larger in magnitude than the bubble rise velocity, the bubble will circulate with the liquid (Albijanic et al., 2007). This minimum superficial liquid velocity usually occurs at U_{Gr} = 3.5-5.0 cm/s (Jones, 2007; Wei et al., 2008) and is described by thorough gas bubble circulation (complete bubble circulation regime – regime 3 in Figure 6.4). It should be noted that regime 3 is by far the most commonly encountered circulation regime. The required gas flow rate for pilot and industrial scale reactors requires very high superficial gas velocities, which all but guarantee circulation (Blazej et al., 2004b; Chisti, 1989). Bubble free (regime 1) and transition (regime 2) regimes are usually avoided because they have poor phase contacting, mixing, and selectivity (Wei et al., 2008). In addition, special attention and effort are required to keep the flow in the bubble free and transition regimes for an industrial-scale reactor.

Reactors operating in regime 1 or possibly early regime 2 are usually found when cultivating mammalian cell structures or highly shear sensitive microorganisms for which shear stress becomes the limiting operational factor; however, designers have found it easier to operate in non-standard designs, which at least partially circulate (see, for example, van Bentham et al. (1999a)).

The transition from regime 2 to regime 3 is not well understood. It is suspected that the transition is initiated by the gas phase entering the heterogeneous or transition flow regime identified for bubble columns. These flow regimes would produce larger bubbles with faster bubble rise velocities, which disengage easier, decrease the downcomer gas holdup, and increase the circulation driving force. This behavior is often confirmed with circulation starting and flow entering the transition flow regime at $U_{Gr} \approx 0.045$ m/s (Joshi et al., 1990; Merchuk et al., 1998). The faster liquid circulation velocity eventually surpasses the gas slip velocity in the downcomer, and gas bubbles are entrained in the downcomer flow. The circulating gas adds to the riser gas holdup, potentially reinforcing the trend.

Complications arise when/if the gas disengagement leads to a smaller riser gas holdup, such that the driving force is not heavily influenced. The gas disengagement process has some geometric influences which cause the transition to regime 3 to occur relatively early in the transition flow regime or well into the heterogeneous flow regime. A second complication is that the recirculated gas can lead to more frequent bubble collisions and coalescence so that the riser gas holdup may decrease early in regime 3 until the flow structure stabilizes. This case requires the downcomer gas holdup to decrease at a faster rate than the riser gas holdup. Otherwise, the circulation would stay in regime 2. This behavior makes circulation regime transition highly variable. Interestingly, the transition to regime 3 occurs at a gas holdup of 10-12% regardless of the bubble flow regime, and for reasons and through mechanisms which are not well understood at this time (van Benthum et al., 1999b). The liquid circulation velocity resumes its relationship in regime 3 and increases with

the riser superficial gas velocity. In general, the maximum downcomer gas holdup is about 20% (van Benthum et al., 1999b).

The riser superficial gas velocity at which transition occurs depends significantly on liquid properties. Generally, liquids containing surfactants or alcohols tend to experience circulation relatively early ($U_{Gr} \approx 0.035$ m/s) while water experiences it later ($U_{Gr} \approx 0.045$ m/s) (Albijanic et al., 2007; Jones, 2007; van Benthum et al., 1999b). Large bubbles, 3-5 mm in diameter, are not entrained in the downcomer in a water system until $U_{Gr} \approx 0.20$ m/s. Large, ellipsoidal bubbles at these velocities also form significant wakes which limit the effective interfacial area. This factor is almost always ignored in theoretical gas-liquid mass transfer coefficient correlations or models (Talvy et al., 2007).

A simple measure to correlate liquid circulation velocity to the superficial gas velocity would be through a power law such as (Bello et al., 1984; Merchuk, 1986):

$$U_{Lr} = \alpha U_{Gr}^{\beta} \tag{6.1}$$

where U_{Lr} and U_{Gr} are the riser superficial liquid and gas velocities, and α and β are fitted constants. The coefficient α depends on the reactor geometry and liquid properties while the exponent β is a function of the flow regime and reactor geometry. This base equation can be further enhanced, and terms can be added to account for specific properties or reactor design (Chisti, 1989). The fitted terms are usually positive, implying that the liquid circulation velocity increases with increasing superficial gas velocity; however, if slugging, choking, or throttling occurs, the liquid circulation velocity can actually decrease with increasing superficial gas velocity (Jones, 2007).

A more detailed correlation could be arrived at by accounting for each force. For example, one could balance the hydrostatic pressure difference to reactor specific pressure drops (e.g., head losses due to wall friction, elbows, bends, etc.). This approach would be based on a theoretical foundation, but attempts have not been very successful due to the specific geometric dependence, and empirical correlations are still the most practical approach (Albijanic et al., 2007; Chisti, 1989).

Analysis could be skewed to favor riser versus downcomer data due to the riser cross-sectional area usually being larger than that of the downcomer. A better strategy would be to analyze each section separately. One approach is to assume a large degree of independence, which would work relatively well if the controlling factors in each section are independent of the other. A large effective riser diameter would not impact the riser gas holdup and would cause the riser gas holdup behavior to be a function of just the gas flow rate and liquid properties. A small downcomer diameter, on the other hand, could cause the downcomer to enter the slug flow regime, which would limit circulation. Even larger downcomer diameters can be affected by trapped gas, which can grow with superficial gas velocity. The effect could be a reduction in the effective downcomer cross-sectional area and possible flow choking (Chisti, 1989; Jones, 2007). A single correlation does not take these interactions into account.

6.3 Configuration

The specific reactor configuration has a significant effect on gas holdup and gas-liquid mass transfer performance, as can be seen in Figure 6.5. Other factors, such as downcomer-to-riser cross-sectional area ratio or the gas separator design, can also play significant roles. For example, external-loop airlift reactors use gas separators that allow more time for the gas phase to disengage than in internal-loop airlift reactors. Hence, the downcomer in ELALRs has a negative effect on global or total gas holdup and gas-liquid mass transfer.

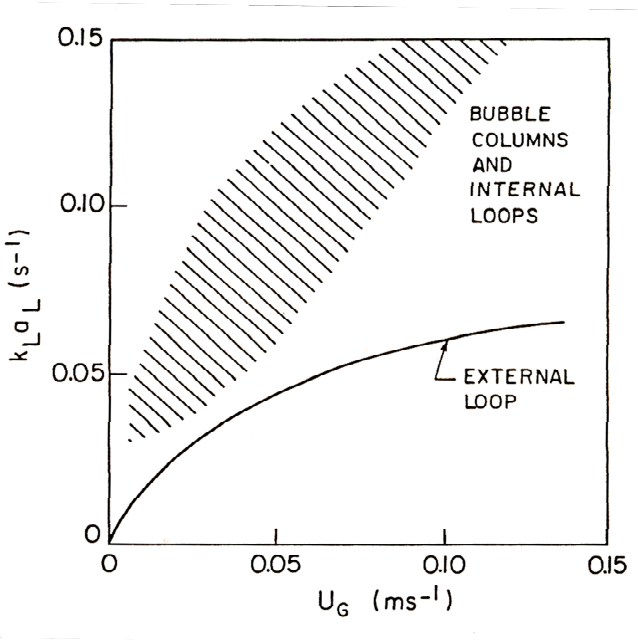

Figure 6.5: Achievable gas-liquid mass transfer in bubble columns and internal-loops versus external-loops (Chisti, 1989).

Furthermore, airlift reactor studies often use an effective riser diameter that is less than 0.15 m, which has been shown to influence the bubble size distribution in bubble columns (Kantarci et al., 2005). Not surprisingly, research work which compares ALR designs based on the reactor diameter use smaller riser and downcomer columns, and find a strong reactor diameter dependence, noting that bubble diameters increase with reactor size (Ruen-ngam et al., 2008). The reactor (riser) diameter effect is expected to be very similar to that of bubble columns, which has been reviewed in Section 5.3.1.

The reactor base is usually not discussed. The understanding is that as long as the base does not interfere with flow and increase frictional losses, one does not pay attention to it; however, some evidence exists that curved or filled bottoms may promote this limited impact (Chisti, 1989). With this in mind, the base height has a minimal impact on ALR operation as well. The only restriction is that a short base height can cause a large pressure drop, which would increase the operational cost. In such a case, gas holdup is expected to increase with bottom clearance (Al-Masry, 1999). Luckily for designers, a restrictive bottom clearance in the experimental scale is often self-corrected during

scaleup such that minimal problems are encountered in the pilot or industrial stage. None of the presented correlations at the end of this chapter attempt to reflect the bottom designs in any form.

6.3.1 Reactor Height

The reactor height can be defined in two ways. The first definition is often termed the effective reactor height and is defined as the distance between the base and the bottom of the gas separator. The second is the unaerated liquid height, which is defined as the distance from the base to the fluid surface prior to aeration. These definitions can be seen in Figure 6.6 for the internal- and external-loop airlift reactor.

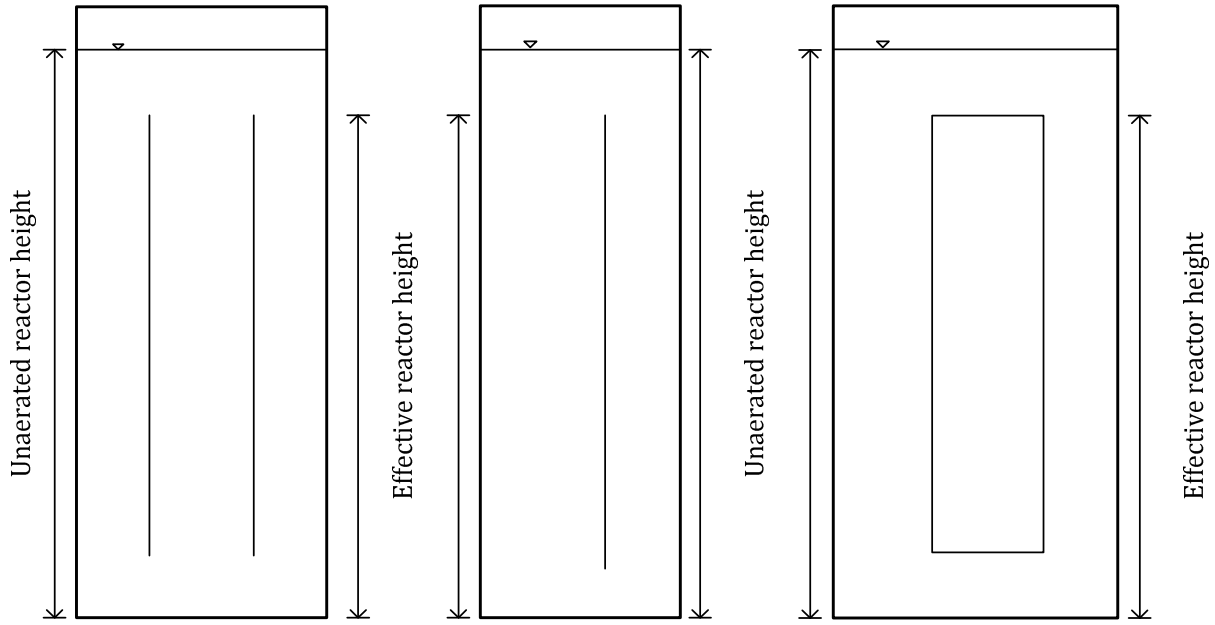

Figure 6.6: Airlift reactor component definitions.

The effective reactor height influences the circulation path, which has many hydrodynamic implications as implied by the liquid circulation velocity defined by Blenke (1979):

$$U_{Lc} = \frac{x_c}{t_c} \tag{6.2}$$

where U_{Lc}, x_c, and t_c are the liquid circulation velocity, circulation path length, and circulation time, respectively. By changing the reactor height, the circulation path length changes. The circulation

length path influences the liquid circulation velocity, gas disengagement, and the hydraulic pressure difference, which drives the circulation flow. As the circulation length path increases, the liquid circulation velocity is expected to increase. The result would be an increase in gas disengagement and decrease in gas holdup and gas-liquid mass transfer. At the same time, a long circulation path or time could be dangerous because it could lead to spent gas or minimal surface renewal in the downcomer (Talvy et al., 2007), possibly leading to microorganism starvation. It should be noted that the circulation time is largely influenced by the riser and downcomer residence times, while the separator and base residence times are oftentimes ignored (Joshi et al., 1990).

Bentifraouine et al. (1997a) varied the effective reactor height from 1-1.6 m and observed a significant increase in the superficial liquid velocity, which was attributed to an increase in the hydrostatic pressure differential. They also concluded that the increase in superficial gas velocity caused a decrease in the gas phase residence time and, hence, gas holdup; however, the other possibility is that the faster liquid velocity is able to prevent the gas from disengaging and may lead to higher gas residence time. This was observed by Snape et al. (1995) who concluded that gas holdup increased and superficial liquid velocity varied minimally with increasing reactor height. In other words, the effective reactor height's influence is dependent on the liquid flow regime and liquid velocities; however, gas-liquid mass transfer is usually seen as increasing with the effective reactor height (Siegel and Merchuk, 1988) unless gas holdup decreases significantly as well. It should be noted that the risk of recirculating used gas increases with higher liquid circulation velocity.

The effect of the unaerated liquid height is more complicated. If the unaerated liquid height was less than the effective reactor height, an increase in the unaerated liquid height would lead to an increase in the superficial liquid velocity and decrease in gas holdup (Bentifraouine et al., 1997a, 1997b; Wei et al., 2008). If, on the other hand, the unaerated liquid height was equal to or greater

than the effective reactor height, gas holdup, superficial liquid velocity, and, hence, ALR operation are not affected (Bentifraouine et al., 1997a, 1997b; Snape et al., 1995).

Wei et al. (2008) concluded that the unaerated liquid height had a negligible influence in the transition from the bubble free (regime 1) to the transition regime (regime 2), but had a very important influence in the shift from the transition to complete bubble circulation regime (regime 3). Bubbles were entrained in the downcomer at approximately the same superficial gas velocity, regardless of unaerated liquid height; however, the flow resistance decreased with increased unaerated liquid height such that bubble penetration also increased in the downcomer, which led to an earlier transition into the complete bubble circulation regime.

The reactor height is often presented in the form of the riser aspect ratio (h_R/d_R). The effect of riser aspect ratio is expected to depend on the gas flow and gas circulation rate. An increase in the riser aspect ratio does not significantly change the liquid circulation velocity. Therefore, the circulation path length and circulation time increases with increasing riser aspect ratio, which allows the gas phase to achieve its equilibrium bubble diameter more efficiently.

If the superficial gas velocity and gas circulation rate are low, such that bubble-bubble interaction is low as well, an increase in the riser aspect ratio is expected to increase the average bubble diameter, decrease the gas holdup, and decrease the gas-liquid mass transfer coefficient. This effect occurs until the reactor is tall enough to achieve equilibrium. Bubble columns achieve this at an aspect ratio of approximately 5 and height of 1-3 m. The airlift reactor, especially the external-loop variant, is expected to require a higher riser aspect ratio due to the limited axial velocity variations. Evidence suggests that the superficial gas velocity is an important variable in this determination and a decrease in gas holdup may be observed up to a riser aspect ratio of 20-40. Therefore, it is fairly common to observe bubble size variations with reactor height in both the draught tube and external-loop airlift reactor (Ruen-ngam et al., 2008). If, on the other hand, the

superficial gas velocity and gas circulation rate is relatively fast, a riser aspect ratio much less than 20 shows a negligible influence (Joshi et al., 1990).

6.3.2 Area Ratio

The area ratio is defined as the ratio of downcomer to riser cross-sectional area, but can also be represented by a downcomer to riser hydraulic diameter ratio. It is a simple representation of the flow restriction that exists in the reactor design since wall friction is of little importance unless viscosity is significantly increased (Chisti, 1989).

The area ratio influences the liquid circulation rate by adjusting the flow restriction. If the downcomer diameter or area ratio is reduced too much, the liquid flow becomes restricted and the liquid circulation velocity is expected to decrease. According to Eqn. (6.2), the gas phase could follow for the same circulation path length (x_c) but the circulation time (t_c) could increase, which would lead to higher gas-liquid mass transfer (Blenke, 1979). Mere scale can have a perceived influence as well, and studies using area ratios higher than 0.25 on the pilot and industrial scale do not observe any restrictive effects. In general, frictional losses decrease with increasing scale such that the losses in a 10.5 liter ILALR are four times higher than those observed in a geometrically similar 200 liter ILALR (Blazej et al., 2004b). Generally, correlations model the area ratio with a negative exponent, meaning that an increase in the downcomer-to-riser area ratio leads to a decrease in gas holdup and the gas-liquid mass transfer coefficient (Garcia-Ochoa and Gomez, 2009); however, very large or very small area ratios often do not follow this rule.

An excessive reduction in the downcomer diameter (very low area ratio) would be too restrictive and reduce the liquid velocity such that the gas phase could easily disengage, which would reduce the amount of available gas (gas holdup), the driving force, and gas-liquid mass transfer. In other words, a restrained system would decrease the liquid circulation velocity, driving force, gas holdup, and gas-liquid mass transfer by decreasing the area ratio. In general, research work has not focused on area ratios below 0.10 with the exception of Jones (2007) who used an

ELALR with an area ratio of 0.063. Popovic and Robinson (1984) confirmed this by increasing the area ratio from 0.11 to 0.44, which increased the superficial liquid velocity about four-fold. Airlift reactors are defined by the riser and very large area ratios result in bubble column-like performance; hence, area ratios beyond 4.0 are rarely used.

Valves are occasionally used to adjust the area ratio for experimentation, such as the research by Bendjaballah et al. (1999). They closed the valve from fully to 40% open without major effects on gas holdup. This would lead to the conclusion that an optimum area ratio exists, which does not impact gas holdup and also minimizes cost. The optimum ratio may not be easily determined since it depends on the scale and operating range, and the installation of a restrictive valve in the downcomer (assuming the optimum area ratio is below the valve-free area ratio) would provide the necessary flexibility and means to get there (Weiland, 1984). Additional losses and dynamics would be introduced by the valve and must also be addressed.

If circulation is a major design goal, Joshi et al. (1990) concluded that an area ratio of about one maximizes the liquid circulation rate in a 10 m^3 volume reactor regardless of sparger location. If the reactor volume is increased to 100 m^3, the optimum area ratio increases to 2. When the area ratio is adjusted, the circulation velocity monotonically decreases with increasing area ratio. In Joshi's work, a reactor with V_L = 10 m^3, h_R/d_R = 40, and P/V_L = 0.3 kW/m^3 experienced a liquid circulation velocity decrease from 3.0 to 0.5 m/s when the area ratio increased from 0.25 to 4.0. The higher liquid velocities at lower area ratio also introduced circulation instabilities, which disappeared at A_d/A_r = 0.3 at 10 m^3 and A_d/A_r = 0.5 at 100 m^3. Hence, a stable and optimum area ratio can be achieved with a riser-to-downcomer diameter ratio of about 1.41 (Joshi et al., 1990). Variations exist for the draught tube internal-loop and external-loop airlift reactor, which depend on the maximizing characteristic and are presented in Section 6.3.4 and 6.3.5, respectively.

6.3.3 Gas Separator

The gas separator is an important design feature which is often ignored. The simple reason is that internal-loop airlift reactors have only a few options, and the design is essentially the same: a vented headspace, which is similar to the tank separator shown in Figure 6.7c. The external-loop airlift reactor, however, is presented with additional design options (shown in Figure 6.7a and 6.7b), which provides the external-loop airlift reactor with some advantages for certain processes.

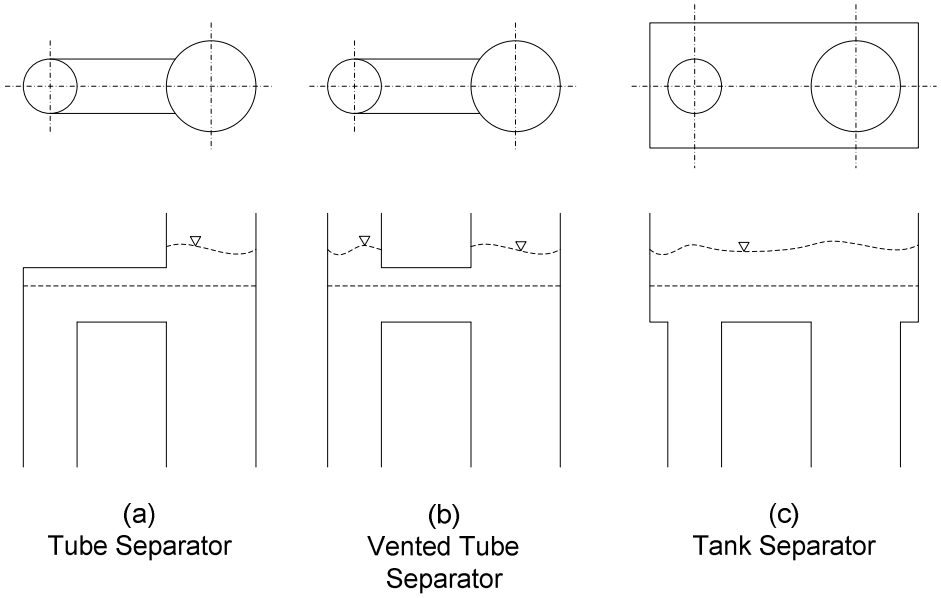

Figure 6.7: Common gas separator designs for external-loop airlift reactors (Jones, 2007).

The tank separator (Figure 6.7c) is the simplest and most common design and is used for both the ELALR and ILALR. It is usually a simple, rectangular vented box that connects the riser to the downcomer. The tank separator, however, has a negative effect in the ELALR. It increases the available gas separation area and gas separator residence time relative to a comparable ILALR design. If a comparison is made between an ELALR and ILALR on the basis of unaerated liquid height, the ELALR will have a shallower separator liquid height and higher rate of gas disengagement. Hence, the ELALR is often cited to have a lower gas holdup and gas-liquid mass transfer performance, as shown in Figure 6.5, but also higher liquid circulation velocity (Chisti, 1989).

The unaerated liquid level is an important feature. Liquid circulation can usually be achieved by injecting more gas and ensuring a sufficiently high aerated fluid level; however, in some extreme cases, additional gas would not cause additional circulation or could actually suppress circulation to the point of no liquid circulation. This may occur when the aerated liquid level is too shallow in the gas separator such that complete gas disengagement is promoted. Therefore, increasing the liquid level to a minimal operational level would allow gas-phase circulation (Merchuk et al., 1999). The operator is expected to have the ability to add enough liquid to have control, and, naturally, research has not gone towards quantifying the necessary unaerated liquid height.

More importantly for operation, the gas residence time in the separator controls disengagement such that decreasing the gas residence time in this region would lead to an increase in the downcomer gas holdup, which could decrease the hydraulic pressure differential and liquid circulation velocity (Siegel et al., 1986). The negative effect would be if the gas residence time in the separator is too long such that gas easily disengages and causes a decrease in gas holdup and gas-liquid mass transfer (Al-Masry, 1999).

One cannot easily quantify the critical fluid level since it is highly dependent on liquid properties, but a simple guideline can be used. If the gas separator residence time is longer than the minimum separation time (time required for the average bubble to rise from the top of the riser to the liquid surface), gas disengagement is encouraged (Al-Masry, 1999). In other words, the separator would encourage gas detachment if bubbles are allowed to spend enough time in the gas separator to rise to the surface given their bubble rise velocity. Hence, increasing the superficial gas velocity could increase the bubble rise velocity and decrease the minimum separation time. Luckily for ELALR operators, this design allows liquid circulation velocity adjustments (Chisti, 1989) so that the described situation may be offset. The gas separator, however, is sometimes designed to decrease the liquid velocity such that spent gas disengages more readily. Such a system might

require a second sparger in the downcomer in order to provide sufficient gas for microorganism viability (Merchuk et al., 1999).

A system specific operational rule could be introduced based on a ratio between tank separator volume to total reactor volume. An optimum volume ratio is expected to minimize power input without affecting downcomer gas holdup, which would lower operational cost and optimize output. Al-Masry (1999) varied separator volume in air-water and air-glycerol systems from 0-37%. He found that the optimum ratio, based on hydrodynamics and power input, was 11% for the air-water system. Increasing the volume ratio did not lead to significantly higher riser or downcomer gas holdup. Decreasing the volume ratio produced higher gas holdup, but it also led to much lower liquid circulation velocities. The air-glycerol system proved more difficult due to coalescence, and a volume ratio of 0% failed to lead to circulation until U_{Gr} = 0.08 m/s. Hence, the airlift reactor acted as a bubble column. Increasing the volume ratio beyond 7% would cause negative effects such that gas holdup was minimal at 37%. The liquid circulation velocity in the air-glycerol system was much lower than in the air-water system, which made the air-water system hydrodynamically superior.

The other gas separator designs offer an alternative such that the gas separator residence time is limited. The (closed) tube (Figure 6.7a) and vented tube (Figure 6.7b) represent the same idea. The tube separator is a simple design that basically increases the separator liquid height (assuming comparable volume as with a tank separator), which increases the amount of time required for bubbles to reach the surface and disengage from the liquid phase; however, in reality, it works too well. Gas often fails to disengage completely and tends to build in the connector and eventually in the downcomer. This accumulation leads to flow choking and reduces the liquid circulation velocity. Another way to interpret the gas accumulation is that it reduces the effective downcomer-to-riser area ratio. Making the situation worse, the downcomer can enter the plug flow regime. Gas holdup increases, but the representative bubbles are very large and gas-liquid mass transfer suffers

greatly. Ultimately, the connector and downcomer could be completely choked, at which point the airlift reactor acts just like a bubble column (Jones, 2007).

The vented tube connector minimizes the problem of gas accumulation, and gas is allowed to separate fairly efficiently. Unfortunately for some processes, the additional separator volume increases the gas separation efficiency relative to an internal-loop airlift reactor for the same reasons as for the tank separator; however, the liquid circulation velocity keeps increasing with superficial gas velocity without a local maximum (Bentifraouine et al., 1997a; Choi, 2001), which may be advantageous for some processes. The vented tube separator is also susceptible to the risk of operating in the slug flow regime and the formation of very large bubbles, which can choke the downcomer flow (Jones, 2007).

The vented tube separator, in turn, can be improved with the introduction of a valve, which allows the overhead pressure to be varied. The valve would introduce an additional circulation control mechanism. As the valve closes, the overhead pressure would increase, and the gas would not disengage as readily. The assumption is that gas disengages too easily in the vented state, while it almost fails to disengage in the tube separator (Jones, 2007; van Benthum et al., 1999a), which a closed valve would imitate. Hence, the optimum would be somewhere in the middle, and a valve adjustment would allow this operational point to be reached. If the initial assumption does not hold true for the design, the valve addition to the vented tube separator would not improve operation.

The connector length (vented or closed) is expected to decrease the separator liquid height and minimum separation time and increase the separation efficiency (Choi and Lee, 1993). Hence, the liquid circulation velocity increases with a longer connector length, which leads to a decrease in downcomer gas holdup. The gas-liquid mass transfer coefficient also decreases with downcomer gas holdup for similar reasons (Choi, 2001). Frictional losses would also increase, but wall losses can be ignored for water-like substances and would only be important in highly viscous liquids (Chisti, 1989).

The flow in the separator is much different than the other airlift components. The riser and downcomer have very well defined flow without backmixing. The separator, on the other hand, has defined regions of up- and down-flow. As with the bubble column, the up-flow region was present in the central region while the down-flow region occurs near the wall. The results are that a stagnant region is present between these flow regions, which may lead to bubble coalescence, and a lower liquid velocity in the separator than in the top of the riser (Lo and Hwang, 2003).

6.3.4 Internal-Loop Airlift Reactor

The internal-loop airlift reactor is a very simple design that presents some advantages for gas-liquid mass transfer. The two basic variants, shown in Figure 6.1, include a vessel separated by a full baffle and a draught tube internal-loop airlift reactor. Regardless of the variant, the internal airlift reactor has very similar gas holdup characteristics to that of a bubble column, as long as the comparison is made within the bubble column's feasible superficial gas velocity range. This similarity is due to the fact that the downcomer gas holdup is 80-95% of the riser gas holdup, and the riser gas holdup is comparable to that of the bubble column. Hence, the global or total ILALR gas holdup is very similar to that of the bubble column (Bello et al., 1984; van Benthum et al., 1999b).

The draught tube ILALR (DT-ILALR) is more efficient than the baffled ILALR at gas-liquid mass transfer, and much more research has been directed towards this variant. This imbalance is due to the advantage that the gas residence time may be up to twice as long in the DT-ILALR than in the baffled ILALR. As a matter of fact, a majority of the correlations for ILALRs, which are presented in Table 6.1 and 6.2, have been developed using draught tubes. The baffled ILALR is usually used to study hydrodynamic behavior. Industrial application seems to be dominated by draught tube ILALRs as well. Baffled ILALRs are a little cheaper, but the advantages of the draught tube far outweigh the costs.

Since the gas phase spends more time in the liquid phase, gas-liquid mass transfer in the ILALR is usually higher than the ELALR (Shariati et al., 2007). Gas-liquid mass transfer coefficients in DT-ILALRs are even slightly higher than in bubble columns due to higher operating gas flow rates. The draught tube diameter can be optimized to minimize costs and maximize a desired variable. General guidelines have been developed for different applications using a draught tube to column diameter ratio (d_D/d_R). A ratio of 0.8-0.9 maximizes mixing and mass transfer. A range of 0.5-0.6 maximizes circulation while 0.6-1.0 minimizes the mixing time (Chisti, 1989). The problem for microorganism applications and the mass transfer guideline (d_D/d_R = 0.8-0.9) is that the downcomer provides minimal contribution to global gas-liquid mass transfer or gas holdup, which runs the risk of starving the microorganisms. If microorganism gas consumption in the downcomer is important, the operator has basically two solutions. First, circulation has to become more important. A tradeoff would have to be struck and the ratio (d_D/d_R) be reduced. The result would be that the microorganisms could spend less time in the oxygen deprived environment or the circulation could be designed to entrain more gas in the downcomer. Second, the microorganisms could be suspended. If the microorganisms are sensitive to shear, they can be suspended in the downcomer. If, on the other hand, the microorganisms require lots of gas, they could be suspended in the riser. Suspension could involve packed particles, porous media, etc.

6.3.5 External-Loop Airlift Reactor

The external-loop airlift reactor has a wide array of variants ranging from the fairly simple, shown in Figure 6.2, to quite complex multistage designs. An important advantage is that the design allows access to all major reactor components, which is a great benefit for troubleshooting reactor performance or visualization (Merchuk et al., 1999); however, this advantage is often not enough, and the ELALR is typically limited for use with shear sensitive cells, photosynthetic microorganisms like algae, or processes requiring fluid recirculation. For example, mammalian cell structure can usually tolerate shear stresses in the range of 0.05-500 N/m^2 (Chisti, 1989), but the sensitivity is

highly variable with cell structure and density such that cells could be highly shear sensitive at low cell density and somewhat resistant at higher densities (Martin and Vermette, 2005). Hence, the reactor operating conditions need to be flexible enough to adjust from very low shear conditions and still potentially operate with a high degree of turbulence (high shear stress).

Stirred tank reactors (discussed in Chapter 4) usually create shear stresses much larger than those that can be tolerated by mammalian cells, and bubble column reactors (discussed in Chapter 5) and ILALRs may reach the high end of the spectrum at best. Bubble-bubble interactions, especially bubble bursts or breakup, create high local shear stresses, which have a negative impact on mammalian cell growth. ELALRs, on the other hand, can maintain low shear rates while still providing a respectable oxygen transfer of 0.6-1.0 mmol/(L min) (Chisti, 1989), which is sufficient even for human skin (0.0011 mmol/(L min) at 10^6 cells/ml) and liver cells (0.005 mmol/(L min) at 10^6 cells/ml) (Martin and Vermette, 2005). This is doable using minimal circulation in the downcomer, and cell suspension on packed material in the lower portion of the downcomer. The cells have minimal bubble-bubble interactions and usually have enough oxygen for growth and liquid flow for waste disposal.

Nonetheless, cell density can become a major problem. For example, mammalian cells are usually 100 μm within a blood capillary for oxygen transfer. Therefore, nature has provided a design limitation. Cells can only be 150-200 μm away from an oxygen source, such as dissolved oxygen in a liquid, because oxygen has a maximum diffusion depth of about 240 μm for cellular material. This may limit the cell density and, in turn, the operational gas flow or local shear rate. Some production problems of critical cells are mitigated by cellular design. Connective tissue cells are elongated and form low density cell structures, while some critical ones, such as liver or kidney cells, operate at high density, but also form many more blood capillaries (Martin and Vermette, 2005). In other words, the ELALR provides the possible production of a wide array of mammalian cell structures as well as shear sensitive microorganism byproducts.

The ELALR can be used for these processes because gas disengagement is very efficient. The bubbles have a relatively fast rise velocity and slow radial velocity. Hence, bubble-bubble interactions are diminished in the ELALR relative to the bubble column or stirred tank reactor, which, in turn, leads to higher gas holdup sensitivity to liquid property variations in bubble columns than in ELALRs (Chisti, 1989; Joshi et al., 1990; Shariati et al., 2007). In other words, the bubble-bubble collision frequency is lower in ELALRs, which makes coalescence adjusting liquid properties, such as viscosity, surface tension, or ionic strength, less important. So, while bubble column and internal-loop airlift reactor gas holdup are usually similar, the downcomer gas holdup in an external-loop airlift reactor is only 0-50% of the riser gas holdup (Bello et al., 1984), which leads to much lower global gas holdup in ELALRs.

The reactor geometry effects in an ELALR can be quite complex and dynamic. As the area ratio increases, the liquid circulation velocity decreases. Hence, the gas phase circulation time decreases and gas holdup increases. The increase in gas holdup leads to an increase in the interfacial area. Some bubble dynamics are reflected in the growth, but, due to the lower bubble-bubble interactions in ELALRs, the increase is fairly continuous, but at a relatively slow rate. For example, Joshi et al. (1990) showed that by increasing the area ratio from 0.25 to 1.0 using a 10 m^3 ELALR at 0.3 kW/m^3 yielded a negligible increase in the interfacial area while a further increase in area ratio to 4.0 increased the interfacial area by about 30%.

The area ratio effects on the liquid-phase mass transfer coefficient are more difficult to predict. Area ratio effects are usually studied by keeping the reactor volume constant, which requires the effective reactor height to be adjusted. As the height is increased, the interfacial solute gas concentration increases as well, which decreases the gas solubility and, in turn, the liquid-phase mass transfer coefficient. In addition, an increase in the area ratio decreases the liquid circulation rate, which increases gas holdup, but may decrease surface renewal. The greater height also raises the pressure drop and power consumption, which increases surface renewal and the liquid-phase

mass transfer coefficient. The extent of these effects is dependent on the operational scale and power level, and it is hard to predict which of the two will dominate.

For example, at a power consumption of 0.3 kW/m^3, Joshi et al. (1990) observed a local maximum when V_L = 10 m^3; this led to the conclusion that the decrease in gas solubility and surface renewal due to the liquid circulation velocity decline was not dominant until the area ratio was increased to about 0.5. The decline, though, was somewhat gradual. At a power consumption of 0.6 kW/m^3, a local maximum was not observed, which suggested the solubility effect was stronger; however, the gas-liquid mass transfer coefficient was about 50% higher at 0.6 kW/m^3 than at 0.3 kW/m^3, which was attributed to a doubling of the interfacial area. Hence, Joshi et al. (1990) concluded that the solubility decrease must have played a more significant role.

6.4 Liquid Properties

Bubble columns and airlift reactors have very similar reaction to liquid properties. Therefore, the information provided and conclusions made in Section 5.5 are applicable for airlift reactors as well.

6.4.1 Viscosity

An increase in viscosity has a much stronger effect on external-loop than internal-loop airlift reactors. At higher viscosities, the lower gas holdup in ILALR is attributed to the lower bubble rise velocity, which causes the bubbles to have a longer circulation time. At lower increases in viscosity, gas entrapment into the downcomer actually becomes easier and may increase gas holdup slightly. This behavior has been observed with a 25% glycerol concentration (Hallaile, 1993). It has also been reported that a viscosity increase in the range of 1.54-19.5 mPa s has a minimal effect on liquid circulation rate and mixing time inside a draught tube airlift reactor (Molina et al., 1999). The experience in the ELALR, however, is opposite. The bubble disengagement efficiency increases because the bubble residence time in the gas separator increases significantly. The result is that if

the viscosity is increased to 14 mPa s through the addition of glycerol, the ELALR experiences a severe gas holdup decrease (McManamey and Wase, 1986; Shariati et al., 2007).

6.4.2 Surface Tension and Additives

Alcohol addition to airlift reactors causes larger amounts of gas being entrained into the downcomer. Hence, the liquid velocity is reduced, and circulation time is increased relative to pure water. The resulting gas holdup and gas-liquid mass transfer tend to be higher. Albijanic et al. (2007) tested the carbon chain length hypothesis, as defined by Zahradnik et al. (1999b), in a draught tube airlift reactor. The circulation time, shown in Figure 6.8, deviated as expected, but only up to 0.07 m/s after which the circulation time converged to a similar value regardless of the aqueous solution. This result was attributed to the downcomer gas holdup in the 1 wt% methanol and n-butanol solutions being 2 and 2.7 times higher than with tap water at U_G = 0.04 m/s. Freitas et al. (2001) detected similar behavior using an aqueous ethanol solution; however, the gas-liquid mass transfer coefficient increased only slightly at U_{Gr} < 0.075 m/s, but was 1.5-2 times higher at higher riser superficial gas velocities. This trend would cease at approximately U_{Gr} = 0.167 m/s because the collision frequency increased sufficiently to allow coalescence to occur more readily and counteract the increasing gas holdup.

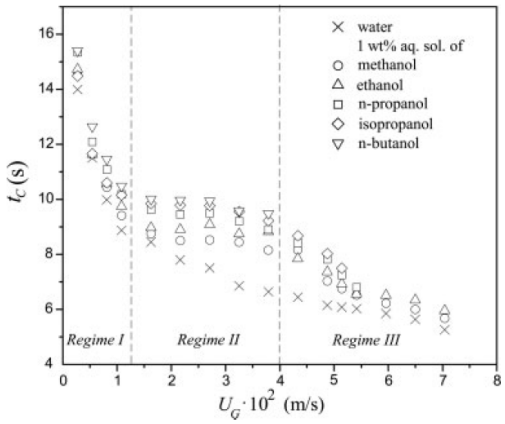

Figure 6.8: Circulation time dependence on alcohol type and superficial gas velocity (Albijanic et al., 2007).

The experimental gas-liquid mass transfer data of Albijanic et al. (2007) are shown in Figure 6.9 for U_{Gr} < 0.05 m/s. The results for the superficial gas velocity at which the circulation time converged were not presented. It is speculated that a convergence to a common gas-liquid mass transfer coefficient would be reached at higher superficial gas velocities, as is suggested by the results presented by Freitas et al. (2001). It should be noted that Albijanic et al. (2007) used a d_D/d_R ratio of 0.51. Gas holdup and gas-liquid mass transfer performance could be optimized at a higher diameter ratio (Chisti, 1989).

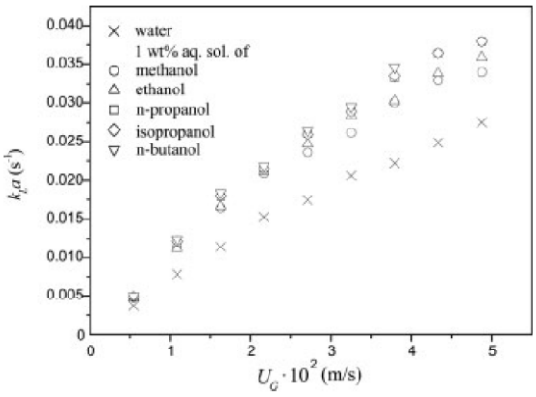

Figure 6.9: Experimental gas-liquid mass transfer coefficient dependence on alcohol type and superficial gas velocity (Albijanic et al., 2007).

6.5 Solid/Slurry Phase Properties

Gas-liquid mass transfer studies in three phase airlift reactors are limited (Freitas and Teixeira, 2001; Muthukumar and Velan, 2006; Nicolella et al., 1998b). A significant amount of information and conclusions are therefore drawn from the slurry bubble column studies and are expected to apply to airlift reactors.

The gas-liquid-solid airlift reactor has a huge advantage for particle suspension (Gjaltema et al., 1997a). Since phase backmixing is limited (Giovannettone et al., 2009), the liquid phase has a clear flow path, which makes suspension much easier and possible at lower gas flow rates (Merchuk et al., 1999). In addition, the low shear rates present in ALRs allow biofilms to grow easier and faster on suspended particles (Gjaltema et al., 1997a; Gjaltema et al., 1997b).

It is also thought that solids decrease gas holdup and gas-liquid mass transfer, especially in the heterogeneous flow regime, due to a decrease in turbulence. Gas-liquid mass transfer correlations for gas-liquid airlift reactors may be applied to gas-liquid-solid airlift reactors if the density difference between the solid and liquid phase is small or if the apparent viscosity is similar, as with bubble column reactors; however, such action does not account for any solid phase effects on the bubble interface, possible surface reaction, and often provides highly variable results. The ability to extend gas-liquid mass transfer correlations in ALRs to gas-liquid-solid systems is due to the particles being fluidized readily and having similar flow behavior if the density difference is small enough. In other words, the particles blend in (van Benthum et al., 2000). The minimal phase backmixing in airlift reactors can add additional complications because the solid distribution may be skewed towards the lower portion of the riser and downcomer. This accumulation may cause a higher rate of coalescence and, in turn, smaller interfacial area and gas-liquid mass transfer coefficients (Freitas and Teixeira, 2001).

The effect and understanding of solid loading on gas-liquid interactions is currently ambiguous, contradictory, or inadequate and requires further research. The main reason is that recent work has shown an important correlation between the dominant flow regime and bubble-particle interactions. In the case of low solids loading (less than 5% by volume), a slurry bubble column indeed acts like a bubble column. As the solids loading increases, the behavior of the SBC starts to deviate from that of the BC. For solids loading up to 25% by volume, the gas holdup decreases significantly. Beyond this concentration, gas holdup increases slightly as small bubbles start to accumulate because of the decrease the bubble rise velocity (Kantarci et al., 2005; van Benthum et al., 2000). This observation is often attributed to a significant increase in the apparent viscosity once the solid holdup increases beyond 20% (van Benthum et al., 2000). This experience is reflected in airlift reactor studies, with some minor differences. Small amounts of drag-reducing polymers could actually enhance fluidization and recirculation, especially in airlift reactors (Chisti,

1989). Airlift reactors tend to have less phase backmixing, and an increase in solid holdup often results in an increase phase buildup in the reactor base and wall regions (Freitas and Teixeira, 2001; Trilleros et al., 2005).

Solid loading shifts the regime transition for the internal-loop airlift reactor to an earlier superficial gas velocity, such that only the complete bubble circulation regime can be observed with high solid loadings. Solid loading also has a strong effect on gas holdup, especially when the solid loading is greater than 20% by volume. It is suspected that a higher solid loading increases the apparent viscosity, which leads to larger bubbles and an increase in the bubble rise velocity. The result is that bubbles spend more time in the gas separator and disengage more efficiently. Hence, the downcomer gas holdup decreases faster than the riser gas holdup (riser gas holdup could even increase), which leads to a higher gas holdup differential and larger circulation driving force (van Benthum et al., 1999b).

Another option is that solids affect flow stability. Low solid loading ($c_s \leq 3\%$ where c_s is the solid volume fraction) tends to stabilize the homogeneous flow regime, increasing the critical flow rate and gas holdup 11-13%, while higher loading ($c_s > 3\%$) leads to instability. At much higher solid loading ($c_s > 20\%$), the solid phase decreases gas-liquid mass transfer by simply occupying too much volume. In effect, bubble-bubble interactions are increased and coalescence is encouraged (Mena et al., 2005). For example, Lu et al. (1995) observed a gas holdup decrease in the downcomer-to-riser gas holdup ratio from 0.88 to 0.68 when solid holdup was increased from 0 to 30%. Van Bentham et al. (1999a) observed a similar trend. Freitas et al. (2001) studied solid loading effects on gas-liquid mass transfer in airlift reactors and observed a decrease of 40 and 60% at solid loading of 20 and 30%, respectively. This may be important if the process requires operation in a specific flow regime. The current problem with gas-liquid-solid systems is that these effects work in parallel. The nature of the relationship is not well-understood such that solids may

increase, decrease, or have a neutral effect on gas holdup and gas-liquid mass transfer, which has led to a variety of discussions, results, and conclusions.

The particle type and size can have a positive effect as it does with the stirred tank reactor. If the particle is wettable, a repelling force is observed against the gas phase, which creates a buffer zone between gas bubbles (Kluytmans et al., 2001), slows film drainage, and suppresses bubble coalescence (Mena et al., 2005). Hence, wettable particles usually increase gas holdup while non-wettable particles decrease it.

Airlift reactor studies examining particle size effects are limited, and the existing research agrees fairly well with the bubble column data. The only problem is that the lack of three phase airlift studies also limits the extent of covered material. Hence, specific conclusions for airlift reactors have been made mostly using bubble column studies and their conclusions. Particles are thought to be too big to contribute to gas-liquid mass transfer in a positive way and simply increase the apparent viscosity; however, fine particles with a particle diameter less than 10 μm are able to penetrate the bubble surface (creating smaller bubbles), increase film density (suppressing bubble coalescence and decreasing bubble rise velocity) (Kluytmans et al., 2001; Mena et al., 2005; Sada et al., 1986), or create reactions at the bubble interface. Another possibility is that the smaller particles stick to the bubble interface, which would block or diminish surface reactions or physically create a resistance to mass transfer. At the same time, the nested particles could increase the active area or destabilize the bubble interface. Very large particles are thought to decrease the bubble rise velocity and increase gas holdup by simply being in the way (Beenackers and Van Swaaij, 1993; Muthukumar and Velan, 2006). The other option is that different effects or studied particle sizes simply have a limited influence on gas-liquid mass transfer (Nicolella et al., 1998a). Studies using fibers would also be of interest in airlift reactors because it could shed more light on the circulation behavior and transition requirements if the microorganism shows flocculation behavior.

6.6 Sparger Design

Gas distributors used in airlift reactors are very similar to those used in bubble columns and include sintered, perforated (most common), or porous plates, membrane or ring-type distributors, arm spargers, and single-orifice nozzles. Airlift reactors may also use ring spargers that are used with stirred tank reactors and bubble columns. Ring spargers are able to produce uniform and stable flow, but are usually unable to produce small bubbles (Deckwer, 1992) and lead to an early transition to heterogeneous flow regime when compared to perforated plates (Schumpe and Grund, 1986). If the sparger is placed within the riser in an airlift reactor, the sparger is often a perforated tube or ring that attempts to mimic the perforated plate performance.

The sparger effect is more pronounced for U_G < 0.15 m/s while it is much less important at U_G > 0.20 m/s and nonexistent at U_G > 0.30 m/s (Han and Al-Dahhan, 2007). Hence, in the case of heterogeneous flow, the sparger has a negligible influence on the bubble size, gas holdup, or gas-liquid mass transfer because the bubble dynamics are determined by the rate of coalescence and breakup, which are controlled by the liquid properties and the nature and frequency of bubble collisions (Chaumat et al., 2005; Merchuk et al., 1998). Since airlift reactors are operated most commonly above 0.15-0.20 m/s, as seen in Figure 6.3, and using rheologically complex fluids, most research work ignores the sparger effect (Merchuk et al., 1998). Of the reviewed work in Tables 6.1 and 6.2, almost all (with very few exceptions) use perforated plate or tube spargers.

The commonly observed high gas flow rates result in correlations that can be fitted across data sets without accounting for sparger design (Kawase and Moo-Young, 1986b). Even a correlation for the liquid circulation velocity can be formed without regard to the sparger, and the results are still within 10%, even for very short vessels (Miyahara et al., 1986). The gas spargers usually do not provide enough kinetic energy from the gas jets to influence the liquid circulation rates (Chisti and Moo-Young, 1987). Hence, the preference and selection for spargers is based on operational

restrictions. The perforated plates and tubes provide the cheapest and most reliable operation, while the others have major drawbacks (Chisti, 1989).

Merchuk et al. (1998) investigated the use of different sparger designs in a draught tube airlift reactor using U_{Gr} = 0-0.20 m/s. Their results concurred with the bubble column experience. If a sparger created a smaller initial bubble diameter, it would lead to higher gas holdup in the homogeneous and transition flow regime and longer mixing times. This dependence diminished with gas flow rate and practically disappeared when U_{Gr} > 0.15 m/s, which was determined to correspond to the transition into the heterogeneous flow regime. A cylindrical perforated-pipe sparger created additional mixing due to a more radial bubble distribution, which interfered with bubble detachment and led to a higher rate of coalescence, especially in the sparger zone, and easier transition to the heterogeneous flow regime. The sparger zone in airlift reactors is defined as the liquid volume up to one column diameter above the sparger location (Giovannettone et al., 2009).

Although the sparger type does not appear to significantly affect ALR performance, sparger position is important and can be optimized. If the gas sparger is left at the bottom of the reactor, the incoming flow tends to interfere and cause a flow imbalance, which in turn leads to accumulation of gas and possible coalescence, as can be seen in Figure 6.10a and 6.10b. If the sparger is placed just within the riser, the incoming fluid flow does not interfere with the incoming gas flow, and the sparged gas is not affected. Elimination of dead zones in the aeration region, as shown by the shaded regions in Figure 6.10c and 6.10d, would also be beneficial. Moving the sparger too close to the surface, however, could lead to surface aeration and a higher rate of gas separation such that gas recirculation could be troublesome. Thus, placing the sparger too far beyond the downcomer inlet does not provide additional benefits.

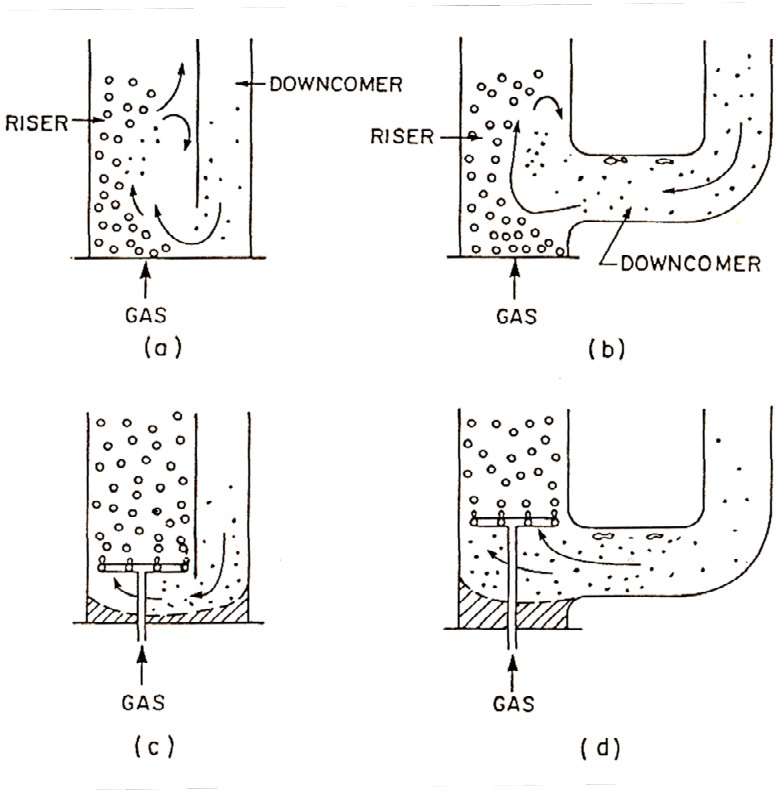

Figure 6.10: Location behavior of gas spargers in airlift reactors (Chisti, 1989).

Placing a sparger in the downcomer can alleviate some problems with oxygen suffocation of microorganisms and circulation, improve control, and reduce energy usage (Merchuk et al., 1999). In effect, the complete bubble circulation regime could be induced earlier and with finer bubbles, which could potentially decrease the bubble diameter and increase the interfacial area; however, downcomer sparging introduces circulation instability, which can only be solved by placing the downcomer sparger at a critical height (h_{DC}).

The critical height can also be used to compare the stability between the different designs. The system is more stable if the critical height is higher. The unfortunate aspect of downcomer sparging is that it is also dependent on the riser and downcomer gas flow rates, which makes the measure highly variable. A higher riser gas flow rate increases the critical height, but the rate of increase decreases with higher downcomer gas flow. Placing the riser sparger farther into the riser may also increase the critical height (Joshi et al., 1990).

According to Joshi et al. (1990), system stability can be optimized by adjusting certain reactor geometries (aspect and area ratio) such that the critical height ratio (h_{DC}/h_R) is the highest possible. The area ratio was easily optimized by Joshi et al. (1990) for this purpose with a critical value of approximately 0.75. The sparger location was then dependent on the power consumption such that the critical height ratio was 0.70 at 0.6 kW/m^3 and 0.60 at 0.3 kW/m^3. In other words, the critical height determined by Joshi et al. (1990) was scale dependent. As a geometrically similar reactor gets larger, the critical height will increase as well.

The aspect ratio is a bit more difficult. Joshi et al. (1990) showed that the critical height rose quickly with aspect ratio up to 10. A change in the aspect ratio from 10 to 40 yielded a relatively minor change in the critical height ratio (from 0.7 to 0.75) with a liquid volume of 10 m^3. In order to achieve h_{DC}/h_R = 0.80, the necessary aspect ratio was about 80, which is usually not used for biological applications. A similar trend was observed with reactor scale (using an aspect ratio of 40). The critical height ratio increased quickly up to 10 m^3 and changed slightly (from 0.7 to 0.75) with a volume increase from 10-100 m^3. A volume of 1000 m^3 was required to achieve h_{DC}/h_R = 0.80 (Joshi et al., 1990).

6.7 Correlations

Approaches used to develop gas-liquid mass transfer correlations in bubble columns have been ported over to airlift reactors, and, unfortunately, they have brought some issues along with them. Airlift reactor correlations are highly empirical, and a unifying development method does not exist. Some correlations attempt to be very specific and use multiple inputs, which are hard to quantify in an industrial setting, or use inputs which are not independent of each other. The suggestion is similar as with the bubble column: experimental units can use these more complicated correlations, but pilot or industrial scale units will have to depend on empirical and design specific correlations.

Further problems are presented by the downcomer and riser. Conditions in the two different sections can be very different, either by design or operation. Gas holdup correlations, which are summarized in Table 6.1, often reflect the different conditions, and two different approaches have been developed. The first approach is to develop correlations and models for the riser. The downcomer is then modeled based on the riser. One such approach has been taken by Bello et al. (1985a) by suggesting

$$\varepsilon_{Gd} = 0.89\varepsilon_{Gr} \tag{6.4}$$

where ε_{Gd} and ε_{Gr} are the downcomer and riser gas holdups, respectively. The other approach is to develop correlations for the riser and downcomer independently. The correlations would use similar inputs such as the riser superficial gas velocity. The assumption is that the downcomer hydrodynamics are ultimately controlled by the riser conditions and its inputs. This approach has been taken by Li et al. (1995)

$$\varepsilon_{Gr} = 0.441 U_{Gr}^{\ 0.841} \mu_a^{\ -0.135} \tag{6.5}$$

$$\varepsilon_{Gd} = 0.297 U_{Gr}^{\ 0.935} \mu_a^{\ -0.107} \tag{6.6}$$

where U_{Gr} and μ_a are the riser superficial gas velocity and the apparent viscosity.

Interestingly, gas-liquid mass transfer correlations for ALRs, presented in Table 6.2, do not differentiate between the reactor components and are displayed in global form. The situation can get troublesome for processes employing microorganisms. Gas holdup correlations have to be used and relied upon to predict the gas-liquid mass transfer conditions in the downcomer, where the danger of starvation is the highest. Although this relationship oftentimes is intact, industrial processes often create surfactants, temperatures, and pressures, which may decouple the relationship.

Gas-liquid mass transfer coefficients follow the gas holdup experience well. As shown in Figure 6.11, k_La increases monotonically with riser superficial gas velocity. The correlations by Chisti et al. (1988b) and Popovic and Robinson (1984) were developed using external-loop airlift reactors, while the others used the draught tube internal-loop airlift reactor. The DT-ILALR has much better performance than the ELALR. It is unfortunate to note that gas-liquid mass transfer correlations are much fewer in number than their gas holdup counterpart.

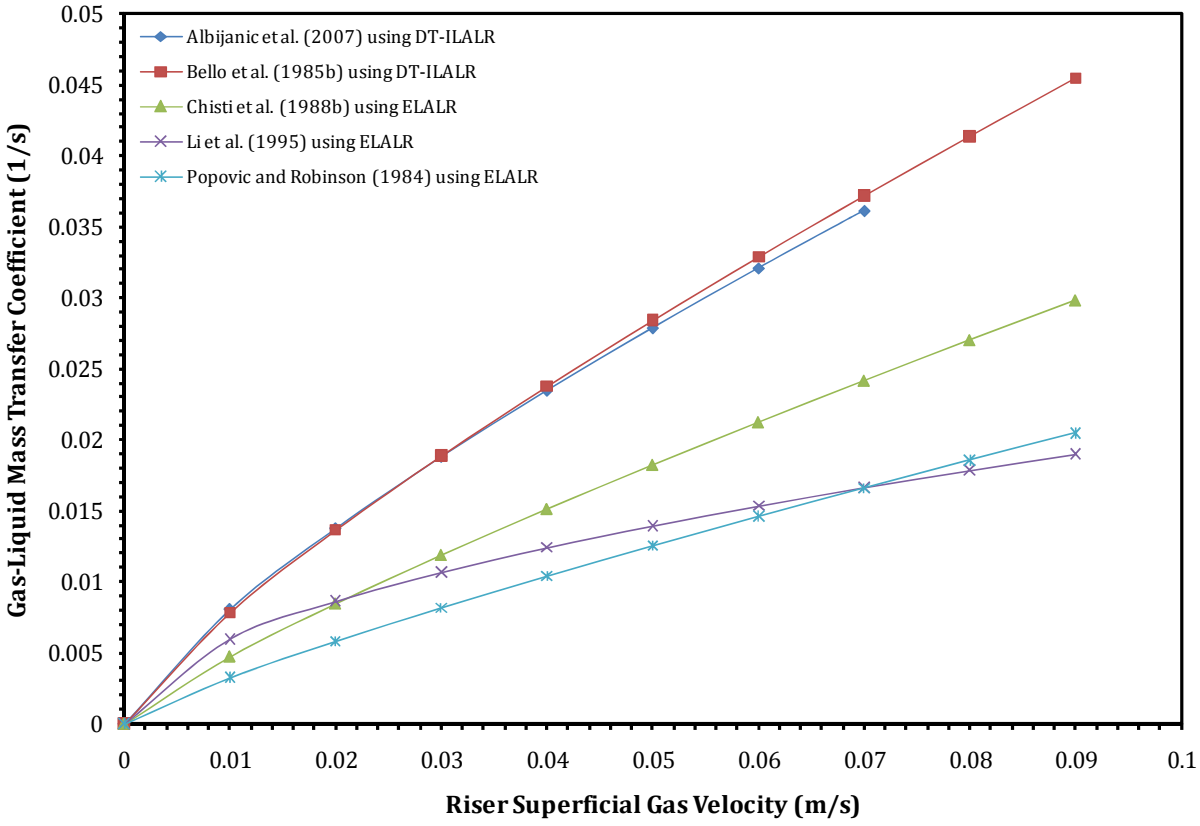

Figure 6.11: Sample gas-liquid mass transfer coefficients for ALRs.

The gas holdup correlations also have a high degree of variability, as shown in Figure 6.12. Correlations are able to reflect the consensus that the internal-loop airlift reactor has better gas holdup performance than the external-loop. This advantage is reflected in the power law presented in the correlations in Table 6.1. The internal-loop airlift reactors consistently have a higher constant and stronger dependence on the superficial gas velocity. As a matter of fact, the ILALR usually has a

U_G power close to unity while the ELALR is usually less than 0.5. A similar observation is made for the gas-liquid mass transfer correlations in Table 6.2. The advantage of the airlift reactor relative to the bubble column also comes through. The bubble column correlations show a leveling effect at higher superficial gas velocities. This trend is not present in the airlift reactor correlations.

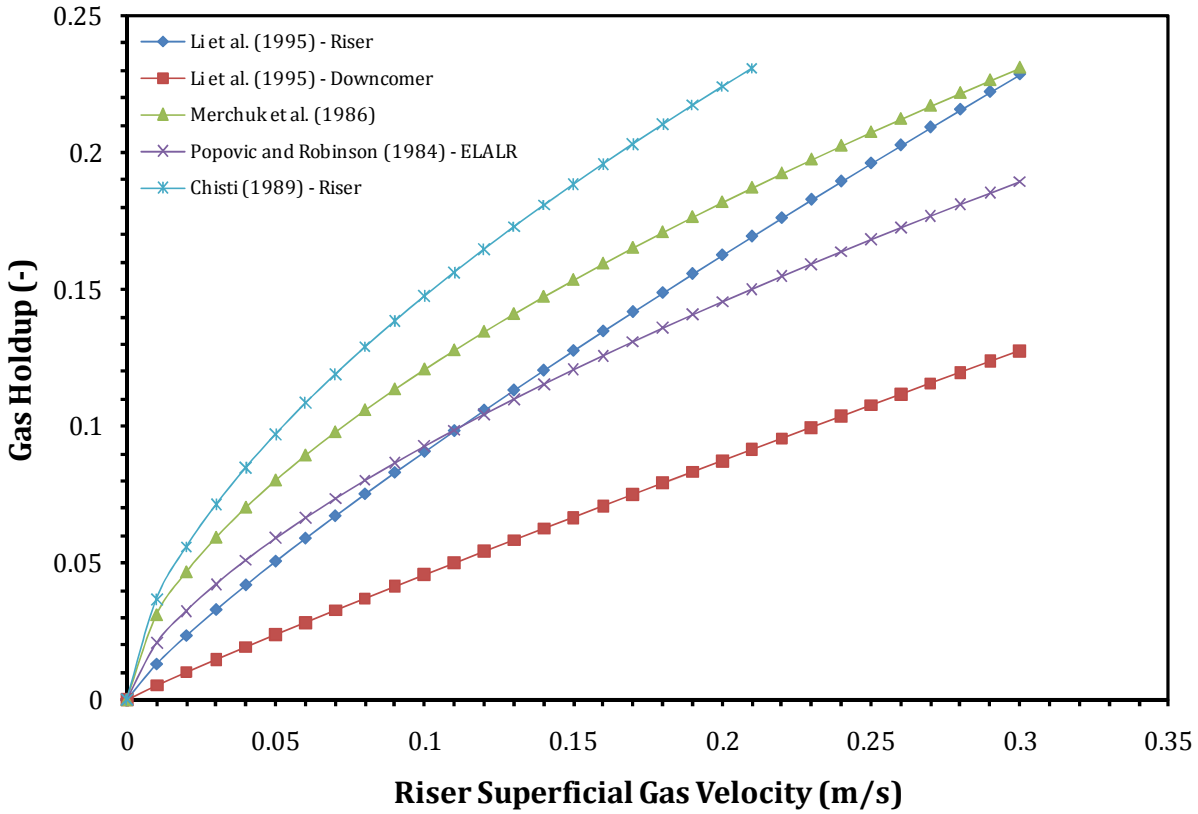

Figure 6.12: Sample gas holdup correlations for the internal-loop airlift reactor.

A significant problem with a large number of available correlations is that they require knowledge of the liquid phase behavior. This need is quite logical, but replication often requires a correlation for the liquid velocity, and additional error would be introduced in the generated gas holdup and gas-liquid mass transfer data.

A few measurement and assumption issues are built into the existing correlations. Gas-liquid mass transfer correlations, which are calculated at high gas flow rates, may be 15% lower than the system experiences because an incorrect assumption of ideal phase mixing is often made (Blazej et

al., 2004a). A further problem is that a normal bubble distribution is often assumed in the analysis, but the truth of this or any other assumption has not been thoroughly verified (Fadavi et al., 2008).

6.8 Needed Research

The research on airlift reactors is relatively young compared to stirred-tank and bubble column reactors. Figure 6.13 and Figure 6.14 have been developed to illustrate this point graphically. The data have been collected using EngineeringVillage2 (EV2) in spring 2009, which allows access to several engineering-related databases and services. The inputs into EV2 are shown in the legend. A moving three year average was used to smooth the data. This simple search reveals some interesting trends. Research performed in stirred tank reactors and bubble columns is currently preferred to airlift reactors. This fact also increases the likelihood of having in-depth research into more specific topics, such as gas-liquid mass transfer, and, perhaps more importantly, reliable sources of information, experts, and established research groups.

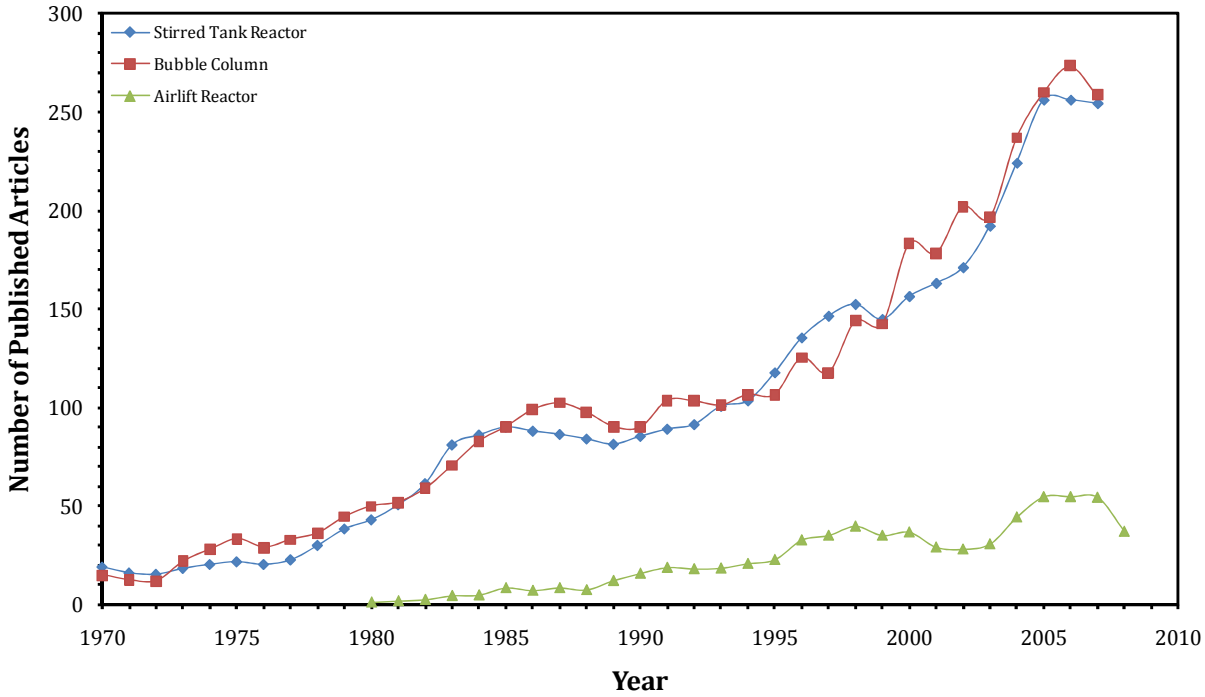

Figure 6.13: General research articles available in the public domain for different reactor types.

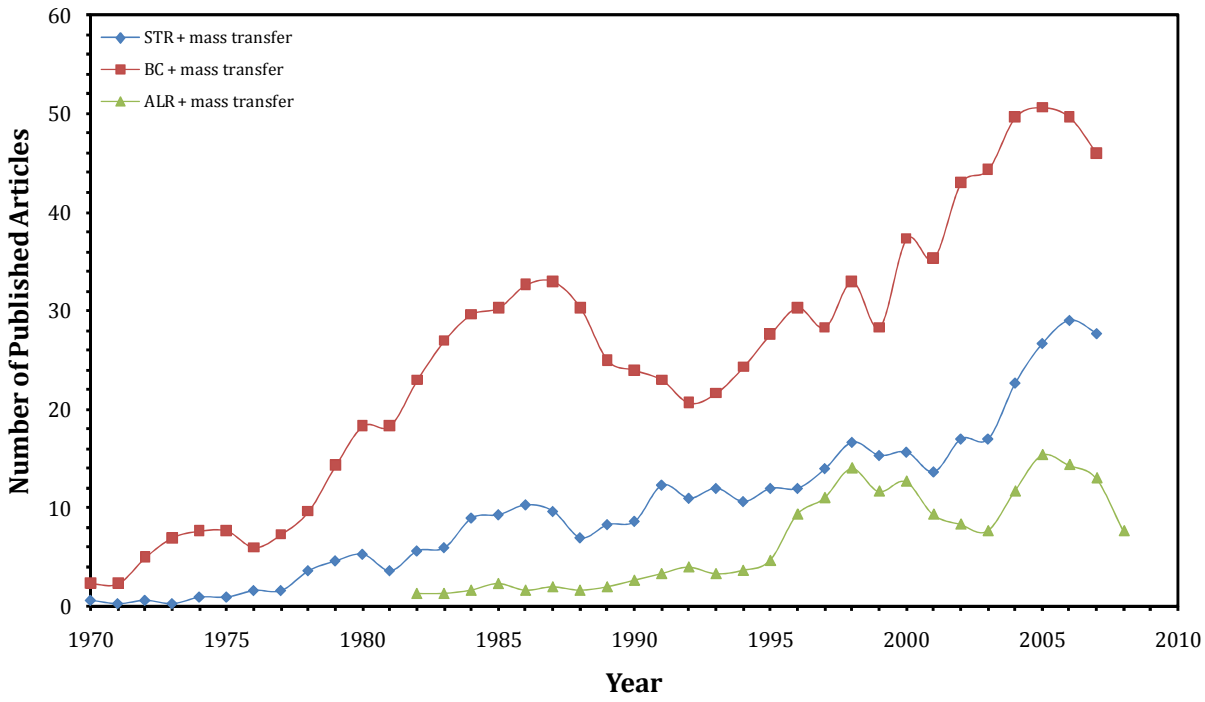

Figure 6.14: Research articles available in the public domain specific to mass transfer for different reactor types.

Figure 6.14 leads to the conclusion that research into mass transfer in airlift reactors, in general, has increased considerably since 1995. The progression seems quite natural. Research in stirred tank reactors had made its short-comings obvious, and the advent of the bubble column was a natural transition. As research into the bubble column matured, some of its issues also came to light, and the solution, the airlift reactor, was seen as the next stage. It may also be concluded that the number of articles related to airlift reactors is suppressed because research in bubble columns can be largely ported to the airlift reactor; however, some major differences do exist.

The liquid circulation behavior differs largely in the airlift reactor, but is still not very well understood. The basic structure and behavior is known, but quantification requires deeper understanding, which is not available at this time. The relationship between the superficial gas and liquid circulation velocity can be ambiguous. The bubble distribution is also not well defined. In other words, the basic principles need more research.

Bioprocessing could also use more specific attention. Research incorporating a solid phase is scarce, and it is unclear how many of the slurry bubble column characteristics would be expected to behave similarly in an airlift reactor. Tissue growth applications could use more extended studies. Current effects of variable local conditions on cellular biochemistry are not understood. As such, cells could be grown to mimic the macroscopic behavior of the desired cells, but still miss the molecular, cellular, and biochemical interactions necessary to mimic the operations of the target cells. Thus, for example, one could grow kidney cells, which do not filter anything. This problem is limited with connective tissue, but only because of the cell function, which does not necessarily require biochemical reactions.

Proper startup procedures, such as initial cell density and distribution, and tracking important or toxic byproducts are also troublesome (Martin and Vermette, 2005). Fiber suspensions have not been widely applied in airlift reactors, but its application would be of interest for suspended cell growth and density propagation. The incorporation of microorganisms in hydrodynamic studies have not been widely attempted even though microorganisms are known to increase the gas-liquid mass transfer coefficient due to a higher rate of oxygen consumption (Garcia-Ochoa and Gomez, 2009), especially at and near the surface.

More focus on consistent variable testing is needed. Oftentimes, multiple variables are adjusted while the analysis is focused on just one. The conclusions are based on one variable, and the changes in the others are ignored. Particle size comparisons are often done based on scale. One group is often referred to as large with a diameter on the millimeter scale, while the small particles are defined by a diameter less than 1 millimeter. In addition, these particles are often constructed of differing materials, such that a density variance is introduced, or are used in different concentrations. These facts make hydrodynamic and gas-liquid mass transfer conclusions highly variable in the literature.

This mistake may be made for scale comparison studies as well. Blazej et al. (2004b), for example, compared vessels with volumes of 10.5, 32, and 200 liters. The 10.5 and 32 liter versions can be classified as experimental scale, while the 200 liter ALR may be considered pilot scale (Garcia-Ochoa and Gomez, 2009). Hence, the results, shown in Figure 6.15, could be very helpful for scaleup. Each vessel, however, was geometrically different with varying downcomer-to-riser area and aspect ratio and bottom clearance. Although the differences were not great and comply with the scaleup procedure of Garcia-Ochoa and Gomez (2009), it introduces an additional dilemma. Which effects are related to the scale and which to the downcomer-to-riser area ratio, or is the difference even significant? If a control study with constant ratios is not done, these questions are much harder to answer and conclusions are based on the experimenters' interpretation and inference.

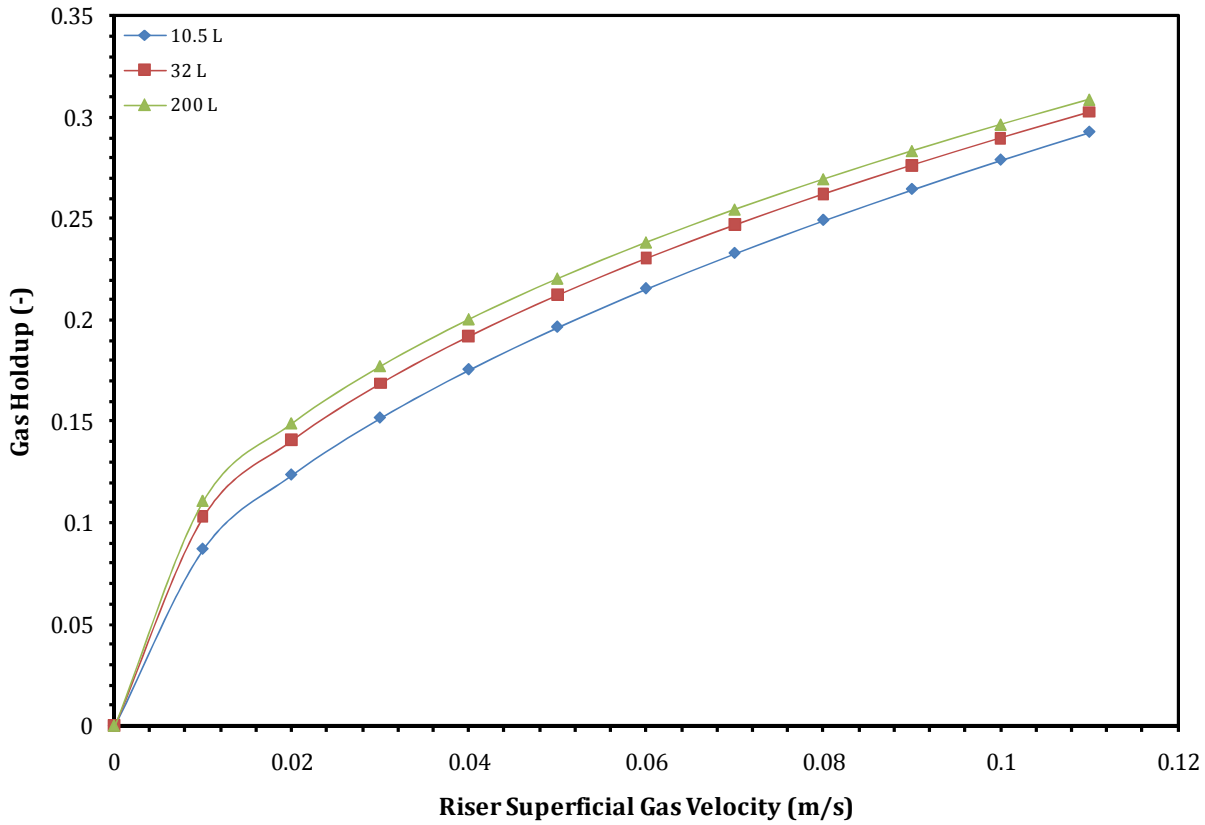

Figure 6.15: Airlift reactor scale effects (adopted from Blazej et al. (2004b)).

6.9 Summary

Bubble column reactors are the main competitor to airlift reactors, and deployment decisions are usually based on a competitive basis that excludes the stirred tank reactor. Hence, studies rarely compare the stirred tank reactor, bubble column, and airlift reactor. Usual comparisons are made either between the stirred tank reactor and the bubble column or the bubble column and the airlift reactor. The first stage in identifying a bioreactor usually involves a comparison between the STR and BC, which clarifies the reactor and process requirements. If the bubble column is found to be competitive, the airlift reactor is introduced to the discussion.

The airlift reactor is often used in cases for which the bubble column lacks the operational flexibility or requirements. In other words, the stirred tank reactor does not have the necessary features, and the bubble column has traits which could have negative effects on the production process. These negative traits often include extensive phase backmixing, undefined flow paths, limited gas flow rates, and potentially damaging shear rates. The airlift reactor can successfully address these issues and can provide further control, such as a downcomer sparger, and access to major reactor components.

The negative aspect of airlift reactors is that research is in its early stages in many respects. A basic hydrodynamic understanding is lacking. For example, the onset of liquid circulation has been reported to vary between U_{Gr} = 0.035-0.050 m/s. It is occasionally reported to coincide with the introduction of the heterogeneous flow regime while the homogeneous flow regime is prevalent in other cases of circulation onset.

Bubble-bubble contacts are regulated by the same forces and interactions as those found in bubble columns, which would imply that the basic behavior should be very similar to bubble columns. This assumption is often invoked, and bubble column research is used in these cases to set expectations and explain outcomes; however, many assumptions have not been tested. The fact that bubble collisions do not occur as frequently in the airlift reactor as in the bubble column leads to

the conclusion that certain aspects of the bubble column may not be applied to airlift hydrodynamics as easily or at all.

These issues, positive and negative, are reflected in the available correlations. These correlations are both highly useful and also limited. Some are useful because the inputs are easily measured and adjusted as needed; however, correlations are mostly empirical or semi-empirical, which means that they are not widely applicable but, rather, are reactor design dependent at best. Hence, geometric similarity is very important. Furthermore, most studies are performed in air-water systems while most industrial processes use much more complicated and time variant liquids. In other words, the airlift reactor correlations have similar problems as those for stirred tank reactors and bubble columns and are due to the fact that they share the "problem" source: bubble-bubble interactions. Bubble-bubble interactions are highly variable and lead to hydrodynamics which, in turn, are difficult to quantify and predict. Hence, the result has been airlift reactor correlations and models that are either system dependent or not adequately constrained.

(Bendjaballah et al., 1999; Bentifraouine et al., 1997a, 1997b; Blazej et al., 2004b; Blenke, 1979; Lu et al., 1995; Popovic and Robinson, 1984; Snape et al., 1995; van Benthum et al., 2000)

Table 6.1: Gas holdup correlations for airlift reactors.

Reference	Reactor Type(s)	Reactor Parameters	Correlations
(Albijanic et al., 2007)	DT-ILALR	Air-(Water, 1 wt% aqueous solutions of methanol, ethanol, n-propanol, isopropanol, and n-butanol) U_G = 0-0.07 m/s	$\varepsilon_G = 1.65 U_G^{0.97}\left[1+\left(\frac{d\sigma}{dC_A}\right)^{0.20}\right]^{1.52}$
(Bello, 1981)[3]	ELALR		$\varepsilon_{Gr} = 0.16\left(\frac{U_G^{\,2}}{U_{Lr}}\right)^{0.56}\left(1+\frac{A_d}{A_r}\right)$ $\varepsilon_{Gd} = 0.89\varepsilon_{Gr}$
(Bello et al., 1985a)[1]	ELALR	Air-(water, NaCl solution) C_{NaCl} = 0.15 kmol/m^3 d_R or d_r = 0.152 m h_D = 1.8 m U_{Gr} = 0.0137-0.086 m/s A_d/A_r = 0.11-0.69	$\varepsilon_{Gr} = 0.16\left(\frac{U_{Gr}}{U_L}\right)^{\alpha}\left(1+\frac{A_d}{A_r}\right)$ $\varepsilon_{Gd} = 0.89\varepsilon_r$ for DT-ILALR $\varepsilon_{Gd} = 0.79\varepsilon_r - 0.057$ for ELALR α = 0.56 for water α = 0.58 for salt solution
(Bello et al., 1985b)[1]	ELALR DT-ILALR BC	Air-(Water, NaCl solution) C_{NaCl} = 0.15 kmol/m^3 d_R or d_r = 0.152 m h_D = 1.8 m U_{Gr} = 0.0137-0.086 m/s A_d/A_r = 0.11-0.69 (ELALR) A_d/A_r = (0.13, 0.35, 0.56) (ILALR) A_d/A_r = 0 (BC)	$\varepsilon_G = 3.4*10^{-3}\left(1+\frac{A_d}{A_r}\right)^{-1}\left(\frac{P_G}{V_D}\right)^{2/3}$
(Bentifraouine et al., 1997a)[2]	?	U_G = 0.002-0.06 m/s U_{Lr} = 0-0.2 m/s	$\varepsilon_{Gr} = 2U_G^{0.88}\left(1-0.97U_{Lr}^{0.49}\right)$
(Blazej et al., 2004b)	ILALR	Air-Water For 10.5 L: d_R = 0.108 m, d_r = 0.070 m h_R = 1.26 m, h_D = 1.145 A_d/A_r = 1.23, h_c = 0.030 m h_R/d_R = 11 For 32 L: d_R = 0.157 m, d_r = 0.106 m h_R = 1.815 m, h_D = 1.710 A_d/A_r = 0.95, h_c = 0.046 m h_R/d_R = 12 For 200 L: d_R = 0.294 m, d_r = 0.200 m h_R = 2.936 m, h_D = 2.700 A_d/A_r = 1.01, h_c = 0.061 m h_R/d_R = 10	For 10.5 L: $\varepsilon_{Gr} = 0.829U_{Gr}^{0.505}$ $\varepsilon_{Gd} = 0.857\varepsilon_{Gr} - 0.0095$ in regime 2 $\varepsilon_{Gd} = 0.432\varepsilon_{Gr} - 0.0139$ in regime 3 For 32 L: $\varepsilon_{Gr} = 0.815U_{Gr}^{0.449}$ $\varepsilon_{Gd} = 0.885\varepsilon_{Gr} + 0.0065$ in regime 2 $\varepsilon_{Gd} = 0.670\varepsilon_{Gr} - 0.0037$ in regime 3 For 200 L (only regime 3 was presented): $\varepsilon_{Gr} = 0.792U_{Gr}^{0.427}$ $\varepsilon_{Gd} = 0.967\varepsilon_{Gr} + 0.0068$
(Cai et al., 1992)[3]	ILALR		$\varepsilon_{Gr} = 2.47U_{Gr}^{0.97}$
(Chakravarty et al., 1973)[1]	DT-ILALR	Air-(Water, sulphate, glycerol, and iso-butyl alcohol solutions) d_R = 0.10 m d_D = (0.074, 0.59, 0.45) m L_D = 0.40 m L_c = 0.026 m	$\varepsilon_{Gr} = \left[\left(\mu_L - \mu_W\right)^{2.75} + 161\frac{73.3-\sigma}{79.3-\sigma}\right]*10^{-4}*U_{Gr}^{0.88}$ $\varepsilon_{Gd} = 1.23*10^{-2}\left[\frac{74.2-\sigma}{79.3-\sigma}\right]\mu_L^{0.45}\left(\frac{A_d}{A_r}\right)^{1.08}U_{Gr}^{0.88}$

[1] Adopted from Chisti (1989)
[2] Adopted from Jones (2007)
[3] Adopted from Merchuk et al. (1999)

Table 6.1 cont.: Gas holdup correlations for airlift reactors.

Reference	Reactor Type(s)	Reactor Parameters	Correlations
(Chakravarty et al., 1974)[3]	ILALR		$\varepsilon_{Gr} = 0.0057\left[\left(\mu_L - \mu_W\right)^{2.75} - 161\frac{73.3-\sigma}{79.3-\sigma}\right]U_{Gr}^{0.88}$
(Chisti and Moo-Young, 1986)[1]	ILALR (rectangular)	Air-(Water, aqueous salt solution)+1-3 dry wt./vol. % KS-1016 cellulose fiber	Homogeneous flow regime: $\varepsilon_G = \left(1.488 - 0.496c_s\right)U_G^{0.892\pm0.075}$ Heterogeneous flow regime: $\varepsilon_G = \left(0.371 - 0.089c_s\right)U_G^{0.430\pm0.015}$
(Chisti et al., 1988a)[3]	ILALR		$\varepsilon_{Gr} = 0.65U_{Gr}^{(0.603+0.078C_0)}\left(1+\frac{A_d}{A_r}\right)^{-0.258}$ $\varepsilon_{Gd} = 0.46\varepsilon_r - 0.0244$
(Chisti, 1989)	ILALR	U_{Gr} = 0.026-0.21 m/s A_d/A_r = 0.25-0.44	$\varepsilon_{Gr} = 0.65\left(1+\frac{A_d}{A_r}\right)^{-0.258}U_{Gr}^{0.603}$ $\varepsilon_{Gr} = 2.4U_G^{0.97}$
(Choi, 2000)[2]	?	U_G = 0.02-0.18 m/s h_R = 0.04-0.20 m A_d/A_r = 0.11-0.53	$\varepsilon_{Gr} = 0.2447U_G^{0.5616}\left(\frac{A_d}{A_r}\right)^{-0.2779}h_R^{-0.0130}$
(Choi, 2001)[2]	ELALR	U_G = 0.02-0.18 m/s L_c/L_h = 0.1-0.5 m A_d/A_r = 0.11-0.53	$\varepsilon_{Gr} = 0.431U_G^{0.580}\left(\frac{A_d}{A_r}\right)^{-0.040}\left(\frac{L_c}{L_h}\right)^{-0.042}$
(Ghirardini et al., 1992)[3]	ELALR		$\varepsilon_G = 0.55U_{Gr}^{0.78}\left(\frac{U_{Ls}}{U_L}\right)^{0.2}d_r^{0.42}$
(Hills, 1976)[2]	?	U_G = 0.4-3.2 m/s U_{Lr} = 0-2.5 m/s	$\varepsilon_{Gr} = \frac{U_G}{0.21 + 1.35\left(U_G + U_{Lr}\right)^{0.93}}$
(Li et al., 1995)[3]	ILALR		$\varepsilon_{Gr} = 0.441U_{Gr}^{0.841}\mu_a^{-0.135}$ $\varepsilon_{Gd} = 0.297U_{Gr}^{0.935}\mu_a^{-0.107}$
(Kawase et al., 1995)[3]	ILALR		$\frac{\varepsilon_{Gr}}{1-\varepsilon_{Gr}} = \frac{U_{Gr}^{n+2/2(n+1)}}{2^{3n+1/n+1}n^{n+2/2(n+1)}\left(\frac{K}{\rho_L}\right)^{1/2(n+1)}g^{n/2(n+1)}\left(1+\frac{A_d}{A_r}\right)^{3(n+2)/4(n+1)}}$
(Kawase and Moo-Young, 1986a)[3]	ILALR		$\varepsilon_G = 0.24n^{-0.6}Fr^{0.84-0.14n}Ga$
(Kawase and Moo-Young, 1986b)[1]	DT-ILALR BC	Air-(Water, pseudoplastic fluids) U_G = 0.008-0.285 m/s d_R = 0.14-0.35 m n=0.28-1 K = 0.001-1.22 Pa s^n	$\varepsilon_G = 0.24n^{-0.6}\left(\frac{U_G}{\sqrt{gd_R}}\right)^{0.84-0.14n}\left(\frac{gd_R^3\rho_L^2}{\mu_a^2}\right)$
(Kawase and Moo-Young, 1987)[3]	ELALR		$\varepsilon_{Gr} = 1.07\left(\frac{U_G^2}{gd_r}\right)^{0.333}$

[1] Adopted from Chisti (1989)

[2] Adopted from Jones (2007)

[3] Adopted from Merchuk et al. (1999)

Table 6.1 cont.: Gas holdup correlations for airlift reactors.

Reference	Reactor Type(s)	Reactor Parameters	Correlations
(Kemblowski et al., 1993)[3]	ELALR		$\varepsilon_{Gr} = 0.203 \frac{Fr^{0.31}}{Mo^{0.012}} \left(\frac{U_{Gr}}{U_{Lr}} \frac{A_r}{A_d} \right)^{0.74}$ Where: $Mo = \frac{g(\rho_L - \rho_G)}{\sigma \rho_L^2} K^4 \left(\frac{8U_{Gr}}{d_r} \right)^{4(n-1)} \left(\frac{3n+1}{4n} \right)^{4n}$ $Fr = \frac{(U_{Lr} + U_{Gr})^2}{g d_r}$
(Koide et al., 1983a)[3]	ILALR		$\frac{\varepsilon_G}{(1-\varepsilon_G)^4} = 0.16 \left(\frac{U_G \mu_L}{\sigma} \right) Mo^{-0.283} \left(\frac{d_r}{d_R} \right)^{-0.222} \left(\frac{\rho_L}{\Delta \rho} \right)^{0.283} \left[1 - 1.61 \left(1 - e^{0.00565 Ma} \right) \right]^{-1}$
(Koide et al., 1985)[3]	ILALR		$\frac{\varepsilon_G}{(1-\varepsilon_G)^4} = \frac{0.124 \left(\frac{U_G \mu_L}{\sigma} \right)^{0.996} \left(\frac{\rho_L \sigma^3}{g \mu_L^4} \right)^{0.294} \left(\frac{d_r}{d_R} \right)^{0.114}}{1 - 0.276 \left(1 - e^{-0.0368 Ma} \right)}$
(Koide et al., 1988)[3]	ILALR		$\varepsilon_{Gr} = \frac{Fr}{0.415 + 4.27 \left(\frac{U_{Gr} + U_{Lr}}{\sqrt{g d_r}} \right) \left(\frac{g \rho_L d_R^2}{\sigma} \right)^{-0.188} + 1.13 Fr^{1.22} Mo^{0.0386} \left(\frac{\Delta \rho}{\rho_L} \right)^{0.0386}}$
(Merchuk, 1986)[2]	?	U_G = 0.002-0.5 m/s	$\varepsilon_{Gr} = 0.047 U_{Gr}^{0.59}$
(Merchuk et al., 1998)	DT-ILALR	Air-Sea water from Almeria Bay U_G = 0-0.21 m/s h_R = 2 m d_R = 0.096 m h_D = 1.5 m A_r = 0.00283 m^2 A_d = 0.00280 m^2	$\varepsilon_{Gr} = \alpha \left(\frac{U_{Gr}}{U_{Lr}} \right)^{\beta}$

Sparger	A	β
PP with 30xd_0 = 1 mm	0.48	1.03
PP with 30xd_0 = 0.5 mm	0.37	0.79
CS with d_0 = 120 μm	0.34	0.69
CS with d_0 = 60 μm	0.33	0.68
PS with d_0 = 120 μm	0.48	1.13
PS with d_0 = 60 μm	0.40	0.99
PS with d_0 = 30 μm	0.38	0.88

[1] Adopted from Chisti (1989)

[2] Adopted from Jones (2007)

[3] Adopted from Merchuk et al. (1999)

Table 6.1 cont.: Gas holdup correlations for airlift reactors.

Reference	Reactor Type(s)	Reactor Parameters	Correlations
(Miyahara et al., 1986)[1]	DT-ILALR	Air-Non-Newtonian CMC solutions ρ_L = 952-1168 kg/m^3 μ_L = 1.0-14.9 mPa s σ = 34.1-72.0 mN/m d_R = 0.148 m L_d = 1.0 m h_R = 1.20 m d_0 = 0.0005-0.0015 m A_d/A_r = 0.128-0.808	$\varepsilon_{Gr} = \frac{0.4\sqrt{Fr}}{1+0.4\sqrt{Fr}\left(1+\frac{U_L}{U_{Gr}}\right)}$ For $\varepsilon_{Gr} < 0.0133\left(\frac{A_r}{A_d}\right)^{-1.32}$: $\varepsilon_{Gd} = 4.51*10^6 Mo^{0.115}\left(\frac{A_r}{A_d}\right)^{4.2} \varepsilon_{Gr}^{4.2}$ For $\varepsilon_{Gr} > 0.0133\left(\frac{A_r}{A_d}\right)^{-1.32}$: $\varepsilon_{Gd} = 0.05 Mo^{-0.22}\left[\left(\frac{A_r}{A_d}\right)^{0.5} \varepsilon_{Gr}\right]^{0.31 Mo^{-0.073}}$
(Shariati et al., 2007)	DT-ILALR	Air-(Distilled water, aqueous isomax diesel) U_G = 0-0.07 m/s d_R = 0.14 m h_D = 1.1 m d_r = 0.1 m h_c = 0.024 m A_d/A_r = 0.906 h_0 = 25x1 mm (PP) ν_L = 46.142*10^{-6} m^2/s	$\varepsilon_G = 4.92 U_{Gr}^{1.066} \nu_L^{-0.355}$ $\varepsilon_{Gd} = 0.788\varepsilon_{Gr} - 0.004$

[1] Adopted from Chisti (1989)

[2] Adopted from Jones (2007)

[3] Adopted from Merchuk et al. (1999)

Table 6.1 cont.: Gas holdup correlations for airlift reactors.

Reference	Reactor Type(s)	Reactor Parameters	Correlations
(Trilleros et al., 2005)	DT-ILALR	Air-Water h_R = 1.25 m d_R = 0.42 m d_{pg} = 0.25 and 1 mm ρ_{pg} = 2.6 g/cm^3 d_{pc} = 3 mm ρ_{pg} = 1.0 g/cm^3 d_0 = 12x1 mm (PP) d_D = (0.044, 0.082, 0.125, 0.240) m h_D = 0.630 and 1.050 m ε_s = 1-7%	<u>Large glass particles:</u> $\frac{U_{Gr}}{\varepsilon_{Gr}} = \left[0.43\left(U_{Gr} + U_{Lr} + U_{Sr}\right)\right] + 0.26$ U_{Gr} = 0.02-0.10 m/s $(U_{Gr} + U_{Lr} + U_{Sr})$ = 0.80-14.05 m/s ε_{Gr} = 0.013-0.14 <u>Small glass particles:</u> $\frac{U_{Gr}}{\varepsilon_{Gr}} = \left[0.35\left(U_{Gr} + U_{Lr} + U_{Sr}\right)\right] + 0.15$ U_{Gr} = 0.006-0.12 m/s $(U_{Gr} + U_{Lr} + U_{Sr})$ = 1.05-14.75 m/s ε_{Gr} = 0.005-0.17 <u>Polystyrene particles:</u> $\frac{U_{Gr}}{\varepsilon_{Gr}} = \left[0.22\left(U_{Gr} + U_{Lr} + U_{Sr}\right)\right] + 0.15$ U_{Gr} = 0.005-0.12 m/s $(U_{Gr} + U_{Lr} + U_{Sr})$ = 0.50-15.20 m/s ε_{Gr} = 0.005-0.16
(Posarac and Petrovic, 1988)[3]	ELALR		$\varepsilon_{Gr} = \frac{0.6\rho_G^{0.062}\rho_L^{0.069}\mu_G^{0.107}}{\mu_L^{0.053}S_L^{0.185}} \frac{U_{Gr}^{0.936}}{\left(U_{Gr} + U_{Lr}\right)^{0.474}}$
(Popovic and Robinson, 1984)[3]	ELALR BC	Air-Non-Newtonian CMC solutions μ_L = 0.015-0.5 Pa s A_d/A_r = (0, 0.11, 0.25, 0.44)	$\varepsilon_{Gr} = 0.465 U_{Gr}^{0.65}\left(1 + \frac{A_d}{A_r}\right)^{-1.06}\mu_a^{-0.103}$
(Vatai and Tekic, 1986)[3]	ILALR		$\varepsilon_{Gr} = \left(0.491 - 0.498\right)U_{Gr}^{0.706}\left(\frac{A_d}{A_r}\right)^{-0.254} d_r \mu_a^{0.0684}$

[1] Adopted from Chisti (1989)

[2] Adopted from Jones (2007)

[3] Adopted from Merchuk et al. (1999)

Table 6.2: Gas-liquid mass transfer coefficient correlations for airlift reactors.

Reference	Reactor Type(s)	Reactor Parameters	Correlations
(Albijanic et al., 2007)	DT-ILALR	Air-(Water, 1 wt% aqueous solutions of methanol, ethanol, n-propanol, isopropanol, and n-butanol) U_G = 0-0.07 m/s	$k_La = 0.28U_G^{0.77}\left[1+\left(\frac{d\sigma}{dC_A}\right)^{0.15}\right]^{0.71}$
(Bello et al., 1985a)[1]	ELALR	Air-(water, NaCl solution) d_R or d_r = 0.152 m h_D = 1.8 m U_{Gr} = 0.0137-0.086 m/s A_d/A_r = 0.11-0.69	$\frac{k_La h_r}{U_L} = 2.28\left(\frac{U_{Gr}}{U_L}\right)^{0.90}\left(1+\frac{A_d}{A_r}\right)^{-1}$
(Bello et al., 1985b)[1]	ELALR DT-ILALR BC	Air-(water, NaCl solution) d_R or d_r = 0.152 m h_D = 1.8 m U_{Gr} = 0.0137-0.086 m/s A_d/A_r = 0.11-0.69 (ELALR) A_d/A_r = (0.13, 0.35, 0.56) (ILALR) A_d/A_r = 0 (BC)	$k_La = 0.76\left(1+\frac{A_d}{A_r}\right)^{-2}U_{Gr}^{0.8}$ $k_La = 5.5*10^{-4}\left(1+\frac{A_d}{A_r}\right)^{-1.2}\left(\frac{P_G}{V_D}\right)^{0.8}$
(Blazej et al., 2004a)	DT-ILALR	(Air, pure oxygen, nitrogen)-(Na_2SO_3 aqueous solution) d_R = 0.157 m d_D = 0.106 m V_L = 40 dm^3 d_0 = 25x1 mm (PP)	$k_La = 0.91\varepsilon_{Gr}^{1.39}$
(Chisti et al., 1988b)[3]	ELALR		$k_La = (0.349-0.102C_s)U_{Gr}^{0.837}\left(1+\frac{A_d}{A_r}\right)^{-1}$
(Freitas and Teixeira, 2001)	DT-ILALR	Low density solids: d_P = 2.131±0.102 mm ρ_s = 1023±+1 kg/m^3 High density solids: d_P = 2.151±0.125 mm ρ_s = 1048±+1 kg/m^3 ε_s = 0-30% U_{Gr} = 0.01-0.5 m/s	<u>Water/low density solids</u> $k_La = \left(-0.93U_{Gr}^2+1.33U_{Gr}-0.012\right)\left(-0.0000016\varepsilon_s^2-0.00099\varepsilon_s+0.054\right)$ <u>Water/high density solids</u> $k_La = \left(-0.33U_{Gr}^2+0.43U_{Gr}-0.0064\right)\left(-0.000080\varepsilon_s^2-0.0056\varepsilon_s+0.17\right)$ <u>Ethanol (10 g/L)/low density solids</u> $k_La = \left(-0.95U_{Gr}^2+1.34U_{Gr}-0.021\right)\left(-0.000072\varepsilon_s^2-0.00079\varepsilon_s+0.075\right)$ <u>Ethanol (10 g/L)/high density solids</u> $k_La = \left(-0.78U_{Gr}^2+1.20U_{Gr}-0.021\right)\left(-0.000074\varepsilon_s^2-0.0035\varepsilon_s+0.081\right)$

[1] Adopted from Chisti (1989)

[2] Adopted from Jones (2007)

[3] Adopted from Merchuk et al. (1999)

Table 6.2 cont.: Gas-liquid mass transfer coefficient correlations for airlift reactors.

Reference	Reactor Type(s)	Reactor Parameters	Correlations
(Kawase and Moo-Young, 1986a)[3]	ILALR		$Sh = 0.68n^{-0.72}Fr^{0.38n+0.52}Sc^{0.38-0.14n}$
(Kawase and Moo-Young, 1986b)[1]	DT-ILALR BC	Air-(Water, pseudoplastic fluids) U_G = 0.008-0.084 m/s d_R = 0.14-0.305 m n=0.543-1 K = 0.00089-2.82 Pa s^n	$\frac{k_L a d_R^{\,2}}{D_L} = 0.68n^{-6.72}\left(\frac{d_R U_G \rho_L}{\mu_a}\right)^{0.38n+0.52}\left(\frac{\mu_a}{D_L \rho_L}\right)^{0.38n-0.14}$
(Koide et al., 1983a)[1]	DT-ILALR	Air-Newtonian fluids μ_L = 0.9-13 mPa s σ = 51-73 mN/m^3 D_L (10^9) = 0.18-2.42 m^2/s U_G = 0.0098-0.156 m/s d_R = 0.10-0.30 m d_D = 0.06-0.19 m L_d = 0.70-2.10 m L = 0.84-2.24 m d_0 = 0.001-0.015 m (SO) d_0 = 7x0.001 m (PP)	$\frac{k_L a d_R^{\,2}}{D_L} = 0.477\left(\frac{\mu_L}{\rho_L D_L}\right)^{0.5}\left(\frac{g d_R^{\,2} D_L}{\sigma}\right)^{0.837}\left(\frac{g d_R^{\,3} D_L^{\,2}}{\mu_L^{\,2}}\right)^{0.257}\left(\frac{d_D}{d_R}\right)^{-0.54}\varepsilon_G^{\,1.36}$ $3.69*10^2 \le \frac{\mu_L}{\rho_L D_L} \le 5.68*10^4$ $1.36*10^3 \le \frac{g d_R^{\,2} D_L}{\sigma} \le 1.22*10^4$ $2.27*10^8 \le \frac{g d_R^{\,3} D_L^{\,2}}{\mu_L^{\,2}} \le 3.32*10^{11}$ $0.471 \le \frac{d_D}{d_R} \le 0.743$ $0.037 \le \varepsilon_G \le 0.21$
(Koide et al., 1983b)[1]	DT-ILALR	Air-Newtonian fluids μ_L = 0.9-13 mPa s σ = 51-73 mN/m^3 D_L (10^9) = 0.18-2.42 m^2/s U_G = 0.0098-0.156 m/s d_R = 0.10-0.30 m d_D = 0.06-0.19 m L_d = 0.70-2.10 m L = 0.84-2.24 m d_0 = 0.001-0.004 m (SO)	$\frac{k_L a \sigma}{D_L g \rho_L} = 2.25\left(\frac{\mu_L}{\rho_L D_L}\right)^{0.5}\left(\frac{\rho_L \sigma^3}{g \mu_L^{\,4}}\right)^{0.136}\left(\frac{d_0}{d_R}\right)^{-0.0905}\varepsilon_G^{\,1.26}$ $3.71*10^2 \le \frac{\mu_L}{\rho_L D_L} \le 6.00*10^4$ $1.18*10^6 \le \frac{\rho_L \sigma^3}{g \mu_L^{\,4}} \le 5.93*10^{10}$ $0.471 \le \frac{d_D}{d_R} \le 0.743$ $7.41*10^{-3} \le \frac{d_0}{d_c} \le 2.86*10^{-2}$ $0.0302 \le \varepsilon_G \le 0.305$
(Koide et al., 1985)[3]	ILALR		$Sh = 2.66Sc^{0.5}Bo^{0.715}Ga^{0.25}\left(\frac{d_r}{d_R}\right)^{-0.429}\varepsilon_G^{\,1.34}$
(Li et al., 1995)[3]	ILALR		$k_L a = 0.0343 U_{Gr}^{\,0.524}\mu_a^{\,-0.255}$
(Merchuk et al., 1994)[3]	ILALR		$Sh = 30000Fr^{0.97}M^{-5.4}Ga^{0.045}\left(1+\frac{A_d}{A_r}\right)^{-1}$

[1] Adopted from Chisti (1989)

[2] Adopted from Jones (2007)

[3] Adopted from Merchuk et al. (1999)

Table 6.2 cont.: Gas-liquid mass transfer coefficient correlations for airlift reactors.

Reference	Reactor Type(s)	Reactor Parameters	Correlations
(Muthukumar and Velan, 2006)	DT-ILALR	Air-(Isoamyl alcohol, benzoic acid, propanol, CMC solution) ε_s = 5-20% d_R = 0.19 m d_r/d_R = (0.34, 0.44, 0.49, 0.59, 0.76) h_R = 2 m h_D = 1.22 m h_c = 0.05 m d_0 = 37x1 mm (PP)	
			For three-phase systems that enhance k_La: $\frac{k_L a d_R}{D_L} = 0.7 c_s^{-0.214} \left(\frac{U_G^2}{g d_R}\right)^{0.49} \left(\frac{d_r}{d_R}\right)^{-0.46} \left(\frac{g d_R^3 \rho_L^2}{\mu_L^2}\right)^{-0.209} \left(\frac{g d_R^2 \rho_L}{\sigma}\right)^{2.515} \left(\frac{\rho_p - \rho_L}{\rho_L}\right)^{-0.144} \left(\frac{U_t \mu_L}{\sigma}\right)^{-0.1}$ For three-phase systems that decrease k_La: $\frac{k_L a d_R^2}{D_L} = 0.64 \varepsilon_s^{-0.214} \left(\frac{U_G^2}{g d_R}\right)^{0.49} \left(\frac{d_r}{d_R}\right)^{-0.46} \left(\frac{g d_R^3 \rho_L^2}{\mu_L^2}\right)^{0.576} \left(\frac{U_t \mu_L}{\sigma}\right)^{-0.343}$ $k_L a = 0.678 U_G^{0.907} \mu_{eff}^{-0.086}$ where: $\mu_{eff} = (5000 U_G)^{n-1}$
(Nicolella et al., 1998a)	DT-ILALR	Air-Water-Biofilm particles U_G = 0.002-0.027 m/s ε_s = 5, 10, 15% d_s = (0.47, 0.91, 1.67, 1.95) mm d_R = 0.060 m d_r = 0.043 m h_R = 0.700 m h_D = 0.360 m	$k_L a = 0.6 \varepsilon_G$
(Popovic and Robinson, 1984)[1, 3]	ELALR BC	Air-Non-Newtonian CMC solutions μ_L = 0.015-0.5 Pa s A_d/A_r = (0, 0.11, 0.25, 0.44)	$k_L a = 1.911 * 10^{-4} U_{Gr}^{0.525} \left(1 + \frac{A_d}{A_r}\right)^{-0.853} \mu_a^{-0.89}$ $k_L a = 0.24 U_{Gr}^{0.837} \left(1 + \frac{A_d}{A_r}\right)^{-1}$
(Ruen-ngam et al., 2008)	DT-ILALR	Air-(Tap and sea water) Salinity = (0, 15, 30, 45) ppm U_G = 0.01-0.07 m/s h_R = 1.2 m L_D = 1 m h_c = 0.05 m d_R = 0.137 A_d/A_r = (0.067, 0.443, 0.661, 1.008) V_L = 1.5 L d_0 = 30x1 mm (PR)	When salinity = 0 ppm $Sh = 0.41 + 1.05 Gr^{0.48}$ When salinity = 15-45 ppm $Sh = 0.41 + 1.04 Gr^{0.16} Sc^{0.3} + 0.13 Re^{0.46} Sc^{0.06}$
(Siegel and Merchuk, 1988)[3]	ELALR		$k_L a = 913 \left(\frac{P}{V_L d_R}\right)^{1.04} U_L^{-0.15}$

[1] Adopted from Chisti (1989)

[2] Adopted from Jones (2007)

[3] Adopted from Merchuk et al. (1999)

7 Fixed Bed Reactors

7.1 Introduction

Fixed bed reactors are three-phase systems for which the solid phase is structurally fixed. There are two basic categories of fixed bed reactors which are defined by the phase flow directions. The first class is the packed bed reactors (PBRs), shown in Figure 7.1. Packed bed reactors are defined by countercurrent phase flow, which can lead to reactor stability and safety issues during exothermic reactions (Yakhnin and Menzinger, 2008). The liquid phase is sprayed from the top while the gas phase is fed from the bottom. The second class is trickle bed reactors (TBRs), shown in Figure 7.2, which have very similar designs, but each component is adjusted to conform to particular phase flow patterns. Trickle bed reactors are defined by cocurrent, downward phase flow – the liquid and gas phases are fed from the top (Maiti and Nigam, 2007; Medeiros et al., 2001). The gas phase is pressurized to improve process efficiency. If the gas and liquid phases flow occurs upward, the reactor is referred to as flooded bed reactor. Although the differences may seem minor, the dynamics can be very different. For example, flooded-bed reactors operate with the packed material being almost or completely submerged while the trickle bed reactor is usually operated with minimal flooding (Al-Dahhan et al., 1997; Kolev, 2006).

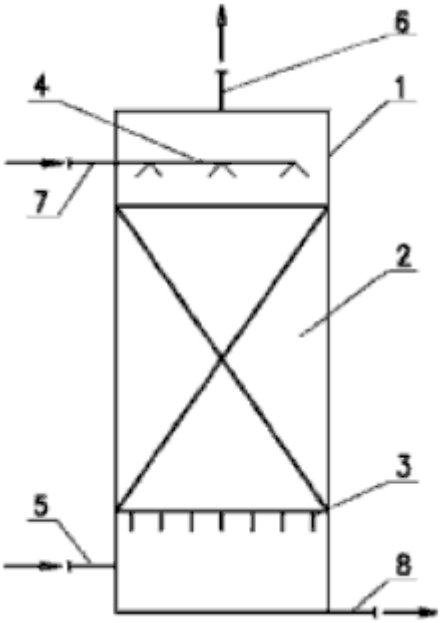

Figure 7.1: Packed bed column internals: (1) vessel, (2) packed material, (3) support plate, (4) liquid distributor, (5) gas input, (6) gas output, (7) liquid input, and (8) liquid output (Kolev, 2006).

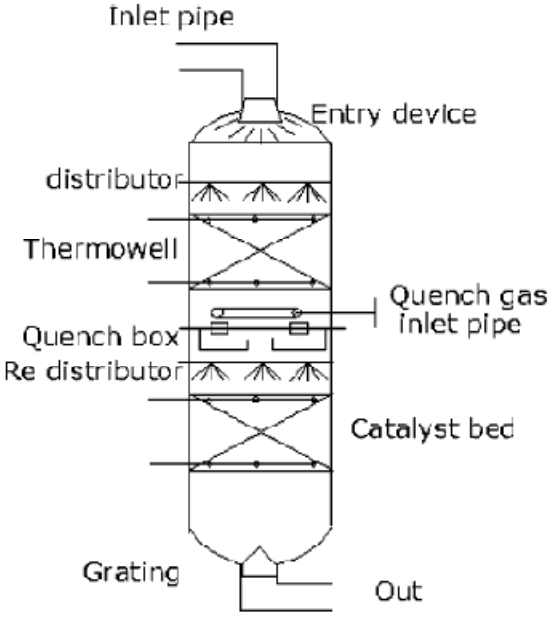

Figure 7.2: Trickle bed reactor schematic (Maiti and Nigam, 2007).

Flooded bed reactors ensure that the entire packing surface is wetted, which is highly important for liquid-phase limited processes and reactions; however, most biological applications are gas-phase limited, which would make the flooded bed reactor less useful in its current state (as used by the chemical industry). This reactor design could be useful for biological applications if the microorganisms require significant substrate flow or are sensitive to gas-liquid interfaces; however, flooded bed reactors are typically not used in industry because they are difficult to design and manage (Maiti and Nigam, 2007).

The exact reactor choice is highly dependent on the type of reaction required by the process. Since biological applications are not very fast, the choice is going to be more dependent on the microorganism's environmental requirements. For biological applications, fixed bed reactors have traditionally been used for shear sensitive microbes and cells (especially mammalian). In contrast, shear resistive strains would be expected to experience better results in a bubble column or airlift reactor since these devices operate at much higher gas and liquid flow rates.

Fixed bed reactors, especially TBRs, are heavily used in industrial practice. They are used by the petroleum, petrochemical, and chemical industries for waste treatment and processing, biochemical and electrochemical processes, and hydrotreatment. Catalysts provide a mechanism to accelerate and channel very complex processes, which would normally require high pressures and/or temperatures and long processing times, into a more manageable reaction and reactor environment. The fixed bed reactor is the perfect reactor-of-choice to achieve these goals such that the trickle bed reactor has been used to process approximately 1.6 billion metric tons of products by the petroleum industry in 1991 alone (Al-Dahhan et al., 1997). Hence, large amounts of research and development have and will continue to go into these reactors because even marginal improvements can yield significant profitability increases.

The negative aspects of fixed bed reactors are often tied to the performance, behavior of the particular catalyst, and potentially difficult design and scaleup (Nacef et al., 2007). If the catalyst is

deactivated or spent fairly quickly, construction of the fixed bed reactors makes the processes impractical. The catalyst would have to be replaced too frequently, leading to high labor and packing costs. One of the main objectives is to ensure that the packing material experiences optimal wetting. Catalysts that do not wet provide inefficient reaction sites. Hence, the flow has to stay within an acceptable pattern. Flow channeling is quite problematic since it can cause inactive catalyst and performance and economic losses (Doan et al., 2008; Maiti and Nigam, 2007). On the extreme, flow channeling can lead to runaway reactions and potentially to combustion/explosion (Al-Dahhan et al., 1997).

A related issue is that identifying flow problems or catalyst utilization is often hard to accomplish in an industrial setting. There are two basic approaches. The first involves measuring pressure drop and/or temperature differentials in the reactor; however, this technique is useful only if flow channeling is significant to cause variations, and it often does not account for wetting problems. The second is to visually inspect the catalyst, but this is often done once the catalyst is spent, which can take up to 2-3 years (Maiti and Nigam, 2007). After the inspection and determination of catalyst inactivity, a plan is made to correct the flow, but the soundness of those corrections cannot be determined until the next inspection. There are other methods to investigate liquid maldistribution, but these can often be complicated or expensive (see Llamas et al. (2008) for an example).

Each reactor type has specific operational parameters. Trickle bed reactors are usually operated adiabatically at high pressure (20-30 MPa) and temperature and employ U_G < 30 cm/s and U_L < 1 cm/s (Al-Dahhan et al., 1997; Attou et al., 1999; Nigam and Larachi, 2005) although research work is often conducted at atmospheric pressures (Attou et al., 1999). Packed bed columns use similar phase velocity ranges, but those can be increased up to U_G < 3.5 m/s and $U_L \sim 0.11$ m/s for some special reactor configurations (Kolev, 2006). Biological operation, however, may call for much

lower velocities. If the fixed bed reactor is used as a biofilter, U_G < 0.001 m/s and U_L < 0.005 m/s are common (Maldonado et al., 2008).

7.2 Column Geometry and Components

The packed bed and trickle bed reactors have very similar construction. Both devices are made of a cylindrical vessel, but the internal construction varies greatly between the designs, engineering firm, or even application. The basic components consist of a support mechanism for the packed material and phase distributors and extractors. The major difference for trickle bed reactors is that they tend to use packaged gas-liquid distributors rather than separate units. Other parts are basically the same although the flooded bed reactor has a different collection system.

The packed bed reactors consist of support plates, hold-down plates, liquid (re)distributors, gas or vapor distributors, gas deflection plates, and screen mesh. The identity and type of the particular parts is dependent largely on reactor scale (Figure 7.1). The gas deflection plates and screen mesh are used in a cross-flow cascade packed column, which is only useful for chemical processes. The support plates are primarily for structural integrity. They simply hold the packed material in place and allow the gas and liquid to pass through. Since the packed bed reactor is sectioned into multiple stages in industrial applications, as shown in Figure 7.1, the support plates also have to prevent phase maldistribution, which is usually accomplished with proper plate leveling. Uneven packing loading may cause support plate bending and flow maldistribution is likely (Kolev, 2006; Maiti and Nigam, 2007). As with aeration plates in bubble columns, the uniform liquid distribution objective is important, difficult, and often not completely achieved.

The design direction often involves using the lightest and least obstructive support plates in order to achieve packed material and flow stability. Since the packed bed reactors are mainly used by the chemical industry, fouling and erosion are important side effects of the reactants. Hence, the chemical industry requires ready access to the packed material and support plates that are easily removed and changed. This requirement would most likely be necessary for biological applications

as well. The support plate is usually fastened to a supporting ring, which is welded to the vessel, due to possible pressure surges, which could potentially lift the support plate and the supported packing.

Support plates are classified according to the type of packing (random or structured) used in the reactor. Support plates used for random packing have inclined walls to support free solid particles and ensure that these stay static. Some examples include the SP 1 (Figure 7.3), 2, and 3 Multibeam support plates. The SP 1 is used for packed bed columns with a diameter larger than 1200 mm while the SP 2 and 3 (Figure 7.4) are used for diameters of 100-300 mm and 300-1200 mm, respectively.

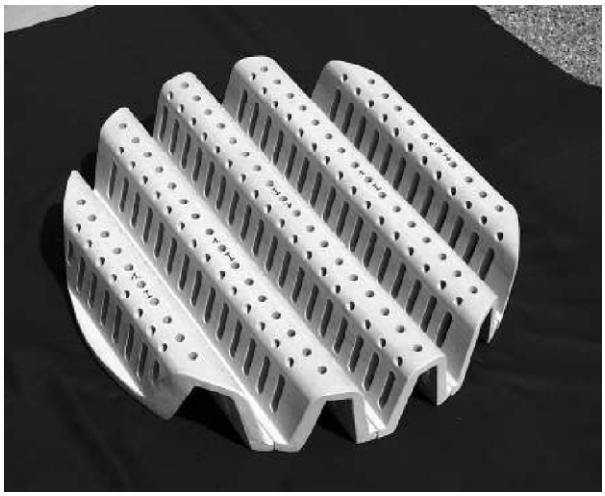

Figure 7.3: SP 1 Multibeam support plate used for columns with d_R > 1200 mm (Raschig Jaeger Technologies, 2006).

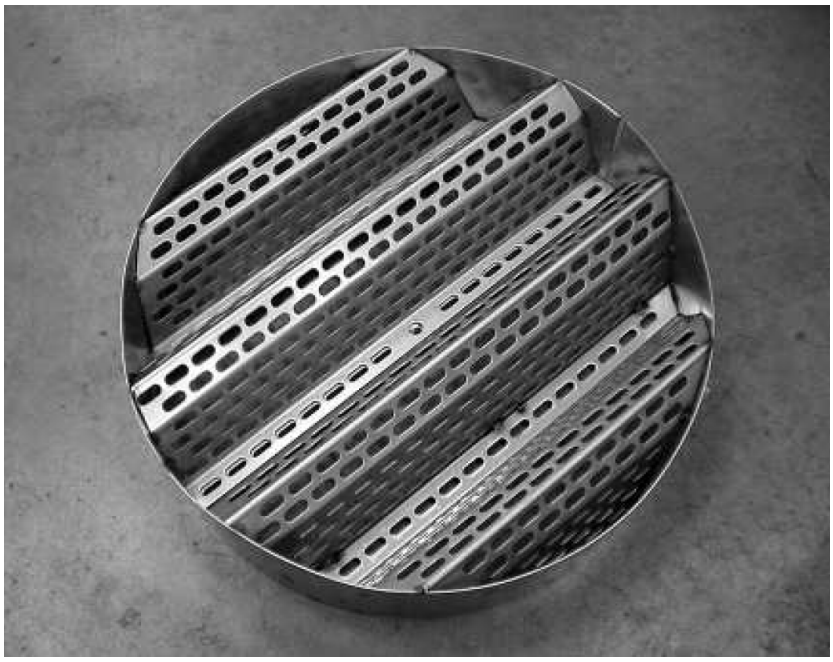

Figure 7.4: SP 2 and 3 Multibeam support plates used for 100 < d_R < 300 mm and 300 < d_R < 1200 mm, respectively (Raschig Jaeger Technologies, 2006).

The column diameter and geometry of the support plates also impose a minimum packing size. The support plate height is dependent on material construction. For example, carbon and stainless steel call for a height of 265 mm while thermoplastic support plates have a height of 300 mm. Due to material properties, larger columns (with larger amounts of supported packing) require further strengthening of the support plates.

The downside of these Multibeam support plates is that they are plagued by fouling and uncontrolled growth, which can lead to improper flow distribution and inefficient reactor operation. Hence, biological processes might find it more advantageous to use a more open support plate such as the hexa-grid (SP-HG) or cross-flow-grid (SP-CF) support plate; however, these plates are usually flat and are more applicable to structured packings. The SP-HG, shown Figure 7.5, is preferred for mass transfer processes while the SP-CF, as shown in Figure 7.6, ensures a more uniform gas distribution. Other possibilities include the flat bar plate (exclusively for structured packing), vapor distributing packing (used to reduce vapor velocity), or ceramic packing (used for corrosive processes) support plates.

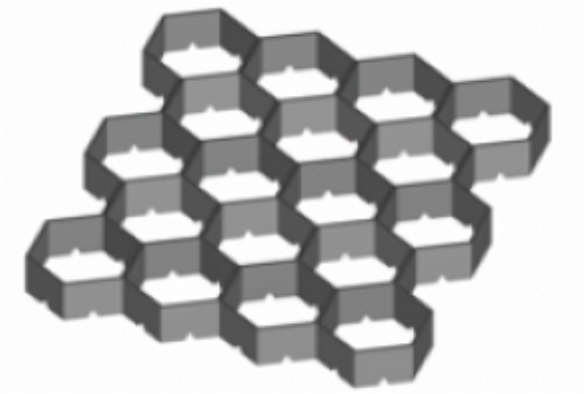

Figure 7.5: SP-HG support plate (Raschig Jaeger Technologies, 2006).

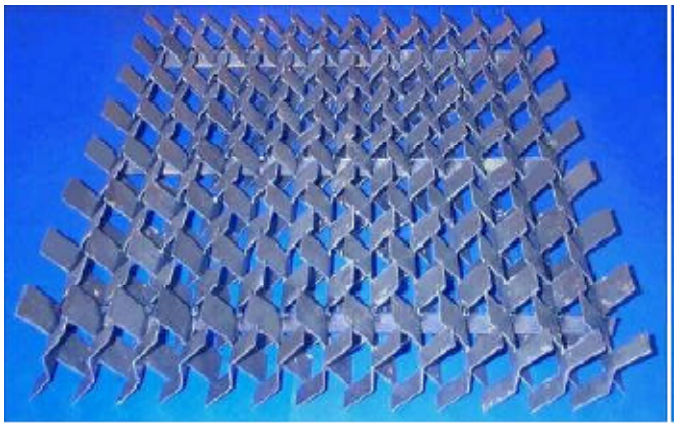

Figure 7.6: SP-CF support plate (Raschig Jaeger Technologies, 2006).

Hold-down plates are used to secure packing in case of flooding or pressure surges. In these situations, it is possible that the packing would wash away and enter the output stream. The standard hold-down plate (HP-1) is constructed from a frame with a metal screen. This hold-down plate is not meant to interfere with the liquid flow, but is also not designed to stabilize the packed material. Hence, more fragile packing, such as ceramics or carbon steel, cannot use the HP-1 plate without a breakage or grinding risk. As such, fragile packing should use the HP-2 hold-down plates, which has a grid-like structure that inhibits packing movement. Structured packing typically utilize hold-down plates (HP-P), which are bolted to the vessel and are designed to prevent movement within the bed or packing wash-out. An example of the hold-down plate is the grid-like Raschig grid

(RG) or HP-1, shown in Figure 7.7. Plates are intended for larger vessels (d_R > 3000 mm), but can also be designed for some smaller ones (d_R = 500-3000 mm).

Figure 7.7: HP-1 hold-down plate (Raschig Jaeger Technologies, 2006).

Since packed bed columns are mainly designed for the chemical industry, a lot of attention is paid to liquid phase distribution, because the liquid distributor design is crucial while gas-phase distribution gets less attention. If the liquid distribution operates or performs poorly, the packing is not going to be wetted effectively, which is important for soluble gases. Nonwetted packing leads to reactor underperformance (Maiti and Nigam, 2007). Although biological systems would also need significant attention, these processes could mostly do with simpler options.

There are two basic options for liquid distribution: single stream and spray distributors. Single stream distributors basically feed the liquid phase through a perforated pipe to channels, which, in turn, distribute the liquid over the cross-sectional area. This is shown in Figure 7.8. Some examples of these are the shower type (perforated) distributor, trough distributor, distributor with weirs, bottom-hole distributor, splash-plate distributor, channel-type distributor, distributor with gas risers, or pipe liquid distributors. Spray distributors are used for processes requiring large amounts of liquid surface, gas cooling, or homogeneous liquid distribution. Since the droplets are smaller, the spray distributors are also better at wetting particles, which produces more efficient packing operation.

Figure 7.8: Example of liquid distributor (Raschig Jaeger Technologies, 2006).

Liquid redistributors are often used to correct liquid flow to a more uniform pattern and/or to add more liquid to the reactor. Liquid distributors are often used to redistribute the liquid phase as well, but a simpler option, shown in Figure 7.9, would be a perforated plate with directional facing. Liquid collectors are used to channel the liquid into the liquid outlet in order to prevent converted/used liquid to stay in the column bottom. The hardest portion of designing a collector is to not interfere with gas distribution, and the available designs are quite wide and diverse. Trickle bed reactors, on the other hand, tend to use liquid collectors, which are only used for collecting and extracting liquid.

Figure 7.9: Example of a liquid redistributor (Raschig Jaeger Technologies, 2006).

Gas distributors are also an important component of packed bed columns and influence phase distribution. The design issue is to ensure uniform flow distribution through the column or a necessary ratio relative to the liquid phase. The liquid-gas ratio is only important if the process requires a chemical reaction of the liquid phase induced by the gas phase. The packing, on the other

hand, is responsible for the pressure drop profile and, hence, the downstream gas phase distribution.

The simplest gas distributor is a perforated pipe. Since the pipe creates a significant amount of flow irregularity in the distributor region, the packed material is usually placed a distance away from the gas inlet to ensure the gas flow becomes more uniformly distributed upon entering the packed region. The separation distance is dependent on the column diameter such that a column of 1 m requires a distance of about 0.4 m. Columns with d_R = 1-2 m require a separation distance of 0.7 m while larger columns should have a distance of about 1 m (Kolev, 2006). An actual rule, which is often linear, can be developed to quantify a column diameter to separation distance ratio, but this rule would be dependent on the level of turbulence. This turbulence can be represented by a ratio of inlet to column gas velocity.

Other gas distributor options include more complicated systems such as a guided vane gas distributor, which attempts to create a more uniform gas distribution through higher turbulence, or a liquid collector-gas distributor combination; this design is more appropriate for high pressure columns, especially if multiple packed beds are necessary. For example, the process may require the product to be extracted and more liquid/gas phase to be input into the column. Hence, such a device would be necessary. Trickle bed reactors share the basic designs with packed bed reactors and make more extensive use of combination devices. Examples of combination distributors for the trickle bed reactors include perforated plate (Figure 7.10), chimney tray, bubble cap tray, and vapor assist lift distributors.

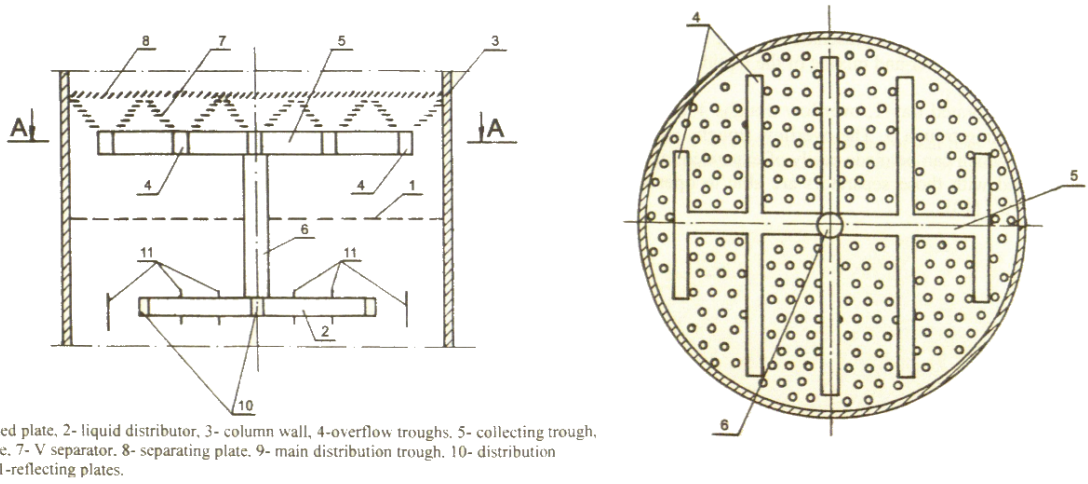

1- perforated plate, 2- liquid distributor, 3- column wall, 4-overflow troughs, 5- collecting trough, 6- join pipe, 7- V separator, 8- separating plate, 9- main distribution trough, 10- distribution troughs, 11-reflecting plates.

Figure 7.10: Example of a combination liquid collector-gas distributor system (Kolev, 2006).

A simple choice is the perforated plate while the chimney is useful if vapors are present. If the perforated plate is used and flow uniformity is desired, the number of drip points should be as large and as close as possible. The problem with most perforated devices is that coking or accumulation of other materials may clog the holes and lead to the initial liquid flow maldistribution. Secondly, the perforated plate requires a certain minimal liquid loading. If the minimal liquid amount is not present, some perforations will stay dry and once again lead to initial liquid maldistribution. The perforated plate cannot be designed for some minimal and universally used value because the pressure drop at nominal operation has to be minimized. Hence, the plate is usually designed for normal state of operation while turndown conditions may be a challenge. A quick summary of available devices for trickle bed reactors is presented in Table 1 (Maiti and Nigam, 2007).

Table 7.1: Distributor comparison (Adopted from Maiti and Nigam (2007)).

Type	Spacing Density	Level Sensitivity	Liquid Rangeability	Vapor-Liquid Flexibility	LiquidVapor Mixing
Perforated Plate	Best	Worst	Worst	Worst	Worst
Chimney	Average	Poor	Poor	Poor	Poor
Multiport Chimney	Average	Average	Average	Average	Poor
Bubble Cap	Worst	Average	Good	Good	Best
Gas-Lift Assisted	Best	Best	Best	Best	Best

The negative aspects and age of perforated plate distributors have led to improvements over the years. A historical performance summary is presented in Figure 7.11. The chimney-type distributors attempt to improve gas-liquid contacting and prevent clogging issues. The liquid is injected as jets while the air is used to break up the liquid into smaller droplets. Unfortunately, chimney-type distributors are highly sensitive to the liquid level and have a limited number of liquid entry points. Bubble caps are distributors which do not use the liquid hydraulic head to perform liquid distribution duties. Bubble caps, in turn, use the gas flow to distribute the liquid. Therefore, the bubble cap trays allow much wider liquid flow rates, but the design requires a larger diameter, which leads to even fewer drip points than the chimney-type distributors. Vapor-lift tubes, as the name implies, use the gas phase to push the liquid from an established level through a U-tube and distribute droplets onto the packing. The biggest advantages of the vapor-lift tubes are that they are smaller, simpler, and cheaper to construct, provide more wall coverage, and increase wetting efficiency. Hence, vapor-lift tubes are expected to become dominant for chemical processes, but a perforated plate might be good enough for biological applications. Graphical examples of combination devices for trickle bed reactors are shown in Figure 7.12 (Maiti and Nigam, 2007).

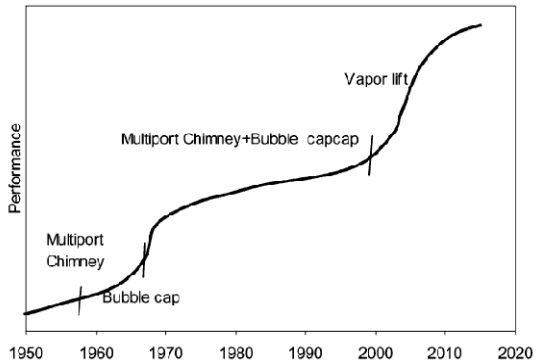

Figure 7.11: Historical distributor performance changes (Maiti and Nigam, 2007).

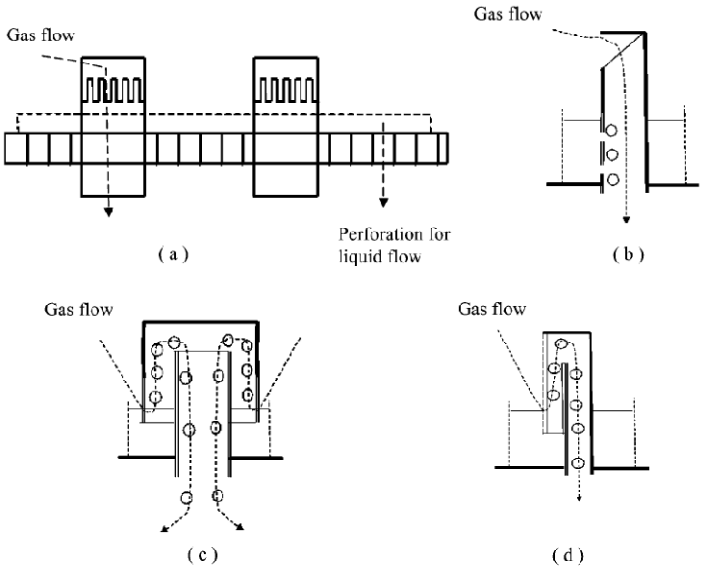

Figure 7.12: Examples of (a) perforated plate, (b) chimney, (c) bubble cap, and (d) vapor-lift tube used in TBRs (Maiti and Nigam, 2007).

7.3 Flow Regime

Packed and trickle bed reactors (PBRs and TBRs, respectively) share some basic flow characteristics, but major differences exist, which lead to differing reactor performance and application. At very low superficial gas velocities, the superficial liquid velocity has a significant impact on the relative gas velocity for both PBR and TBR operation. Furthermore, liquid holdup is solely a function of the superficial liquid velocity (Alix and Raynal, 2008). Under PBR operation, increasing the superficial liquid velocity causes an increase in the relative gas velocity. This effect, in turn, increases the pressure drop of wetted to dry packing. TBR operation, on the other hand, leads to the opposite effect.

By increasing the superficial gas velocity in packed bed reactors, a critical superficial gas velocity is reached at which the friction between the gas and liquid phases leads to an increase in liquid holdup. This critical point also represents the inflection shown in Figure 7.13 and is caused by the emerging and powerful influence of the superficial gas velocity on the liquid holdup. This point is referred to as the loading point.

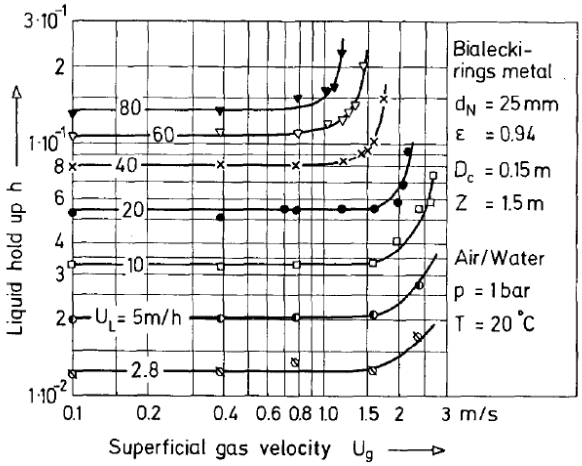

Figure 7.13: Representation of the loading point in packed bed columns (Stichlmair et al., 1989).

As the superficial gas velocity is increased, the liquid holdup increases as well until another critical point, the flooding point, is reached. At the flooding point, the slope of the pressure drop versus superficial gas velocity line becomes exponential. The drag force of the gas phase becomes the dominating influence on the pressure drop (Kolev, 2006; Stichlmair et al., 1989). The effect of the loading and flooding points and the transition on the pressure drop and slope can be seen in Figure 7.14. The identification of these boundaries allow for optimal operation, which is observed between the loading and flooding points for most industrial processes, such that mass transfer is maximized while operating costs are minimized.

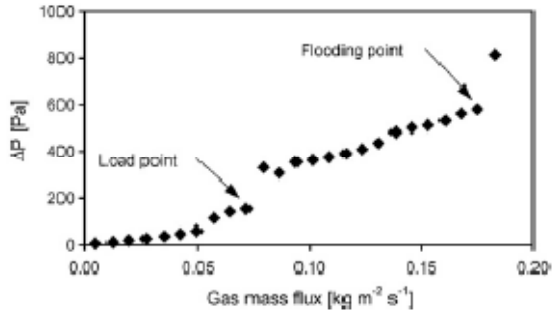

Figure 7.14: Example illustrating loading and flooding points (Breijer et al., 2008).

The operating range between the loading and flooding points is referred to as the loaded regime. The loaded regime is important for mass transfer purposes. One way to judge mass transfer efficiency in fixed bed reactors is with the height equivalent to a theoretical plate (HETP). A theoretical plate is an abstract stage in which two phases are capable of establishing an equilibrium. Thus, having an actual height that is lower at the same superficial gas velocity implies a more efficient mass transfer process. In the same line of reasoning, having the same equivalent height with a higher superficial gas velocity implies that more mass has been transferred, and the reaction occurs under more optimal circumstances.

Figure 7.15 represents the effect of increasing the liquid rate in direct proportion with the vapor (gas) rate. The important markers are points C, E, G, and F. Point A illustrates a minimal liquid loading or a minimal liquid and vapor rate at which the column converts the feed. If the vapor rate is lower than the critical value at point A, the HETP increases such that a practical column is not operable. Points C and F represent the loading and flooding points, respectively. The region between points B and C define the constant separation efficiency region, where the interaction between the liquid and vapor is weak. Point E represents the minimal HETP, which would yield the operating condition for the shortest and smallest column; however, a more efficient point can be obtained at point G, which represents the maximal efficiency capacity (MCE). The maximal efficiency capacity provides the most stable operations while also maximizing the mass transfer potential. Increasing the vapor rate beyond point G yields an inefficient result such that the column requires larger and larger scale in order to achieve the same result (Kolev, 2006) – not something designers and operators look for.

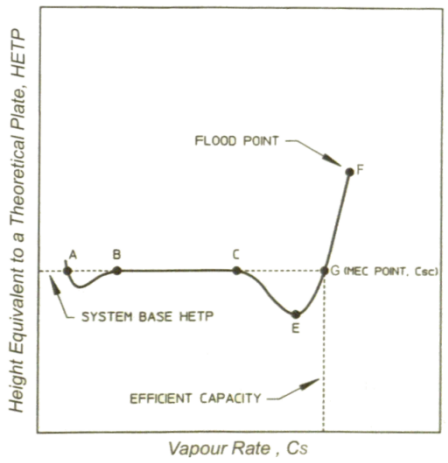

Figure 7.15: Packed bed reactor operating regimes (Kolev, 2006).

Another way to define the flow in packed bed reactors is using the Reynolds number, which is defined by the packing diameter and superficial (gas) velocity. Creeping flow is observed at Reynolds numbers less than 1. This region is defined by a linear pressure drop with increasing interstitial velocity. A steady laminar inertial flow is observed within a Reynolds range of 10-150 where the pressure drop develops a nonlinear relationship with interstitial velocity. An unsteady laminar inertial flow develops at Reynolds numbers of 150-300; this region is defined by laminar wake oscillations in the pores. Furthermore, vortices start developing at a Reynolds number of approximately 250. At Reynolds numbers above 300, the flow becomes unsteady and resembles turbulent flow. It should be noted that experimental scale vessels experience Reynolds numbers in the creeping and steady laminar inertial flow while industrial scales operate at higher Reynolds numbers (Schuurman, 2008).

In trickle bed operation, the frictional force acts in the flow direction, decreasing the liquid holdup. For TBR operation, the flooding point does not exist in the same sense as in a PBR. Instead, the same critical ("flooding") point in the trickle-flow regime is defined by a decreasing slope relative to dry packing (Kolev, 2006; Stichlmair et al., 1989). Hence, the trickle bed reactor is not affected by flooding or loading conditions and can be applied to wider gas and liquid phase flow ranges (Breijer et al., 2008). The trickle-flow reactor is only limited by the pressure drop, which

causes economic constraints for TBR application. The downside is that the packed bed reactor is necessary for equilibrium reactions, which are not easily carried out in a trickle bed reactor due to the countercurrent nature of the phase flow directions (Al-Dahhan et al., 1997; Kolev, 2006).

The general PBR flow structure is highly dependent on the initial liquid phase flow distribution, liquid velocity, particle shape, particle size, and packing method. The fact that the packing method is influential can be somewhat troubling with random packing as results are harder to replicate once the packing is replaced. On a smaller scale, the flow structure is affected by start-up procedure, wettability, flow modulation, and particle coordination number (number of touching neighbors per particle). The level of the nonuniformity is largely controlled by reactor internals. A properly designed and operated reactor is expected to have uniform flow distribution or at least become stable relatively quickly (Doan et al., 2008; Maiti and Nigam, 2007).

Nonuniform flow has several causes. The first cause is that the initial liquid distribution is not uniform such that the liquid does not enter the packing volume uniformly (shown in Figure 7.16a). If the liquid is not well-distributed and adjustments are not effective or easily implemented, a layer of inert packing particles on top of the reactive packing may lead to some flow improvement. The more common cause is that the packing has not been packed well, damaged, or that its shape makes the flow unstable (shown in Figure 7.16b). The shape may lead to liquid maldistribution in the case that the reactor-to-particle diameter is too small (i.e., the particles are too large relative to the reactor diameter). For example, if the ratio is less than 20, the liquid starts to show maldistribution near the wall region at higher superficial liquid velocities. Hence, the reactor-to-particle diameter should be at least 20 to ensure proper liquid distribution for nominal liquid velocities (Metaxas and Papayannakos, 2008). If axial dispersion is problematic, a ratio larger than 50 minimizes the influence of axial variations (Schuurman, 2008). It should be noted that liquid flow at the wall requires a bed height-to-diameter ratio of at least 4.0 (Doan et al., 2008). The unfortunate result is that the packing is not properly wetted (shown in Figure 7.16c), and the mistake is often not

realized until the packing is replaced, which may not occur for at least 2-3 years (Maiti and Nigam, 2007).

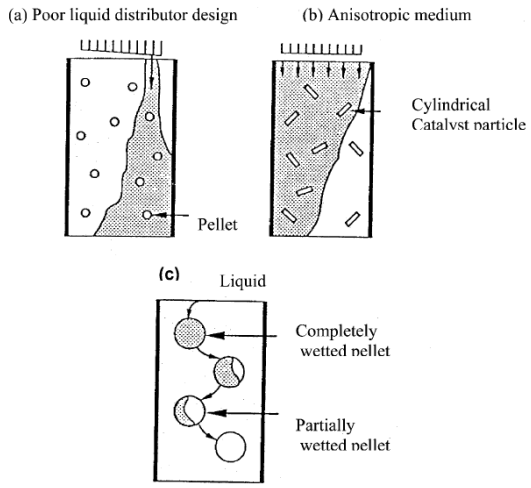

Figure 7.16: (a) Initial liquid maldistribution and (b) restrictive packing leading to (c) different levels of wetted pellets (Maiti and Nigam, 2007).

Packing manufacturers develop and test their packing extensively, but oftentimes do not have the expertise or infrastructure to test packing flow behavior. Engineering firms have the expertise, but are missing the infrastructure and incentives to test packing. Hence, the customer and end-user is expected to experience some trouble that usually requires on-site adjustment (Maiti and Nigam, 2007).

The trickle bed reactor hydrodynamics are influenced by the operating conditions, reactor design, reactor internals, distributor design, and phase properties (Nacef et al., 2007). There are four basic flow regimes in a TBR. At low superficial liquid and gas velocities, the liquid trickles onto the packing, forming streams and films, while the gas phase flows through the residual voids; this is called the trickle regime. The trickle bed reactor performance in the trickle regime is dependent on the pressure gradient and liquid saturation. A significant portion of the packing is unwetted in the trickle regime, which is addressed by increasing the superficial liquid velocity. The extent of unwetted packing may be used to identify flow nonuniformity and its causes (Liao et al., 2008) since the packing should be completely wetted during the transition from the trickle to pulsing flow

regime. The liquid holdup can be increased by increasing the liquid flow rate, while increasing the gas flow rate leads to a decrease in the holdup (Burghardt et al., 1995).

At higher superficial liquid velocity, the pulsing regime is formed because the liquid blocks the flow paths and forces alternating liquid- and gas-rich regions in the reactor volume. This is very similar to the slug flow regime in bubble columns. An interesting behavior in the pulsing flow regime is that the liquid holdup is mostly independent of the liquid flow rate although it is still negatively affected by an increase in the gas flow rate (Burghardt et al., 1995). The identification of the pulsing regime is achieved by using the transition between the trickling and pulsing regimes. This transition is defined by a temporary decrease in drift flux (velocity) as the superficial gas velocity is increased, as seen in Figure 7.17. Correlations have been developed that attempt to model the velocity at which the transition may occur; however, these correlations are limited to only a few important parameters (phase velocities, liquid viscosity, particle diameter, and bed height) (Nacef et al., 2007) such that more complicated processes, such as those involving non-Newtonian liquids, are almost impossible to predict.

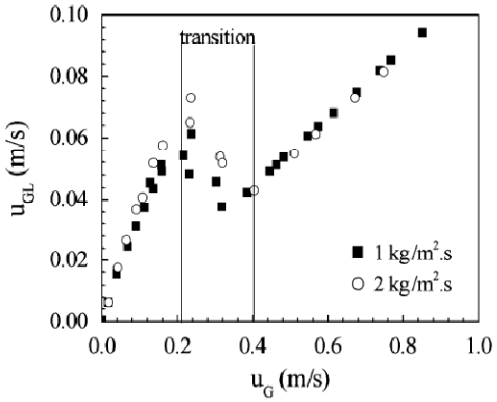

Figure 7.17: Flow regime detection in trickle bed reactors (Nacef et al., 2007).

At high superficial gas and low superficial liquid velocities, a spray regime occurs that is defined by the liquid phase being turned into droplets by the continuous gas phase. At low superficial gas and higher superficial liquid velocities, the dispersed bubble (gas) regime is observed and defined by a continuous liquid phase, which entrains the gas phase as bubbles (Attou et al., 1999). The dispersed bubble is most often used in the trickle bed reactor, but pulsing regime operation is also common (Burghardt et al., 1995). Biological application would benefit the most from the dispersed bubble regime while the pulsing regime may cause damage to the microorganisms as well as potential exposure to the gas-liquid interface. A generalized regime map has not been developed because the regime transitions are dependent on material properties like wettability, size, shape, packing, etc. (Maldonado et al., 2008).

7.4 Liquid Properties

Liquid properties influence the behavior of the bubble interface and, consequently, have a strong effect on both the liquid-phase mass transfer coefficient and the interfacial area. Research using organic liquids, which would be very useful for bioreactor and gas-liquid mass transfer optimization, is almost nonexistent for fixed bed reactors.

It should be noted that packed bed reactors operate differently than other gas-liquid reactors covered so far. In the other reactor designs, the gas phase is dispersed in the liquid phase such that bubbles are formed from which the gas phase is transferred to the liquid. The surface area through which the transfer occurs is the bubble's. In packed bed reactors, general operation yields droplets immersed in the gas phase, which causes the main transfer surface to be the droplet-gas interface. In order to increase the mass transfer interface, smaller droplets have to be produced. This process is often turbulent and may result in liquid droplet breakup and coalescence, which may be destructive to some microorganisms (specifically those that are shear sensitive).

A unique property of fixed bed reactors in general is that the wetted particles also become part of the mass transfer interface. This difference is not too important for chemical systems due to the commonly used packing designs, but biological systems may have additional problems. For example, the packing serves as a supporting mechanism for the microorganisms. Hence, the microorganisms feed and breath through the liquid layer on top of the colonies. If the liquid droplets do not touch or interact in some way with the liquid-microbial interface, mass transfer may not occur. Another design objective has to be added to biological systems that stipulates that the packing is refreshed with liquid and that the liquid's interaction with the microbial interface is optimized. The liquid properties play a crucial role in this process. The viscosity of the liquid determines the stickiness or the wettability of the packing. The degree to which this property is important is highly variable with the specific microbial needs, and research determining this requirement in fixed bed reactors is nonexistent; however, if trickle- or flooded-bed reactors are used, gas bubbles are the mass transfer mechanisms, and the same bubble behavior and interactions are to be expected as with (three-phase) bubble columns and airlift reactors (Nacef et al., 2007).

Unfortunately for biological applications, the liquid property influence is often ignored in fixed bed reactor research. Approximately half the data for fixed bed reactors has been obtained using air-water systems with glass bead packing (Nacef et al., 2007). Hence, a significant problem arises. The available data is biased towards a situation that does not occur in industrial settings or biological applications, even if they are for experimental purposes. To make matters worse, experimental phase flow ranges oftentimes differ significantly from industrial practice (Burghardt et al., 1995) such that those results by themselves would have little meaning for real-world application. Furthermore, these test systems experience constant properties, such as liquid viscosity or particle density. This state is often not observed in biological systems since

microorganisms change the liquid properties and consume or colonize the solid phase. Hence, the effective liquid viscosity and particle density may be unsteady.

7.5 Packing Material

Packing is the solid and fixed phase in the reactor volume. It is often used to judge reactor performance and utilization. The wettability or wetting efficiency is the representative parameter of choice and is defined as the ratio of wetted-to-external particle surface area (Metaxas and Papayannakos, 2008). The external area is not equal to the total surface area because the external area excludes the contact areas (Burghardt et al., 1995). The wetting efficiency is a function of phase flow rates, pressure, liquid properties, and packing diameter. In most cases, the wetting efficiency varies between 0.6 and 1.0. The most common approach to measuring wettability is by using tracers and visual inspection. Reaction methods can be used, but are difficult to implement from a theoretical point of view (Nigam and Larachi, 2005). The type of packing generally does not determine wettability directly, but rather influences the liquid distribution, which may lead to non-wetting if flow maldistribution occurs.

As summarized by Nigam and Larachi (2005), wettability may be modeled using saturated pores and solid surfaces. At low wettability, the liquid volume per unit wetted surface area is large (represented by Figure 7.18A). As the wettability increases and the liquid volume per unit wetted surface area decreases, and the contact angle and the wetting efficiency increases (Figure 7.18B); however, this is followed by a small contact angle and decrease in efficiency (transition between Figure 7.18B and C) and then a resumption of the nominal increase (Figure 7.18C). A further increase in wettability causes a steep contact angle and quick increase in wetting efficiency (transition between Figure 7.18C and D), which is followed again by a contact angle and efficiency decrease (Figure 7.18D). As the wetted pores reach each other, the contact angle becomes stationary and further liquid flattening is not possible such that wetting efficiency is abnormally high (transition between Figure 7.18D and E). If there are any partially solid surfaces left, the liquid

film ruptures and a quick decrease in wetting efficiency is observed (Figure 7.18F). The result of higher wetting efficiency is a thinner liquid film, which would also represent a smaller resistive mass transfer force (Liao et al., 2008; Nigam and Larachi, 2005). Hence, porosity has a significant impact on wetting efficiency and hysteresis behavior.

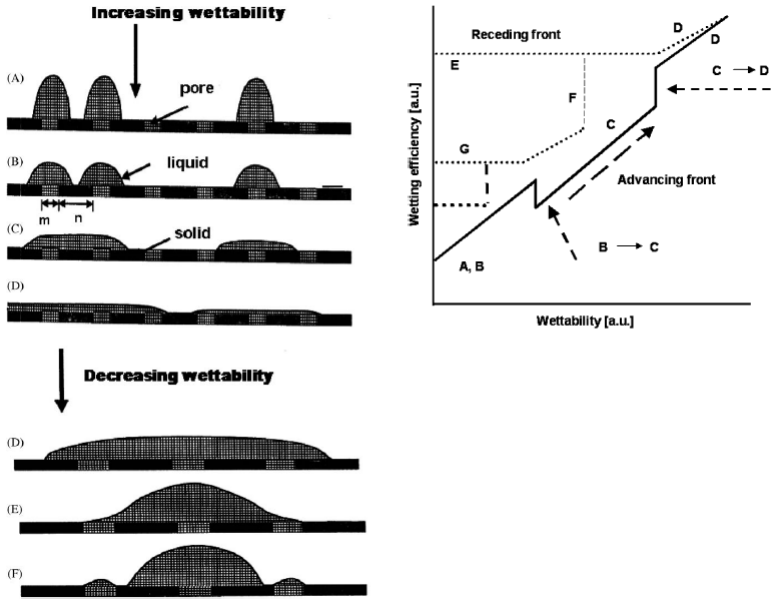

Figure 7.18: Wetting efficiency dependence on the contact angle movement (Nigam and Larachi, 2005).

The startup procedure for fixed bed reactors often involves prewetting the packing in order to limit operational variations. Interestingly, reactors may demonstrate better or worse performance due to a different startup procedure. In other words, the pressure drop or liquid holdup are not good indicators of flow uniformity, but rather shows significant dependence on the startup and prewetting procedure. The possible startup procedures include a dry, Levec, Kan liquid, Super, and Kan gas mode. The dry mode starts the process with the packing dry. The Levec mode prewets the packing for about 20 minutes by flooding the reactor volume and then allowing the liquid to drain out after which the liquid is reintroduced and the process is allowed to start normal operation. The Kan liquid mode prewets the packing by cycling the reactor between the pulsing regime and the operating set point. The Super mode simply floods the reactor volume and then reduces the phase

flow rates to the operational set points. The Kan gas mode prewets the packing by operating in the pulsing regime. The pulsing regime is achieved by increasing gas flow to the critical pulsing point after which the phase flow rates are adjusted to the operational set point (van der Westhuizen et al., 2007). Prewetting has not been studied with biological media so that its influence is currently unknown for this application.

7.5.1 Random Packing

There are two basic types of packing materials: random and structured packings. Random packings are commonly formed from different shapes such as rings, shown in Figure 7.19, or saddles, shown in Figure 7.20. They are constructed out of ceramic, metal, plastics, or coke with the most popular metal application being stainless steel. A chemical treatment may be applied to the surface in order to increase the wettability and process efficiency (Kolev, 2006; Strigle, 1994).

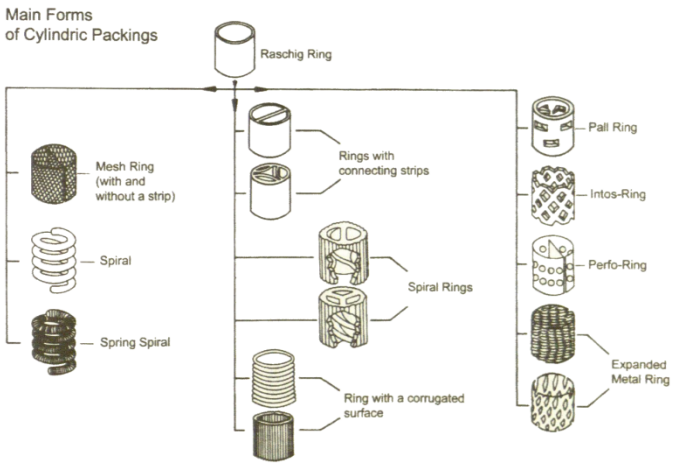

Figure 7.19: Raschig ring packing examples (Reichelt, 1974).

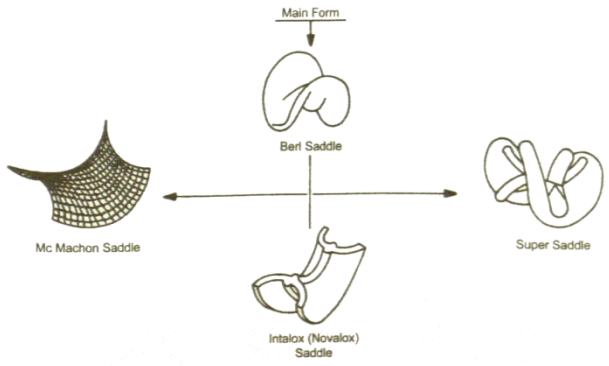

Figure 7.20: Saddle-type packing examples (Reichelt, 1974).

The simplest random packings are spherical, but are not used very often in industry. The most commonly used packing are the Raschig rings and its descendents. The historical development of random packing is summarized in Figure 7.21. Each alteration stems from the need to improve packing performance for the particular process. The most common goal is to increase the surface area available for mass transfer and reaction. The great advantage of random packing is the ease with which it can be produced and loaded into the column. Typically, the packing is simply loaded from the top onto the support plate and secured by the hold-down plates. On the other hand, the random and unstructured distribution of the packing also leads to poor phase distribution, possible flow channeling, and higher pressure drop (Kolev, 2006; Strigle, 1994). The pressure drop, on the other hand, may also be an advantage as it leads to a higher level of turbulence and, hence, higher gas-liquid mass transfer efficiency relative to structured packing (Schultes, 2003).

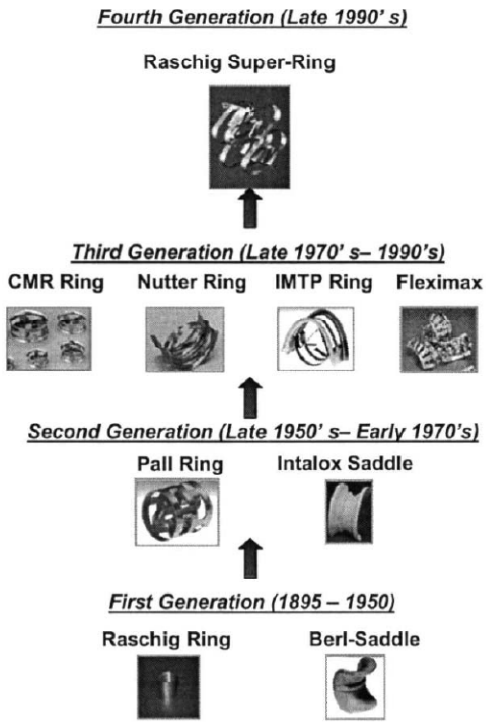

Figure 7.21: Historical random packing development (Schultes, 2003).

The first and most logical adaptation has been to add dividers, internal spirals, and corrugated surfaces to the Raschig ring. Although these rings effectively increase the area, the pressure losses and gas clogging/slugging can be significant, which may limit the operating range. The second adaptation has been to make the rings out of mesh and spirals. Lastly, the rings can be perforated. Interestingly, the pall ring has been determined to fulfill most mass transfer requirements and a better random packing has not been found in the last 30 years; however, other options, such as the Hiflow ring, Ralu-Flow, IMTP, Nutter ring, and Raschig Super Ring, are available and provide satisfactory mass transfer results. Although statistics and performance measures are collected, they are highly dependent on the column diameter such that results presented in the literature may vary greatly and be a challenge to reproduce (Kolev, 2006).

The mass transfer requirement stipulates that the patella (connecting strip) cannot be larger than 5 mm in width. If the patella is larger than that, a droplet will form on the surface, which will effectively reduce the wetted surface available for the reaction. If the patella is less than 5 mm in width, the liquid is capable of moving over the surface without accumulating. The result is that the operating range is widened. The downside is that as the width is decreased, the pressure drop increases. This increase may limit the economics of the process.

7.5.2 Structured Packing

Structured packing is constructed to provide optimal phase channeling and uniform phase distribution. Structured packing material is very similar to the random packing and includes metals, ceramics, plastics, and other materials like wood. Structured packing is usually subdivided into smooth-walled packing, packing with turbulizers, expanded metal packing, corrugated metal sheet packing, and packing for very low superficial liquid velocities (Kolev, 2006; Strigle, 1994).

Smooth-walled packing is constructed using vertical walls, which attempts to limit the pressure losses for a given operating condition. As such, they provide the lowest pressure drop per mass transfer unit for a given volumetric mass transfer coefficient. The first generation of structured packing were fixed rings, such as Raschig rings. Although the construction was very simple, a significant problem became apparent early on. The interior ring channel (labeled 1 in Figure 7.22) is much larger than the exterior ring channel (labeled 2 in Figure 7.22). This discrepancy leads to flow channeling and a dry packing surface. Hence, the natural evolution has been to construct structured packing using similar members and forming them into symmetrical arrangements. Some popular formations are shown in Figure 7.23. Honeycomb has quickly become very popular, largely because they are able to provide a lower pressure drop for a given volumetric mass transfer coefficient. For example, honeycomb packing (Honeycomb No. 1) provide a pressure drop that was 8.3 times lower than the Raschig rings (Kolev, 2006).

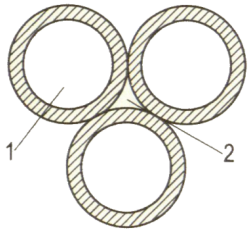

Figure 7.22: Cross-section of structured (Raschig) ring packing (Kolev, 2006).

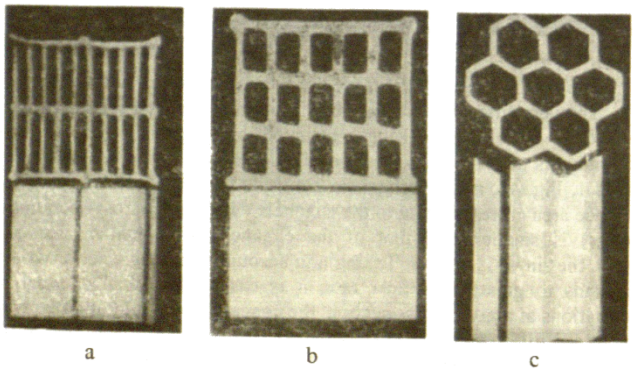

Figure 7.23: Examples of a) slit block, b) grid block, and c) honeycomb block packing structures (Kolev, 2006).

Packing with turbulizers, referred to as Turbo-pack, is made by thermo-pressing or stamping plates such that the packing surface is ribbed, which increases turbulence near the wall. This increased turbulence leads to better heat and mass transfer performance. Turbulizers are usually made in the horizontal direction in order to achieve axial flow uniformity. The result of using turbulizers is that the operable superficial gas and liquid velocities are increased. For example, P15-235 (type of structured packing with turbulizers) allows for superficial gas and liquid velocities up to 3.5 and 0.11 m/s (in PBRs), respectively (Kolev, 2006). The interesting behavior of these turbulizers is that at low superficial liquid velocity, the pressure drop of the wetted packing is half the pressure drop experienced by the dry packing. At high superficial liquid velocity, the pressure drop equalizes for wetted and dry packing.

Expanded metal packing is constructed by stamping or otherwise forming a channel from metal plates. The greatest advantage of this type of packing is that the channels are exclusively in the vertical direction such that the pressure drop is lower relative to the other packing types. Another derived advantage is that this also allows for very high superficial gas velocities, potentially reaching 2.5-3.5 m/s. In order to achieve even higher gas velocities, the gas phase is input and extracted horizontally from the vessel, which allows operational superficial gas velocities up to 6 m/s. The most important disadvantage is that the vertical channel leads to the liquid preferentially wetting the leading edges. Hence, this packing requires more rigorous collection and redistribution than the other options. The exact behavior of the expanded metal packing is highly dependent on its construction, which can vary significantly. Major design considerations are the pitch, step height, and the existence and extent of perforations. The pitch, for example, can be designed so that the packing may be almost completely wet at relatively low superficial liquid velocities or able to handle an extreme (relative to other packing) amount of liquid (Kolev, 2006; Strigle, 1994).

The structured packing of corrugated sheets attempts to fix a major disadvantage of the smooth-walled packing: the possibility of free-falling liquid through the open cross-sectional area. The corrugated sheets are designed to intercept liquid (usually within half of one wave) and enhance axial mixing (Kolev, 2006). The downside is that the pressure drop is larger relative to other structured packing options, but lower than random packing.

Certain processes, such as those relying on equilibrium absorption with low initial concentration of highly soluble gases, require very low superficial liquid velocities in the countercurrent configuration such that existent packing does not perform well. The operator has the option of using very easily wettable materials or using a highly specific packing form. This circumstance is rarely encountered for biological application.

7.6 Biological Considerations

Biocatalysis and microorganisms have become great hopes and are seen as possible solutions to a multitude of problems. As such, research efforts are starting to turn towards suspending microorganisms on packing material to perform similar roles as reactive packing or perhaps completely new functions (Llamas et al., 2008). Biological microorganisms are typically attached to the packing surface since the microorganisms either perform better when cell adhesion occurs or when the cells are highly shear sensitive and need to be protected. Hence, fixed bed reactor performance is highly dependent on the liquid distribution uniformity. It should be noted that the liquid phase usually serves as the food source for the microorganisms. So, if the packing is not wetted, microorganisms will not colonize that section of the reactor. This, in turn, can severely limit reactor performance (Doan et al., 2008).

In addition, column internals may be of significant importance. Even though the perforated plate is a simple and effective device, it tends to provide minimal wall wetting and tends to channel liquid through the central region. This effect can cause interesting performance variations at different liquid flow rates and may make comparisons between different research work difficult. If the outer regions need to have liquid exposure, a better liquid distributor should be selected. Similar channeling can also be experienced by uneven cellular growth rates within the reactor volume.

Biomass and microorganism tend to have a positive effect on fixed bed performance. Packing is usually judged on the basis of wettability, which biomass seems to increase. Doan et al. (2008) compared the wettability of plastic spheres with the same plastic spheres in the presence of microorganisms. The result has been that the liquid holdup increased by approximately 20% in the presence of microorganisms.

Liquid flow distribution and gas solubility issues can be enhanced with periodic liquid flushing of the reactor volume. The flushing tends to renew interfaces and reduce the gas-phase transport resistance (Nigam and Larachi, 2005). This practice may also have additional benefits in controlling microorganism growth. If the microorganisms do very well, the colonies might grow too thick and kill the lower cell layers. In order to prevent buildup in the reactor volume, a flushing cycle could be performed to detach a specific region or amount of microbial growth.

7.7 Correlations

Correlations for fixed bed reactors, which are shown in Tables 7.2 and 7.3, are currently available for specific operating regimes and packing types. Some aspects can be generalized; however, correlations are developed for either random or structured packing even though the same major theories are used to explain gas-liquid mass transfer and behavior (Larachi et al., 2008). Current fixed bed correlations are very design specific, and any broad correlations produce highly variable and sometimes impractical results. This has been at least partially the result of many experiments being conducted at much lower pressure than those observed during industrial application (Attou et al., 1999). Kolev (2006) collected gas-liquid mass transfer correlations for the packed bubble column for his book on packed bed columns; however, the number of correlations is small because research is limited on gas-liquid mass transfer in packed bed reactors. The most recent correlation (other than Kolev's) is from Billet (1989). Most of the work seems to have been done in the 1950s and 60s. Since then, correlations have been seldom formed.

Perhaps the reason for the lack of correlations is twofold. First, the more important information for chemical engineers is the pressure and temperature predictions. With these in hand, chemical engineers are able to predict the other factors of importance. Biological processes are not expected to behave like this, and more work would need to be done for this purpose.

A second reason is perhaps the research group represented by Professor Larachi at Laval University. They have been at the forefront of providing correlations capable of predicting fixed bed performance for a wide variety of packing and designs. Their approach has been based on developing a large database, which incorporates 861 and 4291 experiments for structured and random packings, respectively, and the use of a neural network to determine the most important factors in predicting the necessary output. The resulting average error varies between 20.9-29.2% among six different mass transfer parameters. They have created separate correlation Excel files for the packed, flooded, and trickle bed reactors, which can be accessed from Professor Larachi's homepage at the Laval University (Larachi et al., 2008; Piché et al., 2001a; Piché et al., 2001b; Piché et al., 2001c); the link to this site is http://www.gch.ulaval.ca/bgrandjean/pbrsimul/pbrsimul.html. This is currently the best and most comprehensive resource for gas-liquid mass transfer information applicable to fixed bed opeartion.

7.8 Needed Research

Fixed bed reactors have been largely used by the chemical and related industries. Industrial biological applications are limited. Since fixed bed reactors operate at lower superficial gas and liquid velocities, it is going to be very hard for these reactor types to compete with bubble columns, airlift reactors, or membrane reactors (Gottschalk, 2008). A second competitive problem is that interfacial area in fixed bed reactors is made of liquid droplets and wetted packing. If fixed bed reactors are to be used in biological applications, more research needs to be directed towards increasing the surface area available for mass transfer. One solution that could use more investigation is operation in the flooded regime, which would allow for more bubbles and a larger interfacial area; however, the problem with this approach is that such operation may be described as more bubble column than fixed bed reactor. So far, biological research has been concentrated on waste treatment and providing a support mechanism for highly shear sensitive media such as

mammalian cell structures. In other words, if the microorganism is tough enough for a bubble column or airlift reactor, the fixed bed reactor is not effective.

The current research effort in fixed bed reactors is directed towards the improvement of packing. The view is that the packing choice can make or break the success of the operation and that current operations are so large that even minimal improvements would yield tremendous savings. Although the reactive function is very important given the supporting role packing has in chemical reactions, biological systems are going to be less dependent on this packing function and would be better served with packing that supports larger amounts of microorganisms.

7.9 Summary

Fixed bed reactors use packed, fixed material with the purpose of achieving higher reaction rates than would be possible with two-phase interaction alone. In order to conform to different types of reactions, several styles and forms of fixed bed reactors and packing are in use. The packed bed reactor is a countercurrent model, which injects the liquid from the reactor top and gas from the bottom. The trickle bed reactor is a downward flowing cocurrent reactor. If the flow occurs in the upward direction, it is referred to as a flooded bed reactor. As far as the packing goes, the designer and operator have a wide array of options, which are mainly due to a tremendous amount of customization that has occurred over the years. This experimentation has led to dozens of different packing materials and classifications.

Generally speaking, fixed bed reactors are not able to transfer as much mass as the previously covered reactor types because the phase flow rates in fixed beds is usually much lower. This is due to the fact that the pressure drop across the bed would increase to a value that would make almost any operation either unprofitable or nonreactive. Hence, the general application of fixed bed reactors is to provide a support structure on which microorganisms can grow. Another application of the fixed bed reactors is to serve as biofiltration devices.

There is still a lot of work – including more basic research – left to do on fixed bed reactors for biological applications. Most of the data, conclusions, and designs have been developed for chemical processes and reactions, which usually require very high pressures and temperatures. Microorganisms often have very different requirements and interactions, which have not been explored very deeply, if at all. For example, there isn't a single gas-liquid mass transfer correlation that is directly applicable to microbial design mainly because most of them have been developed in the 1940-60s. So, if the fixed bed reactor limitations are kept in mind, the design can be adapted to serve roles currently supplied by chemical reactions or open the doors to new applications.

Table 7.2: Gas-liquid mass transfer correlations for fixed bed reactors (Adopted from Kolev (2006)).

Researcher(s)	Reactor	Packing	Correlation
(Billet, 1989)		RP	$k_L a = C_L \frac{a^{2/3}}{d_h^{0.50}} D_L^{0.50} \left(\frac{g\rho_L}{\mu_L}\right)^{1/6} U_L^{1/3} \frac{a_e}{a}$ where C_L is an experimental, packing dependent constant
(Fujita and Hayakawa, 1956)	PBR	Rings 5-35 mm Saddles 13-40 mm	$Sh_L = 0.025\left(\frac{h_P}{\delta}\right)^{-0.19} Re_L^{0.67} Sc_L^{0.50}$
(Kasatkin and Ziparis, 1952)	PBR	Rings 8-20 mm	$Sh_L = 0.0021 Re_L^{0.75} Sc_L^{0.50}$
(Hikita and Ono, 1959)	PBR	Wetted single element	$Sh_L = 0.27\left(\frac{d_P}{\delta}\right)^{-0.50} Re_L^{0.545} Sc_L^{0.50}$
(Krevelen and Hoftijzer, 1948)	PBR	Rings, coke, and others	$Sh_L = 0.00595 Re_L^{0.67} Sc_L^{0.33}$
(Koch et al., 1949)	PBR	RP	$k_L a = 0.25 L_m^{0.96}$ $k_L a = 0.0085 U_L$
(Kolev, 1976)		RP	$Sh_L = 0.030 Re_{Le}^{0.50} Ga_L^{0.28} Sc_L^{0.50}$ $Re_{Le} = \frac{4U_L}{a_e \nu_L}$ Sh_L and Ga_L determined by d_P
(Kolev and Daraktschiev, 1976)		Holpack	$Sh_L = 0.00113 Re_L^{0.635} Sc_L^{0.5} Ga_{Lh}^{0.366} (s/t_P)^{4.0} (at_P)^{0.1}$
(Kolev and Semkov, 1983)		RP	$Sh_L = 0.0115 Re_L^{0.33} Ga_L^{0.42} Sc_L^{0.5} (ad_P)^{-0.37}$
(Kolev and Nakov, 1994)		FP with turbulizers	$Sh_L = 0.0077 Sc_L^{0.5} Re_L^{0.70} (ah_P)^{-0.29} (as)^{-0.19}$
(Larachi and Grandjean, 2001)	Correlation Excel files available at http://www.gch.ulaval.ca/bgrandjean/pbrsimul/pbrsimul.html		
(Mangers and Ponter, 1980)		RP	$\frac{k_L a}{D_L} = 0.0039\left(\frac{U_L\rho_L}{\mu_L}\right)^{\alpha}\left(\frac{\mu_L}{\rho_L D_L}\right)^{0.50}\left(\frac{\rho_L^2 g d_P^3}{\mu_L^2}\right)^{0.70}\left(\frac{\rho_L\sigma^3}{\mu_L^4 g}\right)^{0.33}\left(\frac{1}{MWR}\right)^{1.67}$ $\alpha = 0.484 MWR^{0.108}$ $MWR = 1.12\left[(1-\cos\theta_\theta)^{0.60}\left(\frac{\rho_L\sigma^3}{\mu_L^4 g}\right)^{0.20}\right]$ where θ_θ is the contact angle
(Onda et al., 1961)		RP	$Sh_L = 0.01 Re_L^{0.50} Sc_L^{0.50}$
(Onda et al., 1958)	PBR	Rings 6-10 mm	$Sh_L = 0.00625 Re_L^{0.50} Sc_L^{0.50}$
(Onda et al., 1959)	PBR	Rings 6-10 mm	$Sh_L = 0.0107 Re_L^{0.90} Sc_L^{0.50}$
(Ramm and Chagina, 1965)	PBR	FP	$k_L a = 11.6 U_L^{0.768} h_P^{-0.185}$
		Raschig rings 25 and 50 mm	$Sh_L = 0.00216 Re_L^{0.77} Sc_L^{0.50}$
		Pall rings 50 mm	$Sh_L = 0.0036 Re_L^{0.77} Sc_L^{0.50}$
(Raschig LTD)		FP	$Sh_L = 0.01019 Re_L^{1.1-0.4\varepsilon} Sc_L^{0.5} Ga_L^{-0.01} (ah_P)^{-0.35\varepsilon} \varepsilon^{2.9}$ $Sh_L = 0.0026 Re_L^{0.66-0.4(1-\varepsilon)} Sc_L^{0.5} Ga_L^{0.07-0.25(1-\varepsilon)} (ah_P)^{-0.41+0.6(1-\varepsilon)} (1-\varepsilon)^{-0.2}$

Table 7.2 cont.: Gas-liquid mass transfer correlations for fixed bed reactors (Adopted from Kolev (2006)).			
Researcher(s)	**Reactor**	**Packing**	**Correlation**
(Scherwood and Holloway, 1940)	PBR	Rings 25-50 mm	$Sh_L = 0.00204 Re_L^{0.78} Sc_L^{0.50}$
		Rings 12,5 mm	$Sh_L = 0.00333 Re_L^{0.65} Sc_L^{0.50}$
		Saddles 12.5-38 mm	$Sh_L = 0.00285 Re_L^{0.72} Sc_L^{0.50}$
(Shulman et al., 1955)		RP	$Sh_L = 5\left(\frac{F_f^{2/3}}{1-\varepsilon}\right)^{0.55} Re_L^{0.45} Sc_L^{0.50} (a\delta)^{0.33}$ $F_f = \frac{4.83 \nu_L^{2/3}}{a_s}$
(Yoshida and Koyanagi, 1962)	PBR	Rings 15-25 mm Saddles 12-25 mm	$Sh_L = 0.236\left(\frac{d_P}{\delta}\right)^{-0.50} Re_{Le}^{0.50} Sc_L^{0.50}$ $Re_{Le} = \frac{4U_L}{a_e \nu_L}$

Table 7.3: Liquid-phase mass transfer correlations for fixed bed reactors (Adopted from Kolev (2006)).			
Researcher(s)	**Reactor**	**Packing**	**Correlation**
(Billet, 1993)		RP	$k_L = C\left(\frac{D_L}{4\varepsilon}\right)^{0.5}\left(\frac{\rho_L g}{\mu_L}\right)^{1/3} \mu_L^{1/3}$ where C is an experimental, packing dependent constant
(Billet and Schultes, 1993)		RP	$k_L = C_{LB} 12^{1/16}\left(\frac{U_L}{\varepsilon_L}\right)^{0.5}\left(\frac{D_L}{d_h}\right)^{0.5}$ *where* C_{LB} is an experimental, packing dependent constant
(Kolev and Daraktschiev, 1976)		Holpack	$\frac{k_L t_P}{D_L} = 0.00113 Re_L^{0.635} Sc_L^{0.5} Ga_{Lh}^{0.366} (s/t_P)^{4.0} (at_P)^{0.1}$ $Re_L = \frac{4U_L}{a_e \nu_L}$ and $Ga_{Lh} = \frac{g t_P^3}{\nu_L^2}$
(Norman and Sammak, 1963)	Disk column	RP	$\frac{k_L d_d}{d_R} = 0.13\left(\frac{4U_{Ll}}{\mu_L}\right)^{0.61}\left(\frac{\mu_L}{\rho_L d_R}\right)^{0.50}\left(\frac{\rho_L^2 g d_d^3}{\mu_L^2}\right)^{0.17}$
(Onda et al., 1959)		RP	$k_L = 0.0051\left(\frac{\mu_L g}{\rho_L}\right)^{1/3}\left(\frac{U_L \rho_L}{a_e \mu_L}\right)^{2/3}\left(\frac{D_L \rho_L}{\mu_L}\right)^{0.5}(a d_P)^{0.4}$
Shi and Mersmann (288)		RP	$k_L = 0.91\left(\frac{6D_L}{\pi d_P}\right)^{0.5} \frac{U_L^{0.19} g^{0.22} \varepsilon^{0.2} \rho_L^{0.23}}{\mu_L^{0.23} a^{0.4}}\left(\frac{\sigma}{\rho_L}\right)^{0.05}(1-0.93\cos\theta_\theta)^{1/3}$
(Zech, 1978)		RP	$k_L = C\left(\frac{\rho_L g d_P^2}{\sigma}\right)^{-0.15}\left(\frac{U_L g d_P}{3}\right)^{1/6}\left(\frac{6D_L}{\pi d_P}\right)^{0.5}$ where C is an experimental, packing dependent constant

8 Novel Reactors

8.1 Introduction

Novel reactors are nonstandard devices, which attempt to deliver better performance, bring new features, or introduce production through a new method. Novel designs accomplish these tasks by either introducing new or significantly adjusting components in standard devices or by introducing a completely new approach and/or concept into the production. This section will concentrate on both aspects of novel reactor design, but more attention will be paid to novel reactor design strategies.

8.2 Novel Bubble-Induced Flow Designs

Novel bubble-induced flow designs apply a plethora of mechanisms that help differentiate each specific design from other novel and standard devices. Some changes are structural and include using different materials and internals. Others include the use of novel methods to excite the bubble interface and induce gas-liquid mass transfer. Novel methods will exclude devices that are created to study specific events relating to standard devices. For example, the study by Sotiriadis et al. (2005) using a specially designed bubble column where the phases move downwards to specifically study bubble behavior, bubble size, and gas-liquid mass transfer in the downcomer of airlift reactors would fall in the excluded devices.

Perhaps the simplest variation to aerated designs is to inject the phase(s) using the jetting principle. Such devices are often grouped as jet reactors. It should be noted that jet reactors do not necessarily share any other commonalities besides the phase input techniques. The reactor internals and phase flow can vary significantly. Jet reactors use liquid jets and injection devices in order to achieve high liquid velocities and turbulence. The higher turbulence generally yields to better gas-liquid mass transfer performance, which is its largest advantage. On the other hand, the shear rates, especially in the injection vicinity, tend to be much higher than the average. Microorganism growth could produce uneven reactor performance. Furthermore, the generated

shear stresses are potentially too high for microorganisms to survive. Hence, the current application of jet reactors is limited to strictly chemical processes, and research with microorganisms is limited.

Some examples of jet reactors include submerged- and plunging-jet reactors, ejector reactors, hydrocyclones, and venturi devices. Plunging-jet reactors throw a liquid jet through a gas phase, which is usually reactive, into the liquid volume. In other words, these reactors attempt to transfer the gas phase by creating gas entrainment at the liquid surface. This jet reactor requires jet velocities of up to 30 m/s (Charpentier, 1981). Submerged-jet reactors pump a liquid phase through a venture where the liquid is combined with the gas phase. The result is a mixture that has a very bubbly appearance. The generated bubbles are very small and would be expected to have a large gas-liquid surface area. Varley (1995) reported a Sauter mean diameter of 0.29-1.92 mm in a 72 liter submerged-jet reactor using U_L = 3-12 m/s.

The ejector reactor uses a similar injection device as the submerged-jet reactor, but the created jet is injected into an airlift-like vessel. The gas-liquid mixture is allowed to go through a riser and into a separator. Since the gas phase separates, a density difference is created and liquid recirculates into the injection zone. These reactors are capable of operating with liquid velocities of at least 20 m/s. With this kind of turbulence, the ejector reactor outperforms stirred tank reactors at equivalent operating conditions (Charpentier, 1981).

Venturi-based reactors work similarly to submerged-jet and ejector reactors, but the big difference is that the liquid is injected into a high velocity gas phase field whereas the ejector reactors inject gas into a high velocity liquid phase field. Hence, the venturi-based reactors create small liquid droplets similar to an atomizer. Venturi-based reactors are used as scrubbers or with quantities of gas phase present in the reactor volume. In contrast, ejector reactors create small bubbles that are used in liquid phase dominated reactor volumes (Charpentier, 1981).

Jet injectors may also be combined with monolith reactors as shown in Figure 8.1. Monoliths are usually tube reactors with channeled flow. The reaction occurs at the gas-liquid interface as well as on the channel wall, which are usually catalytic or coated with catalytic material. Monoliths can be made into vertical (similar to bubble column) or horizontal tubes, airlift devices (whereby the riser would a monolith), or even into a mechanically stirred device. Usually, however, monoliths are designed like bubble columns or airlift reactors (Broekhuis et al., 2001).

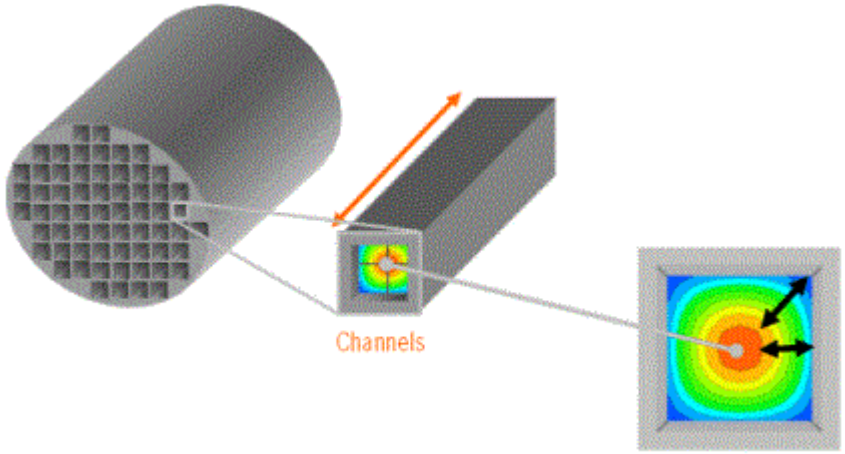

Figure 8.1: Monolith reactor example (Process Systems Enterprise Limited, 2009).

Monolith reactors could be considered a novel class on their own. The problem is that the monolith reactor relies on the catalytic properties of the wall in order to have better mass transfer and reaction performance than the other reactor types. If these properties do not exist, as they are not expected to with biological applications, the channels are too small and cause gas to slug. Hence, a monolith reactor would be limited by the amount of biological media and phase flow media, specifically the gas phase. If the microorganisms grow well, the channels could be plugged and extensive cleaning may be necessary. For most biological applications, monoliths do not provide theoretical advantages to a fixed bed reactor, bubble column, or airlift reactor. This fact is reflected in the lack of biological application of traditional monolithic reactors; however, monolith-like principles are sometimes hidden within fixed bed reactors. In these cases, the monolith-like packing is used as a support mechanism for cellular growth. For biological studies that are available,

monolith reactors tend to compete with trickle-down (fixed bed) or membrane reactors. For example, the 2007 AIChe Annual Meeting held in Salt Lake City, UT had a conference section dedicated to monoliths and membranes (Bauer et al., 2007). It is also a popular option to design monolith microreactors (Schönfeld et al., 2004), which are basically scaled-down versions of large-scale reactors.

Researchers have also combined reactor types. Guo et al. (1997), for example, designed an external loop airlift reactor that incorporates a fluidized bed within the downcomer section, shown in Figure 8.2. The fluidized bed section is used to immobilize microorganisms on carrier particles in order to protect them from damage. The design is meant for the production of enzymes, biofluidization, and wastewater treatment. Although shear rates were minimized, bubbles were not entrained within the downcomer. Furthermore, the gas-liquid mass transfer coefficient was observed to increase with gas holdup. The result is that the gas-liquid mass transfer is limited due to the fact that global gas holdup for the reactor is strictly defined by the riser gas holdup without any addition by the downcomer.

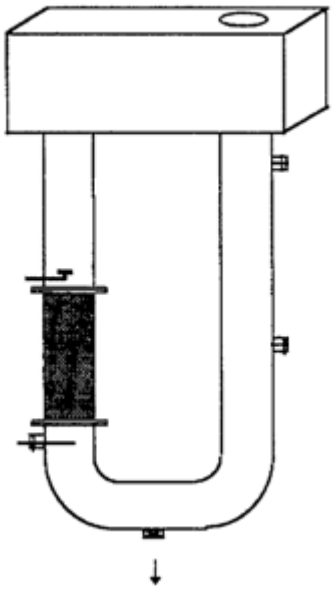

Figure 8.2: Novel external loop airlift reactor designed by Guo et al. (1997).

Wastewater treatment plants oftentimes use vessels that combine the (slurry) bubble column with a mechanical extractor and/or mixer. The mechanical extractor is used to scrape heavy residue at strategically located divider walls. Such a system implies that the liquid flows across the gas flow field. Siemens' proprietary Attached Growth Airlift Reactor (AGAR)-Moving Bed Bioreactor is an example of such a device (Figure 8.3).

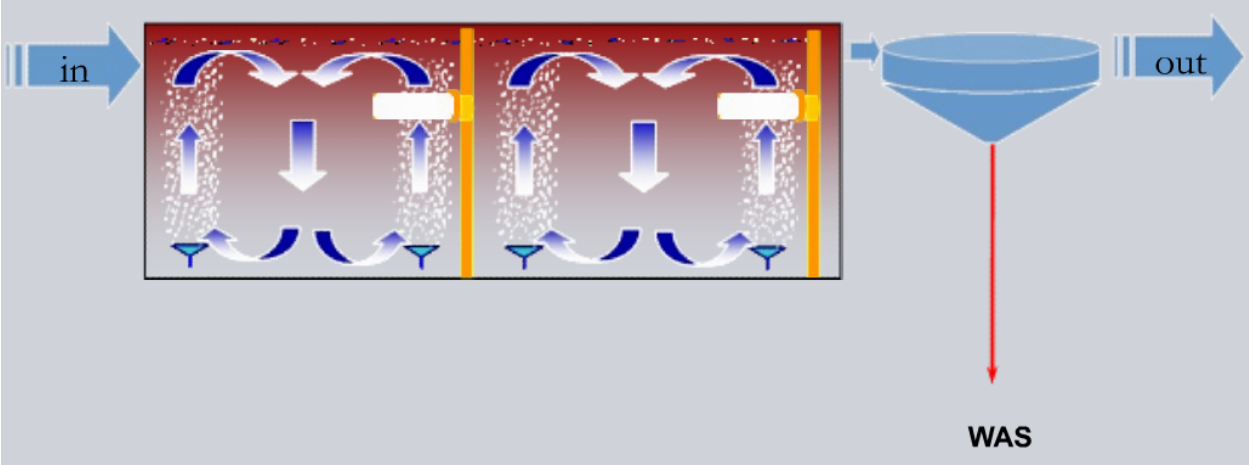

Figure 8.3: Siemens AGAR system (Siemens Water Technologies, 2009).

Wastewater treatment may also require the use of UVA-UVB rays as a mechanism to kill any unwanted cellular material. Unsparged photoelectrochemical reactors, which resemble unsparged slurry bubble columns, are standard devices for such an operation. Harper et al. (2001), however, experimented with a modified aerated airlift reactor, shown in Figure 8.4. The design uses an UVA-UVB lamp core around which the photochemical reaction is allowed to occur. The liquid and gas can be recirculated to maximize output and conversion and optimize residence times. A similar design could be very useful for photosynthetic microorganism growth, such as algae, but no information on such a system has been found in the open literature.

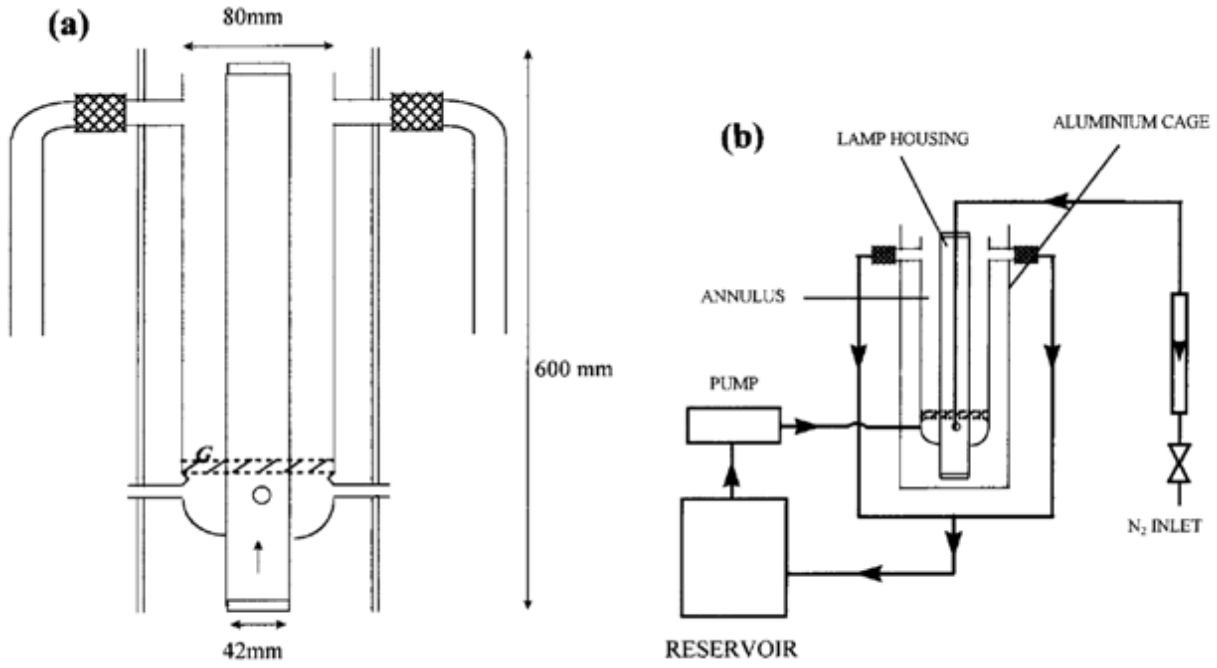

Figure 8.4: (a) Novel sparged photoelectrochemical reactor cross-section and (b) schematic diagram used by Harper et al. (2001).

Ellenberger and Krishna (2002) introduced vibrations in order to reduce the bubble rise velocity, destabilized the bubble surface, and reduced surface tension forces. These changes lead to an improved liquid-phase mass transfer coefficient and, hence, gas-liquid mass transfer coefficient. This goal has been accomplished using mechanical vibration devices in previous studies cited by the authors. In contrast, Ellenberger and Krishna (2002) introduces sinusoidal pressure variations at a frequency on the order of 100 Hz and amplitude of 0.0025-0.01 mm; this leads to a reduction in the bubble diameter by 40-50% and an increase of 100-300% in gas holdup and 200% in the gas-liquid mass transfer coefficient when compared to the no pressure variation system.

Another less commonly applied adjustment with bubble columns and airlift reactors is to introduce additional turbulence by pumping or mechanically exciting the liquid phase. Such adjustments have long been viewed as being advantageous and increasing gas-liquid mass transfer, but they have also been seen as very expensive options (Lundgren and Russel, 1956). The advantage of such a system is that it allows more control of the liquid phase flow, but the cost is

usually represented by the additional power required by the pump or impeller motor. The need for such a device stems from the potentially limiting suspension capabilities, liquid circulation rates, and axial nutrient gradients provided by standard airlift reactors. These issues are exaggerated with height. The pumped circulation column is shown in Figure 8.5. As expected, the high liquid flow rate (Q_L = 2 m^3/h) used by Fadavi and Chisti (2005) added to the turbulence and nearly doubled gas-liquid mass transfer relative to an airlift reactor. Liquid flow in an airlift reactor generally does not contribute significantly to bubble breakage, but the fast liquid flow in the pumped variant did so and led to a smaller average bubble diameter.

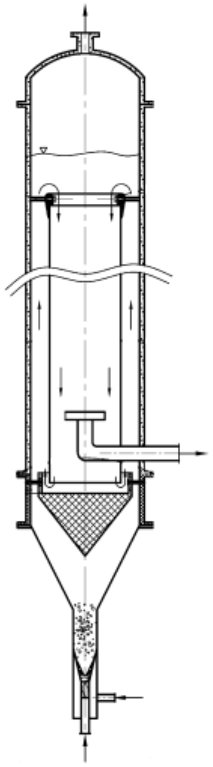

Figure 8.5: Experimental pumped circulation column proposed by Fadavi and Chisti (2005).

A mechanically induced circulation loop reactor is shown in Figure 8.6. This variant works on similar principles as the pumped circulation column. The mechanically induced circulation loop reactor attempts to increase liquid velocity using impeller sets. Chisti and Jauregui-Haza (2002) accomplished this by imbedding a down-pumping Prochem Maxflo T hydrofoil impeller. Air is injected into the annular region of the reactor for several reasons. First, the impellers may flood

with the higher gas flow rates usually applied in airlift reactors. Second, the operational set becomes easier to handle if the impellers are placed in the reactor center. Lastly, the impellers are used to increase the liquid velocity rather than bubble breakage. So, the impellers used for pumping, such as the Prochem Maxflo T, do not necessarily handle gas well and placing them in the riser would make the situation unnecessarily more complicated. Additionally, the riser flow is already influenced by the gas flow rate. It should be noted that many airlift reactor issues can be solved with proper airlift reactor design and phase flow rates; however, these hybrid variants are useful when high gas flow rates are not possible or for more control. Generally, mechanically agitated airlift reactors are still seen as economically inhibitive except for a set of specialized cases.

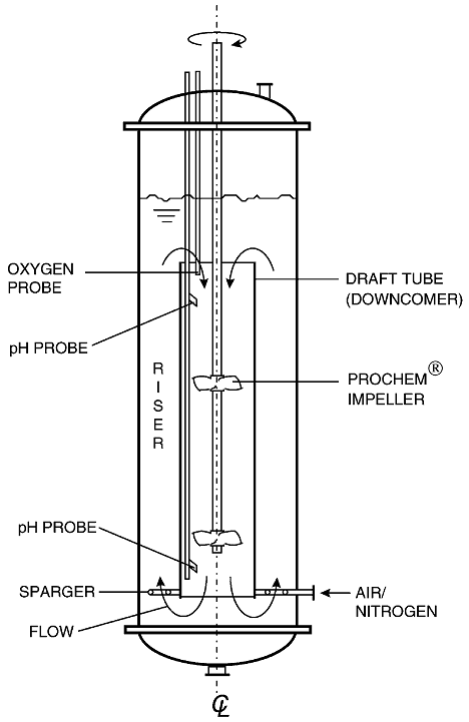

Figure 8.6: Experimental mechanically induced circulation loop reactor proposed by Chisti and Jauregui-Haza (2002).

Another area of reactor modifications has been to add or adjust column internals. For airlift reactors, some research has gone into replacing the draught-tube with a net draught-tube that would allow for bubble breakage near the wall region (Fu et al., 2004; Fu et al., 2003). This additional bubble breakage leads to a smaller bubble diameter in the riser, which in turn leads to

higher gas-liquid mass transfer. If the process is mass transfer limited, it is expected that an increase in productivity would be observed. Although the net draught-tube reactor has the potential to easily increase gas-liquid mass transfer, it also has the potential to be easily plugged by biomass growth or otherwise foul in an industrial setting.

Static mixers can be installed in bubble columns or airlift reactors to provide additional mixing efficiency. Such devices are used to break bubbles before they have a chance to coalesce. The performance of these devices range greatly, but increase in gas-liquid mass transfer of 500% has been observed (Chisti et al., 1990; Fadavi and Chisti, 2005). Such increases, however, are to be expected with highly viscous media. Viscosities that are nearer to water are going to see much smaller performance increases. So, operators interested in adding static mixers to their bubble column or airlift reactor also have to consider the additional cleaning requirements that may come from such devices. In other words, static mixers may not provide enough of an improvement in low viscosity fluids to pay for their additional maintenance costs.

8.3 Miniaturized Reactors

Miniaturized reactors can be divided into two categories based on scale: Micro- and nanoreactors. These reactors present several fundamental advantages and open new venues. Miniaturized reactors allow for personal-scale chemical and biochemical production, which can be used by researchers. They also allow for cost effective production when smaller quantities of a chemical is required. Other larger reactors are often not feasible because the production is not cost effective if the product is not very valuable or if the production is not consistent or pure enough for higher value chemicals. Miniaturized reactors, however, provide a great deal of control over reaction kinetics and hydrodynamics.

Another very important advantage of miniaturized reactors is that scale-up takes on a different form. The scaleup procedure for standard reactors and miniaturized reactors is compared in Figure 8.7. The scaleup procedure for standard reactors involves a complicated iteration processes. A laboratory reactor is designed as a proof-of-concept. Next, an experimental-scale reactor is designed to ensure production viability. After a few iterations, a small-scale pilot plant is constructed to test and finalize the production process, equipment placement, and economic viability. Once this step is accomplished, a large-scale plant is constructed. The iteration requirement stems from the significant hydrodynamics and/or reaction kinetics changes that are experienced as scale is increased (Watts and Wiles, 2007).

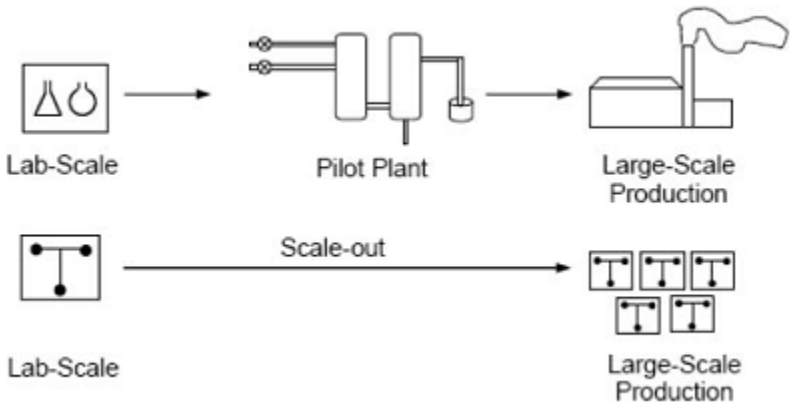

Figure 8.7: Scaleup procedure comparison (Watts and Wiles, 2007).

With miniaturized reactors, however, scale-up is a much simpler process. The procedure involves putting miniaturized reactors into series and/or parallel in order to produce larger output quantities. This approach keeps the reaction kinetics and hydrodynamics predictable for each component regardless of plant scale. Hence, the process is often referred to as “numbering-up”. In other words, the laboratory reactor is very similar to the industrial production with the reactor quantity and controls being the most significant differences. This property keeps the startup and development costs lower and more flexible (Ehrfeld et al., 2000; Watts and Wiles, 2007).

The numbering-up method also introduces another potential advantage. The scaled model operates as a continuous reactor rather than batch while providing the operator with the same control advantages of the batch operation at the same time. Therefore, the process time is expected to be shorter with miniaturized reactors since most standardized reactors use a process time that is longer than the kinetic minimum. Safety is also increased tremendously since the process can be stopped at any point in the process flow (Ehrfeld et al., 2000). These controls can be instituted automatically without the need for human supervision.

8.3.1 Microreactors

Microreactors are defined by their size rather than construction. Microreactors are miniaturized with channels between the (sub-)millimeter and nanometer scale. Microreactors mix the gas and liquid phases pneumatically or mechanically. The size of the complete reactor construction is less important. A microreactor example is shown in Figure 8.8. Microreactors are generally compounded into microreactor elements, which are placed into mixing units. These units are placed into microreactor devices, which have inputs and outputs for all the microreactor units placed within it. Microreactor devices are placed in parallel or series in order to achieve the necessary conversion. Finally, the output is treated (Ehrfeld et al., 2000; Watts and Wiles, 2007). Typical microreactor assembly is shown in Figure 8.9.

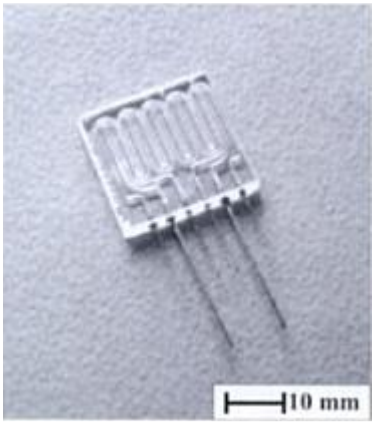

Figure 8.8: Microreactor example (Ehrfeld et al., 2000).

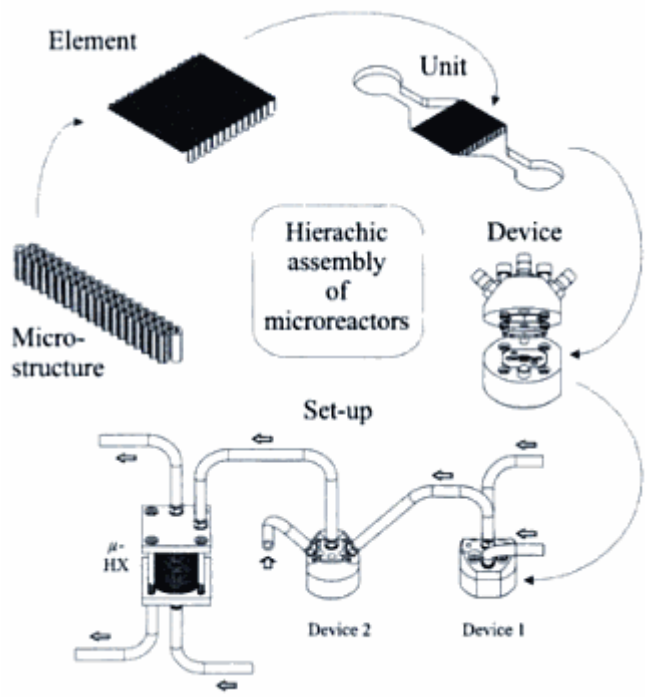

Figure 8.9: Microreactor assembly (Ehrfeld et al., 2000).

Microreactor construction can be accomplished using numerous tools. Costs, however, dominate the construction options. Hence, possible construction techniques are defined by channel flow scale, precision, reliability, and material selection. Naturally, as the reactor scale becomes smaller and precision requirements higher, the costs tend to increase as well. An accepted approach when constructing microreactors out of metals, ceramics, or plastics is using lithography, electroplating, and molding (LIGA). LIGA is a three step process by which a laser, electron beam, ion beam, UV-ray lithography, or X-ray lithography is used to print microstructures. Then, electroforming is used to generate a metal layer onto the microstructure. This metal structure can be used as a mold or embossing tool for mass manufacture (Ehrfeld et al., 2000; Hruby, 2002; Wirth, 2008). The available construction techniques are summarized in Figure 8.10. Ehrfeld et al. (2000) and Wirth (2008) are good and recent sources for the current construction techniques and their applications.

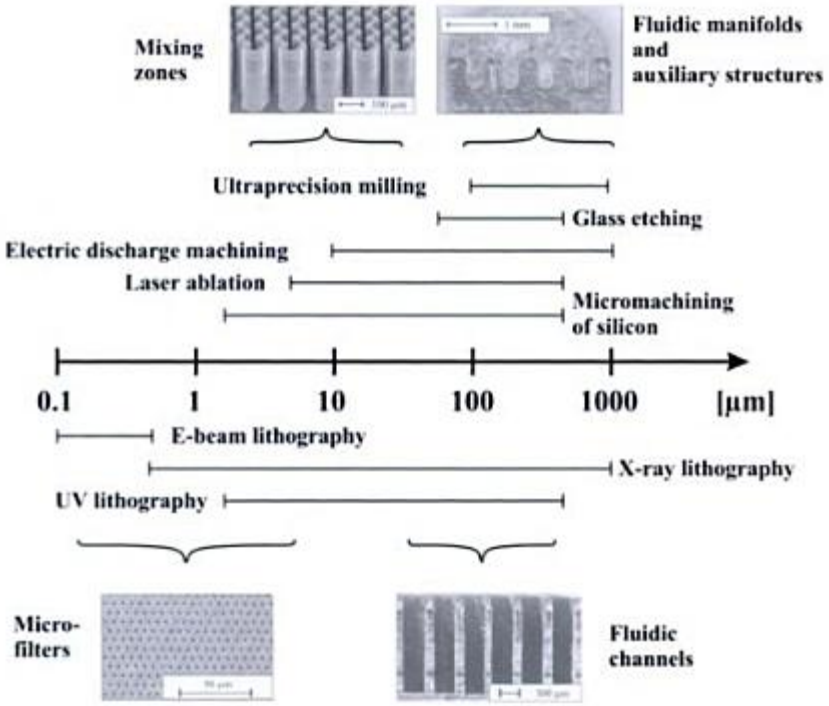

Figure 8.10: Microreactor construction techniques (Ehrfeld et al., 2000).

Mixing in microreactors is almost exclusively assumed to be laminar due to the small flow channel width. Laminar flow through microchannels requires the phase flow to be alternated in some fashion in order to create the mixing environment. This operation is important because mass transfer, in this case, is driven only by molecular diffusion. Hence, the creation of larger gas-liquid interfaces is the only practical course of action for gas limited operations. Miniaturized bubble columns are able to accomplish this task well. For example, a standard reactor can create interfacial areas in the range of 2000 m^2/m^3 while a single channel micro bubble column and micro bubble column with channel arrays can create interfacial areas of 1,700-25,300 and 5,100-16,600 m^2/m^3, respectively (Ehrfeld et al., 2000).

Unfortunately, the extreme numbers are somewhat misleading. In order to properly understand their context for biological application, an understanding of micro bubble column flow regimes is necessary. Bubble velocity in microreactors is defined by a gas space velocity. This velocity is

similar to the superficial gas velocity, but it tends to be slower due to very significant wall effects. So, the gas space velocity is approximated using a sample bubble velocity.

Bubbles in micro bubble columns are observed to be separated by a liquid film from the wall at almost all gas space velocities. At low gas space velocities, the micro bubble column experiences bubbly flow. The bubbly flow is defined by microbubbles, which are spherical and as large as the channel diameter. Since bubbles this size are highly unstable without surfactants, the gas space velocity has to be low enough to allow enough space between bubbles in order to prevent coalescing.

As the gas space velocity is increased, bubbles tend to coalesce and a slug flow regime develops. The slug flow regime is defined by bubbles that are longer than the channel diameter and are still separated by some amount of liquid. Increasing the gas space velocity leads to the slugs coalescing even further, and a slug-annular flow regime is observed. The slug-annular regime experiences very long bubbles, which are separated by a very small amount of liquid. Increasing the gas space velocity more combines the elongated bubbles into an annular gas flow (annular flow regime).

The extreme interfacial values are experienced by the latter two regimes and are most likely useless for biological applications. The channel diameters are very small to begin with, and the liquid film that develops in the slug, slug-annular, and annular flow regimes is not sufficient to support microorganisms. In order to have microorganisms survive in micro bubble columns, the reactor would almost certainly have to be operated in the bubbly regime, which experiences interfacial areas of 1,700-5,100 m^2/m^3. Lower values are observed with micro bubble columns with a diameter of 1,100 μm while the larger values are experienced with a channel diameter of approximately 300 μm (Ehrfeld et al., 2000). Even though these values are higher than those for standard equipment, the advantage for micro bubble columns is not astronomical, and competition and performance are likely to be more comparable and competitive.

Although micro bubble columns are popular, other microreactor mixing methods exist, such as the falling film principle. In such a system, the liquid phase would be input into the microreactor's reaction chamber from the top while the gas phase input is at the bottom. The principle is very similar to the annular flow regime in the micro bubble columns. The liquid would line the reactor walls while the gas phase would move through the annular region. The difference with the falling film reactor is that the liquid is fed at a rate and way that it would guarantee flow only at the wall region and would prevent the liquid phase from mixing into the gas phase (Zhang et al., 2009).

In addition to the micro bubble column and falling film microreactor, several other theoretical schemes exist in order to achieve proper mixing conditions of two phases. The simplest mechanism is defined by the phases entering a tee intersection either as single streams, shown in Figure 8.11a, or numerous substreams, shown in Figure 8.11d. Control over the mixing is provided by the phase flow rates. A more energetic method is to collide high energy (velocity) streams in order to create large interfacial areas due to atomization or spraying (Figure 8.11b). This method is most likely not useful for biological applications as it would most likely damage the microorganisms. It could, however, be used as a phase premixer for semi-suspended microorganisms. One of the phases could also be broken down into substreams, which are then injected into a larger stream of the other phase (Figure 8.11c). For example, gas could be injected into a liquid stream in order to generate bubbles with liquid intervals.

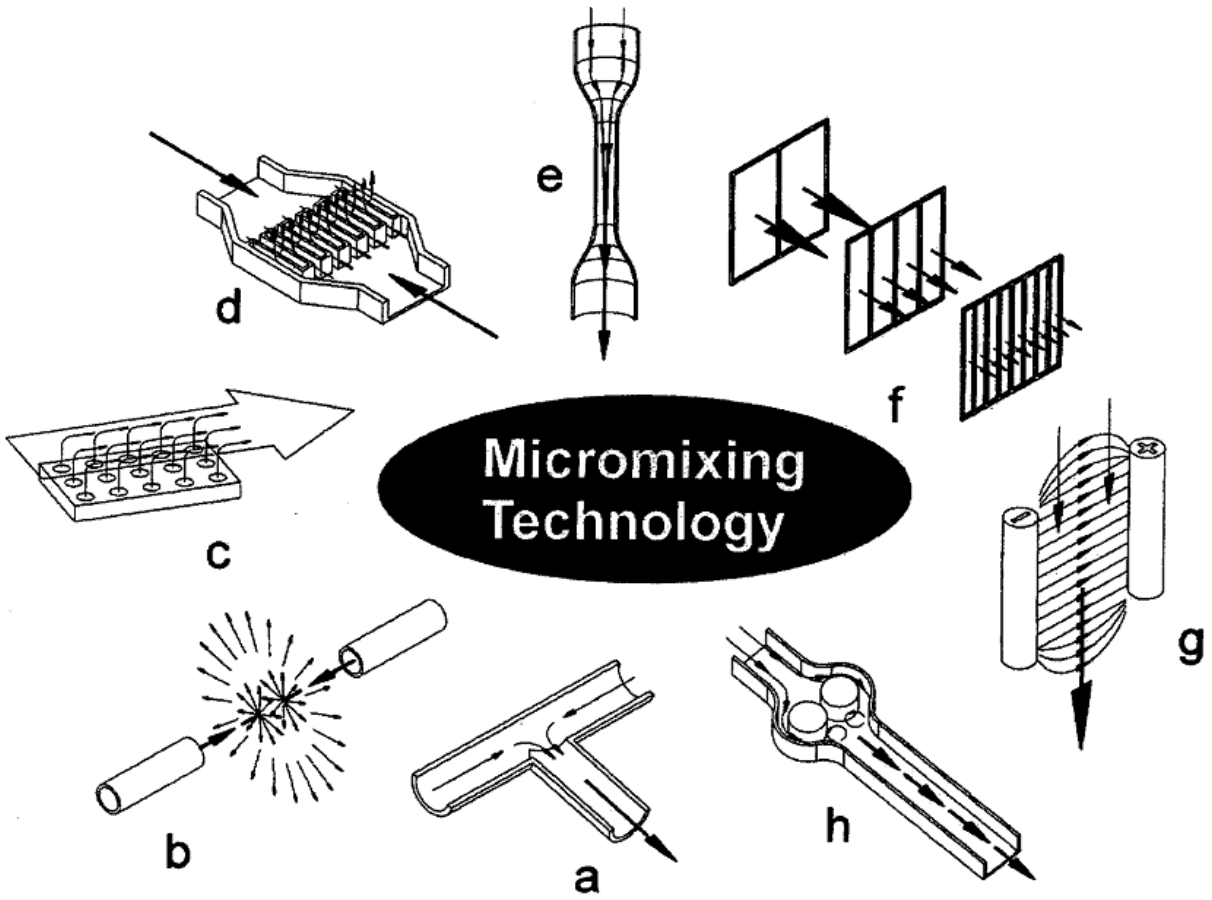

Figure 8.11: Micromixing arrangements: (a) substream contacting, (b) high energy substream contacting, (c) multiple substream injection into major stream, (d) multiple substream contacting, (e) flow restriction, (f) stream splitting, (g) forced mass transfer, and (h) periodic fluid injection (Löwe et al., 2000).

An interesting method for mass transfer problems is to channel the phase flows into a constricted area, which would increase velocity and decrease the diffusion path (Figure 8.11e). Although useful in this regard, it could create problems in biological systems by either damaging the microorganisms or not allowing enough room for the microorganisms to pass through. A more popular approach is to use splitting arrays (Figure 8.11f). The phases would be mixed into a single stream and then continuously broken apart by alternating horizontal and vertical splitters, which get finer as the mixture moves along. Although this method is popular in the chemical industry, microorganism growth would most likely cause blockage. Naturally, these methods can be combined into a single, more complex device. These mixing schemes have been applied to liquid-

liquid contacting problems, but only substream tee contacting and substream injection have been tested for gas-liquid problems (Ehrfeld et al., 2000).

The natural cause for a lack of microreactor research in gas-liquid processes is that most miniaturized reactor research is concentrated on problems experienced in the chemical industry, specifically catalyzed liquid-liquid reactions. Gas-liquid and especially biological reactions have not been widely attempted since the field of microreactor engineering is emerging to fulfill the highest margin needs first. Biological applications are still being mastered with standardized equipment, and economic viability using microreactors seems to be some distance away. Another issue is that much of the work is still not published. For example, Ehrfeld et al. (2000) includes numerous unpublished reports and correspondences, such as the interfacial areas data. The same information for standard reactors, on the other hand, is easily obtained across different print media.

8.3.2 Nanoreactors

A differentiation between nanoscaled and microscaled miniaturized reactors is necessary because the naming convention is not universally applied. Nanoscaled reactors were introduced in the late 90s and are a possible microreactor alternatives for the chemical industry (Ostafin and Landfester, 2009). An example of a nanoreactor in nature is the mitochondrion, which is the energy producing portion in most complex cells. Nanoreactors are more accurately described as molecular reactors, and the reactor volume is defined by the number of molecules confined within the reactor rather than a standard volumetric measurement. Nanoreactor's biological applications, however, will most likely stay very limited. The nanoreactor has some critical faults and problematic characteristics for biological application. The first and largest problem is that the channel size is too small for most microorganisms of interest, such as bacteria. Nanoreactors are on usually on the nanometer scale while smaller bacteria are in the micrometer scale. Hence, no additional discussion on nanoreactors will be presented.

8.4 Membrane Reactor

Some products or intermediaries in biological processes are highly shear sensitive. Standard reactors may not be able to protect the microorganisms sufficiently. Membrane reactors allow for semi-suspension of cells by placing the cellular material within or between (semi)permeable membranes. Membranes are not novel ideas for the chemical industry for which membranes have $9 billion in component sales in 2006 (Nunes and Peinemann, 2006), but their biological application is novel. The chemical industry, however, has used membrane technology for experiments since the 1920s and for industrial applications since the 1960s while the membrane bioreactor concept has been first defined in the literature in 1979 (Hall et al., 2001; Nunes and Peinemann, 2006). It should be noted that permeation and membrane concepts were first scientifically described in 1748 (Baker, 2004).

The initial membrane bioreactors cross-flowed the liquid phase through the membrane, which increased energy costs significantly. Currently viable membrane bioprocesses submerged the membrane in the liquid phase whereby the liquid flows parallel to the membrane matrices. This creates low pressure drops and makes the economic viability a reality. Current membrane reactors also tend to vary the volumetric membrane amount or carrier particles at 60-70% (Leiknes and Odegaard, 2007).

Membranes allow the gas phase to transfer to the microorganisms without exposing the microorganisms to the bubble interface or other potentially high shear areas. This allows high cell densities which, in turn, allows for higher conversion effectiveness (Ko et al., 2008). The membrane may also allow the product to permeate away to a collection area. Since the microorganisms have little exposure to bubbles and the gas has to travel through the membrane, the membrane reactor allows for relatively small amount of gas-liquid mass transfer to occur and almost any other reactor types outperform it on that measure. Unfortunately, some microorganisms, such as animal cells, are

so shear sensitive that they are able to survive only in a membrane protected environment (Bellgardt, 2000).

The most significant disadvantages of membrane bioreactors is that they are very costly to construct and maintain, and their long-term viability is yet to be proven (Dudukovic, 1999; Kumar et al., 2008). For example, microporous membranes have to be replaced every 3 years, which leads to operating and maintenance costs that are approximately 10 times higher than with a conventional gas treatment options (Kumar et al., 2008). Long-term viability is an issue because the current membrane technology has permeate mass fluxes which are an order of magnitude too small to be competitive on volumetric productivity basis. Furthermore, membranes provide an additional heat transfer barrier, which introduces temperature control issues that are generally not present in standard reactor designs (Dudukovic, 1999).

Mass transfer through a membrane occurs at several steps, which differentiate it from mass transfer in standard reactors. The first two processes are very similar. First, the gas is injected into the reactors volume. Then, the gas is transported into the liquid phase. This is usually accomplished by molecular diffusion. The mixing is not turbulent enough for bubble interface excitement. The diffused gas phase transports through the membrane, which adds a significant mass transfer barrier. Membrane transportation is a two part process whereby the gas phase is first absorbed by the membrane and then diffuses through the membrane. This process may lead to separation of the transfer material, which is an advantageous property of membranes for specific product removal. For example, this property would allow separate gas phases to enter the biofilm at different rates or would allow for protein separation (Gottschalk, 2008) or filtration (Ko et al., 2008). Hence, membrane reactors can be split into permselective and nonpermselective categories (Dudukovic, 1999).

The dissolved gas phase then has to diffuse through the biofilm, and the reaction is allowed to occur. The biofilm is usually attached to the membrane rather than being allowed to float (Henstra et al., 2007). Additional problems are created because any byproducts, which may be toxic if they are allowed to concentrate, have to leave the reactor through the same manner. In other words, microbial operation may have significant effects on the gas phase concentrations (gas-liquid mass transfer driving force), which could become an additional restriction on total gas-liquid mass transfer (Kumar et al., 2008).

Membranes can be classified by either geometry (symmetrical or anisotropic) or construction (dense, porous, or composite). Membrane selection becomes the main design criterion for a membrane bioreactor. The membrane can be very dense and complex, which would allow for a high degree of selectivity while microporous materials would allow gas, regardless of identity, to permeate easier. Composite membranes have been developed, which attempt to allow the gas phase to permeate easily while allowing a high degree of selectivity. Biological applications make extensive use of microporous membranes, and some attempts have been made to incorporate composite membranes. The most commonly encountered problem with microporous membranes is that they easily plug, which leads to even higher maintenance costs (Kumar et al., 2008). In such a case, the operation becomes limited by the net material accumulation at or within the membrane. This accumulation can be controlled if the fouling is reversible by backwashing; however, some fouling is irreversible and requires chemical treatment, which would force the membrane bioreactor to be shut down and then restarted after the cleaning procedure (Leiknes and Odegaard, 2007).

Hence, issues have led the membrane bioreactor to be a perfect choice for a select few problems. Interestingly, even with its advantages for those shear sensitive microorganisms, their industrial viability and application has yet to be proven. In practical terms, membrane bioreactors have to compete with fixed bed bioreactors, hybrid systems (fixed bed incorporated into an airlift),

bubble columns, and airlift reactors, all of which are able to provide much higher gas-liquid mass transfer rates. In other words, production could be optimized within an environment that is less friendly than the membrane bioreactor simply because the higher productivity due to higher amounts of gas-liquid mass transfer could offset the productivity losses due to microorganism shear damage. More information on membrane technology for chemical and biological applications can be found in Baker (2004), Nunes and Peinemann (2006), and Peinemann and Nunes (2008a, 2009b).

8.5 Summary

Novel bioreactors can be represented by many different designs and variations, but the most novel and promising approach may turn out to be miniaturized reactors. Novel mechanical or bubble-induced flow designs are not trend setters nor do they solve many of the scaleup and gas-liquid mass transfer problems. Miniaturized reactors, however, could decrease process design and implementation significantly. The numbering-up scaleup method for these reactors reduces the time and amount of work necessary for scaleup to simply figuring the process out for the one experimental unit. The rest of the work is spent on the industrial and economics problems rather than hydrodynamic.

9 Figures of Merit

Figures of merit are quantities that are used to compare reactor performance across all reactor types or just the different designs of stirred tank bioreactors. This section summerizes some reactor specific figures of merit and problems which have prevented meaningful and significant figures of merit being developed as well as some possibilities that could be considered for further research. The figures of merit are also oriented towards stirred tank reactors, bubble columns, and airlift reactors since these are the most common gas-liquid and gas-liquid-solid bioreactors. Fixed bed reactors use a much smaller gas and liquid flow rate so that they are not able to compete with the other reactors unless the microorganisms have to be suspended or otherwise protected.

Figures of merit for stirred tank reactors are especially difficult because of the wide variety of equipment and arrangements used and the high degree of phase interaction complexity. Although the impeller is always used for gas breakup, mixing, and dispersion, the effects of different impellers, setups, inputs, or microorganisms make universal conclusions on hydrodynamics almost impossible. The varieties of microorganisms also make predictions on production or conversion very difficult. Furthermore, a practical model describing conditions for stirred tank reactors across wide operational ranges and scales is currently unavailable. Since this underlying information is not available, a figure of merit, which is applicable across a wide variety of designs, control variables, inputs, and microorganisms, is also not easily within reach and rarely addressed in available research.

The task, however, is not impossible. A practical representation of the mass transfer performance is $\frac{k_L a}{P_G / V_L}$. It represents the mass transfer rate per unit power input. This figure of merit does not attempt to predict output or conversion, but that outcome is implied if the process is still gas-liquid mass transfer limited. If other microorganisms' performance measures are important, a

time dependent representation of output in terms of systems size (units of $\frac{Mass}{Liter-Hour}$) can be used. Its downfall is that design or control variables are not accounted for, but it can still be used in tandem with the previous mass transfer based figure of merit or as a long-term assessment tool.

These same measures have not been extended to the different reactors designs, but they certainly could be. A few fundamental issues exist. The first arises from the fact that variable costs differ significantly between the reactor designs. For example, the stirred tank reactor power draw increases to the fifth power with the impeller diameter and third power with the impeller speed. Hence, increasing the scale of a stirred tank reactor increases the power usage at a fast pace. At the same time, larger mechanical systems, such as the motor and gear systems, may require more or more expensive maintenance. These properties ultimately lead to the operational cost growing faster than with the bubble column or airlift reactor; however, the stirred tank reactor may be able to produce smaller bubbles if it is properly designed and setup. As scale increases, a theoretical inflection point would exist at which the stirred tank reactor advantages are outstripped by the power usage and the bubble column or airlift reactor become a superior economic alternative. This inflection point has not been studied, and such comparisons between stirred tank reactor, bubble column, and/or airlift reactors are very rare. So, such a study could produce a map that could be microorganism specific, which shows the prefered reactor for a given scale and gas or liquid flow rate(s). Many variations and variables would not be accounted for, but a process specific guide could be developed.

A second issue with figures of merit is more of a derived problem. The scaleup procedure for any given reactor design is highly variable. The stirred tank reactor alone has numerous alternatives such as constant power density, impeller velocity, impeller tip speed, or a variation/combination of these variables. Bubble column scaleup might be even harder since the gas and liquid hydrodynamics are not easily controlled or predicted. The airlift reactor scaleup is

perhaps easier due to the more controlled gas and liquid flow patterns. Regardless, the scaleup for each reactor design varies significantly, and, more importantly, the reactors do not have a standard, optimal, or commonly applied and agreed upon scaleup procedure. For example, bubble columns have to be scaled up by increasing the experimental reactor by a factor of 5-10 for each iteration. By approximately 300 L, the reactor is supposed to be scale independent and a pilot plant can be seriously considered. The airlift reactors seem to show this property at a much earlier point, 32 L (see Figure 6.17). The stirred tank reactor, on the other hand, may never lose its scale dependence (after accounting for the power usage). In other words, comparison of industrial bubble columns and airlift reactors could be well defined, but the experimental and pilot scaled reactors may not be. Since most research is done with experimental (small) reactors, figures of merit are often not attempted.

It is clear that a defined winner among the reactor designs does not exist. More importantly, the reactors may not be interchangable and design competition is not clearly defined. The previously discussed issues shed light on the lack of interchangability. The specific project or process helps to further explain the lack of figures of merit in published research. Many of the reactor applications are process or project specific. Without having an idea of the microorganism requirements or its influence on the liquid properties over time, it may be difficult to predict which reactor would be better without experience. At best, some reactors could be ruled out.

An example of the problem difficulty can be simulated by assuming economic product qualities. Let's assume that the product of interest is highly valuable and that its quality impacts the earned price significantly. The reactor for such a product should be chosen on the its ability to consistently produce the same product quality. In other words, the reactor design, which accomplish this task, can get away with costing more (feed, maintenance cost, variable cost, capital cost, etc.) on an annualized output basis. Specifically, it can cost more on a marginal or variable basis since the marginal product price would be able to at least cover those expenses. Such a product also implies a

certain degree of pricing power on the part of the producer. An example of such production is often encountered with patented products (proteins, antibiotics, medicines,etc.). Such a producer may be perfectly happy employing stirred rank reactors regardless of scale.

A commoditized product, on the other hand, requires the marginal product cost be optimize using whatever method works. The producer does not have significant pricing power. If the cost of capital is low or the economies of scale large, the reactor of choice may be quite complicated and the facility may be very large such as many refinaries in the United States. If the cost of capital is high, input prices variable, and the price risks not easily accounted for, producers may be interested in smaller facilities with a smaller initial investment and higher variable cost such as many of the early ethanol facilities. The reactor choice becomes dependent on preference, economic resourcefulness, and a reflection of the producer's risk appetite. The reactor selection for such a producer becomes much more important. It should be noted that competitive markets theory calls for commodity producers to optimize the marginal cost rather than the average.

Some figures of merit, however, could be defined without accounting for the economic impact and trying to judge a reactor's efficiency and feasibility for a given process. The scale of interest for such figures of merit would not be industrial. By the time a process reaches even the pilot stage, the designer has to start considering the economic impact, and the economic decisions become more and more important. The efficiency and feasibility of production has to be decided early in the experimental and scaleup portion of the project. Hence, figures of merit are going to be highly dependent on the reactor scaleup procedures and knowledge thereof. So, more research would need to be directed into producing a unified or at least more uniform scaleup procedure set in order to predict and compare the potential output gains between the reactors.

Cost analysis is usually implemented based on a previous project which used similar components. A size ratio is introduced to relate the base design to the current one. A scaling factor is used to properly represent the equipment relative to its scale basis. The scale basis is determined

by the type of equipment and process and commonly includes flow, volume, area, power, etc. An installation multiplier is introduced which is based on the material cost and type of equipment. This factor hopes to account for the necessary machining, design, and installation costs. For example, a carbon steel agitator has a multiplier of 1.3 while a stainless steel version has one of 1.2. If different equipment has a higher design and installation cost, such as heat exchangers, they carry a higher multiple (2.1 in this case) (Aden et al., 2002; Wooley et al., 1999).

In order to account for inflation in the monetary supply and fluctuations in equipment costs due to technology and commodity prices, an equipment index, such as the Chemical Engineering Purchased Equipment Index (CE Index), is used. This index in particular is popular because bioreactors are completely based on chemical reactor principles such that the index properly reflects fluctuations for bioreactor equipment. Proper usage should project prices to the year when purchasing decisions and commitments are to be made. A formula for the practice can be summarized by (Aden et al., 2002; Wooley et al., 1999):

$$Cost=InstalledBaseCost*\left(\frac{Base}{Current}\right)^{ScalingExp}*InstallationFactor*\left(\frac{CEIndexBase}{CEIndexCurrent}\right) \quad (4.15)$$

Equation (4.15) assumes economies of scale, which is only true for relatively cheap materials such as mild steal. If the material is more expansive, this relationship breaks down. For medium material costs (~$10/kg), a breakeven point (diminishing returns) develops such that larger reactors prove too costly in terms of capital, but smaller reactors are too energy intensive such that the variable costs are higher. As the material becomes more expensive, the breakeven point shifts towards a smaller scale. The opposite is true for cheaper material costs. Capital and input (labor, electricity, or feed) costs also induce similar behavior. As the cost of capital increases, operators prefer smaller scales such that continued operation is used to pay for variable costs which occur during the same period (may be offset due to payment arrangements). Therefore, lower capital and input costs induce larger scales (Patwardhan and Joshi, 1999).

Economies of scale also explain industrial practices for processes which turn from low viscosity Newtonian to viscous and/or non-Newtonian liquids. If feed costs are reduced, the process is more likely to yield a positive return with scale (Ogut and Hatch, 1988) even though the amount of unused volume and discarded feed would increase as well. The rate of diminishing returns would be dependent on product price(s), material costs, and other input costs (electricity, labor) such that the operator may be inclined to halt operation (Ogut and Hatch, 1988) once the power draw becomes economically unbearable. On the other hand, if input costs are too high, the reactor design would require maximum conversion and recycling, leading to diminishing returns such that the amount of equipment may limit the scale of operation.

Equipment selection and recommendations are dependent on a proper cash flow analysis that includes costs and price shocks to inputs, capital costs (debt facilities, lines of credit), and products (Aden et al., 2002; Patwardhan and Joshi, 1999; Wooley et al., 1999). The ultimate goal hinges on investment criteria. Operation can be optimized to meet a certain level of output, maximize profit, maximize the return on equity/capital, or a combination of those which would depend on the investors and their priorities.

10 Concluding Remarks

The interesting aspect of the reactor design developments has been that the different designs are more complementary than competitive in nature. For example, the stirred tank reactor is capable of producing small bubbles, but costs too much to operate at a large scale. The fix has been the bubble column. The bubble column has too much backmixing. The solution is the airlift reactor. If suspension is necessary, one can use a fixed bed reactor. Ultimately, these relationships may be a significant cause that research work rarely attempts to describe more than 2 reactor designs. In addition, any comparisons that are done have been accomplished at the experimental scale where the stirred tank reactor weaknesses are not as apparent.

For gas-liquid mass transfer purposes, the stirred tank reactor ranks better than the bubble column or airlift reactor, and the bubble column outperforms the airlift reactor most of the time. The fixed bed reactors cannot compete unless the microorganisms or biological material is highly shear sensitive. On a cost basis, the bubble column is the cheapest followed by the airlift reactor. The stirred tank reactors have a high power costs associated with impeller scaling while the fixed bed reactors tend to have significant pressure drops and packing and maintenance costs. On the other hand, the airlift reactor is the easiest to scale based on hydrodynamics. The bubble column is harder to scale effectively while the stirred tank reactor has the largest variety of published scaleup procedures. These procedures also tend to have variable success as defined by the process and depend on the reference and final scale.

The ultimate success of the reactor will depend on the comfort and wellbeing of the microorganisms in the bioreactor. In addition to gas-liquid mass transfer, the bioreactor also has to provide efficient mixing, a friendly shear environment, and proper pressure and temperature controls so that the microorganism output can be optimized. Hence, bioreactor design can have significant variation depending on the microorganism employed by the process.

The information that is available for the different reactor designs provides a good understanding of each reactor operation, construction, advantages, and disadvantages. These aspects have been summerized qualitatively in Table 10.1 for each reactor design. A summary of some of the less common or novel reactor options is presented in Table 10.2.

Table 10.1: Reactor comparison.

	Reactor Type	Brief Description	Econ	Ops/Maint.	Hydro-dynamics	Design	Scalability	Comments
Gas-Liquid	Bubble Column (BC)	Column reactor in which the medium is aerated and mixed by gas introduced at its base.	+++	++	++	+++	---	Lack of control; High shear gradients; Reactor of choice for gas conversion; No moving parts
	Airlift Reactor (ALR)	Modified BC with a channel for up- and downflow. Driving force is supplied by a density difference between these sections. More control than BC. Two major variants.						Flow defined by reactor design; Minimum fluid level; Modifications possible leading to further improvements
	Internal Loop Airlift Reactor (ILALR)	ILALR has an internal flow separator creating channels for up- and downflow.	++	++	+++	++	++	Limited flow control
	External Loop Airlift Reactor (ELALR)	ELALR has distinct conduits for fluid flow which are connected at the base and gas separator sections.	+	+++	+++	++	++	Even more control and design flexibility; Better hydrodynamics than ILALR
	Stirred Tank Reactor (STR)	Mechanically agitated and mixed vessel with flow dependent on impeller design. High power consumption.	--	-	+++	++	+	High shear gradients; Ideally mixed; Limited economical operating range
	Packed-Bed Reactors	Reactor in which liquid flows over immobilized solid material also known as packing material. Solids cannot be present in input or product.						Large units possible; Usually countercurrent configuration which is limited by flooding
	Trickle-Bed Reactor (TBR)	Liquid is sprayed over packing with product extraction at the bottom of the reactor.	+	--	+	-	+	
	Packed-Bubble Column (PBC)	Packed BC.	+	--	+	-	+	Liquid flow is negligible
Gas-Liquid-Solid	Slurry Bubble Column (SBC)	G-L-S or G-S Bubble Column. The G-S SBC has analogous hydrodynamic behavior as the G-S Bubbling FBR.	+++	++	+	+++	---	
	Fluidized Bed Reactor (FBR)	Reactor in which the solid phase is suspended in medium.						Many variants available; Usually operated as gas-solid system.
	Bubbling	BC variant that can also be operated in G-S mode.	+++	++	+	+++	---	
	Circulating	ALR variant.	++	++	+++	++	++	Internal or external

Table 10.2: Summary of less important and novel reactors.

	Description	Comments
Others:		
Jet Reactors	Reactor in which the liquid (submerged-jet reactor) or gas (ejector reactor) is introduced at a high velocity. Another variant, the venturi scrubber reactor, injects liquid into a high velocity gas stream causing the liquid to atomize.	Large interfacial areas allowing high mass and heat transfer; Not applicable to most organic substances
Membrane Reactor	G-L-S or G-L reactor in which liquid is diffused through a membrane and converted by the biofilm, which is attached to the membrane, to the final product. Biofouling or clogging is possible. High construction and operating cost.	Four membrane types: Microporous, porous, dense, and composite.
Plate Columns	Liquid is channeled by plates (such as a muffler) and run countercurrently with the gas phase. Able to handle large variations in flow rates and high pressures.	Two major variants: Bubble-cap and sieve plates
Tube Reactors	Cocurrent BC variant with pipelines or coils serving as guidelines. Very similar to heat exchanger.	horizontal, vertical, or coiled; variety of flow regimes
Spray Towers/Column	Usually treated as a Gas-Liquid reactor. Liquid is sprayed countercurrently to gas flow. Used for corrosive and liquids containing substantial amount of solid materials.	Higher energy usage and capital investment
Torus Reactor	Mechanically agitated loop reactor. Lower power consumption, better mixing, and good heat transfer capacity than STR.	Many variants based on different cross-sectional shapes
Wetted Wall Reactor	Vertical reactor with liquid phase entering at the top and flowing along its wall with gas flowing through its core.	
Novelty:		
Magnetically Stabilized FBR	FBR in which a magnetic field is used to stabilize magnetic particles in the fluidized bed.	
Dually Injected Turbulent Separation FBR	FBR variant in which large and small particles are injected separately allowing for separate residence times.	Reactor size and cost is minimized
Continuous Centrifugal Bioreactor	FBR variant in which cells are fluidized using centrifugal forces. Allows high density cell cultivation.	May not be suitable for three phase fermentation
Inverse FBR	FBR variant in which low density particles with a biofilm are used. The biofilm causes a change in its thickness over time causing the bed to growing downward.	Superior to ALR for aerobic wastewater treatment with certain cultures
Blenke-Cascade Reactor	Baffled tower separating the reactor into different sections being mixed by upward flowing gas. Similar to Plate Columns.	Liquid or liquid-solid mixture can be operated co- or countercurrently
Contained FBR	FBR variant which uses a retaining mesh or grid to contain solids and allow a liquid-only product.	
Double Entry FBR	FBR variant which uses top and bottom inlets to minimize gas logging (gas phase lifts solids to reactor surface)	

Nomenclature

a	Gas-liquid interfacial area (per unit liquid volume)	($m^2\ m^{-3}$)
a_e	Effective surface area (per unit liquid volume)	($m^2\ m^{-3}$)
a_s	Surface area of a single element	(m^2)
A	Constant	(-)
A_d	Downcomer cross-sectional area	(m^2)
A_r	Riser cross-sectional area	(m^2)
B	Constant	(-)
B_W	Baffle width	(m)
b_1	Constant	(-)
b_2	Constant	(-)
C	Experimental constant	(-)
C_B	Experimental constant	(-)
C_i	Impeller clearance	(m)
C_L	Experimental constant	(-)
c_s	Solid concentration	($kg\ m^{-3}$)
C_2	Constant	(-)
D_i	Impeller diameter	(m)
d_B	Average bubble diameter	(m)
d_d	Downcomer (hydraulic) diameter	(m)
d_{disc}	Disc diameter of the disc column	(m)
d_D	Draught tube diameter	(m)
D_d	Gas distributor diameter	(m)
d_h	Hydraulic diameter of the packing	(m)
D_L	Liquid diffusivity	($m^2\ s^{-1}$)

d_{Sm}	Sauter mean bubble diameter	(m)
d_p	Average particle diameter	(m)
d_P	Packing diameter	(m)
d_r	Riser diameter	(m)
d_R	Reactor diameter	(m)
D_R	Bubble column diameter	(m)
D_T	Tank diameter	(m)
d_0	Diameter of sparger orifice	(m)
e	Constant	(-)
F	Constant	(-)
F_f	Coefficient of form	(-)
g	Gravitational acceleration	(m s^{-2})
H	Liquid height	(m)
H_b	Liquid height with bubbling	(m)
h_c	Downcomer clearance height	(m)
h_{DC}	Critical downcomer sparger distance	(m)
h_P	Packing height	(m)
h_R	Effective reactor height	(m)
H_0	Liquid height without bubbling	(m)
I	Ion strength	(g-ion L^{-1})
K	Constant	(-)
k_G	Gas-phase mass transfer coefficient	(m s^{-1})
k_L	Liquid-phase mass transfer coefficient	(m s^{-1})
k_La	Gas-liquid mass transfer coefficient	(s^{-1})
L_c	Tube connector length	(-)

L_D	Draught tube length	(-)
L_h	Reactor height; used by Choi (2001)	(-)
L_m	Liquid mass superficial velocity	(kmol m^{-2} s^{-1})
n	Constant	(-)
N	Impeller speed	(rev min^{-1})
N_A	Avogadro's constant	(mol^{-1})
N_{CD}	Impeller speed required for complete dispersion	(rev min^{-1})
N_{CSA}	Critical impeller speed for surface aeration	(rev min^{-1})
N_F	Flooded regime impeller speed	(rev min^{-1})
N_R	Gross recirculation regime impeller speed	(rev min^{-1})
N_0	Constant	(-)
P	Pressure	(MPa)
P_0	Ungassed impeller power draw	(W)
P_g	Gassed impeller power draw	(W)
P_{sat}	Saturation pressure	(MPa)
P_v	Energy dissipation rate	(kW m^{-3})
Q_G	Volumetric gas flow rate	(m^3 s^{-1})
R	Universal gas constant	(kJ K^{-1} $kmol^{-1}$)
R_A	Gas distributor open area ratio	(-)
r_U	Radius of the gas particle	(m)
s	Thickness of the sloped metal sheet	(m)
T	Temperature	(°C)
t_c	Circulation time	(s)
t_P	Thickness of the expanded metal sheets	(m)
U_b	Bubble terminal velocity	(m s^{-1})

U_G	Superficial gas velocity	(m s^{-1})
U_{Gr}	Riser superficial gas velocity	(m s^{-1})
U_L	Superficial liquid velocity	(m s^{-1})
U_{Lc}	Liquid circulation velocity	(m s^{-1})
U_{Ll}	Peripheral liquid flow rate	(kg m^{-1} s^{-1})
U_{Lr}	Riser superficial liquid velocity	(m s^{-1})
U_{Ls}	Liquid velocity in the separator	(m s^{-1})
U_P	Superficial velocity losses to the surroundings	(m s^{-1})
U_R	Bubble rise velocity	(m s^{-1})
U_{sG}	Average slip velocity	(m s^{-1})
U_t	Terminal bubble velocity	(m s^{-1})
U_{trans}	Superficial gas velocity at which flow transitions out of the homogeneous flow regime into the transition flow regime	(m s^{-1})
U_0	Gas velocity in the sparger orifice	(m s^{-1})
U_∞	Terminal rise velocity	(m s^{-1})
$V_L(0)$	Center-line liquid velocity; used by Zehner (1989)	(m s^{-1})
vvm	Gas volume per liquid volume per minute	(m^3 m^{-3} min^{-1})
W	Impeller blade width	(m)
W_L	Found in Kantarci et al. (2005); not defined	(-)
W_s	Found in Kantarci et al. (2005); not defined	(-)
x	Constant	(-)
x_c	Circulation path	(m)

Abbreviations

ALR	Airlift Reactor
A-310	Lightnin A-310 axial flow impeller (hydrofoil)
A-315	Lightnin A-315 axial flow impeller (hydrofoil)
BC	Bubble column
BT-6	Concave blade disc turbine (radial flow impeller)
Carbopol	Carboxypolymethylene
CMC	Carboxymethylcellulose
CS	Cylindrical sintered sparger
DT-ILALR	Draught tube airlift reactor
ELALR	External-loop airlift reactor
FBR	Flooded-bed reactor
FP	Fixed packing
ILALR	Internal-loop airlift reactor
NS	Narcissus impeller (radial flow impeller)
PBT	Pitched blade disc turbine
PBD	Down-pumping pitched blade turbine
PBR	Packed bed reactor
PBU	Up-pumping pitched blade turbine
PP	Perforated plate or tube
PS	(Perforated) Plane sparger (as cited by Merchuk et al. (1998))

RP Random packing

RT Rushton-type impeller (radial flow impeller)

STR Stirred tank reactor

TBR Trickle bed reactor

TX Techmix 335 (axial flow impeller)

TXD Down-pumping Techmix 335

TXU Up-pumping Techmix 335

Greek Symbols

α	Constant and parameter used by Zehner (1989)	(-)
β	Constant (-)	
δ	Modified film thickness, $\delta = \left(\frac{\mu_L^{\,2}}{\rho_L^{\,2} g} \right)^{1/3}$	(m)
γ	Shear rate	(s^{-1})
ε	Bed void fraction	(-)
ε_b	Baseline gas holdup, used by Salvacion et al. (1995)	(-)
ε_G	Gas holdup	(-)
ε_{Gr}	Riser gas holdup	(-)
ε_{Gd}	Downcomer gas holdup	(-)
ε_L	Liquid void fraction	(-)
ε_s	Solid holdup	(-)
ε_0	Gas holdup at atmospheric pressure, used by Kojima et al. (1997)	(-)

λ_L	Liquid thermal conductivity	(W m^{-1} K^{-1})
μ	Liquid dynamic viscosity	(Pa s)
μ_a	Apparent dynamic viscosity	(Pa s)
μ_G	Gas dynamic viscosity	(Pa s)
μ_L	Liquid dynamic viscosity	(Pa s)
μ_w	Dynamic viscosity of tap water	(Pa s)
ν_L	Liquid kinematic viscosity	(m^2 s^{-2})
ρ	Liquid density	(kg m^{-3})
ρ_G	Gas density	(kg m^{-3})
ρ_L	Liquid density	(kg m^{-3})
ρ_m	Slurry density in the absence of gas	(kg m^{-3})
ρ_s	Solids density	(kg m^{-3})
$\Delta\rho$	Phase density difference	(kg m^{-3})
σ	Liquid phase surface tension	(mN m^{-1} or dyn cm^{-1})
σ_w	Surface tension of tap water	(mN m^{-1} or dyn cm^{-1})
θ_θ	Contact angle of wettability	(deg)
φ_s	Volumetric solids fraction	(-)

Dimensionless numbers

Bo	Bond number, $Bo = \frac{\rho_L g D_R^{\,2}}{\sigma}$
Fl_G	Gas flow number, $Fl_G = \frac{Q_G}{ND^3}$

Fr Froude number, $Fr = \frac{U_G}{\sqrt{gD_R}}$

Ga Galileo number, $Ga = \frac{gD_R^{\,3}}{\upsilon_L^{\,2}}$

Ga_L Galileo number, $Ga_L = \frac{g\rho_L^{\,2}}{a^3\mu_L^{\,2}}$

Ga_{Lh} Galileo number, $Ga_{Lh} = \frac{gt_P^{\,3}}{\nu_L^{\,2}}$

Gr Grashof number, $Gr = \frac{d_{Bs}^{\,3}\rho_L\Delta\rho g}{\mu_L^{\,2}}$

Mo Morton number, $Mo = \frac{g\mu_L^{\,4}}{\rho_L\sigma^3}$

Mo Modified Morton number, $Mo_m = \frac{\left(\xi\mu_L\right)^4 g}{\rho_m\sigma^3}$ where

$$\ln\xi = 4.6\varepsilon_s\left\{5.7\varepsilon_s^{\,0.58}\sinh\left[-0.71\exp\left(-5.8\varepsilon_s\right)\ln Mo^{0.22}\right]+1\right\}$$

N_{Pg} Gassed power number, $N_{Pg} = \frac{P_G}{\rho N^3 D^5}$

Re Reynolds number, $Re = \frac{\rho ND^2}{\mu}$

Re_L Liquid phase Reynolds number, $Re_L = \frac{\rho_L U_L D_R}{\mu_L}$

Re_{Le} Reynolds number, $Re_{Le} = \frac{4U_L}{a_e\nu_L}$

Re_P Reynolds number, used by Mena et al. (2005); defined in terms of particle diameter

Re_T Reynolds number, used by Kantarci et al. (2005); not defined

Sc or Sc_L Schmidt number, $Sc = \frac{\nu_L}{D_L}$

Sh Sherwood number, usually $Sh = \frac{k_L a d_R}{D_L}$

Sh_L Sherwood number, usually $Sh_L = \frac{k_L d_P}{D_L}$

We Weber number, $We = \frac{\rho_L U_L^{\ 2} D_R}{\sigma}$

References

Aden, A., Ruth, M., Ibsen, K., Jechura, J., Neeves, K., Sheehan, J., Wallace, B., Montague, L., Slayton, A., and Lukas, J. "Lignocellulosic biomass to ethanol process design and economics utilizing co-current dilute acid prehydrolysis and enzymatic hydrolysis for corn stover." NREL report TP-510-32438. June 2002.

Akita, K., and Yoshida, F. (1973). "Gas holdup and volumetric mass transfer coefficient in bubble columns." *Industrial & Engineering Chemistry, Process Design and Development*, **12**(1): 76-80.

Akita, K., and Yoshida, F. (1974). "Bubble size, interfacial area, and liquid-phase mass transfer coefficient in bubble columns." *Industrial & Engineering Chemistry, Process Design and Development*, **13**(1): 84-91.

Al-Dahhan, M. H., Larachi, F., Dudukovic, M. P., and Laurent, A. (1997). "High-pressure trickle-bed reactors: A review." *Industrial & Engineering Chemistry Research*, **36**(8): 3292-3314.

Al-Masry, W. A. (1999). "Effect of liquid volume in the gas-separator on the hydrodynamics of airlift reactors." *Journal of Chemical Technology & Biotechnology*, **74**(10): 931-936.

Albijanic, B., Havran, V., Petrovic, L., Duric, M., and Tekic, M. N. (2007). "Hydrodynamics and mass transfer in a draft tube airlift reactor with dilute alcohol solutions." *AIChE Journal*, **53**(11): 2897-2904.

Alix, P., and Raynal, L. (2008). "Liquid distribution and liquid hold-up in modern high capacity packings." *Chemical Engineering Research & Design*, **86**(6): 585-591.

Álvarez, E., Gomez-Diaz, D., Navaza, J. M., and Sanjurjo, B. (2008). "Continuous removal of carbon dioxide by absorption employing a bubble column." *Chemical Engineering Journal*, **137**(2): 251-256.

Álvarez, E., Sanjurjo, B., Cancela, A., and Navaza, J. M. (2000). "Mass transfer and influence of physical properties of solutions in a bubble column." *Chemical Engineering Research & Design*, **78**(6): 889-893.

Anabtawi, M. Z. A., Abu-Eishah, S. I., Hilal, N., and Nabhan, M. B. W. (2003). "Hydrodynamic studies in both bi-dimensional and three-dimensional bubble columns with a single sparger." *Chemical Engineering and Processing*, **42**(5): 403-408.

Attou, A., Boyer, C., and Ferschneider, G. (1999). "Modelling of the hydrodynamics of the cocurrent gas-liquid trickle flow through a trickle-bed reactor." *Chemical Engineering Science*, **54**(6): 785-802.

Azbel, D. (1981). *Two-phase flows in chemical engineering*. New York, Cambridge University Press.

Bach, H. F., and Pilhofer, T. (1978). "Variation of gas hold-up in bubble columns with physical properties of liquids and operating parameters of columns." *German Chemical Engineering*, **1**(5): 270-275.

Baker, R. W. (2004). *Membrane technology and applications*. West Sussex, England, John Wiley & Sons, Ltd.

Bakker, A. (1992). "Hydrodynamics of stirred gas-liquid dispersion." PhD Thesis, Delft University of Technology, Delft, The Netherlands.

Bakker, A., and Oshinowo, L. M. (2004). "Modelling of turbulence in stirred vessels using large eddy simulation." *Chemical Engineering Research & Design*, **82**(9 SPEC ISS): 1169-1178.

Barakat, T. M. M., and Sorensen, E. (2008). "Simultaneous optimal synthesis, design and operation of batch and continuous hybrid separation processes." *Chemical Engineering Research & Design*, **86**(3): 279-298.

Bauer, T., Haase, S., Al-Dahhan, M. H., and Lange, R. (2007). 559d Monolithic reactor and particle-packed monolithic reactor for three-phase catalytic reactions. *The 2007 Annual Meeting*. Salt Lake City, UT, AIChe.

Beenackers, A. A. C. M., and Van Swaaij, W. P. M. (1993). "Mass transfer in gas-liquid slurry reactors." *Chemical Engineering Science*, **48**(18): 3109-3139.

Behkish, A., Men, Z., Inga, J. R., and Morsi, B. I. (2002). "Mass transfer characteristics in a large-scale slurry bubble column reactor with organic liquid mixtures." *Chemical Engineering Science*, **57**(16): 3307-3324.

Bellgardt, K.-H. (2000). *Bioreaction engineering: Modeling and control*. New York City, New York, Springer.

Bello, R. A. (1981). "A characterization study of airlift contactors for applications to fermentation." Ph.D. Dissertation, University of Waterloo, Waterloo, Ontario, Canada.

Bello, R. A., Robinson, C. W., and Moo-Young, M. (1984). "Liquid circulation and mixing characteristics of airlift contactors." *Canadian Journal of Chemical Engineering*, **62**(5): 573-577.

Bello, R. A., Robinson, C. W., and Moo-Young, M. (1985a). "Gas holdup and overall volumetric oxygen transfer coefficient in airlift contactors." *Biotechnology and Bioengineering*, **27**(3): 369-381.

Bello, R. A., Robinson, C. W., and Moo-Young, M. (1985b). "Prediction of the volumetric mass transfer coefficient in pneumatic contactors." *Chemical Engineering Science*, **40**(1): 53-58.

Bendjaballah, N., Dhaouadi, H., Poncin, S., Midoux, N., Hornut, J.-M., and Wild, G. (1999). "Hydrodynamics and flow regimes in external loop airlift reactors." *Chemical Engineering Science*, **54**(21): 5211-5221.

Bentifraouine, C., Xuereb, C., and Riba, J.-P. (1997a). "Effect of gas liquid separator and liquid height on the global hydrodynamic parameters of an external loop airlift contactor." *Chemical Engineering Science*, **66**: 91-95.

Bentifraouine, C., Xuereb, C., and Riba, J.-P. (1997b). "An experimental study of the hydrodynamic characteristics of external loop airlift contactors." *Journal of Chemical Technology & Biotechnology*, **69**: 345-349.

Benz, G. T. (2008). "Piloting bioreactors for agitation scale-up." *Chemical Engineering Progress*, **104**(2): 32-34.

Billet, R. (1989). "Packed column analysis and design." Ruhr-Universität Bochum, Bochum, Germany.

Billet, R. (1993). "Process engineering evaluation of packings and the limits of their development." *Chemie-Ingenieur-Technik*, **65**(2): 157-166.

Billet, R., and Schultes, M. (1993). "Physical model for the prediction of liquid hold-up in two-phase countercurrent columns." *Chemical Engineering and Technology*, **16**(6): 370-375.

Birch, D., and Ahmed, N. (1996). "Gas sparging in vessels agitated by mixed flow impellers." *Powder Technology*, **88**(1): 33-38.

Birch, D., and Ahmed, N. (1997). "The influence of sparger design and location on gas dispersion in stirred vessels." *Chemical Engineering Research & Design*, **75**(5): 487-496.

Bisang, J. M. (1996). "Modelling the startup of a continuous parallel plate electrochemical reactor." *Journal of Applied Electrochemistry*, **1997**(27): 379-384.

Blazej, M., Jurascik, M., Annus, J., and Markos, J. (2004a). "Measurement of mass transfer coefficient in an airlift reactor with internal loop using coalescent and non-coalescent liquid media." *Journal of Chemical Technology & Biotechnology*, **79**(12): 1405-1411.

Blazej, M., Kisa, M., and Markos, J. (2004b). "Scale influence on the hydrodynamics of an internal loop airlift reactor." *Chemical Engineering and Processing*, **43**(12): 1519-1527.

Blenke, H. (1979). "Loop reactors." *Advances in Biochemical Engineering*, **13**: 121-214.

Bliem, R., and Katinger, H. (1988a). "Scale-up engineering in animal cell technology: Part I." *Trends in Biotechnology*, **6**(8): 190-195.

Bliem, R., and Katinger, H. (1988b). "Scale-up engineering in animal cell technology: Part II." *Trends in Biotechnology*, **6**(9): 224-230.

Boden, S., Bieberle, M., and Hampel, U. (2008). "Quantitative measurement of gas hold-up distribution in a stirred chemical reactor using X-ray cone-beam computed tomography." *Chemical Engineering Journal*, **139**(2): 351-362.

Bouaifi, M., Hebrard, G., Bastoul, D., and Roustan, M. (2001). "A comparative study of gas hold-up, bubble size, interfacial area, and mass transfer coefficients in stirred gas-liquid reactors and bubble columns." *Chemical Engineering and Processing*, **40**(2): 97-111.

Bouaifi, M., and Roustan, M. (2001). "Power consumption, mixing time and homogenisation energy in dual-impeller agitated gas-liquid reactors." *Chemical Engineering and Processing*, **40**(2): 87-95.

Branyik, T., Vicente, A. A., Dostalek, P., and Teixeira, J. A. (2005). "Continuous beer fermentation using immobilized yeast cell bioreactor systems." *Biotechnology Progress*, **21**(3): 653-663.

Bredwell, M. D., Srivastava, P., and Worden, R. M. (1999). "Reactor design issues for synthesis-gas fermentations." *Biotechnology Progress*, **15**(5): 834-844.

Bredwell, M. D., and Worden, R. M. (1998). "Mass-transfer properties of microbubbles: I. Experimental studies." *Biotechnology Progress*, **14**(1): 31-38.

Breijer, A. A. J., Nijenhuis, J., and van Ommen, J. R. (2008). "Prevention of flooding in a countercurrent trickle-bed reactor using additional void space." *Chemical Engineering Journal*, **138**(1-3): 333-340.

Broekhuis, R. R., Machado, R. M., and Nordquist, A. F. (2001). "The ejector-driven monolith loop reactor -- experiments and modeling." *Catalysis Today*, **69**(1-4): 87-93.

Burghardt, A., Bartelmus, G., Jaroszynski, M., and Kolodziej, A. (1995). "Hydrodynamics and mass transfer in a three-phase fixed-bed reactor with cocurrent gas-liquid downflow." *The Chemical Engineering Journal and the Biochemical Engineering Journal*, **58**(2): 83-99.

Cabaret, F., Fradette, L., and Tanguy, P. A. (2008). "Gas-liquid mass transfer in unbaffled dual-impeller mixers." *Chemical Engineering Science*, **63**(6): 1636-1647.

Cai, J., Nieuwstad, T. J., and Kop, J. H. (1992). "Fluidization and sedimentation of carrier material in a pilot-scale airlift internal-loop reactor." *Water Science & Technology*, **26**(9-11): 2481-2484.

Calderbank, P. H., and Moo-Young, M. B. (1961). "The continuous phase heat and mass-transfer properties of dispersion." *Chemical Engineering Science*, **16**(1-2): 39-54.

Canadian Process Technologies. (2008). "Sparging systems." Retrieved August 7, 2008, from http://www.cpti.bc.ca/files/sparintro.html.

Chakravarty, M., Begum, S., Singh, H. D., Baruah, J. N., and Iyengar, M. S. (1973). "Gas holdup distribution in a gas-lift column." *Biotechnology and Bioengineering Symposium*, **4**: 363-378.

Chakravarty, M., Singh, H. D., Baruah, J. N., and Lyengar, M. S. (1974). *Indian Chemical Engineer*, **16**: 17-22.

Chand Eisenmann Metallurgical. (2008). "Spargers." Retrieved August 07, 2008, from http://www.chandeisenmann.com/products/spargers.asp.

Charpentier, J.-C. (1981). "Mass-transfer rates in gas-liquid absorbers and reactors" in *Advances in Chemical Engineering*. Edited by Drew, T. B., Cokelet, G. E., Hoopes, J. W., Jr. and Vermeulen, T. New York City, New York, Academic Press. **11:** 1-133.

Chaumat, H., Billet-Duquenne, A. M., Augier, F., Mathieu, C., and Delmas, H. (2005). "Mass transfer in bubble column for industrial conditions: Effects of organic medium, gas and liquid flow rates and column design." *Chemical Engineering Science*, **60**(22): 5930-5936.

Chen, R. C., Reese, J., and Fan, L. S. (1994). "Flow structure in a three-dimensional bubble column and three-phase fluidized bed." *AIChE Journal*, **40**(7): 1093-1104.

Chen, Z. D., and Chen, J. J. J. (1999). "Comparison of mass transfer performance for various single and twin impellers." *Chemical Engineering Research & Design*, **77**(2): 104-109.

Cheng, H., and Sabatini, D. A. (2007). "Separation of organic compounds from surfactant solutions: a review." *Separation Science and Technology*, **42**(3): 453 - 475.

Chisti, M. Y. (1989). *Airlift Bioreactors*. New York, NY, Elsevier Science Publishing Co., Inc.

Chisti, M. Y., Halard, B., and Moo-Young, M. (1988a). "Liquid circulation in airlift reactors." *Chemical Engineering Science*, **43**(3): 451-457.

Chisti, M. Y., and Moo-Young, M. (1987). "Airlift reactors: Characteristics, applications, and design considerations." *Chemical Engineering Communications*, **60**: 195-242.

Chisti, Y., Fujimoto, K., and Moo-Young, M. (1988b). *Biotechnology Progress*, **5**: 72-76.

Chisti, Y., and Jauregui-Haza, U. J. (2002). "Oxygen transfer and mixing in mechanically agitated airlift bioreactors." *Biochemical Engineering Journal*, **10**(2): 143-153.

Chisti, Y., Kasper, M., and Moo-Young, M. (1990). "Mass transfer in external-loop airlift bioreactors using static mixers." *Canadian Journal of Chemical Engineering*, **68**(2): 45-50.

Chisti, Y., and Moo-Young, M. (1986). "Disruption of microbial cells for intracellular products." *Enzyme and Microbial Technology*, **8**(4): 194-204.

Cho, J. S., and Wakao, N. (1988). "Determination of liquid-side and gas-side volumetric mass transfer coefficients in a bubble column." *Journal of Chemical Engineering of Japan*, **21**(6): 576-581.

Choi, J. H., and Lee, W. K. (1993). "Circulating liquid velocity, gas holdup and volumetric oxygen transfer coefficient in external-loop airlift reactors." *Journal of Chemical Technology & Biotechnology*, **56**: 51-58.

Choi, K. H. (2001). "Hydrodynamic and mass transfer characteristics of external-loop airlift reactors without an extension tube above the downcomer." *Korean Journal of Chemical Engineering*, **18**(2): 240-246.

Cockx, A., Roustan, M., Line, A., and Hebrard, G. (1995). "Modelling of mass transfer coefficient k_L in bubble columns." *Chemical Engineering Research & Design*, **73**(A6): 627-631.

Daly, J. G., Patel, S. A., and Bukur, D. B. (1992). "Measurement of gas holdups and Sauter mean bubble diameters in bubble column reactors by dynamics gas disengagement method." *Chemical Engineering Science*, **47**(13-14): 3647-3654.

Deckwer, W.-D. (1992). *Bubble Column Reactors*. New York, NY.

Deglon, D. A., O'Connor, C. T., and Pandit, A. B. (1998). "Efficacy of a spinning disc as a bubble break-up device." *Chemical Engineering Science*, **53**(1): 59-70.

Demirel, B., and Yenigün, O. (2002). "Two-phase anaerobic digestion processes: a review." *Journal of Chemical Technology & Biotechnology*, **77**(7): 743-755.

Deshpande, N. S., and Barigou, M. (1999). "Performance characteristics of novel mechanical foam breakers in a stirred tank reactor." *Journal of Chemical Technology & Biotechnology*, **74**(10): 979-987.

Dhaouadi, H., Poncin, S., Hornut, J. M., and Midoux, N. (2008). "Gas-liquid mass transfer in bubble column reactor - Analytical solution and experimental confirmation." *Chemical Engineering and Processing: Process Intensification*, **47**(4): 548-556.

Díaz, M. E., Montes, F. J., and Galán, M. A. (2008). "Experimental study of the transition between unsteady flow regimes in a partially aerated two-dimensional bubble column." *Chemical Engineering and Processing: Process Intensification*, **47**(9-10): 1867-1876.

Dionysiou, D. D., Burbano, A. A., Suidan, M. T., Baudin, I., and Laine, J.-M. (2002). "Effect of oxygen in a thin-film rotating disk photocatalytic reactor." *Environmental Science & Technology*, **36**(17): 3834-3843.

Doan, H. D., Wu, J., and Eyvazi, M. J. (2008). "Effect of liquid distribution on the organic removal in a trickle bed filter." *Chemical Engineering Journal*, **139**(3): 495-502.

Domingues, L., and Teixeira, N. L. J. A. (2000). "Contamination of a high-cell-density continuous bioreactor." *Biotechnology and Bioengineering*, **68**(5): 584-587.

Donati, G., and Paludetto, R. (1999). "Batch and semibatch catalytic reactors (from theory to practice)." *Catalysis Today*, **52**(2-3): 183-195.

Dudukovic, M. P. (1999). "Trends in catalytic reaction engineering." *Catalysis Today*, **48**(1-4): 5-15.

Ehrfeld, W., Hessel, V., and Lowe, H. (2000). *Microreactors: New technology for modern chemistry*. New York, NY, Wiley-VCH.

Ellenberger, J., and Krishna, R. (2002). "Improving mass transfer in gas-liquid dispersions by vibration excitement." *Chemical Engineering Science*, **57**(22-23): 4809-4815.

Fadavi, A., and Chisti, Y. (2005). "Gas-liquid mass transfer in a novel forced circulation loop reactor." *Chemical Engineering Journal*, **112**(1-3): 73-80.

Fadavi, A., Chisti, Y., and Chriascarontel, L. (2008). "Bubble size in a forced circulation loop reactor." *Journal of Chemical Technology & Biotechnology*, **83**(1): 105-108.

Fair, J. R. (1967). "Designing gas-sparged reactors." *Chemical Engineering*, **74**(14): 67-74.

Figueiredo, M. M. L. d., and Calderbank, P. H. (1979). "The scale-up of aerated mixing vessels for specified oxygen dissolution rates." *Chemical Engineering Science*, **34**: 1333-1338.

Fogler, H. S. (2005). *Elements of chemical reaction engineering*. Upper Saddle River, NJ, Prentice Hall.

Ford, J. J., Heindel, T. J., Jensen, T. C., and Drake, J. B. (2008). "X-ray computed tomography of a gas-sparged stirred-tank reactor." *Chemical Engineering Science*, **63**(8): 2075-2085.

Freitas, C., and Teixeira, J. A. (2001). "Oxygen mass transfer in a high solids loading three-phase internal-loop airlift reactor." *Chemical Engineering Journal*, **84**(1): 57-61.

Fu, C.-C., Lu, S.-Y., Hsu, Y.-J., Chen, G.-C., Lin, Y.-R., and Wu, W.-T. (2004). "Superior mixing performance for airlift reactor with a net draft tube." *Chemical Engineering Science*, **59**(14): 3021-3028.

Fu, C.-C., Wu, W.-T., and Lu, S.-Y. (2003). "Performance of airlift bioreactors with net draft tube." *Enzyme and Microbial Technology*, **33**(4): 332-342.

Fujasova, M., Linek, V., and Moucha, T. (2007). "Mass transfer correlations for multiple-impeller gas-liquid contactors. Analysis of the effect of axial dispersion in gas and liquid phases on "local" k_La values measured by the dynamic pressure method in individual stages of the vessel." *Chemical Engineering Science*, **62**(6): 1650-1669.

Fujita, S., and Hayakawa, T. (1956). "Liquid-film mass transfer coefficients in packed towers and rod-like irrigation towers." *Kagaku Kogaku*, **20**(3): 113-117.

Fukuma, M., Muroyama, K., and Yasunishi, A. (1987). "Specific gas-liquid interfacial area and liquid-phase mass transfer coefficient in a slurry bubble column." *Journal of Chemical Engineering of Japan*, **20**(3): 321-324.

Gagnon, H., Lounes, M., and Thibault, J. (1998). "Power consumption and mass transfer in agitated gas-liquid columns: A comparative study." *Canadian Journal of Chemical Engineering*, **76**(3): 379-389.

Garcia-Ochoa, F., and Gomez, E. (2009). "Bioreactor scale-up and oxygen transfer rate in microbial processes: An overview." *Biotechnology Advances*, **27**(2): 153-176.

Garcia-Ochoa, F. F., and Gomez, E. (1998). "Mass transfer coefficient in stirred tank reactors for xanthan gum solutions." *Biochemical Engineering Journal*, **1**(1): 1-10.

Garcia-Ochoa, F. F., and Gomez, E. (2004). "Theoretical prediction of gas-liquid mass transfer coefficient, specific area and hold-up in sparged stirred tanks." *Chemical Engineering Science*, **59**(12): 2489-2501.

Gestrich, W., Esenwein, H., and Kraus, W. (1978). "Liquid-side mass transfer coefficient in bubble layers." *International Chemical Engineering*, **18**(1): 38-47.

Gestrich, W., and Rahse, W. (1975). *Chemie-Ingenieur-Technik*, **47**(1): 8.

Gezork, K. M., Bujalski, W., Cooke, M., and Nienow, A. W. (2000). "The transition from homogeneous to heterogeneous flow in a gassed, stirred vessel." *Chemical Engineering Research & Design*, **78**(3): 363-370.

Gezork, K. M., Bujalski, W., Cooke, M., and Nienow, A. W. (2001). "Mass transfer and hold-up characteristics in a gassed, stirred vessel at intensified operating conditions." *Chemical Engineering Research & Design*, **79**(8): 965-972.

Ghionzoli, A., Bujalski, W., Grenville, R. K., Nienow, A. W., Sharpe, R. W., and Paglianti, A. (2007). "The effect of bottom roughness on the minimum agitator speed required to just fully suspend particles in a stirred vessel." *Chemical Engineering Research & Design*, **85**(5): 685-690.

Ghirardini, M., Donati, G., and Rivetti, F. (1992). "Gas lift reactors : hydrodynamics, mass transfer, and scale up." *Chemical Engineering Science*, **47**(9-11): 2209-2214.

Gill, N. K., Appleton, M., Baganz, F., and Lye, G. J. (2008). "Quantification of power consumption and oxygen transfer characteristics of a stirred miniature bioreactor for predictive fermentation scale-up." *Biotechnology and Bioengineering*, **100**(6): 1144-1155.

Giovannettone, J. P., Tsai, E., and Gulliver, J. S. (2009). "Gas void ratio and bubble diameter inside a deep airlift reactor." *Chemical Engineering Journal*, **149**(1-3): 301-310.

Gjaltema, A., Marel, N. v. d., Loosdrecht, M. C. M. v., and Heijnen, J. J. (1997a). "Adhesion and biofilm development on suspended carriers in airlift reactors: Hydrodynamic conditions versus surface characteristics." *Biotechnology and Bioengineering*, **55**(6): 880-889.

Gjaltema, A., Vinke, J. L., Loosdrecht, M. C. M. v., and Heijnen, J. J. (1997b). "Abrasion of suspended biofilm pellets in airlift reactors: Importance of shape, structure, and particle concentrations." *Biotechnology and Bioengineering*, **53**(1): 88-99.

Godbole, S. P., Honath, M. F., and Shah, Y. T. (1982). "Holdup structure in highly viscous Newtonian and non-Newtonian liquids in bubble columns".

Godbole, S. P., and Shah, Y. T. (1986). "Design and operation of bubble column reactors" in *Encyclopedia of Fluid Mechanics: Gas-Liquid Flows*. Edited by Cheremisinoff, N. P. Houston, Gulf Publishing Company. **3:** 1216-1239.

Gogate, P. R., and Pandit, A. B. (1999). "Mixing of miscible liquids with density differences: Effect of volume and density of the tracer fluid." *Canadian Journal of Chemical Engineering*, **77**(5): 988-996.

Gonzalez, J., Aguilar, R., Alvarez-Ramirez, J., and Barren, M. A. (1998). "Nonlinear regulation for a continuous bioreactor via a numerical uncertainty observer." *Chemical Engineering Journal*, **69**(2): 105-110.

Gottschalk, U. (2008). "Bioseparation in antibody manufacturing: The good, the bad and the ugly." *Biotechnology Progress*, **24**(3): 496-503.

Grover, G. S., Rode, C. V., and Chaudhari, R. V. (1986). "Effect of temperature on flow regime and gas hold-up in a bubble column." *Canadian Journal of Chemical Engineering*, **64**(3): 501-504.

Guo, Y. X., Rathor, M. N., and Ti, H. C. (1997). "Hydrodynamics and mass transfer studies in a novel external-loop airlift reactor." *Chemical Engineering Journal*, **67**(3): 205-214.

Guy, C., Carreau, P. J., and Paris, J. (1986). "Mixing characteristics and gas hold-up of a bubble column." *Canadian Journal of Chemical Engineering*, **64**(1): 23-35.

Hadjiev, D., Sabiri, N. E., and Zanati, A. (2006). "Mixing time in bioreactors under aerated conditions." *Biochemical Engineering Journal*, **27**(3): 323-330.

Hall, D. W., Scott, K., and Jachuck, R. J. J. (2001). "Determination of mass transfer coefficient of a cross-corrugated membrane reactor by the limiting-current technique." *International Journal of Heat and Mass Transfer*, **44**(12): 2201-2207.

Hallaile, M. (1993). "Biotechnology." Ben-Gurion University of the Negev, Beer-Sheva, Israel.

Hammer, H. (1984). *Frontiers in chemical reaction engineering*. New Delphi, India, Halsted Press.

Han, L., and Al-Dahhan, M. H. (2007). "Gas-liquid mass transfer in a high pressure bubble column reactor with different sparger designs." *Chemical Engineering Science*, **62**(1-2): 131-139.

Haque, M. W., Nigam, K. D. P., and Joshi, J. B. (1986). "Hydrodynamics and mixing in highly viscous pseudo-plastic non-Newtonian solutions in bubble columns." *Chemical Engineering Science*, **41**(9): 2321-2331.

Harnby, N., Edwards, M. F., and Nienow, A. W. (1992). *Mixing in the process industry*. Boston, Butterworth-Heinemann Ltd.

Harper, J. C., Christensen, P. A., Egerton, T. A., and Scott, K. (2001). "Mass transport characterization of a novel gas sparged photoelectrochemical reactor." *Journal of Applied Electrochemistry*, **31**: 267-276.

Heijnen, P., and Lukszo, Z. (2006). "Continuous improvement of batch wise operation: A decision support framework." *Production Planning & Control*, **17**(4): 355-366.

Henstra, A. M., Sipma, J., Rinzema, A., and Stams, A. J. (2007). "Microbiology of synthesis gas fermentation for biofuel production." *Current Opinion in Biotechnology*, **2007**(18): 200-206.

Hikita, H., Asai, S., Tanigawa, K., Segawa, K., and Kitao, M. (1980). "Gas hold-up in bubble columns." *Chemical Engineering Journal*, **20**(1): 59-67.

Hikita, H., Asai, S., Tanigawa, K., Segawa, K., and Kitao, M. (1981). "The volumetric liquid-phase mass transfer coefficient in bubble columns." *Chemical Engineering Journal*, **22**(1): 61-69.

Hikita, H., and Kikukawa, H. (1974). "Liquid-phase mixing in bubble columns: Effect of liquid properties." *Chemical Engineering Journal and the Biochemical Engineering Journal*, **8**(3): 191-197.

Hikita, H., and Ono, Y. (1959). "Mass transfer into a liquid film flowing over a packing piece." *Kagaku Kogaku*, **23**(12): 808-813.

Hoffmann, A., Mackowiak, J. F., Gorak, A., Haas, M., Loning, J. M., Runowski, T., and Hallenberger, K. (2007). "Standardization of mass transfer measurements: a basis for the description of absorption processes." *Chemical Engineering Research & Design*, **85**(1): 40-49.

Hoffmann, R. A., Garcia, M. L., Veskivar, M., Karim, K., Al-Dahhan, M. H., and Angenent, L. T. (2008). "Effect of shear on performance and microbial ecology of continuously stirred anaerobic digesters treating animal manure." *Biotechnology and Bioengineering*, **100**(1): 38-48.

Hruby, J. (2002). "Overview of LIGA microfabrication". *5th Workshop on High Energy Density and High Power RF*, Snowbird, Utah (USA), American Institute of Physics.

Hughmark, G. A. (1967). "Holdup and mass transfer in bubble columns." *Industrial & Engineering Chemistry Process Design and Development*, **6**(2): 218-220.

Idogawa, K., Ikeda, K., Fukuda, T., and Morooka, S. (1987). "Effect of gas and liquid properties on the behavior of bubbles in a column under high pressure." *International Chemical Engineering*, **27**(1): 93-99.

Ityokumbul, M. T., Kosaric, N., and Bulani, W. (1994). "Gas hold-up and liquid mixing at low and intermediate gas velocities: 1. Air-water system." *The Chemical Engineering Journal and the Biochemical Engineering Journal*, **53**(3): 167-172.

Jakobsen, H. A., Lindborg, H., and Dorao, C. A. (2005). "Modeling of bubble column reactors: Progress and limitations." *Industrial & Engineering Chemistry Research*, **44**(14): 5107-5151.

Jean, R.-H., and Fan, L.-S. (1987). "On the particle terminal velocity in a gas-liquid medium with liquid as the continuous phase." *Canadian Journal of Chemical Engineering*, **65**(6): 881-886.

Jones, S. T. (2007). "Gas-liquid mass transfer in an external airlift loop reactor for syngas fermentation." PhD Dissertation, Iowa State University, Ames, IA.

Jordan, U., and Schumpe, A. (2001). "The gas density effect on mass transfer in bubble columns with organic liquids." *Chemical Engineering Science*, **56**(21-22): 6267-6272.

Jordan, U., Terasaka, K., Kundu, G., and Schumpe, A. (2002). "Mass transfer in high-pressure bubble columns with organic liquids." *Chemical Engineering & Technology*, **25**(3): 262-265.

Joshi, J. B., Ranade, V. V., Gharat, S. D., and Lele, S. S. (1990). "Sparged loop reactors." *The Canadian Journal of Chemical Engineering*, **68**(October): 705-741.

Joshi, J. B., and Sharma, M. M. (1979). "Circulation cell model for bubble columns." *Chemical Engineering Research & Design*, **57**(4): 244-251.

Kang, Y., Cho, Y. J., Woo, K. J., and Kim, S. D. (1999). "Diagnosis of bubble distribution and mass transfer in pressurized bubble columns with viscous liquid medium." *Chemical Engineering Science*, **54**(21): 4887-4893.

Kantarci, N., Borak, F., and Ulgen, K. O. (2005). "Bubble column reactors." *Process Biochemistry*, **40**(7): 2263-2283.

Kapic, A. (2005). "Mass transfer measurements for syngas fermentation." M.S. Thesis, Iowa State University, Ames, IA.

Kapic, A., and Heindel, T. J. (2006). "Correlating gas-liquid mass transfer in a stirred-tank reactor." *Chemical Engineering Research & Design*, **84**(3A): 239-245.

Kapic, A., Jones, S. T., and Heindel, T. J. (2006). "Carbon monoxide mass transfer in a syngas mixture." *Industrial & Engineering Chemistry Research*, **45**(26): 9150-9155.

Karamanev, D. G., Chavarie, C., and Samson, R. (1996). "Hydrodynamics and mass transfer in an airlift reactor with a semipermeable draft tube." *Chemical Engineering Science*, **51**(7): 1173-1176.

Kasatkin, A. G., and Ziparis, I. N. (1952). *Chim Prom*, **7**: 203.

Kato, Y., and Nishiwaki, A. (1972). "Longitudinal dispersion coefficient of a liquid in a bubble column." *International Journal of Chemical Reactor Engineering*, **12**(1): 182-7.

Kawase, Y., Halard, B., and Moo-Young, M. (1987). "Theoretical prediction of volumetric mass transfer coefficients in bubble columns for Newtonian and non-Newtonian fluids." *Chemical Engineering Science*, **42**(7): 1609-1617.

Kawase, Y., and Moo-Young, M. (1986a). "Influence of non-Newtonian flow behaviour on mass transfer in bubble columns with and without draft tubes." *Chemical Engineering Communications*, **40**(1-6): 67-83.

Kawase, Y., and Moo-Young, M. (1986b). "Mixing and mass transfer in concentric-tube airlift fermenters: Newtonian and non-Newtonian media." *Journal of Chemical Technology and Biotechnology*, **36**(11): 527-553.

Kawase, Y., and Moo-Young, M. (1987). "Heat transfer in bubble column reactors with Newtonian and non-Newtonian fluids." *Chemical Engineering Research & Design*, **65**(2): 121-126.

Kawase, Y., and Moo-Young, M. (1988). "Volumetric mass transfer coefficients in aerated stirred tank reactors with Newtonian and non-Newtonian media." *Chemical Engineering Research & Design*, **66**(3): 284-288.

Kawase, Y., and Moo-Young, M. (1992). "Correlations for liquid-phase mass transfer coefficient in bubble column reactor with Newtonian and non-Newtonian fluids." *Canadian Journal of Chemical Engineering*, **70**(1): 48-54.

Kawase, Y., Tsujimura, M., and Yamaguchi, T. (1995). "Gas hold-up in external-loop airlift bioreactors " *Bioprocess and Biosystems Engineering*, **12**(1-2): 21-27.

Kawase, Y., Umeno, S., and Kumagai, T. (1992). "The prediction of gas hold-up in bubble column reactors: Newtonian and non-Newtonian fluids." *Chemical Engineering Journal*, **50**(1): 1-7.

Kemblowski, Z., Przywarski, J., and Diab, A. (1993). "An average gas hold-up and liquid circulation velocity in airlift reactors with external loop." *Chemical Engineering Science*, **48**(23): 4023-4035.

Khudenko, B. M., and Shpirt, E. (1986). "Hydrodynamic parameters of diffused air systems." *Water Research*, **20**(7): 905-915.

Kim, S. D., Baker, C. G. J., and Bergougnou, M. A. (1972). "Hold-up and axial mixing characteristics of two and three phase fluidized beds." *Canadian Journal of Chemical Engineering*, **50**(6): 695-691.

Kluytmans, J. H. J., Kuster, B. F. M., and Schouten, J. C. (2001). "Gas holdup in a slurry bubble column: Influence of electrolyte and carbon particles." *Industrial & Engineering Chemistry Research*, **40**(23): 5326-5333.

Kluytmans, J. H. J., van Wachem, B. G. M., Kuster, B. F. M., and Schouten, J. C. (2003). "Mass transfer in sparged and stirred reactors: influence of carbon particles and electrolyte." *Chemical Engineering Science*, **58**(20): 4719-4728.

Ko, C.-H., Chiang, P.-N., Chiu, P.-C., Liu, C.-C., Yang, C.-L., and Shiau, I.-L. (2008). "Integrated xylitol production by fermentation of hardwood wastes." *Journal of Chemical Technology & Biotechnology*, **83**(4): 534-540.

Koch, H. A., Stutzman, L. F., Blum, L. F., and Hutchings, H. A. (1949). "Liquid transfer coefficients for the carbon dioxide-air-water system." *Chemical Engineering Progress*, **45**(11): 677-682.

Koide, K., Horibe, K., Kawabata, H., and Ito, S. (1985). "Gas holdup and volumetric liquid-phase mass transfer coefficient in solid-suspended bubble column with draught tube." *Journal of Chemical Engineering of Japan*, **18**(3): 248-254.

Koide, K., Kimura, M., Nitta, H., and Kawabata, H. (1988). "Liquid circulation in bubble column with draught tube." *Journal of Chemical Engineering of Japan*, **21**(4): 393-399.

Koide, K., Kurematsu, K., Iwamoto, S., Iwata, Y., and Horibe, K. (1983a). "Gas holdup and volumetric liquid-phase mass transfer coefficient in bubble column with draught tube and with gas dispersion into tube." *Journal of Chemical Engineering of Japan*, **16**(5): 413-418.

Koide, K., Morooka, S., Ueyama, K., Matsuura, A., Yamashita, F., Iwamoto, S., Kato, Y., Inoue, H., Shigeta, M., Suzuki, S., and Akehata, T. (1979). "Behavior of bubbles in large scale bubble column." *Journal of Chemical Engineering of Japan*, **12**(2): 98-104.

Koide, K., Sato, H., and Iwamoto, S. (1983b). "Gas holdup and volumetric liquid-phase mass transfer coefficient in bubble column with draught tube and with gas dispersion into annulus." *Journal of Chemical Engineering of Japan*, **16**(5): 407-413.

Koide, K., Takazawa, A., Komura, M., and Matsunaga, H. (1984). "Gas holdup and volumetric liquid-phase mass transfer coefficient in solid-suspended bubble columns." *Journal of Chemical Engineering of Japan*, **17**(5): 459-466.

Kojima, H., Sawai, J., and Suzuki, H. (1997). "Effect of pressure on volumetric mass transfer coefficient and gas holdup in bubble column." *Chemical Engineering Science*, **52**(21-22): 4111-4116.

Kolev, N. (1976). "Wirkungsweise von Füllkörperschüttungen." *Chemie-Ingenieur-Technik*, **48**(12): 1105-1112.

Kolev, N. (2006). Packed Bed Columns: For absorption, desorption, rectification and direct heat transfer. Amsterdam, The Netherlands, Elsevier.

Kolev, N., and Daraktschiev, R. (1976). "Issledobanie massoobmena w gorizontalbnoi listowoi nasadke." *Theoretical Fundamentals of Chemical Technology*, **10**(4): 611-614.

Kolev, N., and Nakov, S. (1994). "Performance characteristics of a packing with boundary layer turbulizers. III. Liquid film controlled mass transfer." *Chemical Engineering and Processing*, **33**(6): 437-442.

Kolev, N., and Semkov, K. (1983). "Axial mixing in the liquid phase in packed columns." *Verfahrenstechnik*, **17**(8): 474-479, 488.

Krevelen, D. V. V., and Hoftijzer, P. J. (1948). "Kinetics of simultaneous absorption and chemical reaction." *Chemical Engineering Progress*, **44**(7): 529-536.

Krishna, R., Urseanu, M. I., and Dreher, A. J. (2000). "Gas hold-up in bubble columns: Influence of alcohol addition versus operation at elevated pressures." *Chemical Engineering and Processing*, **39**(4): 371-378.

Krishna, R., van Baten, J. M., and Urseanu, M. I. (2001). "Scale effects on the hydrodynamics of bubble columns operating in the homogeneous flow regime." *Chemical Engineering & Technology*, **24**(5): 451-458.

Kumar, A., Degaleesan, T. E., Laddha, G. S., and Hoelscher, H. E. (1976). "Bubble swarm characteristics in bubble columns." *Canadian Journal of Chemical Engineering*, **54**(6): 503-508.

Kumar, A., Dewulf, J., and Van Langenhove, H. (2008). "Membrane-based biological waste gas treatment." *Chemical Engineering Journal*, **136**(2-3): 82-91.

Laari, A., and Turunen, I. (2005). "Prediction of coalescence properties of gas bubbles in a gas-liquid reactor using persistence time measurements." *Chemical Engineering Research & Design*, **83**(7): 881-886.

Larachi, F., Levesque, S., and Grandjean, B. P. A. (2008). "Seamless mass transfer correlations for packed beds bridging random and structured packings." *Industrial & Engineering Chemistry Research*, **47**(9): 3274-3284.

Lau, R., Peng, W., Velazquez-Vargas, L. G., Yang, G. Q., and Fan, L. S. (2004). "Gas-liquid mass transfer in high-pressure bubble columns." *Industrial & Engineering Chemistry Research*, **43**(5): 1302-1311.

Lee, D.-H., Grace, J. R., and Epstein, N. (2000). "Gas holdup for high gas velocities in a gas-liquid cocurrent upward-flow system." *Canadian Journal of Chemical Engineering*, **78**(5): 1006-1010.

Leiknes, T., and Odegaard, H. (2007). "The development of a biofilm membrane bioreactor." *Desalination*, **202**(1-3): 135-143.

León-Becerril, E., Cockx, A., and Liné, A. (2002). "Effect of bubble deformation on stability and mixing in bubble columns." *Chemical Engineering Science*, **57**(16): 3283-3297.

León-Becerril, E., and Liné, A. (2001). "Stability analysis of a bubble column." *Chemical Engineering Science*, **56**(21-22): 6135-6141.

Levin, Y., and Flores-Mena, J. E. (2001). "Surface tension of strong electrolytes." *Europhysics Letters*, **56**(2): 187-192.

Li, G. Q., Yang, S. Z., Cai, Z. L., and Chen, J. Y. (1995). "Mass transfer and gas-liquid circulation in an airlift bioreactor with viscous non-Newtonian fluids." *The Chemical Engineering Journal and the Biochemical Engineering Journal*, **56**(2): b101-b107.

Li, H., and Prakash, A. (1997). "Heat transfer and hydrodynamics in a three-phase slurry bubble column." *Industrial & Engineering Chemistry Research*, **36**(11): 4688-4694.

Li, H., and Prakash, A. (2000). "Influence of slurry concentrations on bubble population and their rise velocities in a three-phase slurry bubble column." *Powder Technology*, **113**(1-2): 158-167.

Liao, Q., Tian, X., Chen, R., and Zhu, X. (2008). "Mathematical model for gas-liquid two-phase flow and biodegradation of a low concentration volatile organic compound (VOC) in a trickling biofilter." *International Journal of Heat and Mass Transfer*, **51**(7-8): 1780-1792.

Linek, V., Kordac, M., Fujasova, M., and Moucha, T. (2004). "Gas-liquid mass transfer coefficient in stirred tanks interpreted through models of idealized eddy structure of turbulence in the bubble vicinity." *Chemical Engineering and Processing*, **43**(12): 1511-1517.

Linek, V., Kordac, M., and Moucha, T. (2005a). "Mechanism of mass transfer from bubbles in dispersions: Part II. Mass transfer coefficients in stirred gas-liquid reactor and bubble column." *Chemical Engineering and Processing*, **44**(1): 121-130.

Linek, V., Moucha, T., and Kordac, M. (2005b). "Mechanism of mass transfer from bubbles in dispersions: Part I. Danckwerts' plot method with sulphite solutions in the presence of viscosity and surface tension changing agents." *Chemical Engineering and Processing*, **44**(3): 353-361.

Linek, V., Moucha, T., and Sinkule, J. (1996a). "Gas-liquid mass transfer in vessels stirred with multiple impellers--I. Gas-liquid mass transfer characteristics in individual stages." *Chemical Engineering Science*, **51**(12): 3203-3212.

Linek, V., Moucha, T., and Sinkule, J. (1996b). "Gas-liquid mass transfer in vessels stirred with multiple impellers--II. Modelling of gas-liquid mass transfer." *Chemical Engineering Science*, **51**(15): 3875-3879.

Lines, P. C. (1999). "Gas-liquid mass transfer: surface aeration in stirred vessels with dual impellers." *Institution of Chemical Engineers Symposium Series*, (146): 199-216.

Lines, P. C. (2000). "Gas-liquid mass transfer using surface-aeration in stirred vessels, with dual impellers." *Chemical Engineering Research & Design*, **78**(3): 342-347.

Llamas, J.-D., Pérat, C., Lesage, F., Weber, M., D'Ortona, U., and Wild, G. (2008). "Wire mesh tomography applied to trickle beds: A new way to study liquid maldistribution." *Chemical Engineering and Processing: Process Intensification*, **47**(9-10): 1765-1770.

Lo, C.-S., and Hwang, S.-J. (2003). "Local hydrodynamic properties of gas phase in an internal-loop airlift reactor." *Chemical Engineering Journal*, **91**(1): 3-22.

Lockett, M. J., and Kirkpatrick, R. D. (1975). "Ideal bubbly flow and actual flow in bubble columns." *Transactions of the Institution of Chemical Engineers*, **1975**(53): 267-273.

Löwe, H., Ehrfeld, W., Hessel, V., Richter, T., and Schiewe, J. (2000). Micromixing technology. *4th International Conference on Microreaction Technology*. Atlanta, GA, AIChe**:** 31-47.

Lu, W.-J., Hwang, S.-J., and Chang, C.-M. (1995). "Liquid velocity and gas holdup in three-phase internal loop airlift reactors with low-density particles." *Chemical Engineering Science*, **50**(8): 1301-1310.

Lundgren, D. G., and Russel, R. T. (1956). "An air-lift laboratory fermentor." *Applied and Environmental Microbiology*, **4**(1): 31-33.

Luo, X., Lee, D. J., Lau, R., Yang, G., and Fan, L.-S. (1999). "Maximum stable bubble size and gas holdup in high-pressure slurry bubble columns." *AIChE Journal*, **45**(4): 665-680.

Maiti, R. N., and Nigam, K. D. P. (2007). "Gas-liquid distributors for trickle-bed reactors: A review." *Industrial & Engineering Chemistry Research*, **46**(19): 6164-6182.

Majirova, H., Pinelli, D., Machon, V., and Magelli, F. (2004). "Gas flow behavior in a two-phase reactor stirred with triple turbines." *Chemical Engineering & Technology*, **27**(3): 304-309.

Maldonado, J. G. G., Bastoul, D., Baig, S., Roustan, M., and Hébrard, G. (2008). "Effect of solid characteristics on hydrodynamic and mass transfer in a fixed bed reactor operating in co-current gas-liquid up flow." *Chemical Engineering and Processing: Process Intensification*, **47**(8): 1190-1200.

Mangers, R. J., and Ponter, A. B. (1980). "Effect of viscosity on liquid film resistance to mass transfer in a packed column." *Industrial & Engineering Chemistry, Process Design and Development*, **19**(4): 530-537.

Martín, M., García, J. M., Montes, F. J., and Galán, M. A. (2008a). "On the effect of the orifice configuration on the coalescence of growing bubbles." *Chemical Engineering and Processing: Process Intensification*, **47**(9-10): 1799-1809.

Martín, M., Montes, F. J., and Galan, M. A. (2008b). "Influence of impeller type on the bubble breakup process in stirred tanks." *Industrial & Engineering Chemistry Research*, **47**(16): 6251-6263.

Martin, Y., and Vermette, P. (2005). "Bioreactors for tissue mass culture: Design, characterization, and recent advances." *Biomaterials*, **26**(35): 7481-7503.

Mashelkar, R. A. (1970). "Bubble columns." *British Chemical Engineering*, **1970**(15): 1297-1304.

McFarlane, C. M., and Nienow, A. W. (1995). "Studies of high solidity ratio hydrofoil impellers for aerated bioreactors. 1. Review." *Biotechnology Progress*, **11**(6): 601-607.

McFarlane, C. M., and Nienow, A. W. (1996a). "Studies of high solidity ratio hydrofoil impellers for aerated bioreactors. 3. Fluids of enhanced viscosity and exhibiting coalescence repression." *Biotechnology Progress*, **12**(1): 1-8.

McFarlane, C. M., and Nienow, A. W. (1996b). "Studies of high solidity ratio hydrofoil impellers for aerated bioreactors. 4. Comparison of impeller types." *Biotechnology Progress*, **12**(1): 9-15.

McFarlane, C. M., Zhao, X.-M., and Nienow, A. W. (1995). "Studies of high solidity ratio hydrofoil impellers for aerated bioreactors. 2. Air-water studies." *Biotechnology Progress*, **11**(6): 608-618.

McManamey, W. J., and Wase, D. A. J. (1986). "Relationship between the volumetric mass transfer coefficient and gas holdup in airlift fermentors." *Biotechnology and Bioengineering*, **28**(9): 1446-1448.

Medeiros, E. B. M., Petrissans, M., Wehrer, A., and Zoulalian, A. (2001). "Comparative study of two cocurrent downflow three phase catalytic fixed bed reactors: Application to the sulphur dioxide catalytic oxidation on active carbon particles." *Chemical Engineering and Processing*, **40**(2): 153-158.

Mehrnia, M. R., Towfighi, J., Bonakdarpour, B., and Akbarnejad, M. M. (2005). "Gas hold-up and oxygen transfer in a draft-tube airlift bioreactor with petroleum-based liquids." *Biochemical Engineering Journal*, **22**(2): 105-110.

Mena, P. C., Ruzicka, M. C., Rocha, F. A., Teixeira, J. A., and Drahos, J. (2005). "Effect of solids on homogeneous-heterogeneous flow regime transition in bubble columns." *Chemical Engineering Science*, **60**(22): 6013-6026.

Merchuk, J. C. (1986). "Gas hold-up and liquid velocity in a two-dimensional air lift reactor." *Chemical Engineering Science*, **41**(1): 11-16.

Merchuk, J. C., Contreras, A., García, F., and Molina, E. (1998). "Studies of mixing in a concentric tube airlift bioreactor with different spargers." *Chemical Engineering Science*, **53**(4): 709-719.

Merchuk, J. C., Glutz, M., Negev, B.-G. U. o. t., and Beer-Sheva, I. (1999). "Bioreactors: Air-lift Reactors" in *Encyclopedia of Bioprocess Technology: Fermentation, Biocatalysis, and Bioseperations*. Edited by Flickinger, M. C. and Drew, S. W. New York City, New York, John Wiley & Sons, Inc. **1:** 320-353.

Merchuk, J. C., Ladwa, N., Cameron, A., Bulmer, M., and Pickett, A. (1994). "Concentric-tube airlift reactors: effects of geometrical design on performance." *AIChE Journal*, **40**(7): 1105-1117.

Mersmann, A. (1977). "Auslegung und Maβstabsvergrösserung von Blasen- und Tropfensäulen." *Chemie-Ingenieur-Technik*, **49**(9): 679-691.

Metaxas, K., and Papayannakos, N. (2008). "Gas-liquid mass transfer in a bench-scale trickle bed reactor used for benzene hydrogenation." *Chemical Engineering & Technology*, **31**(10): 1410-1417.

Micromold Products. (2008). "PTFE ring sparger." Retrieved August 31, 2008, from http://catalog.micromold.com/product/pipe-tube-fittings-specials/n-and-custom-plastic-fabrication-ptfe-ring-sparger.

Miller, D. N. (1974). "Scale-up of agitated vessels gas-liquid mass transfer." *AIChE Journal*, **20**(3): 445-453.

Mishra, V. P., and Joshi, J. B. (1994). "Flow generated by a disc turbine: Part IV: Multiple impellers." *Chemical Engineering Research & Design*, **72**(A5): 657-668.

Miyahara, T., Hamaguchi, M., Sukeda, Y., and Takehashi, T. (1986). "Size of bubbles and liquid circulation in a bubble column with draught tube and sieve plate." *Canadian Journal of Chemical Engineering*, **64**: 718-725.

Moilanen, P., Laakkonen, M., Visuri, O., Alopaeus, V., and Aittamaa, J. (2008). "Modelling mass transfer in an aerated 0.2 m^3 vessel agitated by Rushton, Phasejet and Combijet impellers." *Chemical Engineering Journal*, **142**(1): 95-108.

Mok, Y. S., Kim, Y. H., and Kim, S. Y. (1990). "Bubble and gas holdup characteristics in a bubble column of CMC solution." *The Korean Journal of Chemical Engineering*, **7**(1): 31-39.

Molina, E., Contreras, A., and Chisti, Y. (1999). "Gas holdup, liquid circulation and mixing behaviour of viscous Newtonian media in a split-cylinder airlift bioreactor." *Food and Bioproducts Processing*, **77**(1): 27-32.

Moo-Young, M., and Blanch, H. W. (1981). "Design of biochemical reactors mass transfer criteria for simple and complex systems." *Advances in Biochemical Engineering*, **19**: 1-69.

Moucha, T., Linek, V., and Prokopova, E. (2003). "Gas hold-up, mixing time and gas-liquid volumetric mass transfer coefficient of various multiple-impeller configurations: Rushton turbine, pitched blade and Techmix impeller and their combinations." *Chemical Engineering Science*, **58**(9): 1839-1846.

Mouza, A. A., Dalakoglou, G. K., and Paras, S. V. (2005). "Effect of liquid properties on the performance of bubble column reactors with fine pore spargers." *Chemical Engineering Science*, **60**(5): 1465-1475.

Murthy, B. N., Ghadge, R. S., and Joshi, J. B. (2007). "CFD simulations of gas-liquid-solid stirred reactor: Prediction of critical impeller speed for solid suspension." *Chemical Engineering Science*, **62**(24): 7184-7195.

Muthukumar, K., and Velan, M. (2006). "Volumetric mass transfer coefficients in an internal loop airlift reactor with low-density particles." *Journal of Chemical Technology & Biotechnology*, **81**(4): 667-673.

Nacef, S., Poncin, S., Bouguettoucha, A., and Wild, G. (2007). "Drift flux concept in two- and three-phase reactors." *Chemical Engineering Science*, **62**(24): 7530-7538.

Nakanoh, M., and Yoshida, F. (1980). "Gas absorption by Newtonian and non-Newtonian liquids in a bubble column." *Industrial & Engineering Chemistry Process Design and Development*, **19**(1): 190-195.

Nauman, E. B., and Buffman, B. A. (1983). *Mixing in Continuous Flow Systems*. New York, John Wiley & Sons.

Nedeltchev, S. (2003). "Correction of the penetration theory applied for prediction of mass transfer coefficients in a high-pressure bubble column operated with gasoline and toluene." *Journal of Chemical Engineering of Japan*, **36**(5): 630-633.

Ni, X., Gao, S., Cumming, R. H., and Pritchard, D. W. (1995). "A comparative study of mass transfer in yeast for a batch pulsed baffled bioreactor and a stirred tank fermenter." *Chemical Engineering Science*, **50**(13): 2127-2136.

Nicolella, C., van Loosdrecht, M. C. M., and Heijnen, J. J. (1998a). "Mass transfer and reaction in a biofilm airlift suspension reactor." *Chemical Engineering Science*, **53**(15): 2743-2753.

Nicolella, C., van Loosdrecht, M. C. M., van der Lans, R. G. J. M., and Heijnen, J. J. (1998b). "Hydrodynamic characteristics and gas-liquid mass transfer in a biofilm airlift suspension reactor." *Biotechnology and Bioengineering*, **60**(5): 627-635.

Nielsen, J., and Volladsen, J. (1993). "Description and modelling" in *Bioprocessing*. Edited by Rehm, H.-J., Reed, G., Puehler, A. and Stadler, P. New York, NY, VCH. **3:** 79-102.

Nienow, A. W. (1996). "Gas-liquid mixing studies: A comparison of Rushton turbines with some modern impellers." *Chemical Engineering Research & Design*, **74**(A4): 417-423.

Nienow, A. W. (1998). "Hydrodynamics of stirred bioreactors." *Applied Mechanics Reviews*, **51**(1): 3-32.

Nienow, A. W., Kendall, A., Moore, I. P. T., Ozcan-Taskin, G. N., and Badham, R. S. (1995). "The characteristics of aerated 12- and 18-blade Rushton turbines at transitional Reynolds numbers." *Chemical Engineering Science*, **50**(4): 593-599.

Nienow, A. W., Warmoeskerken, M. M. C. G., Smith, J. M., and Konno, M. (1985). "On the flooding/loading transition and the complete dispersal condition in aerated vessels agitated by a Rushton-turbine", Wuerzburg, West Germany, BHRA, Cranfield, England.

Nienow, A. W., Wisdom, D. J., and Middleton, J. C. (1977). The effect of scale and geometry on flooding, recirculation, and power in gassed stirred vessels. *Second European Conference on Mixing*. Cambridge, England**:** F1 1-16.

Nigam, K. D. P., and Larachi, F. (2005). "Process intensification in trickle-bed reactors." *Chemical Engineering Science*, **60**(22): 5880-5894.

Nishikawa, M., Nakamura, M., and Hashimoto, K. (1981). "Gas absorption in aerated mixing vessels with non-Newtonian liquid." *Journal of Chemical Engineering of Japan*, **14**(3): 227-232.

Nishikawa, M., Nishioka, S., and Kayama, T. (1984). "Gas absorption in an aerated mixing vessel with multi-stage impellers." *Journal of Chemical Engineering of Japan*, **17**(5): 541-543.

Nocentini, M. (1990). "Mass transfer in gas-liquid, multiple-impeller stirred vessels: a discussion about experimental techniques for k_La measurement and models comparison." *Chemical Engineering Research & Design*, **68**(3): 287-294.

Nocentini, M., Fajner, D., Pasquali, G., and Magelli, F. (1993). "Gas-liquid mass transfer and holdup in vessels stirred with multiple Rushton turbines: Water and water-glycerol solutions." *Industrial & Engineering Chemistry Research*, **32**(1): 19-26.

Nocentini, M., Pinelli, D., and Magelli, F. (1998). "Analysis of the gas behavior in sparged reactors stirred with multiple Rushton turbines: Tentative model validation and scale-up." *Industrial & Engineering Chemistry Research*, **37**(4): 1528-1535.

Norman, W. S., and Sammak, F. Y. Y. (1963). "Gas absorption in a packed column Part I: The effect of liquid viscosity on the mass transfer coefficient." *Transactions of the Institution of Chemical Engineers*, **41**(3): 109-116.

Nouri, L. h., Legrand, J., Benmalek, N., Imerzoukene, F., Yeddou, A.-R., and Halet, F. (2008). "Characterisation and comparison of the micromixing efficiency in torus and batch stirred reactors." *Chemical Engineering Journal*, **142**(1): 78-86.

Nunes, S. P., and Peinemann, K.-V., Eds. (2006). *Membrane technology in the chemical industry*. Weinheim, Germany, Wiley-VCH Verlag GmbH & Co. KGaA.

Ogut, A., and Hatch, R. T. (1988). "Oxygen transfer into Newtonian and non-Newtonian fluids in mechanically agitated vessels." *Canadian Journal of Chemical Engineering*, **66**(1): 79-85.

Oldshue, J. Y. (1983). *Fluid mixing technology*. New York, NY, McGraw-Hill Publications Co.

Olmos, E., Gentric, C., and Midoux, N. (2003). "Numerical description of flow regime transitions in bubble column reactors by a multiple gas phase model." *Chemical Engineering Science*, **58**(10): 2113-2121.

Onda, K., Sada, E., and Murase, Y. (1959). "Liquid-side mass transfer coefficients in packed towers." *AIChE Journal*, **5**(2): 235-239.

Onda, K., Sada, E., and Otubo, F. (1958). "Liquid-side mass-transfer coefficient for a tower packed with Raschig rings." *Kagaku Kogaku*, **22**(4): 194-199.

Onda, K., Sada, E., and Saito, M. (1961). "Gas-side mass transfer coefficients in packed tower." *Kagaku Kogaku*, **25**(N11): 820-828.

Ostafin, A., and Landfester, K., Eds. (2009). *Nanoreactor Engineering*. Engineering in Medicine & Biology. Boston, Artech House.

Ozturk, S. S., Schumpe, A., and Deckwer, W. D. (1987). "Organic liquids in a bubble column: Holdups and mass transfer coefficients." *AIChE Journal*, **33**(9): 1473-1480.

Patwardhan, A. W., and Joshi, J. B. (1998). "Design of stirred vessels with gas entrained from free liquid surface." *Canadian Journal of Chemical Engineering*, **76**(3): 339-364.

Patwardhan, A. W., and Joshi, J. B. (1999). "Design of gas-inducing reactors." *Industrial & Engineering Chemistry Research*, **38**(1): 49-80.

Paul, E. L., Atiemo-Obeng, V. A., and Kresta, S. M., Eds. (2004). *Handbook of Industrial Mixing*. Hoboken, New Jersey, John Wiley & Sons, Inc.

Peinemann, K.-V., and Nunes, S. P., Eds. (2008a). *Membranes for energy conversion*. Membrane Technology. Weinheim, Germany, Wiley-VCH Verlag GmbH & Co. KGaA.

Peinemann, K.-V., and Nunes, S. P., Eds. (2008b). *Membranes for life sciences*. Membrane Technology. Weinheim, Germany, Wiley-VCH Verlag GmbH & Co. KGaA.

Piché, S., Larachi, F., and Grandjean, B. P. A. (2001a). "Flooding capacity in packed towers: Database, correlations, and analysis." *Industrial & Engineering Chemistry Research*, **40**(1): 476-487.

Piché, S., Larachi, F., and Grandjean, B. P. A. (2001b). "Loading capacity in packing towers: Database, correlations and analysis." *Chemical Engineering & Technology*, **24**(4): 373-380.

Piché, S. R., Larachi, F., and Grandjean, B. P. A. (2001c). "Improving the prediction of irrigated pressure drop in packed absorption towers." *The Canadian Journal of Chemical Engineering*, **79**(4): 584-594.

Pollack, J. K., Li, Z. J., and Marten, M. R. (2008). "Fungal mycelia show lag time before re-growth on endogenous carbon." *Biotechnology and Bioengineering*, **100**(3): 458-465.

Poorte, R. E. G., and Biesheuvel, A. (2002). "Experiments on the motion of gas bubbles in turbulence generated by an active grid." *Journal of Fluid Mechanics*, **461**: 127-154.

Popovic, M., and Robinson, C. W. (1984). "Estimation of some important design parameters for non-Newtonian liquids in pneumatically-agitated fermenters". *Proceedings of the 34th Canadian Chemical Engineering Conference*, Quebec City, Canada.

Posarac, D., and Petrovic, D. (1988). "An experimental study of the minimum fluidization velocity in a three-phase external loop airlift-reactor." *Chemical Engineering Science*, **43**(5): 1161-1165.

Pramparo, L., Pruvost, J., Stuber, F., Font, J., Fortuny, A., Fabregat, A., Legentilhomme, P., Legrand, J., and Bengoa, C. (2008). "Mixing and hydrodynamics investigation using CFD in a square-sectioned torus reactor in batch and continuous regimes." *Chemical Engineering Journal*, **137**(2): 386-395.

Process Systems Enterprise Limited. (2009). "Advanced process modelling for reaction systems." Retrieved Sept 27, 2009, from http://www.psenterprise.com/gproms/applications/reaction/catalyst_monolith.html.

Puthli, M. S., Rathod, V. K., and Pandit, A. B. (2005). "Gas-liquid mass transfer studies with triple impeller system on a laboratory scale bioreactor." *Biochemical Engineering Journal*, **23**(1): 25-30.

Ramaswamy, S., Cutright, T. J., and Qammar, H. K. (2005). "Control of a continuous bioreactor using model predictive control." *Process Biochemistry*, **40**(8): 2763-2770.

Ramesh, K. V., Raju, G. M. J., Sarma, G. V. S., and Sarma, C. B. (2009). "Effect of internal on phase holdups of a three-phase fluidized bed." *Chemical Engineering Journal*, **145**(3): 393-398.

Ramm, W. M., and Chagina, Z. W. (1965). "Issledowanie teplootdachi pri powerxnostnom kipenii rastworow neletuchix weshestw." *Khimicheskaia Promyshlennost*, **23**: 219-222.

Raschig Jaeger Technologies (2006). "Product Bulletin 1100." *Raschig Jaeger Technologies Brochures*, (1100): 1-20.

Raschig LTD. "Prospectus of Packings."

Reddy, G. P., and Chidambaram, M. (1995). "Near-optimal productivity control of a continuous bioreactor." *IEE Proceedings: Control Theory and Applications*, **142**(6): 633-637.

Reichelt, W. (1974). Stromung und Stoffaustausch in Fullkorperapparaten bei Gegenstrom einer flussigen und einer gasformigen Phase. Weinheim/Bergstr, Verlag Chemie.

Reilley, I. G., Scott, D. S., De Bruijin, T., Jain, A., and Pixkorz, J. (1986). "A correlation for gas holdup in turbulent coalescing bubble columns." *Canadian Journal of Chemical Engineering*, **1986**(64): 705-717.

Rewatkar, V. B., Deshpande, A. J., Pandit, A. B., and Joshi, J. B. (1993). "Gas hold-up behavior of mechanically agitated gas-liquid reactors using pitched blade downflow turbines." *Canadian Journal of Chemical Engineering*, **71**(2): 226-237.

Rewatkar, V. B., and Joshi, J. B. (1993). "Role of sparger design on gas dispersion in mechanically agitated gas-liquid contactors." *Canadian Journal of Chemical Engineering*, **71**(2): 278-291.

Ros, M., and Zupancic, G. D. (2002). "Thermophilic aerobic digestion of waste activated sludge." *Acta Chimica Slovenica*, **49**(4): 931-943.

Roy, N. K., Guha, D. K., and Rao, M. N. (1963). "Fractional gas holdup in two-phase and three-phase batch-fluidized bubble-bed and foam-systems." *Indian Chemical Engineer*, **1963**: 27-31.

Roy, S., and Joshi, J. B. (2008). "CFD study of mixing characteristics of bubble column and external loop airlift reactor." *Asia-Pacific Journal of Chemical Engineering*, **3**(2): 97-105.

Ruckenstein, E. (1964). "On mass transfer in the continuous phase from spherical bubbles or drops." *Chemical Engineering Science*, **19**(2): 131-148.

Ruen-ngam, D., Wongsuchoto, P., Limpanuphap, A., Charinpanitkul, T., and Pavasant, P. (2008). "Influence of salinity on bubble size distribution and gas-liquid mass transfer in airlift contactors." *Chemical Engineering Journal*, **141**(1-3): 222-232.

Ruzicka, M. C., Drahos, J., Fialová, M., and Thomas, N. H. (2001a). "Effect of bubble column dimensions on flow regime transition." *Chemical Engineering Science*, **56**(21-22): 6117-6124.

Ruzicka, M. C., Drahos, J., Mena, P. C., and Teixeira, J. A. (2003). "Effect of viscosity on homogeneous-heterogeneous flow regime transition in bubble columns." *Chemical Engineering Journal*, **96**(1-3): 15-22.

Ruzicka, M. C., and Thomas, N. H. (2003). "Buoyancy-driven instability of bubbly layers: Analogy with thermal convection." *International Journal of Multiphase Flow*, **29**(2): 249-270.

Ruzicka, M. C., Zahradník, J., Drahos, J., and Thomas, N. H. (2001b). "Homogeneous-heterogeneous regime transition in bubble columns." *Chemical Engineering Science*, **56**(15): 4609-4626.

Sada, E., Katoh, S., Yoshii, H., Yamanishi, T., and Nakanishi, A. (1984). "Performance of the gas bubble column in molten salt systems." *Industrial & Engineering Chemistry, Process Design and Development*, **23**(1): 151-154.

Sada, E., Kumazawa, H., and Lee, C. H. (1986). "Influences of suspended fine particles on gas holdup and mass transfer characteristics in a slurry bubble column." *AIChE Journal*, **32**(5): 853-856.

Salvacion, J. L., Murayama, M., Ohtaguchi, K., and Koide, K. (1995). "Effects of alcohols on gas holdup and volumetric liquid-phase mass transfer coefficient in gel-particle suspended bubble column." *Journal of Chemical Engineering of Japan*, **28**(4): 434.

Sardeing, R., Aubin, J., Poux, M., and Xuereb, C. (2004a). "Gas-liquid mass transfer: Influence of sparger location." *Chemical Engineering Research & Design*, **82**(9): 1161-1168.

Sardeing, R., Aubin, J., and Xuereb, C. (2004b). "Gas-liquid mass transfer: A comparison of down- and up-pumping axial flow impellers with radial impellers." *Chemical Engineering Research & Design*, **82**(12): 1589-1596.

Scargiali, F., D'Orazio, A., Grisafi, F., and Brucato, A. (2007). "Modelling and simulation of gas-liquid hydrodynamics in mechanically stirred tanks." *Chemical Engineering Research & Design*, **85**(5): 637-646.

Schäfer, R., Merten, C., and Eigenberger, G. (2002). "Bubble size distributions in a bubble column reactor under industrial conditions." *Experimental Thermal and Fluid Science*, **26**(6-7): 595-604.

Scherwood, T. K., and Holloway, F. A. L. (1940). *Transactions of the American Institute of Chemical Engineers*, **36**(1): 21.

Schönfeld, H., Hunger, K., Cecilia, R., and Kunz, U. (2004). "Enhanced mass transfer using a novel polymer/carrier microreactor." *Chemical Engineering Journal*, **101**(1-3): 455-463.

Schultes, M. (2003). "Raschig Super-Ring: A new fourth generation packing offers new advantages." *Chemical Engineering Research & Design*, **81**(1): 48-57.

Schumacher, J. (2000). "A framework for batch-operation analysis within the context of disturbance management." *Computers & Chemical Engineering*, **24**(2-7): 1175-1180.

Schumpe, A., and Deckwer, W. D. (1987). "Viscous media in tower bioreactors: Hydrodynamic characteristics and mass transfer properties." *Bioprocess and Biosystems Engineering*, **1987**(2): 79-94.

Schumpe, A., and Grund, G. (1986). "The gas disengagement technique for studying gas holdup structure in bubble columns." *Canadian Journal of Chemical Engineering*, **64**(6): 891-896.

Schuurman, Y. (2008). "Aspects of kinetic modeling of fixed bed reactors." *Catalysis Today*, **138**(1-2): 15-20.

Shah, Y. T., Kelkar, B. G., Godbole, S. P., and Deckwer, W. D. (1982). "Design parameters estimations for bubble column reactors." *AIChE Journal*, **28**(3): 353-379.

Shariati, F. P., Bonakdarpour, B., and Mehrnia, M. R. (2007). "Hydrodynamics and oxygen transfer behaviour of water in diesel microemulsions in a draft tube airlift bioreactor." *Chemical Engineering and Processing*, **46**(4): 334-342.

Sharma, M., and Yashonath, S. (2006). "Breakdown of the Stokes-Einstein relationship: Role of interactions in the size dependence of self-diffusivity." *The Journal of Physical Chemistry B*, **110**(34): 17207-17211.

Shewale, S. D., and Pandit, A. B. (2006). "Studies in multiple impeller agitated gas-liquid contactors." *Chemical Engineering Science*, **61**(2): 489-504.

Shpirt, E. (1981). "Role of hydrodynamic factors in ammonia desorption by diffused aeration." *Water Research*, **15**(6): 739-743.

Shulman, H. L., Ulrich, C. E., Proulz, A. Z., and Zimmerman, L. O. (1955). "Wetted and effective: Interfacial areas, gas- and liquid-phase mass transfer rates." *AIChE Journal*, **1**(2): 253-258.

Siegel, M. H., and Merchuk, J. C. (1988). "Mass transfer in a rectangular air-lift reactor: Effects of geometry and gas recirculation." *Biotechnology and Bioengineering*, **32**(9): 1128-1137.

Siegel, M. H., Merchuk, J. C., and Schugerl, K. (1986). "Air-lift reactor analysis: Interrelationships between riser, downcomer, and gas-liquid separator behavior, including gas recirculation effects." *AIChE Journal*, **32**(10): 1585-1596.

Siemens Water Technologies. (2009). "Integrated and advanced biological wastewater systems." Retrieved October 7, 2009, from http://www.water.siemens.com/en/products/biological_treatment/integrated_advanced_wastewater_systems/Pages/Zimpro_AGAR.aspx.

Simon, J., Wiese, J., and Steinmetz, H. (2006). "A comparison of continuous flow and sequencing batch reactor plants concerning integrated operation of sewer systems and wastewater treatment plants." *Water Science & Technology*, **54**(11): 241-248.

Smith, D. N., Fuchs, W., Lynn, R. J., and Smith, D. H. (1983). "Bubble behavior in a slurry bubble column reactor model", Washington, DC, USA, ACS.

Smith, J. M., Van't Riet, K., and Middleton, J. C. (1977). Scale-up of agitated gas-liquid reactors for mass transfer. *Proceedings of the Second European Conference on Mixing*. Stephens, H. S. and Clarke, J. A. Crafield, U. K., BHRA Fluid Engineering.

Smith, J. M., and Warmoeskerken, M. M. C. G. (1985). "Dispersion of Gases in Liquids with Turbines", Wuerzburg, West Germany, BHRA, Cranfield, England.

Snape, J. B., Zahradnik, J., Fialova, M., and Thomas, N. M. (1995). "Liquid-phase properties and sparger design effects in an external-loop airlift reactor." *Chemical Engineering Science*, **50**(20): 3175-3186.

Sokol, W., and Migiro, C. L. C. (1996). "Controlling a continuous stirred-tank bioreactor degrading phenol in the stability range." *The Chemical Engineering Journal and the Biochemical Engineering Journal*, **62**(1): 67-72.

Sokolov, V. N., and Aksenova, E. G. (1983). *Journal of Applied Chemistry of the USSR*, **55**(10): 2158.

Sotelo, J. L., Benitez, F. J., Beltran-Heredia, J., and Rodriguez, C. (1994). "Gas holdup and mass transfer coefficients in bubble columns. 1. Porous glass-plate diffusers." *International Chemical Engineering*, **34**(1): 82-90.

Sotiriadis, A. A., Thorpe, R. B., and Smith, J. M. (2005). "Bubble size and mass transfer characteristics of sparged downwards two-phase flow." *Chemical Engineering Science*, **60**(22): 5917-5929.

Stegeman, D., Ket, P. J., Kolk, K. A. v. d., Bolk, J. W., Knop, P. A., and Westerterp, K. R. (1995). "Interfacial area and gas holdup in an agitated gas-liquid reactor under pressure." *Industrial & Engineering Chemistry Research*, **34**(1): 59-71.

Stenberg, O., and Andersson, B. (1988a). "Gas-liquid mass transfer in agitated vessels: I. Evaluation of the gas-liquid mass transfer coefficient from transient-response measurements." *Chemical Engineering Science*, **43**(3): 719-724.

Stenberg, O., and Andersson, B. (1988b). "Gas-liquid mass transfer in agitated vessels--II. Modelling of gas-liquid mass transfer." *Chemical Engineering Science*, **43**(3): 725-730.

Stichlmair, J., Bravo, J. L., and Fair, J. R. (1989). "General model for prediction of pressure drop and capacity of countercurrent gas/liquid packed columns." *Gas Separation & Purification*, **3**(March): 19-28.

Strigle, R. F. J. (1994). Packed Tower Design and Applications: Random and Structured Packings. Houston, TX, Gulf Publishing Company.

Su, X. (2005). "Gas holdup in gas-liquid-fiber semi-batch bubble column." PhD. Dissertation, Iowa State University, Ames, IA.

Su, X., and Heindel, T. J. (2004). "Gas holdup behavior in nylon fiber suspensions." *Industrial & Engineering Chemistry Research*, **43**(9): 2256-2263.

Su, X., and Heindel, T. J. (2005a). "Effect of perforated plate open area on gas holdup in rayon fiber suspensions." *Journal of Fluids Engineering*, **127**(4): 816-823.

Su, X., and Heindel, T. J. (2005b). "Modeling gas holdup in gas-liquid-fiber semibatch bubble columns." *Industrial & Engineering Chemistry Research*, **44**(24): 9355-9363.

Su, X., Hol, P. D., Talcott, S. M., Staudt, A. K., and Heindel, T. J. (2006). "The effect of bubble column diameter on gas holdup in fiber suspensions." *Chemical Engineering Science*, **61**(10): 3098-3104.

Syeda, S. R., Afacan, A., and Chuang, K. T. (2002). "Prediction of gas hold-up in a bubble column filled with pure and, binary liquids." *Canadian Journal of Chemical Engineering*, **80**(1): 44-50.

Talvy, S., Cockx, A., and Liné, A. (2007). "Modeling of oxygen mass transfer in a gas-liquid airlift reactor." *AIChE Journal*, **53**(2): 316-326.

Tang, C., and Heindel, T. J. (2005a). "Effect of fiber type on gas holdup in a cocurrent air-water-fiber bubble column." *Chemical Engineering Journal*, **111**(1): 21-30.

Tang, C., and Heindel, T. J. (2005b). "Gas-liquid-fiber flow in a cocurrent bubble column." *AIChE Journal*, **51**(10): 2665-2674.

Tang, C., and Heindel, T. J. (2006a). "A gas holdup model for cocurrent air-water-fiber bubble columns." *Chemical Engineering Science*, **61**(10): 3299-3312.

Tang, C., and Heindel, T. J. (2006b). "Similitude analysis for gas-liquid-fiber flows in cocurrent bubble columns". *Proceedings of FEDSM06: ASME Joint US-European Fluids Engineering Summer Meeting*, Miami, Florida.

Tang, C., and Heindel, T. J. (2007). "Effect of fiber length distribution on gas holdup in a cocurrent air-water-fiber bubble column." *Chemical Engineering Science*, **62**(5): 1408-1417.

Tatterson, G. B. (1991). *Fluid Mixing and Gas Dispersion in Agitated Tanks*. New York, McGraw-Hill, Inc.

Tatterson, G. B. (1994). *Scaleup and Design of Industrial Mixing Processes*. New York, McGraw-Hill, Inc.

Tecante, A., and Choplin, L. (1993). "Gas-liquid mass transfer in non-Newtonian fluids in a tank stirred with a helical ribbon screw impeller." *Canadian Journal of Chemical Engineering*, **71**(6): 859-865.

Titchener-Hooker, N. J., and Hoare, P. D. M. (2008). "Micro biochemical engineering to accelerate the design of industrial-scale downstream processes for biopharmaceutical proteins." *Biotechnology and Bioengineering*, **100**(3): 473-487.

Torré, J.-P., Fletcher, D. F., Lasuye, T., and Xuereb, C. (2007). "An experimental and computational study of the vortex shape in a partially baffled agitated vessel." *Chemical Engineering Science*, **62**(7): 1915-1926.

Trilleros, J., Díaz, R., and Redondo, P. (2005). "Three-phase airlift internal loop reactor: Correlations for predicting the main fluid dynamic parameters." *Journal of Chemical Technology & Biotechnology*, **80**(5): 515-522.

Tse, K., Martin, T., McFarlane, C. M., and Nienow, A. W. (1998). "Visualisation of bubble coalescence in a coalescence cell, a stirred tank and a bubble column." *Chemical Engineering Science*, **53**(23): 4031-4036.

Ulbrecht, J. J., and Patterson, G. K. (1985). *Mixing of liquids by mechanical agitation*. New York, Gordon and Breach Science Publishers.

Ungerman, A. J. (2006). "Mass transfer enhancement for syngas fermentation." M.S. Thesis, Iowa State University, Ames, IA.

Ungerman, A. J., and Heindel, T. J. (2007). "Carbon monoxide mass transfer for syngas fermentation in a stirred tank reactor with dual impeller configurations." *Biotechnology Progress*, **23**(3): 613-620.

van Benthum, W. A. J., van den Hoogen, J. H. A., van der Lans, R. G. J. M., van Loosdrecht, M. C. M., and Heijnen, J. J. (1999a). "The biofilm airlift suspension extension reactor. Part I: Design and two-phase hydrodynamics." *Chemical Engineering Science*, **54**(12): 1909-1924.

van Benthum, W. A. J., van der Lans, R. G. J. M., van Loosdrecht, M. C. M., and Heijnen, J. J. (1999b). "Bubble recirculation regimes in an internal-loop airlift reactor." *Chemical Engineering Science*, **54**(18): 3995-4006.

van Benthum, W. A. J., van der Lans, R. G. J. M., van Loosdrecht, M. C. M., and Heijnen, J. J. (2000). "The biofilm airlift suspension extension reactor. Part II: Three-phase hydrodynamics." *Chemical Engineering Science*, **55**(3): 699-711.

van der Meer, A. B., Beenackers, A. A. C. M., Burghard, R., Mulder, N. H., and Fok, J. J. (1992). "Gas/liquid mass transfer in a four-phase stirred fermentor: Effects of organic phase hold-up and surfactant concentration." *Chemical Engineering Science*, **47**(9-11): 2369-2374.

van der Schaaf, J., Chilekar, V. P., van Ommen, J. R., Kuster, B. F. M., Tinge, J. T., and Schouten, J. C. (2007). "Effect of particle lyophobicity in slurry bubble columns at elevated pressures." *Chemical Engineering Science*, **62**(18-20): 5533-5537.

van der Westhuizen, I., Du Toit, E., and Nicol, W. (2007). "Trickle flow multiplicity: The influence of the prewetting procedure on flow hysteresis." *Chemical Engineering Research & Design*, **85**(12): 1604-1610.

van Elk, E. P., Knaap, M. C., and Versteeg, G. F. (2007). "Application of the penetration theory for gas-liquid mass transfer without liquid bulk: Differences with systems with a bulk." *Chemical Engineering Research & Design*, **85**(4): 516-524.

Vandu, C. O., and Krishna, R. (2004). "Influence of scale on the volumetric mass transfer coefficients in bubble columns." *Chemical Engineering and Processing*, **43**(4): 575-579.

Varley, J. (1995). "Submerged gas-liquid jets: Bubble size prediction." *Chemical Engineering Science*, **50**(5): 901-905.

Vasconcelos, J. M. T., Orvalho, S. C. P., Rodrigues, A. M. A. F., and Alves, S. S. (2000). "Effect of blade shape on the performance of six-bladed disk turbine impellers." *Industrial and Engineering Chemistry Research*, **39**(1): 203-213.

Vasquez, G., Antorrena, G., Navaza, J. M., Santos, V., and Rodriguez, T. (1993). "Adsorption of CO_2 in aqueous solutions of various viscosities in the presence of induced turbulence." *International Chemical Engineering*, **1993**(4): 649-655.

Vatai, G., and Tekic, M. N. (1986). "Effect of pseudoplasticity on hydrodynamic characteristics of air-lift loop contactor." *Rheologica Acta*, **26**: 271.

Vázquez, G., Cancela, M. A., Riverol, C., Alvarez, E., and Navaza, J. M. (2000). "Application of the Danckwerts method in a bubble column: Effects of surfactants on mass transfer coefficient and interfacial area." *Chemical Engineering Journal*, **78**(1): 13-19.

Vazquez, G., Cancela, M. A., Varela, R., Alvarez, E., and Navaza, J. M. (1997). "Influence of surfactants on absorption of CO_2 in a stirred tank with and without bubbling." *Chemical Engineering Journal*, **67**(2): 131-137.

Veera, U. P., and Joshi, J. B. (1999). "Measurement of gas hold-up profiles by gamma ray tomography: Effect of sparger design and height of dispersion in bubble columns." *Chemical Engineering Research & Design*, **77**(4): 303-317.

Veera, U. P., Kataria, K. L., and Joshi, J. B. (2004). "Effect of superficial gas velocity on gas hold-up profiles in foaming liquids in bubble column reactors." *Chemical Engineering Journal*, **99**(1): 53-58.

Verma, A. K., and Rai, S. (2003). "Studies on surface to bulk ionic mass transfer in bubble column." *Chemical Engineering Journal*, **94**(1): 67-72.

Vesselinov, H. H., Stephan, B., Uwe, H., Holger, K., Günther, H., and Wilfried, S. (2008). "A study on the two-phase flow in a stirred tank reactor agitated by a gas-inducing turbine." *Chemical Engineering Research & Design*, **86**(1): 75-81.

Vial, C., Laine, R., Poncin, S., Midoux, N., and Wild, G. (2001). "Influence of gas distribution and regime transitions on liquid velocity and turbulence in a 3-D bubble column." *Chemical Engineering Science*, **56**(3): 1085-1093.

Waghmare, Y. G., Rice, R. G., and Knopf, F. C. (2008). "Mass transfer in a viscous bubble column with forced oscillations." *Industrial & Engineering Chemistry Research*, **47**(15): 5386-5394.

Walter, J. F., and Blanch, H. W. (1986). "Bubble break-up in gas-liquid bioreactors: Break-up in turbulent flows." *Chemical Engineering Journal*, **32**(1): B7-B17.

Watts, P., and Wiles, C. (2007). "Micro reactors: A new tool for the synthetic chemist." *Organic and Biomolecular Chemistry*, **5**(5): 727-732.

Wei, C., Xie, B., and Xiao, H. (2000). "Hydrodynamics in an internal loop airlift reactor with a convergence-divergence draft tube." *Chemical Engineering & Technology*, **23**(1): 38-45.

Wei, Y., Tiefeng, W., Malin, L., and Zhanwen, W. (2008). "Bubble circulation regimes in a multi-stage internal-loop airlift reactor." *Chemical Engineering Journal*, **142**(3): 301-308.

Weiland, P. (1984). "Influence of draft tube diameter on operation behavior of airlift loop reactors." *German Chemical Engineering*, **7**(6): 374-385.

Westerterp, K. R., and Molga, E. J. (2006). "Safety and runaway protection in batch and semibatch reactors: A review." *Chemical Engineering Research & Design*, **84**(A7): 543-552.

Wilkinson, P. M. (1991). "Physical aspect and scale-up of high pressure bubble column." PhD Thesis, University of Groningen, Groningen, Netherland.

Wilkinson, P. M., Spek, A. P., and van Dierendonck, L. L. (1992). "Design parameters estimation for scale-up of high-pressure bubble columns." *AIChE Journal*, **38**(4): 544-554.

Williams, J. A. (2002). "Keys to bioreactor selection." *Chemical Engineering Progress*, **98**(3): 34-41.

Wirth, T., Ed. (2008). *Microreactors in organic synthesis and catalysis*. Weinheim, Germany, Wiley-VCH Verlag GmbH & KGaA.

Wooley, R., Ruth, M., Sheehan, J., Ibsen, K., Majdeski, H., and Galvez, A. "Lignocellulosic biomass to ethanol process design and economics utilizing co-current dilute acid prehydrolysis and enzymatic hydrolysis current and futuristic scenarios." NREL report TP-580-26157. July 1999.

Worden, R. M., and Bredwell, M. D. (1998). "Mass transfer properties of microbubbles: II. Analysis using a dynamic model." *Biotechnology Progress*, **14**(1): 39-46.

Yakhnin, V. Z., and Menzinger, M. (2008). "Estimating spectral properties of the thermal instability in packed-bed reactors." *Chemical Engineering Science*, **63**(6): 1480-1489.

Yawalkar, A. A., Pangarkar, V. G., and Beenackers, A. A. C. M. (2002). "Gas hold-up in stirred tank reactors." *The Canadian Journal of Chemical Engineering*, **80**: 158-166.

Yoshida, F., and Koyanagi, T. (1962). "Mass transfer and effective interfacial areas in packed columns." *AIChE Journal*, **8**(3): 309-316.

Zahradnik, J., Fialová, M., and Linek, V. (1999a). "The effect of surface-active additives on bubble coalescence in aqueous media." *Chemical Engineering Science*, **54**(21): 4757-4766.

Zahradnik, J., Fialová, M., Ruzicka, M., Drahos, J., Kastánek, F., and Thomas, N. H. (1997). "Duality of the gas-liquid flow regimes in bubble column reactors." *Chemical Engineering Science*, **52**(21-22): 3811-3826.

Zahradnik, J., and Kastanek, F. (1979). "Gas holdup in uniformly aerated bubble column reactors." *Chemical Engineering Communications*, **3**(4-5): 413-429.

Zahradnik, J., Kuncová, G., and Fialová, M. (1999b). "The effect of surface active additives on bubble coalescence and gas holdup in viscous aerated batches." *Chemical Engineering Science*, **54**(13-14): 2401-2408.

Zech, J. B. (1978). "Liquid flow and mass transfer in an irrigated packed column." PhD Thesis, TU Munchen, Munchen, Germany.

Zehner, P. (1989). "Mehrphasenstromungen in Gas-Flussigkeits-Reaktoren." *Dechema-Monograph*, **1989**(114): 215-233.

Zeng, A.-P., and Deckwer, W.-D. (1996). "Bioreaction techniques under microaerobic conditions: from molecular level to pilot plant reactors." *Chemical Engineering Science*, **51**(10): 2305-2314.

Zhang, H., Chen, G., Yue, J., and Yuan, Q. (2009). "Hydrodynamics and mass transfer of gas-liquid flow in a falling film microreactor." *AIChE Journal*, **55**(5): 1110-1120.

Zou, R., Jiang, X., Li, B., Zu, Y., and Zhang, L. (1988). "Studies on gas holdup in a bubble column operated at elevated temperatures." *Industrial & Engineering Chemistry Research*, **27**(10): 1910-1916.